A MODEL STUDY OF CLAY MOBILISATION AND PERMEABILITY REDUCTION DURING OIL RESERVOIR FLOODING

by

S. BAKHSH, BSc

This thesis is submitted in partial fulfilment of the regulations for the award of the degree of
Doctor of Philosophy
of the
Loughborough University of Technology

August 1991

Supervisor: Dr R J Akers

Department of Chemical Engineering

Dedicated to my parents for
their guidance and affectionate love

* * * * *

ACKNOWLEDGEMENTS

I would like to thank:

My supervisor, Dr R.J. Akers for his patience and guiding help throughout the course of the research and in the past few years.

Professor D.C. Freshwater, for the provision of the research facilities; Mr P.J. Lloyd, my Director of Research and Dr J.I.T. Stenhouse for their interest and support; colleagues and staff in the Department; Professor B. Scarlett, at the University of Delft, for much encouragement when I needed it; and Mrs Janet Smith for efficiently typing the script.

The Science and Engineering Research Council for financial support of the research programme; the British Petroleum Research Centre, Sunbury-on-Thames, where Dr E.L. Neustadter, Dr J.H. Clint and Dr. J. Heaviside made available equipment, facilities, and offered much useful advice.

Many friends who have encouraged me; Dr C.P.S. Johal and Dr M. Naaem for their help in so many ways; Hamid, Siyyara, Sabina and Sadiya for putting up with me; my family; and finally to my brothers and sisters: Javed, Sohail, Shahid, Umber, Zahid, Nekhaar, Siyyara and Asma to all of whom I owe so much.

ABSTRACT

Formation damage effects have been reported in a number of oil reservoirs in secondary and enhanced recovery stages of production. The loss in permeability has been widely attributed to the swelling or pore-plugging action of colloidal clay minerals which are present in varying quantities in the pore spaces of reservoir rocks. This research has been aimed at predicting the action of non-swelling clay particles such as those commonly found in North Sea reservoir sandstones.

The literature from the areas of formation damage, colloidal suspensions, and deep bed filtration has been examined with particular attention being given to the subject of clay mineralogy. An experimental test rig was designed, comprising a cylindrical packed sand bed used as a model reservoir to study the permeability changes associated with the action of clay fines under various flooding regimes. The pH, salinity and valency of ionic species present in the flooding fluids were found to be the controlling factors for clay mobilisation. Fines dispersal coincided with spontaneous decrease in permeability when sandpacks treated with monovalent brine were subjected to fresh water flow. Analysis showed that the fines released from the bed were primarily kaolinite in the size range 1-5 micron. A minimum critical salinity of flooding water was shown to exist, above which particle dispersal is prevented. Further experimental work provided a measure of the ion exchange capacity of the clay fines in the sandpack as well as of pure clay materials.

The close-range interaction of kaolinite particles with silica surfaces was measured in a continuous flow glass apparatus which allowed in-situ observation and measurement by optical microscopy. Particle deposition in this system was found to be very sensitive to the method of cleaning of the silica surface. Deposition was also a function of the suspension flowrate. Clay mobilisation behaviour, as observed in the sandpack experiments, was confirmed with suspension pH, salinity and flowrate to a lesser extent, governing the particle release process.

The research has identified the conditions under which clay mobilisation is initiated. It is proposed that any model of permeability reduction should be adapted to include the effects of specific ion-exchange processes between clays and flooding liquids.

TABLE OF CONTENTS

Errata

Page, Para, Line	
1,1,2	*for* capillary forces *read* capillary forces and gravity
5,2,1	*for* by D'arcy[10] as *read* by Darcy[10], for horizontal, laminar flow as
6,4,1	*for* form *read* from
10,2	*for* NH_4 *read* NH_4^+
13,4,6	*for* a charge deficit *read* a negative charge
15,2,6	*for* meg *read* meq
24	*Eqn. 3 to read:* $\frac{\partial \sigma}{\partial t} = \begin{pmatrix} k\sigma(u-u_c) & for \quad u > u_c \\ 0 & for \quad u < u_c \end{pmatrix}$
29,3	*Eqn. 5, read* 25 nm *for* 25mm
31	*Eqn. 10, first term on RHS to read* N_-
31,1,3	*for* this *read* thus
32	*Eqn. 11, for* z, *read* -z
33	*Eqn. 17, for* k_x *read* kx
34	*Eqn. 17, for* nKT *read* nkT
37,3,10	*denominator of equation defining* K2 *to read* εkT
41,3,4 & 6	*for* D'Arcy *read* Darcy
41,3,6	*omit* in the
42,1,5	*for* Kuwabara[103] *read* Kuwabara[104]
43,1,2	*for* e1 = porosity *read* e = porosity
46,1,2	*for* P_1^* *read* ΔP_1^*
48,1,3	*for* stream function *read* stream function ψ,
48,5,2	*for* 100 m^2 *read* 100 μm^2
49,3,7	*for* o = initial flux *read* J_o = initial flux
50	*Eqn. 36, LHS to read* B_e
52	*Eqn. 39 to read* $F_A = \varepsilon a$
56	*Eqn. 46 to read* $G = \frac{(\rho_p - \rho_w) g d_p^2}{18 \mu v_0}$
59	*Eqn. 49, on RHS read + for =*
60	*Eqn. 50 to read* $F_D = 6\pi\mu a V + F_{D,P}$
60	*Eqn. 51 to read* $F_{D,P} = (F_{D,P})_{\parallel} \cos^2\theta + (F_{D,P})_{\perp} \sin^2\theta$

72,1,9	*for* where *read* was
76,1,5	*for* MNaCl *read* 1M NaCl
103,2,5	*for* D'Arcy *read* Darcy
Fig 55a	*Angle labelled* O_p *to read* θ_p

CHAPTER 1

INTRODUCTION

Oil reservoirs are porous sandstone or limestone rock structures wherein the oil is held by capillary forces. The rock matrix often contains significant quantities of fine particles, such as, in the case of sandstone reservoirs, quartz rock fragments and a range of mineral species which include colloidal clays. These particles, collectively termed 'fines', are either present as flocculated material in the pore space or are loosely attached to the pore surfaces in single or small multiple units or larger clusters. During primary oil extraction, internal pressure forces oil out of the reservoir to the wellhead where it is separated from the formation water and entrained solids. The reservoir pressure is usually maintained by pumping formation water back into the reservoir. In offshore fields, treated seawater or mixtures of seawater and formation water are used for this purpose whilst onshore, treated fresh water, seawater or artificial formation water is used.

These pressure maintenance operations are generally referred to as secondary recovery or water flooding. Tertiary or enhanced recovery procedures involve the use of surfactants and a range of chemicals in order to improve the oil fraction recovered from mature and depleted reservoirs [1-9]. Polymer solutions and foams [5] are generally used for mobility control of secondary and tertiary floods.

During stages of secondary and enhanced recovery, permeability losses have been observed in many reservoirs. The reaction, or 'water-

sensitivity' of reservoir fines to changes in flooding conditions is considered by many workers to be a primary cause of formation damage[13-22]. Early work in this area suggested that the swelling of certain types of clay as the dominant effect while, more recently, migration of fines and pore blocking have been found to be significant. Even reservoirs known to contain only small amounts of fines have suffered permeability loss during water flooding. Knowledge about why water sensitivity occurs could be useful in the prevention of formation damage problems at an earlier stage in production.

The water sensitivity of reservoir clay is a common reported cause of formation damage in sandstone reservoirs [13-22]. Typically, it occurs when a low salinity fluid is used to displace reservoir fluids, initiating a mobilisation of fines which migrate through the reservoir as a 'front'. The observed loss in permeability is only temporarily recovered when flooding is resumed in the reverse direction, suggesting that pore plugging is the dominant mechanism of permeability reduction in these situations. Damage, often most severe in the near well-bore region of injection and production wells, may also occur deep inside a reservoir where it is likely to be difficult to remedy.

It appears that the specific reasons for the water sensitivity phenomenon have not been identified. Both 'chemical' and 'physical' models of core damage have been proposed. In the latter case, particle release and transport is assumed to be due to fluid flow conditions alone. In one study [42], the flooding velocity was found to be critical for particle plugging and re-entrainment effects. The

'chemical' models attribute greater significance to the interactions between reservoir fluids, the pore surfaces and the fine particles contained in the pore space.

In the vicinity of pore surfaces and constrictions, the interaction of the surface properties of particles and grains is generally considered to have a greater influence than the particle transport. The effect of flocculated fines on flow conditions in a sandstone undergoing flooding has not been reported in any great detail in the literature despite the knowledge that clay particles are often found as 'aggregates' or 'plate-stacks' in a reservoir. This morphology implies a potentially increased resistance to flow and could explain the occurrence of water sensitivity effects in sandstones containing even trace quantities of clay minerals [20].

Despite the considerable amount of work done in the field of particle detachment, migration and pore-plugging, these phenomena remain largely unexplained. Much of this uncertainty is due to the fact that oil reservoirs contain a complexity of fines, differing in shape, size and surface electrochemical properties, making their characterisation a difficult task. It is often assumed that all fines behave in the same way under flooding conditions. In this work an attempt has been made to quantify pore plugging effects specifically due to the non-swelling kaolinite clays. Experiments with packed sand beds have been combined with work on a micromodel deposition and detachment system to provide basic data for the development of a theoretical basis for the prediction of particle capture, detachment and permeability reduction.

In Chapters 2 and 3, an extensive literature review is presented, covering the subject areas of formation damage and reservoir fines mineralogy, with particular reference to colloidal clays and their ion exchange properties. Work in the fields of porous media flow modelling and deep bed filtration is examined in order that fluid forces and particle-surface interactions may be better understood.

The equipment used and experimental procedures developed have been described in Chapter 4. The results of the experimental work are presented in Chapter 5 and discussed in detail in Chapter 6. Also presented here, on the basis of the theoretical and experimental analysis, is the model formulated for clay fines behaviour during flooding in sandstone reservoirs. The conclusions of the research are presented in Chapter 7 with some recommendations for further work.

CHAPTER 2

LITERATURE REVIEW I

2.1 INTRODUCTION

The most important properties of reservoir rocks from an oil production point of view, are their porosity and permeability. Rock porosity, the ratio of pore to bulk rock volume, provides storage capacity for the liquid and gas accumulation while permeability is a measure of the movement of fluids in the reservoir or from the reservoir to a well. Thus, permeability is a measure of the fluid transmitting capacity of the rock and depends on the porosity, the pore size distribution, the degree of interconnection of pores and the presence of void spaces. All of these factors are determined by the geological history of the reservoir.

Permeability has been empirically defined by D'Arcy [10] as:

$$K = \frac{\mu Q L}{A \Delta P} \qquad (1)$$

where K = permeability, Darcy

μ = viscosity, centipoise

L = length of rock sample, cm

A = cross-section of rock sample, cm^2

ΔP = pressure drop across rock sample, atmospheres

Q = flowrate, ml/s

This definition leads to the specific, or single-fluid saturation permeability expressed in terms of darcys. Reservoir rocks possess permeabilities from a few millidarcys to several darcys.

Reservoir rock can contain a three-phase mixture of crude oil, natural gases and connate brine. It is the effective permeability which is the important parameter in determining production performance. The effective permeability falls progressively below the specific permeability as the proportion of the particular fluid in the pore space decreases, tending to zero well before the proportion of that fluid reaches zero.

The degree of pore interconnection in a rock has a marked effect on its permeability. Thus, a formation can be porous whilst displaying low permeability. Effective porosity as opposed to total porosity is a more useful parameter when attempting to characterise permeability. The oil containing zone of a reservoir is often termed the 'pay-zone'. The significant quantity in calculating the oil production from a zone is the summation of the products of zone thickness and permeability often quoted as millidarcy-metres. This takes account of any vertical or lateral heterogeneity in the reservoir.

Reservoir rocks commonly have porosities in the range form 5% to 30%. The coarser-grained sedimentary rocks such as sands and sandstones, are the most typical reservoir rocks, possessing relatively high porosities. Limestone ('carbonate') reservoirs are generally less porous. However, even low porosity limestones can have reasonably high permeabilities particularly when they possess faults or fractures which have high fluid transmission capabilities. The permeability of reservoir rock is increased when naturally occurring or artificially

induced fractures exist in the rock. Fractures can also result in effects such as 'fingering' and leakage which are detrimental to production performance.

Within the reservoir, the fluids present are distributed vertically in order of their densities where the reservoir pore structure is homogeneous. Thus a reservoir may be divided into zones in which gas will be found above condensate, oil and formation brines.

The existence of cap and seat seal rocks prevents or minimises the escape of hydrocarbons from the reservoir. Cap rocks may be composed of layers of salt, as with 'salt-domes', gypsum or other largely impervious deposits [11,12]. Clays, shales and compacted limestones also fulfil the requirements of fine grain and pore size necessary for cap rocks. Generally, cap rocks possess very low permeabilities but more importantly very 'high' capillary pressures which limit the ingress of non-wetting oil or gas phases from the reservoir. Capillary pressure is inversely proportional to pore-throat radii and proportionally dependent on the interfacial tension between the formation water and oil or gas. Thus, provided that the hydrostatic pressure in the reservoir does not exceed some critical value, oil or gas will not enter cap rocks. This critical condition is dependent on the density difference between water and hydrocarbons, the interfacial tension, the pore sizes in the reservoir and pore-throat sizes in the cap rock. When cap rocks are plastic, reservoir fluids are less likely to be lost through them when fracturing techniques are applied.

2.2 RESERVOIR MINERALOGY

This section examines the properties of quartz, clay, and other minerals found in sandstone reservoirs.

The rock structure of oil reservoirs is formed from the fusion of mineral oxides, inorganic and organic materials under conditions of high temperature and pressure, resulting in a porous matrix of varying composition and degrees of heterogeneity. The characterisation of reservoir mineralogy thus occupies an important place in any study of formation damage.

2.2.1 Fines

Reservoir sandstones often contain significant quantities of intergranular materials collectively referred to as 'fines'. Typically, fragments of quartz, feldspar, mica and a wide spectrum of clay particulate matter can be found in the pore spaces, the single particles ranging in size from the sub-micron to a few tens of microns. During flooding, these fines can be mobilised by changes in the ionic strength or chemical constitution of the displacing fluids. Even areas of high permeability can be permanently affected by such migrating fines.

Research carried out to date has not yet identified the types of minerals causing the greatest damage, however it is widely considered that clays make a significant contribution on account of their complex surface electrochemical properties [13-18].

2.2.2 Quartz

This is by far the largest constituent of sandstone reservoir rock, usually greater than 90% by weight, and is composed of highly crystalline silica. This mineral forms the basic porous rock structure through fusion at high temperatures and pressures or cementation by iron and calcium salts. The porous nature of sandstone reservoirs can be attributed to the relative hardness of quartz, producing fewer fragments during laydown although the degree of porosity is a function of a number of factors including the presence of indigenous clays and other minerals.

2.2.3 Clay Minerals

On the basis of size alone, clay has for a long time been defined as all particulate material smaller than 4 microns [24,25]. However, modern analytical techniques, including X-ray diffraction, have shown that clays are crystalline alumino-silicates with identifiable unit structures [26]. The silica and alumina take the form of alternating layers which are integrated into one another to varying degrees, depending on the number of layers required to form the repeating unit structure. The silica layer comprises a silicon atom surrounded by four oxygen atoms or hydroxyl ions, forming a tetrahedral sheet. The alumina forms an octahedral sheet with one aluminium atom at the centre of six hydroxyl ions. Two-layered, three-layered, mixed-layer and amorphous clays all exist in nature.

Although there is no general agreement as to the proper definition of clay, alumino-silicate material finer than 4 μm is commonly considered to be the 'clay fraction' in the context of oil reservoir clay. Clays do exist as larger particles and are also important in terms of formation damage problems.

Thus, to define clay by means of particle size alone is insufficient because other minerals such as quartz, feldspar do occur in the <4 μm size class but do not have many of the other properties associated with the clay minerals. However the <4 μm size fraction of a sandstone generally has a higher proportion of clay minerals of interest when studying formation damage phenomena. The clay minerals in the pores of a reservoir may be affected by their ionic environment so as to cause swelling or migration effects. Other fine materials associated with the clays may then be dislodged thus contributing to the scale of pore blocking.

The structure and composition of the clay minerals gives them unique physical and electrochemical properties. The three-layered clays such as montmorillonite exhibit 'swelling' when in contact with fresh or non-compatible water. Generally, their surfaces are highly active due to charge imbalances within their structures. This factor is the cause of their ion exchange, chemical adsorption and double layer characteristics. Base or ion exchange is the exchange of ions in solution for those in a solid, the commonest exchange ions in the case of clay minerals being Ca^{2+}, Na^{+}, K^{+}, Mg^{2+}, H^{+} and NH_4 [4]. These ions are held in between the layers as well as on the outer surfaces of the structural unit, without any alteration to the basic clay structure [22].

2.2.3.1 Kaolinite

The chemical formula of kaolinite may be written as $Al_4Si_4O_{10}(OH)_8$. Its structure, as shown schematically in Figure 1, consists of one tetrahedral silicon-oxygen sheet and one aluminium-hydroxyl layer. This type of structure is usually referred to as a 1:1 lattice. No expansion of the lattice occurs when kaolinite comes into contact with

aqueous solutions. The replacement of aluminium by iron or magnesium within the structure of this clay mineral has not been reported. X-ray diffraction patterns of a typical kaolinite result in a spacing between the alumina and silica sheets of about 7.2 Angstroms. Kaolinite has been reported to exist in various states of crystallinity which can usually be quantified by differential thermal analysis. The state of disorderliness of kaolinite is thought to contribute to surface properties such as ion exchange [27].

Kaolinite is primarily a product of the weathering of feldspathic rock, though other mechanisms of formation have been recognised [24,25]. It has a composition which can be expressed as [26]:

Silica	46.5%
Alumina	39.5%
Water	14.0%

Particles of kaolinite are recognised by their characteristic hexagonal platelet form in the 0.1-5 micron size range. Individual platelets often are found clumped together as "card-pack" structures. The surface and ion-exchange properties of kaolinite clays are worthy of special mention and have been covered in a later section.

2.2.3.2 Montmorillonite

This mineral is a three-layered clay with the unit cell consisting of a sheet of alumina molecules sandwiched between two layers of silica molecules (Figure 2). Particles of montmorillonite are usually very small (less than 1 micron). They are very susceptible to swelling when in contact with water or polar organic liquids which can penetrate the loose layer structure. Potassium, sodium, calcium and

magnesium ions are readily exchanged by montmorillonites which have the highest cation exchange capacities of the clay mineral group, from ten to fifty times greater than crystalline kaolinite (see Table 1).

2.2.3.3 Illite

This is also a three-layered clay mineral. However it does not display swelling characteristics due to the presence of potassium ions situated between the unit layers. This ion presence balances the charge deficiency inherent in the structure and reduces the cation exchange capacity. Particles of illite are generally irregularly shaped and less than 2 microns in their characteristic dimension. Figure 3 presents the structure of the mineral. It is interesting to note that illite may be degraded when potassium is removed from the structure by the leaching action of slightly acidic water. Degraded illite is susceptible to expansion when water enters between the unit layers as the ion exchange process takes place. In general, illite has a lower base exchange capacity than the montmorillonites (Table 1).

2.2.3.4 Mixed-Layer Allophane Clay

Naturally occurring clay materials may contain particles with mixed or 'interstratified' layers as in the case of some illite and chlorite clays. Such clays have relatively high ion exchange capacities and can display swelling tendencies.

Also referred to as the "amorphous" clays due to the absence of any specific X-ray diffraction patterns, the allophane clays vary widely in composition and are often present in clay masses.

2.2.4 Chlorite, Mica and Feldspar

Chlorite

Though it is not strictly a clay, chlorite is commonly found in a clay fraction. Particles are small, generally sub-micron, and of a structure is similar to that of the three layered clays but with the addition of a layer of brucite (magnesium hydroxide) in between the alumina and silica unit layers.

Mica

The group of lamellar minerals collectively termed 'mica' are commonly associated with clays in nature but are found over a much wider size range. They consist of alumino silicates with weak interlayer forces. Mica has been found often to be closely associated with kaolinite [28].

Feldspar

Feldspar is probably the most abundant mineral in sandstones after quartz, and is widely regarded as the base material for the formation of clay minerals. The potassium form consisting of the block-like crystals is commonest in nature.

2.2.5 Ion Exchange and Clay Minerals

The ion exchange capacity of clay minerals arises from a combination of sources as follows [27]:

i) isomorphous substitution within the crystal structure. This is the process where one ion is replaced by another of similar size without altering the physical structure. Normally, aluminium ions substitute for silicon ions creating a charge deficit at the surface.

ii) preferential adsorption of potential-determining ions, caused by the presence of lattice imperfections and broken bonds.

iii) exposed hydroxyl groups.

The cation exchange capacities of a number of clay minerals of interest are given in Table 1. Table 2 gives a list of sizes of the commonest exchange ions associated with clay structures.

A factor often overlooked and which is particularly relevant to clays in their natural states is the degree of structural crystallinity. The ion exchange capacity of a sample of clay is likely to be much higher when there are a large number of broken bonds and surface imperfections present on the particles and when a clay mass is poorly crystallised [26,27].

In general, clay particles are found to be negatively charged in aqueous solution on account of the deficiency of charge of the mineral structure. The magnitude of the charge varies with pH, fluid salinity and a range of electrochemical properties of the aqueous phase and solid.

Broken bonds around the edges of the silica-alumina units give rise to unsatisfied or excess charges which are balanced by adsorbed ions. Broken bonds tend to occur on the non-cleavage vertical surfaces of clay particles, in the case of kaolinite, on the edges of individual plates (parallel to the c-axis). The number of broken bonds per unit surface area increases as the particles get smaller hence the exchange capacity would be expected to increase. The nature of broken bonds in clay mineral particles has been studied by relatively few clay

specialists. Wiklander concluded that hydroxyl ions would attach to the silicon ions of broken tetrahedral units causing a negative charge on the lattice [29]. Positive charges originate from exposed octahedral groups which act as bases by accepting protons. Thus it would be expected that with rising pH the negative charge would grow due to increased ionization of the acid groups (silicon) and the positive charge would decrease due to lower proton addition to the basic groups. Thus, in the low exchange capacity clays such as kaolinite and well crystallised illite and chlorite, broken bonds at the edges of particles are regarded a major cause of exchange capacity.

The substitution of aluminium (Al^{3+}) for silicon (Si^{4+}) in the tetrahedral sheet and of lower valence ions such as magnesium (Mg^{++}) for aluminium in the octahedral sheet produces net charge deficiencies in clay particles. Such substitutions may either be balanced by intra-lattice changes (OH^- for O^{2-}) or by cation adsorption. Thus, to get a cation exchange capacity of 2 meg/100g of kaolinite, only one silicon unit out of 400 needs to be replaced by an aluminium [30].

The hydrogen of exposed hydroxyl groups could, in principle, be replaced by an exchangeable cation even though it is comparatively tightly held. In kaolinite, the presence of the hydroxyl sheet on one side of the cleavage plane suggests that this cause of ion exchange may be significant [26].

In those minerals containing large numbers of broken bonds, cations could be expected around the edges of flakes (kaolinite) and needles (illite, chlorite). In the three-layered clays e.g. montmorillonite the majority of the ions are found on the basal plane surfaces. This

is also generally true for exchange cations arising from lattice substitution in the two-layered clays. However cations adsorbed due to substitutions in the tetrahedral sheet are more strongly retained. This is because the charges resulting from substitutions on the octahedral sheet must act through a greater distance. It is suggested that these charges exchange cations which are easier to replace than those held by aluminium for silicon substitutions [26]. This would explain why the potassium ions in the mica group minerals seem to be largely non-exchangeable. Evidence for this theory is however not available for all clays.

An interesting proposition relating to kaolinite is that the exchangeable cations occur only on the basal oxygen surface of the silica tetrahedral units and that the cation exchange capacity therefore depends on the thickness of kaolinite platelets [31].

Moore observed that as the amount of exchangeable Ca^{2+} ions on a clay surface decreases, the more difficult is the removable of further ions [22]. Sodium ions however show the reverse relationship. Both replacing power and the strength with which the exchange cation is held are increased by a higher valency of the ion. The relative replacing power of one cation by another was given by the following series:

$$H^{+} > Ca^{++} > Mg^{++} > K^{+} > Na^{+} > Li^{+}$$

The exception to the above replacement rule is the hydrogen ion. Also the series is not valid for all clay minerals due to clay-specific structural differences.

Anion exchange also makes a small contribution to the overall exchange properties of clay minerals. In the case of kaolinite chloride adsorption is proposed constant at about 1 μmol/g over a range of concentration [27]. Chloride adsorption increases with decreasing pH.

The structure of the silica surface in aqueous electrolyte contact is of a major role in mobilisation. The structure of the silica surface in aqueous electrolyte contact is of particular relevance to clay particle behaviour in formation damage and has been investigated [34-36,38], while Sposito has studied the general area of soil chemistry [33]. Some physical properties of clay and other non-metallic minerals have also been compiled [53].

2.3 FORMATION DAMAGE BY CLAY

Most reservoir sandstones contain within their pore spaces significant quantities of particulate matter which can be mobilised during flooding.

Much of the work done to date has been qualitative in nature largely due to difficulties in characterising the behaviour of reservoir fines under different flooding conditions. However, with more sophisticated analytical techniques, better characterisation of reservoir materials has enabled detailed study of the causes of mobile fines problems. The literature in this area is now examined.

2.3.1 Clay Swelling

A number of early investigations attributed formation damage symptoms to a reduction of pore volume from the swelling of the montmorillonite type of clays present in the reservoir. Morris et al flooded

reservoir cores containing on average 8% swelling clays finding an average reduction in permeability relative to air of 92.5% [23]. A swelling test conducted on a core sample, involving prolonged exposure to a weak electrolyte solution, resulted in a visually noticeable increase in the volume of the core after a few hours. Further evidence of the swelling phenomenon was provided in a number of studies. Moore studied cation exchange and flocculation properties of clay minerals [22]. Montmorillonite was found most active in cation exchange processes and most susceptible to hydration effects, illite and kaolinite affected to a lesser degree. It was proposed that monovalent ions could be much more easily removed from clays than divalent ions and that the forces keeping particles flocculated in formation brines could break down allowing dispersion and swelling to take place.

2.3.2 Clay Dispersion

Dodd et al tested core samples for the 'swelling-clay' effect[19]. Core minerals and their water sensitivity were analysed by using the technique of X-ray Diffraction-Peak Intensity measurement. The results were compared with field data. The main conclusion of this study was that non-expandable clay minerals were not a factor in the permeability loss, that only swelling clays and the dispersion of small 'swollen lamellae' leading to pore blockage were the main causes. However, it was recognised that the observed 'increase' in core permeability under reverse flow could not be explained only by the 'swelling clay' theory.

Around the same time, Hewitt suggested that non-swelling clays such as illite and kaolinite also participated in the pore plugging action brought by dispersion [20]. A strongly water sensitive sandstone was

permeability tested and evidence of mobile fines behaviour was found. The clays analysed were reported to exist as 'inter-granular' or 'inter-granular and laminated', the upper size limit taken at 16 microns.

The dispersion and plugging mechanism of formation damage was favoured by Land et al [21]. In the sandstones tested, the fines fraction up to 12 microns accounted for 5-8% wt of the core. Of this approximately 25% was found to be kaolinite. Calcium ions were thought to prevent dispersion and permeability loss.

The study of Jones reported this among three main findings[18]:

a) The increase in clay blocking effects with salinity change.

b) The reduction of dispersion of clay with relatively low concentrations of divalent ions.

c) The low values of electrophoretic mobility of the calcium form of clays compared to the sodium form.

Effects (a) and (b) were demonstrated using core material which was known to be water sensitive. Abrupt salinity reduction when using monovalent ions resulted in damage in all cases, however, when at least 10% of the ions were divalent (calcium or magnesium) the permeability of the core was unaffected. Electrophoretic mobility of a bentonite 'swelling' clay was measured using a Riddick cell. Jones found that the mobility of the calcium clay was approximately half that of the sodium form. The observed permeability reduction in water sensitive reservoirs was attributed to fresh water 'invasion' or 'water shock' caused by osmotic effects as the salinity decreased.

The water sensitivity of the Berea sandstone was determined by Mungan [39]. In core samples subjected to fresh water after brine flooding, the severest damage was found to occur in the upstream sections of the core. Longitudinal mixing was thought to be largely responsible for this observation. Illite and kaolinite clays, both non-swelling types were found in evidence in the effluent produced from damaged cores. Cores were also found to be pH-sensitive, the effect here being the dissolution of grain cementing material like silica and calcite.

Permeability tests were conducted by Gray and Rex on sandstone cores containing little or no swelling clays [13]. Fresh water permeabilities were on average less than 33% of connate water permeability. As well as the absence of swelling, a number of effects were observed which can only be explained by fine particle plugging action:

a) Core permeabilities increased temporarily during flow reversals.
b) Final air permeabilities were lower than initial values.
c) The production of fines in core effluents when fresh water displaced brine.

X-ray Diffraction analysis of core effluent indicated the presence of fine mica 'needles' 1-5 microns long and hexagonal kaolinite platelets 0.1-0.3 microns in diameter. Clay dispersion was attributed to local shear gradients in the core during flooding and to double layer expansion effects caused by a decrease in salinity below a critical threshold. Osmosis was not considered a cause of clay dispersion, as proposed by Jones [18]. Reed also noticed the presence of mica in migratory fines [54].

2.3.3 Pore-Plugging

Mobilised clays from water-sensitised sandstone cores were identified by Neasham as one of three morphological types[17]:

i) Discrete

ii) Pore-lining

iii) Pore-bridging

Using scanning electron microscopy, kaolinite was often found as 'stacked' platelets attached to pore surfaces as discrete particles. Sandstones containing this type of clay were characterised by high 'permeability-porosity' functions. Low permeability sandstones contained illite and chlorite clays as pore-bridging aggregates or fibrous networks. Sandstones in the discrete particle class contained mainly kaolinite fines in concentrations up to 5% wt though some of the cores tested contained up to 20% wt fines. The morphology of illite in reservoir sandstone has been studied [57].

Donaldson and Baker proposed a statistically controlled model of particle transport in sandstones [40]. Particle sedimentation and interception were introduced into the analysis. Diffusion and electrical double layer effects were not considered. Core-floods were then conducted in which ground quartz particles of mean sizes 4, 6 and 7 microns prepared in 1% brine (NaCl), were pumped through sandstone cores possessing mean pore sizes of 10, 15 and 30 microns. Core pressure data and effluent particle size analysis resulted in a number of significant conclusions as follows:

a) larger diameter pores initially contained most of the flow but were first to become plugged;

b) large particles were captured quickly while pressure drop remained constant in this period;

c) cake build-up on grain surfaces was initiated by the larger particles;

d) pore-plugging effects were observed after the flow of at least 150 pore volumes; and

e) in most tests 50% of the particles passing through the core were less than 3 microns in diameter.

In the theoretical model, the size of 'injected' particles was randomly distributed and, using an average diameter of model pore, the differential pore pressure was calculated on the basis of three events:

f) particle passes through core;

g) particle is retained in the core; or

h) all particles are released if a threshold pressure is exceeded.

The authors reported good agreement with experimental results.

Muecke stressed the need for treatment of 'fines' rather than just the clay group of minerals [41]. For US Gold Coast unconsolidated sandstones, fine materials on a less than 37 micron basis accounted for 2-15% wt of the rock and were composed of:

39% quartz

32% amorphous minerals

18% other minerals, and

11% clay minerals.

The clay minerals form the smallest part of the fines fraction, it should be appreciated that the choice of definition of the size range of fines is also an issue here.

In Muecke's experiments, suspensions of calcium carbonate containing particles 2-15 microns in size were pumped through a sealed cell consisting of 200 micron glass chips sintered between two glass plates. Visual observations in single phase flow showed that:

a) particles bridged at intergranular constrictions;
b) the bridging probability is a function of fines concentration; and
c) that fines could be released by flow reversal depending on their deposited condition.

In multiphase experiments the wettability of particle and grain surfaces and the interfacial effects between fluids were found to be the dominant factors in fines behaviour. At the oil-water interface both oil and water-wet particles were mobile while at irreducible saturation conditions fines remained trapped in the stationary phase that wetted them. When both oil and water were mobile, interfacial pressure gradients kept the fines mobile. This was illustrated when injection of oil-water mixtures resulted in fines production. During oil flow alone, water-wet fines remained in the connate water film while in water flow an 'equilibrium' condition was established after some flow where fines remained trapped at the intergranular contact points.

According to Somerton and Radke the surface properties of clays are significant in their behaviour in brine and alkaline flooding conditions, with cation exchange playing a major role in mobilisation [15].

Gruesbeck and Collins suggested that fines related to permeability loss is restricted to the near well-bore region [42,48]. The model proposed, like the model of Neasham [17] considers that pores could be of the small 'plugging-type' or large 'surface-deposition type'. In sandpack flooding tests, surface deposition and particle re-entrainment effects were demonstrated using a large grain diameter to fines size ratios. Calcium carbonate particles 8 micron in diameter were prepared in 2% KCl solution.

Simplified, the theoretical model assumed the local rate of 'surface-type' deposition to be proportional to the concentration of fines in suspension, thus:

$$\frac{\partial \sigma}{\partial t} = \beta * C \qquad (2)$$

where σ = volume of fines deposited/unit initial pore volume

C = concentration of fines in suspension.

β = constant

The entrainment law was defined thus:

$$\frac{\partial \sigma}{\partial t} = \begin{cases} k * \sigma * (u-u_c) & \text{for } u > u_c \\ 0 & \text{for } u < u_c \end{cases} \qquad (3)$$

where u = the fluid volume flux density, or velocity,

u_c = a critical fluid velocity, and

k = a constant.

Experiments in which a 'clean' fluid was pumped through a 'contaminated' bed were conducted in an attempt to verify the entrainment hypothesis. Particle deposition in the small 'plugging' pores was assumed proportional to the amount of particles already deposited:

$$\frac{\partial \sigma_p}{\partial t} = (k_1 + k_2 * \sigma_p) * u_p * C \qquad (4)$$

where σ_p = volume of fines deposit in plugging pathways

u_p = volume flux density for plugging pathways, and

k_1, k_2 = constants

The ratio of pore to particle diameter was used as a guide to the type of deposition that could be expected.

Measurements indicated three types of response of pressure drop in sandpacks which contained mobilised fines:

a) no change - surface type deposition

b) increase then plateau - combined surface and plugging action

c) constant increase - plugging deposition.

Analysis of effluent from Berea core floods showed a fines content on a less than 5 micron basis as:

Mineral	Core 1	Core 2
Quartz	42.5	59.8
Feldspar	10.0	11.5
Kaolinite	23.6	16.2
Illite	20.3	9.9
Chlorite	2.6	2.6
Siderite	1.0	-

Two phase flow was found to give increased particle entrainment.

The water sensitivity phenomenon was studied by Khilar [43,44]. The well-known Berea sandstone was used containing 8% fines, mainly quartz, kaolinite and illite and having a porosity of approximately 19%. The salinity change concept was endorsed by his finding that a critical rate of salinity decrease existed. Above this rate particle dispersal and pore-plugging effects were observed. Increased salinity gradients produced higher concentrations of fines in the core effluent. Spontaneous particle dispersal initiated by double layer expansion in the colloidal clays was proposed as the mechanism of permeability reduction. Critical salt and clay fines concentration levels were suggested as the governing criteria for the dispersal process.

Gabriel and Inamdar investigated chemical and physical mechanisms of formation damage [47]. Flooding tests on Berea cores initially saturated with a 2% KCl solution indicated that existence of a critical flooding velocity of (0.007 cm/s = 0.25 m/hr) above which the permeability declined. At lower velocities fines were thought to be in concentrations not high enough for damage to occur.

Recent studies utilise theoretical and experimental work in formation damage from the last twenty years. Scheurman has attempted to develop guidelines for injection fluid selection in order to alleviate problems of fluid-rock compatibility [45]. It is proposed that the cation concentration, particularly divalent ions, of injection fluids should not be allowed to fall to levels below those dictated by the cation exchange capacities (CEC's) of the clay minerals present. In core tests, swelling clays showed the highest salinity requirement of

about 600 milliequivalents per litre. Well crystallised kaolinite had the lowest exchange capacity at 2 meq/l compared to 17 meq/l for a poorly crystalline type. Well-bore treatment guidelines have also been proposed. Calcium potassium and ammonium ions are suggested as suitable candidates with treatment radii of 1.5-3 metres around the well bore.

Sharma et al have examined the conditions under which deposition and release of clays takes place in sandstones [46]. Constant charge clay surfaces were assumed in their double layer analysis. In conducting electrophoretic mobility measurements for the estimation of the zeta potentials, the surface charge properties of the sandstone were assumed to be largely unaffected by crushing. Particle deposition and release were expressed in terms of the surface potential interaction of the clays with sandstone surfaces. In this way, regions of capture and release were determined. The transition between an equilibrium state and particle deposition was found to be extremely narrow. This was also found to be true for the transition to particle release from a state of particle attachment. It was proposed that, inside the deposition or release regimes, the respective rates are a function of the fluid interstitial velocity. The theoretical analysis also showed that smaller particles would be more difficult to deposit and easier to release, pointing out that experimental work has not yet shown this to be true.

The control of pH of flooding liquids with the specific purpose of clay stabilisation is not a regular practice in field operations. This is often due to the fact that formation brines are themselves at neutral or near-neutral conditions. A number of workers propose that the release of fines can be prevented by adjusting the pH and there is

a critical pH below which no particle release can occur. These workers propose that the ion exchange process is influenced by pH. In the work by Kia [49], the electrophoretic mobilities of kaolinite clay and crushed sandstone were measured. The calcite content of the sandstone was removed so that its dissolution would not alter the pH and ionic strength during measurement. In the initial stage of a fresh water core flood, the pH was observed to rise before attaining the pH of the water injected. This effect was attributed to the replacement of sodium ions on clay surfaces by hydrogen ions from the water. The authors concluded that, as the pH is lowered, permeability loss is reduced and that, at pH values less than 4.8 no permeability reduction occurs when fresh or low salinity water is contacted with sandstone cores.

Injectivity studies have been conducted from the viewpoints of fluid-rock compatibility and filter cake formation [50]. The Barkman-Davidson theory has been used as a basis for the theoretical development [51], with the conclusion that the existing theory for calculating the life of injection wells is too pessimistic.

The contribution of colloid science in investigating clay damage has been emphasised by Lauzon [52]. Porter has recently overviewed formation damage by presenting experience of suitable and harmful drilling and injection fluids [14]. Loose and tightly packed kaolinite platelets were shown to exist. An interesting observation was that inorganic Si-OH and Al-OH polymers could be formed in many drilling mud systems. Their effects on the viscosity of mud filtrate and formation water could be significant.

The use of surfactants, polymers, their mixtures and a number of chemical flood treatments continues in efforts to increase oil/water

ratios [55,56]. Ion adsorption and exchange phenomena and salinity criteria for these chemical floods have also received some attention [58-61].

2.4 ELECTROCHEMICAL FORCES IN COLLOIDAL CLAY SUSPENSIONS

Colloidal clay particles in suspension are subject to Van der Waals attraction, double layer and other less well understood short-range electrical forces. These electrical forces have been reviewed.

2.4.1 Van der Waals Forces

Van der Waals forces are intermolecular and arise as a result of dipole and charge oscillation electrical (dispersion) effects. As illustrated in Figure 6(a), the interaction between a particle and a much larger collector can be approximated by the adhesion force between a sphere and a plate [62] :

$$F_A = AR/6H^2 \quad \text{for } R >> H \quad \text{and} \quad H < 25 \text{ mm} \tag{5}$$

where A is the Hamaker constant which is a function of the material properties of the constituent molecules

R is the sphere radius, and

H is the sphere-plate separation distance.

The interaction energy between the sphere and plate is given by:

$$V_A = -\frac{A}{6}\left[\frac{2R(R+H)}{H(H+2R)} - \ln\frac{(H+2R)}{H}\right] \tag{6}$$

which reduces to,

$$V_A = -\frac{AR}{6H} \qquad \text{for} \qquad R >> H \tag{7}$$

The interaction between two flat plates, Figure 6(b), can be expressed as:

$$P_A = \frac{A}{6\pi H^3} \qquad \text{for} \qquad H < \frac{3\lambda}{2\pi} \tag{8}$$

where P_A = force of adhesion per unit surface area

λ = the principal absorption wavelength of the material (typically 100 mm)

Gregory estimated the Van der Waals attraction between two plates as [63]:

$$F_A = \frac{A}{12\pi H^3}\left(\frac{15.96H/\lambda + 2}{(5.32H/\lambda + 1)^2}\right) \tag{9}$$

Van der Waals forces operate in polar and non-polar solutions and are a function of the dielectric constants of the interacting materials(contained in the Hamaker constant) and magnitude of particle-collector separation.

2.4.2 The Electrical Double Layer

If a solid is dispersed in a polar liquid, the solid-liquid interface will usually acquire a small electrical charge, which may be either positive or negative. The charge may be caused by the ionisation of a surface molecule, or by preferential adsorption of one ionic species of the solid surface. It is well known that fine clay materials carry

a net negative charge on their surfaces when in neutral aqueous suspension.

The surface charge is compensated by an accumulation of ions of opposite charge (counterions) in the liquid phase adjacent to the particle surface. The situation this arising is shown in Figure 4(a) for a model spherical clay particle. Counterions, whilst being attracted to the particle surface also tend to diffuse away from it in the direction of their concentration gradient. An equilibrium distribution of counterions is thus established known as the 'diffuse' or Guoy layer after one of the early proponents[cited in 27]. Ions in the liquid possessing a like charge to the surface ('co-ions') are repelled from the surface so that the diffuse layer contains an excess of counterions and a deficiency of co-ions. The counterion and diffuse layers are known as the double layer.

Gouy (and independently, Chapman) performed an analysis of a double layer system by making a series of simplifying assumptions [27,64]:

i) The surface is flat and infinitely large
ii) The surface has a uniform charge per unit area
iii) The ions in the diffuse layer are point charges
iv) The diffuse layer has a uniform dielectric constant
v) The liquid contains ions of equal and opposite charge +z and -z.
vi) The ions in the diffuse layer are distributed according to the Boltzmann equation:

$$N_x = N \exp\left[\frac{ze[\psi_x - \psi_\infty]}{kT}\right] \qquad (10)$$

where z = ion valency

e = the electronic charge

N_x = the number of ions at a distance x from the interface

ψ = the electrical potential, and

k = the Boltzmann constant and T the absolute temperature.

Therefore

$$N_x^+ = N_\infty \exp\left[\frac{ze\,\psi_x}{kT}\right] \tag{11}$$

and

$$N_x^- = N_\infty \exp\left[\frac{+ze\psi_x}{kT}\right] \tag{12}$$

The net charge density ρ at x is given by

$$\rho_x = ze\,[N_x^+ - N_x^-] \tag{13}$$

Therefore

$$\rho_x = -2N_\infty\, ze \sinh \frac{ze\,\psi_x}{kT} \tag{14}$$

The potential, ψ, is related to the charge density ρ by Poissons equation,

$$\nabla^2 \psi_x = -\frac{\rho_x}{\varepsilon\ \varepsilon_o} \tag{15}$$

Therefore,

$$\frac{d^2\psi_x}{dx^2} = \frac{2ze\ N_\infty}{\varepsilon\ \varepsilon_o} \mathrm{Sinh}\ \frac{ze\ \psi_x}{kT} \tag{16}$$

where ε = the dielectric constant of the medium

ε_o = the permittivity of vacuum.

Therefore

$$\psi_x = \psi_o \exp(-k_x) \tag{17}$$

where ψ_o the electrical potential at the solid-liquid interface.

and $$K = \frac{2 N_\infty z^2 e^2}{\varepsilon \varepsilon_o kT} \tag{18}$$

Thus the potential drops exponentially with distance.

The Guoy-Chapman model of the double layer leads to very high charge densities near the surface because it assumes ions as point charges neglecting their size. Stern [65] proposed a modification of the theory whereby the closest approach of an ion is limited by its size. Thus in the Stern model the counter-ions are located at a very small but fixed distance from the surface of the particle. Stern could then assume the simplification, that in this region, the 'Stern layer', the electrical potential drops linearly with distance from ψ_o at the surface to ψ_s at the edge of the layer where δ is the thickness of the Stern layer. This scheme is shown in Figure 5. Outside the Stern layer is the diffuse layer whose ion concentration decreases exponentially to the bulk ion concentration.

Modern concepts of the nature of electrical double layers continue to be developed and applied to existing knowledge about the double layers of colloidal clays [75,76]. As shown in Figure 5, the double layer

around a clay particle consists of the inner Stern layer and an outer 'diffuse' or Guoy layer. Within this system there are three planes of significance: the clay surface or clay-water interface, the outer Helmholz plane (OHP) and the plane of shear.

The OHP is the plane that defines the outer limit of the Stern layer i.e. the layer of counter ions condensed on the particle surface. The plane of shear is the plane on which shear occurs between the envelope of fluid that moves with the particle and the bulk fluid. In the Stern layer the ions are assumed to oscillate about fixed adsorption sites whereas in the diffuse layer they are assumed to undergo Brownian motion.

In applying double layer theory to clays, the Stern layer is often ignored in order to simplify the analysis which is then based solely on the description of the diffuse layer.

In aqueous solution the repulsive forces due to the interaction of the double layers around similar particles can overcome the Van der Waals attraction and hence affect the deposition and condition of attachment of particles. The classical DLVO theory (Derjaguin, Landau, Verwey, Overbeek) considers the effect of double layer interaction on the stability of hydrophobic colloidal sols [66,67,74]. Their theory calculates the double layer interaction for the conditions of constant surface potential or constant surface charge, these conditions being determined by the properties of the surface. Double layer thickness was assumed to be small compared to particle radii and it was also assumed that the potentials of interacting particles could be equated with the zeta potential of the individual particles. The summation of Van der Waals and double layer forces for varying ionic

strengths enabled the calculation of the total interaction energy for coagulation. The DLVO theory is used as a basis for the study of many particle-surface interaction systems.

The zeta-potential of a clay particle or surface is the potential at the plane of shear. It is often assumed to be equal to the Stern potential, ψ_s where δ is the thickness of the Stern layer. The difference between these two potentials is generally regarded as being insignificant [27]. The zeta-potential, often used as a measure of the double layer thickness, is estimated by measurements of the electrophoretic mobility of particles. Electrophoresis involves the measurement of the velocity of particles in a suspension which is subjected to an electrical field. Smoluchowski [77] developed an expression to calculate the zeta potential from mobility data:

$$u = \frac{\varepsilon \ \psi_z}{4 \ \pi \ \mu} \qquad (19)$$

where u = particle mobility, $m^2 s^{-1} V^{-1} m$

ε = permittivity of medium, $kg^{-1} m^{-3} A^2 sec^4$

μ = viscosity of the suspension, $kgm^{-1} s^{-1}$

ψ_z = zeta-potential, V

The expression holds for the condition that the particle radius is at least two hundred times the double layer thickness.

James and Williams measured the particle interactions in kaolinite suspensions for a range of pH values and NaCl concentrations from 10^{-4}M-10^{-1}M [78]. Zeta-potentials were determined under these conditions (Table 3). Their analysis concluded that face-edge and edge-edge are the likeliest forms of association in clay suspensions.

Extensive work has been done on the characterisation of kaolinite suspensions with respect to their zeta-potentials and ion exchange properties [79-85].

Double layer interactions are significant in the determination of adhesion forces between similar and dissimilar particles. Hogg et al, studying the stability of colloidal dispersions of dissimilar spherical particles, reduced the problem to a development of the plate-plate system for which the interaction potential can be approximated by, for potentials less than about 25 mV [68]:

$$\frac{d^2\psi}{dx^2} = K^2\psi \qquad (20)$$

where $K = 8\pi ce^2z^2/\varepsilon kT$, the Debye-Huckel parameter

and ψ = surface potential in esu (electrostatic charge units)

c = bulk ion concentration, ions/cm^3

ε = permittivity of the medium

e = electronic charge

z = valence of ionic species

k = Boltzmann's constant

T = absolute temperature, and

ψ, c and z referring to each ionic species in turn.

For a spherical particle system, the interaction potential is:

$$V_R = \int_o^\infty 2\pi h\, V_1\, dh \qquad (21)$$

where V_1 = interaction potential energy for plate-plate system under similar conditions.

h = separation distance.

The general solution of this can be simplified for the case of identical, spherical particles to give the interaction potential energy as:

$$V_R = \frac{\varepsilon a \psi_o^2}{2} \ln [1 + \exp (- KH_o)] \qquad (22)$$

where a = particle radius

ψ_o = surface potential of the particles.

H_o = the shortest distance between the surfaces of the particles

Their analysis confirmed the accuracy of the linear Debye-Huckel approximation for low surface potentials.

Gregory more recently estimated the double layer force between two plates as [69]:

$$F_{DL} = nKT [(2Y_1Y_2 \cosh KH - Y_1^2 - Y_2^2)/\sinh^2 KH] \qquad (23)$$

where n = number of ions per unit volume

k = Boltzmann's constant

T = absolute temperature

Y_i = ze ψ_i/kT, the reduced surface potential

z = the valency of counterions,

e = the electronic charge, and

ψ_i = the surface potential of particle i

K = the Debye-Huckel reciprocal length parameter given in,

$K^2 = 2e^2nz^2/ kT$, where,

ε = the permittivity of the medium.

Visser used a concentric cylinders technique to determine the effect of pH on the adhesive force between submicron carbon black particles and a cellulose surface [70]. From deposition and centrifuge removal experiments, the adhesion force was found to be a maximum at a pH = 3.3 whilst a state of zero charge for this system was also found to occur at this pH. It was shown that, under these conditions, only Van der Waals dispersion forces were operating.

Double layer repulsive forces were found to be solely dependent on the surface potential of the flat cellulose surface in a further investigation in which colloidal polystyrene particles were used, Visser [71].

The adhesion behaviour of dissimilar surfaces, termed heterogeneous interaction, has also been studied by Amelina et al [72], and Revut et al, who correlated the zeta potential with time of existence of an adhesion bond [73]. Short-range electrical forces have been little studied [88].

Ion adsorption characteristics of minerals have recently received some attention [76,86]. Results from these works have introduced concepts of 'surface-complexation' for describing the binding of counterions in the double layer. The classical Guoy-Stern double layer model continues to be extended by theories of ion adsorption.

2.4.2.1 The Double Layer on Edge Surfaces of Clay Plates

At the edges of clay particles, the silica and alumina crystal sheet structures are disrupted and primary bonds broken. An electric double layer is created by the adsorption of potential determining ions in such cases. Where the octahedral sheet is broken, the edge surface

is comparable to the surface of an alumina particle. Alumina surfaces have positive double layers in acid solution with aluminium ions potential determining and negative double layers in alkaline solution with hydroxide ions acting as potential determining. However the zero point of charge is not at neutral pH; this is found to vary with crystal structure, so in neutral clay suspensions it is possible that a POSITIVE double layer exists on edge surfaces due to the exposed alumina sheet. This double layer may become more positive with decreasing pH and vice versa, but the net electrophoretic charge of a clay particle is ALWAYS negative due to the predominant effect of the flat surface in electrophoresis experiments. A classic demonstration of this is the adhesion of gold particles to the edges of clay plates [87]. A similar effect was observed with mica particles, with the negatively charged gold sticking to the positive flat surfaces of the platelets.

Where the silica sheet is disrupted compares with the surface of a silica particle. Silica surfaces are normally negatively charged but can become positive in the presence of even small amounts of aluminium ions [27]. Since a clay suspension will contain aluminium ions by dissolution, a positive double layer on the broken silica surface edge can exist. Also the silica sheet can be broken at points where the aluminium ions have substituted in, although there is no evidence for this. However it can be seen that the silica surface can behave as an alumina surface, thus the whole edge area may be negatively charged and thus carry a POSITIVE double layer.

Clays show a small anion exchange capacity under certain conditions e.g. kaolinite shows a small anion adsorption capacity in slightly acid conditions but not in alkaline pHs. The positive double layer is

then responsible for the adsorption of anions as counter ions. The small cation exchange capacity observed is due to the negative double layer on the flat surface resulting from isomorphous substitutions in the kaolinite lattice.

CHAPTER 3

LITERATURE REVIEW II

3.1 INTRODUCTION

The fluid flow conditions in a reservoir during water flooding can have a marked effect on the detachment, migration and subsequent re-capture of colloidal fines. Flooding velocities in the well-bore region are usually maintained high enough in order to keep entrained solids in suspended state. Away from the well-bore, velocities are of the order of a few metres per day. These are comparable to those found in deep-bed filtration processes. Work reviewed in Chapter 2 has shown the existence of a critical velocity for pore-plugging. This Chapter presents a review of general porous media flow models and an application of these models to particle behaviour in deep bed filtration.

3.2 FLUID FLOW MODELS

Models describing flow in porous media are generally based on the Stokes equations of laminar fluid flow.

The solutions to the Stokes equations for straight cylindrical tubes (the Hagen-Poiseuille relation) were employed by Kozeny and Carman in the modelling of a packed bed by a bundle of capillary tubes[as cited in 106]. The D'Arcy equation (Equation 1) which gives a linear relationship between pressure drop and flow rate is an empirical expression. The permeability, K, from the D'Arcy equation in the can be found in the Kozeny-Carman equation which relates permeability to the porosity and particle size thus:-

$$K = \frac{1}{k} \frac{e^3}{(1-e)^2} \frac{1}{S^2} \qquad (24)$$

where e = porosity

S = specific surface area

k = Kozeny-Carman constant (usually equal to 5).

At high solids concentrations the effect of increased particle interactions on the resistance to flow is marked and non-linearity in the flow rate-pressure drop relation occurs requiring high values of the constant k. To take account of these factors, Happel [103,110] and Kuwabara [103] independently developed theoretical models to represent the relative motion of any assemblage of particles in a fluid. In these models particles in an assemblage are represented as spheres each surrounded by a fluid envelope or shell which contains a volume of fluid equal to the relative volume of fluid to particles in the whole assemblage (or porosity).

The following boundary conditions were applied:

i) a frictionless surface of the fluid envelope i.e. no tangential stress

ii) no radial flow of fluid across this surface, and

iii) no slip at the particle (inner sphere) surface.

Happel [103] used the general solution of the Stokes creeping motion equations to derive the relative particle-fluid velocity in terms of particle dimensions only:

$$V/V_o = \left(\frac{3 - \frac{a}{2}\gamma + \frac{a}{2}\gamma^5 - 3\gamma^6}{3 + 2\gamma^5}\right) \frac{\Delta P}{\Delta P_o} \qquad (25)$$

where $$\gamma = \frac{\text{particle radius}}{\text{fluid sphere radius}} = \frac{a}{b}$$

and $e = 1 - \gamma^3$, where e_1 = porosity.

The subscript 'o' represents the dilute solutions 'no interaction' condition when $P = P_o$. In the case of porous media,

$$V = V_o$$

as the particles comprising the medium are fixed. The model takes particle interactions into account to a greater degree in that, as the porosity decreases the fluid shell around each particle shrinks. However, the extent of the distortion has not been evaluated in the model, each cell being assumed to remain spherical. Also the assumption of a free surface means that disturbances within any cell are not transmitted to neighbouring cells. The Happel model agrees well with the Kozeny-Carman theory for porosities from 0.2-0.6.

The shear and lift forces acting on small particles near larger surfaces have been studied by a number of workers [134,136-7]. The shear force experienced by a particle very close to a surface can be approximated by:

$$F_{SH} = 6\pi\mu a_p^2 \frac{3 A_s U \sin\theta_p}{2 a_s} (H_D+1) F(H_D) \qquad (26)$$

where a_p = particle radius

a_s = collector radius

A_s = a dimensionless function of porosity given in Happel's model [138]

U = superficial velocity

θ_p = angle of incidence of flow (Figure 55a)

H_D = dimensionless gap (= h/a_p)

$F(H_D)$ = a universal function of H_D

For flow in consolidated media (e.g. sandstone) there is increased resistance to flow due to the existence of sealed pore channels which do not affect the porosity but may reduce the permeability. For porous media in general, the flow regime can be described by the modified Reynolds number

$$Re_p = \frac{\rho \, v \, dp}{\mu e} \qquad (27)$$

where e = porosity, and

dp = average pore diameter (often taken as the average particle diameter).

μ = viscosity of liquid

ρ = density of liquid

The laminar flow theory as employed in the Carman-Kozeny and Happel models does not consider the random inertial forces which arise in porous structures as a consequence of pore size distribution. Collins [105] and others [106-8] have reported a transitional Reynolds number for the onset of inertial effects which is in the range from one to ten.

Scheidegger stresses the disorder of porous media and that any model representing flow should be based on statistical methods [109].

Payatakes [111] with other workers [112] takes this into account and proposes a porous bed model consisting of a series of unit bed elements each made up of a series of unit cells resembling constricted tubes arranged in parallel. This was simplified to a description of the flow through a periodically constricted tube which was considered to represent the nature of a flow channel in a packed bed. Their theory defines geometric parameters for the constricted tube as follows:

i) Periodicity, $\ell = [\frac{\pi}{6(1-e)} d_g^3]^{1/3}$

where d_g = diameter of spherical grains

and e = porosity.

ii) Constriction size distribution (CSD), and

iii) Number of constrictions/unit cross-sectional area of bed.

Using the geometric factors in the solutions of the Stokes Navier equations, in which the inertia terms were included, a correlation was obtained between the packed bed friction factor expressed as:

$$f_s = - \frac{d_g \Delta P}{2\rho \ell v_s^2} \qquad (28)$$

where v_s = superficial velocity,

and the superficial Reynolds number:

$$(N_{Re})_s = \frac{d\, g^v\, s}{\mu} \tag{29}$$

as follows:

$$f_s = -\left[\frac{2\, d_c\, d_g}{N_c\, \pi \ell\, d_c^3}\right] \frac{\Delta P_1^*}{(N_{Re})_s} \tag{30}$$

where d_c = an effective average constriction diameter

d_g = an effective average grain diameter

P_1^* = dimensionless pressure drop

N_c = number of constrictions per unit cross-section of bed

Calculated and experimental friction factor values were compared over the range of Reynolds numbers from one to ten.

For beds of glass spheres agreement between model and experiment was reported to be -4% whilst for a bed of sand grains this was +12%. Although the model accounts for inertial effects at the higher Reynolds number values and therefore is more suited to gas and aerosol flow, it was not applied over the whole range of porosities as was the Happel model and hence its validity for all systems is uncertain.

Rajagopalan and Tien [113] combined the constricted tube model and the Happel spherical cell approach whereby the former was used for pressure drop estimation in a packed bed and the latter for particle deposition studies. This approach reduced the excessive computation involved in the numerical solution of the flow and trajectory equations used in the constricted tube model.

3.3 PARTICLE SURFACE INTERACTIONS

3.3.1 The Rotating Disc

The rate of particle transport and deposition onto a collector surface has been studied by many workers with the aid of experiments using the rotating disc apparatus [89-96]. The apparatus consists of a collector surface rotating at constant speed in a dilute particle suspension. A rigorous theory of the hydrodynamics of the flow near the collector [89] has ensured the use of this technique for classical particle deposition studies.

3.3.2 Stagnation Point Flow

Recent work on the deposition of colloidal particles has advanced existing experimental techniques by enabling an optical observation of deposition in situ under specified hydrodynamic conditions [97-8]. The technique has been developed from work in the area of impinging jets of both liquids and gases [99-102].

In the apparatus, a stream of colloidal dispersion flows up through a tube, impinging and depositing particles on a glass slide placed normal to the flow. Unlike the rotating disc methods, which involve removal of the surface from the suspension, the collector surface remains undisturbed throughout an experiment. Observations and particle counts were made from above the slide.

The theoretical treatment assumes laminar flow conditions with the existence of a stagnation point near the deposition surface. The flux of particles to the surface was obtained by defining the flow field in the following steps:

i) vorticity $w = \frac{\partial v_r}{\partial z} - \frac{\partial v_z}{\partial r}$ (31)

and,

ii) the stream function , as

$$v_z = \frac{1}{r}\frac{\partial \psi_s}{\partial r} \quad \text{and} \quad v_r = -\frac{1}{r}\frac{\partial \phi}{\partial z} \tag{32}$$

The terms w and ψ are applied in the Navier-Stokes flow equations for steady-state, non-inertial flow.

iii) The flow field near the stagnation point is then described by considering the diffusion layer thickness to be much smaller than the laminar flow boundary layer thickness.

iv) The mass transfer problem is simplified by assuming that attractive forces near the surface are cancelled by the increased hydrodynamic resistance here, thus, for a negligible energy barrier, the flux is represented by a non-dimensional Sherwood Number (Sh), in terms of a dimensionless Peclet Number (Pe) and gravity number (Gr).

v) A force balance is conducted to account for the electric double layer force, F_e, the London dispersion (Van der Waals) force, F_d and the gravitational force F_g. These are summed for the z direction resulting in the force balance,

$$F_z = F_e + F_d + F_g \tag{33}$$

Deposition, which was measured as the number of particles deposited per 100 m^2, denoted by the coating density S, was found to decrease

with time and with decreasing Reynolds number. Two factors were proposed to explain this non-linearity,

i) particle detachment, and
ii) blocking or masking effects.

Double layer interactions were considered insignificant as there was little change in the zeta-potentials of the colloidal particles and surface. For a sodium chloride electrolyte concentration of 10^{-3}M, the suspensions were stable hence coagulation effects were also negligible.

The effects of 'masking' and 'escape' of particles were introduced as coefficients, β_m and β_e where

$$\beta_m = \pi a^2 \gamma J_o \qquad (34)$$

surface blocked per particle

where a = particle radius

γ = a dimensionless coefficient expressing the number of particle cross-sections blocked per particle, and

$_o$ = initial flux given by

$$Sh = J_o \frac{a}{D_o C_o} \qquad (35)$$

where D_o = diffusion coefficient of particles in the bulk solution

C_o = initial particle concentration.

β_e combines transport and interaction energy effects

$$e = Sh \frac{D_o}{a \int_{h_1}^{h_2} \exp\,[-\phi(h)]\, dh} \qquad (36)$$

where $\phi(h)$ is a dimensionless interaction energy function such that

$$\phi(h) \to 0, \text{ as } h \to \infty$$

where h is the distance away from the surface h_1 can be taken as very small for convergence, and h_2 at points depending on the existence of energy maxima or minima. Thus the coating density,

$$S(t) = \frac{J_o}{\beta_m + \beta_e} [1 - \exp\{-(\beta_m + \beta_e)t\}] \qquad (37)$$

The observed 'blocking' effects when deposited particles hinder deposition in an area of 20 to 30 times their cross-sectional area were reported as 'shadowing' effects by Pendse et al [123]. This illustrates the significance and extent of particle-particle interactions in the deposition process in addition to the particle-surface effects which have been widely studied.

The importance of microscopically smooth surfaces was stressed, since the 'micro-roughness' of both particle and deposition surface can change double layer interactions and cause abnormal charge distribution. It is possible that where the surface roughness dimension of particles and surface are approximately the same, conditions are favourable for deposition. Alternatively mechanical interaction may occur, interfering with the electrical interaction forces.

3.3.3 Particle Entrainment

It is not yet known how changes in the parameters (diffusion, hydrodynamic, and electrochemical) which bring about particle capture can influence the escape of these particles from collecting surfaces.

Dabros and Van de Ven [98] proposed that thermal motion and turbulent flow effects explained particle removal and the consequent non-linearity of deposition. Detachment was observed under both turbulent and laminar flow conditions and the depth of the potential energy minimum was considered significant.

Turbulence was initially proposed as a factor in detachment by Cleaver and Yates [133] based on the occurrence of random lift forces near a surface. They proposed that for detachment to occur the lift forces F_L must overcome the adhesion forces F_A.

For a spherical particle deposited on a pipe wall, the lifting force due to turbulent bursts was given as:

$$F_L = k_t \rho \, v^2 \, (\frac{av^*}{\nu})^3 \qquad (38)$$

where k_t is a constant in the range 0.1 to 10

and ρ is the fluid density

v^* is the Blasius friction velocity

a is the particle radius

ν is the liquid viscosity.

The adhesion force could be approximated by:

$$F_A = \varepsilon a \qquad (39)$$

where ε is a constant incorporating separation distance, the Hamaker constant and surface potentials.

For the case of London-Van der Waals force only, $\varepsilon = A$, the Hamaker constant. Thus it was shown that,

$$a > \left(\frac{A\nu}{6\, k_t\, h_o^2 \rho v^{*3}}\right)^{1/2} \qquad (40)$$

where h_o is the shortest distance between sphere and collector surface.

Turbulence induced forces could explain the observations of Ison and Ives [117] who noticed that kaolinite particles flowing in solution through a packed bed of glass spheres 'drifted laterally' in the bed. These effects, also observed by Hunter and Alexander [83], were partly attributed to inertial effects, which are usually ignored in deep bed filtration on the basis that $Re \leqslant 1$. However, detachment and lateral migration have been reported even under low Reynolds number conditions [116]. Saffman had already investigated the lift force on a sphere in low Reynolds number flow [134].

The approach by Ison and Ives [117] in identifying different Reynolds number groups, depending on the nature of the flow, is significant. They proposed the use of four more Reynolds numbers as follows:

$$Re_\Omega = \frac{\Omega e^2 \rho}{\mu}, \qquad Re = \frac{Ve}{\mu}\rho$$

$$Re_K = \frac{ke^2\rho}{\mu} \quad \text{and} \quad Re_W = \frac{we^2\rho}{\mu}$$

where e = effective diameter of suspension particle

Ω = angular velocity of suspension particle in shear flow

v = superficial or approach velocity

k = fluid velocity shear gradient, and

w = frequency of flow pulsation

Although this approach has not found widespread support, it is evident that the Reynolds parameter can be better correlated with the detachment, migration and secondary deposition effects which have been reported. In porous media flow these phenomena appear to be sensitive to 'local' flow patterns and velocity gradients which generate point to point variations in the value of the Reynolds number.

The microscopic surface roughness of porous media particles, as already mentioned, also influences the behaviour of small particles. Dabros has introduced this factor as a dispersion (Van der Waal's force) retardation term [98], as follows:

$$(1 + 0.5\ b/\delta) \qquad (41)$$

where b = thickness of an 'outer rough shell' of the particle, and

δ = closest distance between surfaces.

In this respect, two factors are significant:

i) the comparative size of 'roughness' and particle, and

ii) the relationship between the roughness and the Reynolds number.

It is apparent that a more rigorously calculated Reynolds number near the surfaces of a particles and grain surfaces is needed before the effect of turbulence can be evaluated.

3.4 DEEP BED FILTRATION

3.4.1 Clean Filter Beds

The capillary, cell and constricted tube models for fluid flow have all been applied to describe the phenomenon of particle deposition in granular deep bed filtration. This process, is used primarily in water and waste water filtration but also has applications in porous media flow in general. The efficiency of the process is normally characterised by:

i) the filtration or particle removal efficiency, and
ii) the pressure drop characteristics as a function of time.

Iwasaki carried out an experimental study on the filtration through sand beds, of water contaminated with bacteria and suspended matter [114]. He defined and obtained values for a "penetration coefficient" or "impediment modulus" for different sand grain and suspended matter sizes and at varying filter velocities.

The mechanisms of particle capture in liquids were only understood after work had been done on aerosol and gas filtration through fibrous media, one of the main contributors being Langmuir [115] in his report on smokes and filters. Extensive work has since been done on the nature of particle capture processes in deep-bed filters [126-130]. Herzig has developed a mathematical model of deposition and pressure drop in the deep-bed filtration of suspensions [131]. Work has also been done in this area using kaolinite [132].

Yao et al [116] developed the particle-collector concept for granular filtration and analysed particle capture in two stages:

i) a transport step in which suspended particles are brought into close proximity with the collector, and

ii) an attachment step.

Only transport mechanisms were considered, these being identified as:

iii) Brownian diffusion

iv) gravitational settling, and

v) interception.

Diffusion effects were significant only for sub-micron particles, the magnitude being given by the diffusion coefficient, D, in the Stokes-Einstein approximation

$$D = kT/3\pi\mu d \qquad (42)$$

where k is the Boltzmann constant, T the absolute temperature, μ the viscosity and d the particle diameter. The gravitational and interception mechanisms take account of respectively,

i) the particle-fluid relative density causing a denser particle to deviate from fluid streamlines, and

ii) the particle size which determines the path of the "limiting particle trajectory" from which a particle will be just captured.

The model conducts a mass balance about an elemental volume of suspension

$$\frac{\partial C}{\partial t} + v.\nabla C = D\nabla^2 C + \left(1 - \frac{\rho w}{\rho_p}\right) \frac{mg}{3\pi\mu d_p} \frac{\partial C}{\partial z} \qquad (43)$$

where D is the diffusion coefficient, C is the local concentration of suspended particles, v is the velocity of water, ρ_w and ρ_p are the densities of water and particle respectively, and z is the coordinate in the direction of gravitational force. The numerical solution of this equation involves the single collector efficiency

$$\eta = \frac{\text{rate at which particles strike collector}}{\text{rate at which particles flow towards collector}}$$

which determines the overall filter efficiency.

The analytical solution of the mass balance equation was limited to the determination of the single collector efficiencies for the diffusion, interception and gravitation mechanisms operating individually,

$$\eta_D = 4.04\ Pe^{-2/3} = 0.9\ (\frac{kT}{\mu dp\ d\ v_o})^{2/3} \tag{44}$$

$$\eta_I = \frac{3}{2}\ (\frac{dp}{d})^2 \tag{45}$$

$$\eta_G = \frac{(p_o - p)g{d_r}^2}{18\mu v_o} \tag{46}$$

and it was proposed that the overall filter efficiency

$$\eta = \eta_D + \eta_I + \eta_G \tag{47}$$

as an approximation of the result of the numerical solution.

It was experimentally shown using latex particles and glass beads that there exists a size of suspended particles for which the removal efficiency is a minimum and that this size is typically 1 μm for water filtration. These observations were confirmed in the theoretical model. The diffusion, gravitation and interception mechanisms were each found to be at their respective minima for this size of suspended particle.

The theory was formulated on the assumption that particles are captured by the collector at the first contact and, once captured, remain in the same position on the collector. However, the effect of the accumulation of deposits on the hydrodynamic conditions in the bed was not evaluated, since only clean filter beds were modelled.

Two main conclusions were reached:

i) the removal efficiency of a packed bed is independent of the initial suspended particle concentration, and

ii) destabilising chemicals including some polymers, enhance attachment in filtration

Ison and Ives [117] simulated granular filtration by flowing kaolinite suspensions through beds of glass spheres. An additional removal mechanism, that of impaction, was considered along with, in dimensionless groups, the diffusion, gravitation and interception factors. A dimensionless removal coefficient was obtained:

$$\Lambda = K \left(\frac{\rho v d}{\mu}\right)^{-2.7} \left(\frac{e}{d}\right)^{-2.3} \left(\frac{\overline{\sigma - \rho}\ e^2\ g}{18\ \mu v}\right)^{1.3} \qquad (48)$$

where K is a constant

e is the effective diameter of suspension particles

$\overline{\sigma - \rho}$ is the relative particle-to-fluid density.

The effect of inertial impaction, proposed as a mechanism, was found to be negligible for the experiments carried out in which low values (< 1) of Reynolds number were used. As in the previous model, initial clean filter conditions were considered only. Therefore, with the accumulation of deposits inertial effects would be expected to increase due to disturbances in fluid streamlines. The importance of the Reynolds number and non-linear inertia terms in the fluid flow equations was emphasised.

The 'capture on contact' principle used by previous workers was discussed by Gimbel and Sontheimer in a study of particle deposition in sand filters [118]. It was pointed out that for large particles of size ≅ 35 μm, experimentally obtained removal efficiencies were much lower than model values. This suggested use of capture probabilities of considerably less than unity. For small particles (≅ <3μm) model values were much lower than experimental values and this was attributed to surface roughness of the sand grains. Model results taking these factors into account showed closer agreement with experimental results for negligible double layer repulsion (this was obtained by dosing with 16 μg/l optimum dose of a cationic polyelectrolyte). Colloidal particles were not considered in the model.

3.4.2 Clogging filter beds

Discrepancies between theoretical models and experimentally derived results are marked after the initial 'clean' filter period. Thus recent work has concentrated on the dynamic behaviour of deep bed filters.

Tien et al studied earlier experimental investigations on the nature of deposition in aerosol streams in fibre filtration [119]. They proposed that deposition could be described by two factors:

i) suspended particle size, and

ii) the random position of particles in the flowing stream.

The deviation of fluid pathlines (and therefore particle trajectories) by a deposited particle results in a "shadowing" effect giving reduced deposition in the surrounding area. However, the chance of a chain or dendritic formation of particles increases due to the protruding particle which increases the projected surface area of the collector. The deviation of fluid streamlines approaching a deposited particle or dendrite and the inability of suspended particles to follow the streamlines was proposed as a cause of dendrite formation. The authors observed that dendrites were usually composed of particles of roughly similar sizes. The authors used bulk particle concentrations and random numbers to describe the positions of particles approaching a collector. All contacts were assumed to result in a stable deposition. Primary deposition, that is deposition directly onto a grain and secondary deposition, onto a dendrite, were identified. The increase in drag force was modelled by Pendse et al [120] for,

a) singly attached particles

b) ideal particle dendrites, and

c) particle clusters.

Their model used Faxen's drag force equation:

$$F_D = 6\pi \mu a \left[V_{(0)} = \frac{a^2}{6} \nabla^2 V_{(0)}\right] \qquad (49)$$

where a = radius of the stationary sphere, and subscript '0' represents conditions at the centre of the sphere.

The total drag on the collector particle system was given by,

$$F_D = 6 \pi a \, Cl + F_{D,P} \tag{50}$$

where

$$F_{D,P} = (F_{D,P})_{11} \, Cl^2\theta + (F_{D,P})_1 . Sin^2\theta \tag{51}$$

The authors proposed that:

i) for ideal particle dendrites there is a relative reduction in drag force increase as the number of particles in the chain increases;

ii) deposited particles greater than 10 particle radii distance cause negligible drag force increase;

iii) interaction effects can be limited to the two <u>closest</u> neighbouring particles for any given particle, and

iv) the pressure drop increase across a clogged filter bed can be given by:

$$\frac{\Delta p}{\Delta p_o} - 1 = \frac{1}{F_{D_o}} \sum_{i=1}^{N} F_{D_i} \tag{52}$$

where subscript 'o' refers to clean conditions and ΔF_{D_i} are the drag force contributions due to the i^{th} particle for N deposited particles on the collector.

Chiang and Tien [121] applied this work to characterise:

i) the filter coefficient, and

ii) pressure gradient.

They proposed the relations:

$$\frac{\lambda}{\lambda_o} = F_1(\alpha, \sigma); \quad \frac{\partial p/\partial z}{(\partial p/\partial z)_o} = F_2(\rho, \sigma) \tag{53}$$

where subscript 'o' represents clean filter conditions

σ is the specific deposit

and α, β are constants.

The adhesion probability, also used by Gimbel and Sontheimer [118] was also utilised in the model. Their stochastic analysis predicts much higher collection efficiencies than given by other models compared with experimental results. Functions F_1 and F_2 were found to be independent of bed depth.

The effects of deposited particles on the macroscopic properties of packed beds, were investigated by O'Melia and Ali [122] and others [123-124].

O'Melia suggested that for a clean filter the particle removal efficiency is independent of the influent concentration or in equation form,

$$\frac{\partial C}{\partial L} = -\lambda C \quad \text{where } \lambda \neq f(C_o) \tag{54}$$

However, the removal efficiency increases with increasing influent concentration after the initial period. This is due to the retained particles acting as collectors as they present an increased surface area to the flowing suspension.

Suspended particle size was found to be inversely proportional to the pressure drop increase. Thus sub-micron particles were found to cause the largest head losses. Earlier work by Yao [116] had showed that 1 μm particles were found to have the lowest removal efficiencies. This suggests that deposition mechanisms for this size of particle are less effective generally.

A network model approach was described by Leitzelement et al [125] in a study of particle deposition in a two-dimensional square array of tubes of randomly determined sizes. The effects of deposition on the permeability were related to:

i) the pore size distribution, and
ii) the interconnection of pores.

Dispersion effects and the formation of "preferential" paths through the network were proposed. However, the combination of random tube size distributions and 'regular' array interconnections meant that the flow resistance could not be accurately modelled. The process of averaging pore sizes also introduced some error. It was concluded that a much larger network model was needed.

CHAPTER 4

EXPERIMENTAL WORK

4.1 INTRODUCTION

An experimental investigation was conducted to determine the cause and effect of clay mobilisation. Sandpacks were used as model reservoirs. The flooding parameters were, the salinity of fluids, their pH, contact time and flowrate. The interaction of kaolinite particles with silica surfaces was studied in a specially designed apparatus, under comparable conditions to those used in the sandpack tests. The analytical techniques included Atomic Spectroscopy, clay composition and size analysis and work with the Scanning Electron Microscope.

4.2 RESERVOIR CORE FLOODING

Despite the unsuitability of reservoir core material for extensive tests, it was important to conduct at least one experiment on a core-flooding rig. This was done in order to place water sensitivity effects in the context of actual reservoir permeabilities and flooding rates.

A non-extracted core (1" x 1") from a suspected water-sensitive sandstone in the North Sea Forties field was tested*. The test rig, shown in Figure 10 was enclosed in an isothermal cabinet operating at 25^{o}C. The core sample was placed in the sleeved core-holder. An

---

* BP Research Centre, Petroleum Engineering Branch, Sunbury-on-Thames, Middlesex.

external pressure of 30 bar was applied to the sleeve. Filtered fluids were supplied to the core with an Altex twin-cylinder pump. The fluid flow sequence is listed in Table 9. The measured variables were the inlet pressure and effluent flowrate.

4.3 USE OF SANDPACKS

Previous researchers have used either core or sandpack-flooding experiments to study formation damage behaviour. In the case of core-flooding, reservoir cores obtained from drilling operations are tested in sleeved holders under simulated reservoir temperatures and pressures. In packed bed studies, unconsolidated sand or glass ballotini is flooded under single or multiphase conditions. The disadvantage with the use of ballotini beds has been the problem of achieving adhesion between clay and ballotini surface [117]. Moreover, it is doubtful whether the nature of adhesion of clay on natural sands can be represented in these systems. The use of capillary-network models has been successful in the study of oil-water interfacial phenomena and multiphase flow behaviour, however their application in formation damage studies has so far been limited because such models are not well-suited to the study of hydrodynamic and ionic effects. In selecting the best method of permeability testing, the difficulty in maintaining similar core properties on a run to run basis was considered a major disadvantage of the core flooding technique. Reservoir sandstone is invariably a heterogeneous and isotropic material. The scarcity of cores and their cost is an added disadvantage. The flooding of unconsolidated sandpacks at velocities prevailing during waterflooding offered some similarity with the type of flow in a reservoir formation, despite an order of magnitude difference in permeability. A further significant advantage

of the use of sandpack flooding as a basis of permeability analysis was that, with careful preparation, the sandpacks would be homogeneous and reproducible.

The degree of complexity of the experimental system, and hence the analytical techniques required to interpret the results obtained, was further minimised by the selection of single phase experiments throughout the programme.

4.3.1 Selection of Sand

A test sand was desired with grain properties and clay mineralogy which were similar to those of the Forties sandstone in the UK North Sea. Secondly a packed bed of the sand should be of porosity and permeability characteristics giving measurable pressure drops during flooding. A size fraction of sand produced with oil and separated out at the wellhead was a candidate for a test sand.

4.3.1.1 Reservoir Separator Sand

Produced oil contains entrained solids which are separated at the wellhead by sieving and sedimentation processes. These solids consist of the finer grades of sand, silt, clay and organic matter. The sand fraction is normally cleaned for experimental use by a standard technique which does not hydrate any clays present. This fraction, termed separator sand, has been and continues to be used as an important material for formation damage studies.

The composition, sieve and BET surface area analysis of the Forties separator sand from the North Sea are given in Tables 5 and 7. Scanning electron micrographs of separator sand grains (Plates 1-2) illustrate the characteristic features of crystalline grain structure

in the well defined edges and clear faces on generally semi-rounded grains. The average grain diameter can be seen from Figure 8 to be 116 microns, with a grain size distribution from 50 to 150 microns. Evidence of fine clay materials can be seen in the grain surface crevices and where high surface roughness of the sand grain occurs.

The fines content of separator sand, measured as alumino-silicate materials less than 45 microns, was in the region of 5-6% wt and consisted primarily of quartz fragments, kaolinite, illite, mica and some feldspar. The analysis is shown in Table 7 and Plate 14 examines the clay fraction of separator sand with the electron microscope.

Although it was intended to use separator sand as a basis of the permeability testing, preliminary tests showed that some batches were water-wet while others remained oil-wet, making a case for representative testing difficult. This was possibly due to the cleaning procedures it had undergone. This initiated the search for other sands with similar properties especially with respect to grain size and the clay analysis.

4.3.1.2 Redhill and Chelford Sands

A number of sands were used to identify the most suitable from an experimental point of view. These sands included commercial grades of sand used in the building industry and as moulding sands*. Their sieve analysis and composition results are given in Tables 6 and 8.

As can be seen from these data, such sands were incompatible with reservoir separator sand in terms of mineralogical composition (low kaolinite content) and grain properties.

---

* British Industrial Sands Ltd.

The analyses show that the Chelford 95 grade contained approximately 10% of fines, mainly as feldspar and mica. The lack of kaolinite and illite clays in the fines fraction, which were of primary interest, made this sand unsuitable. The Redhill 110 sand possessed similar properties to the reservoir separator sand in its grain surface structure and fines composition. However, the total fines amounted to approximately 2%, a value which was slightly lower than acceptable when compared with separator sand on BET surface area tests.

4.3.1.3 Fine-Grey Sand

A sand which possessed roughly similar properties to reservoir separator sand was selected after consultation with the British Geological Survey*. The sand was located at an open quarry site near Ightam, Kent**. The sieve and composition analysis of the 'Fine-Grey' (FG) sand is shown in Tables 5 and 7 where it may be compared against reservoir separator sand. Plate 3 and scanning electron micrographs (Plates 16-17) show features similar to Forties Separator and grains with respect to their surface structure and the morphology of fines associated with the sand grains. Fine-Grey sand is a water wetted sand with 5-8% wt associated fine materials, mainly quartz, illite and kaolinite.

4.3.2 Preparation of Sandpacks

An often used method of bed preparation in flooding tests is dry packing, compacting and evacuating before allowing fluid to flow into the bed. This can only be done with a steel column which has the drawback that the quality of the packed bed cannot be observed.

---

* British Geological Survey, Nottingham
** Ightam Sand Pits Ltd, Ightam, Kent

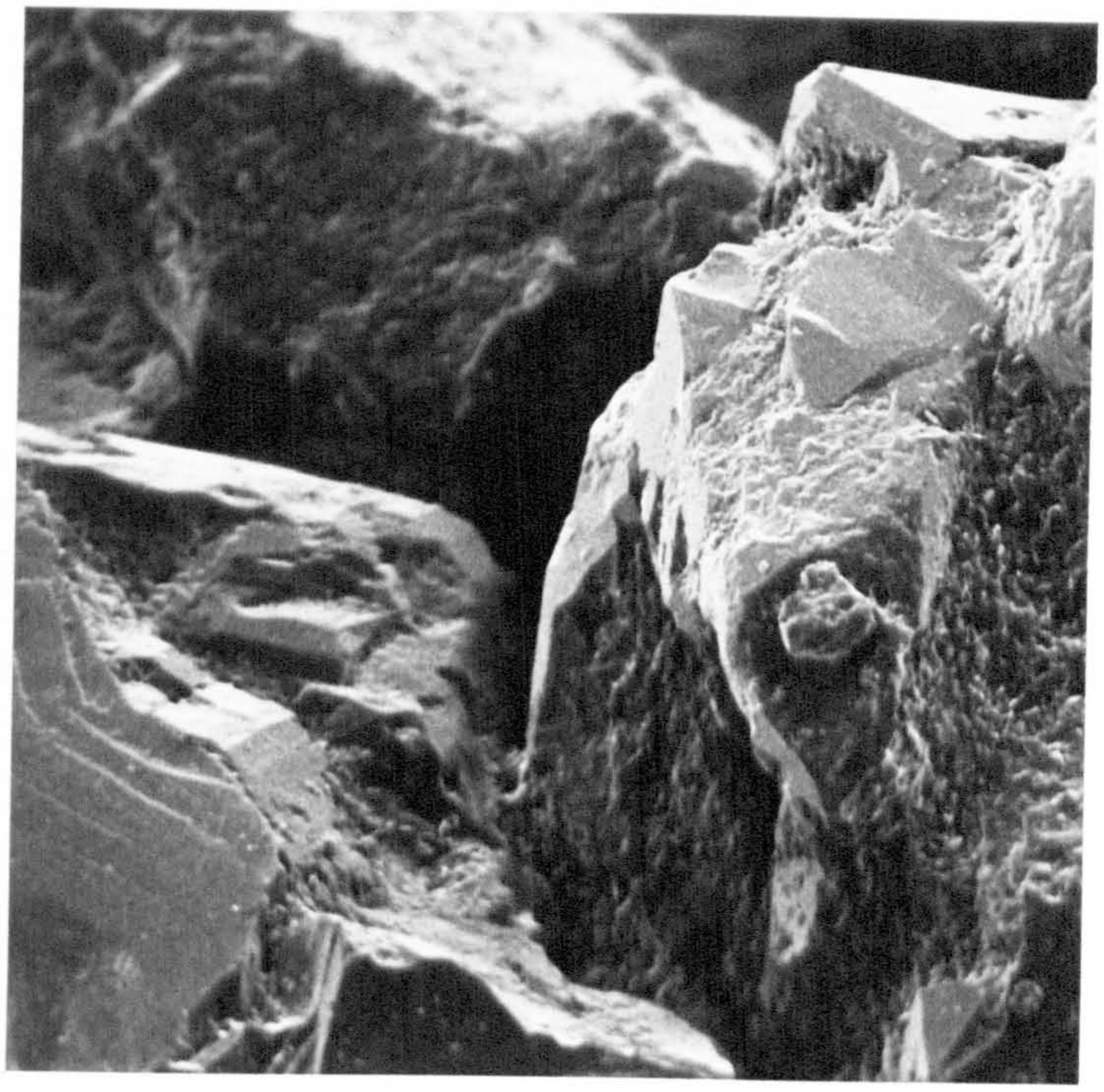

PLATE 1 A NORTH SEA RESERVOIR SEPARATOR SAND (x500)

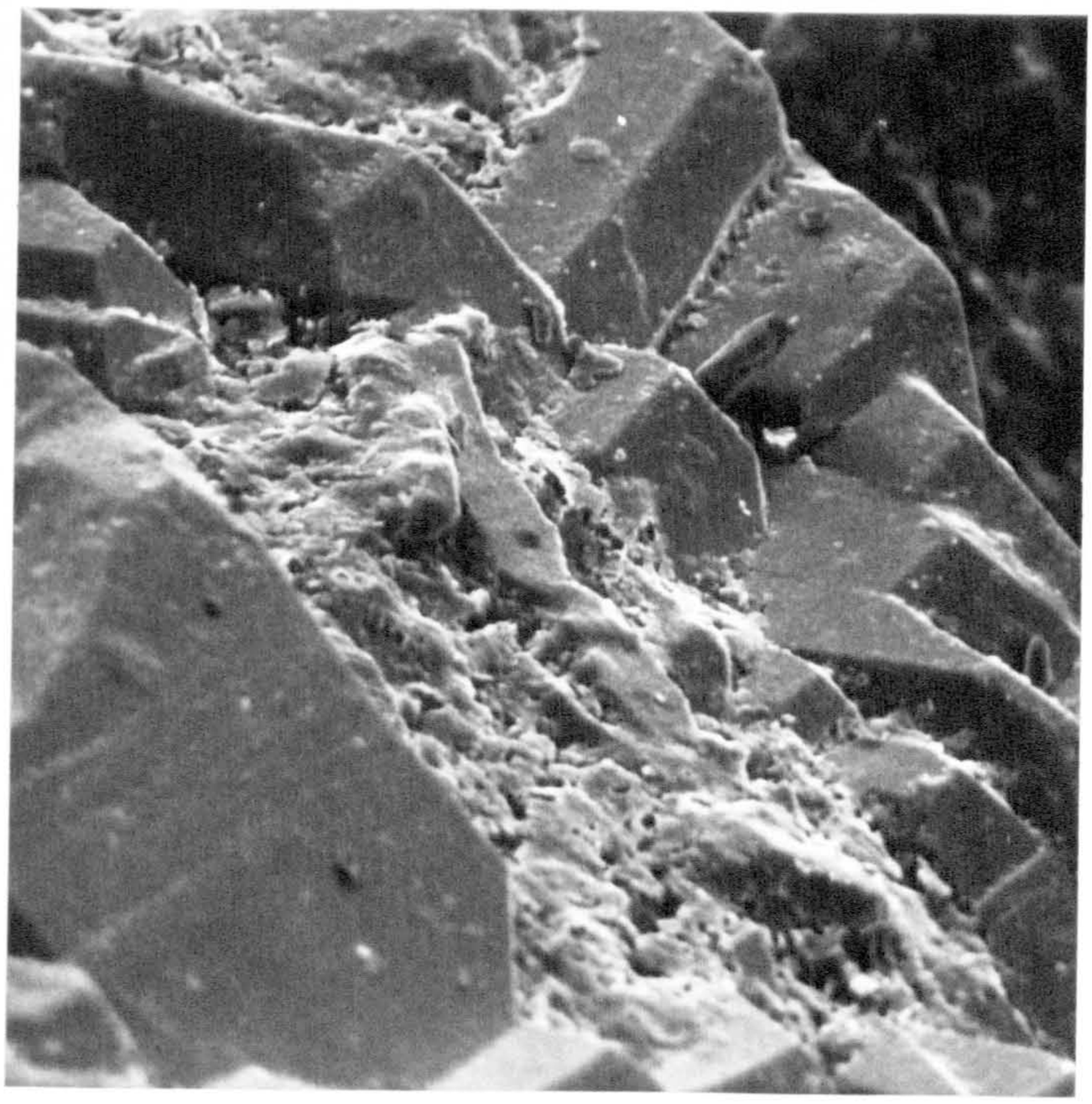

PLATE 2 SEPARATOR SAND GRAIN SURFACE SHOWING CLAY MATERIALS IN CREVICES (x2000)

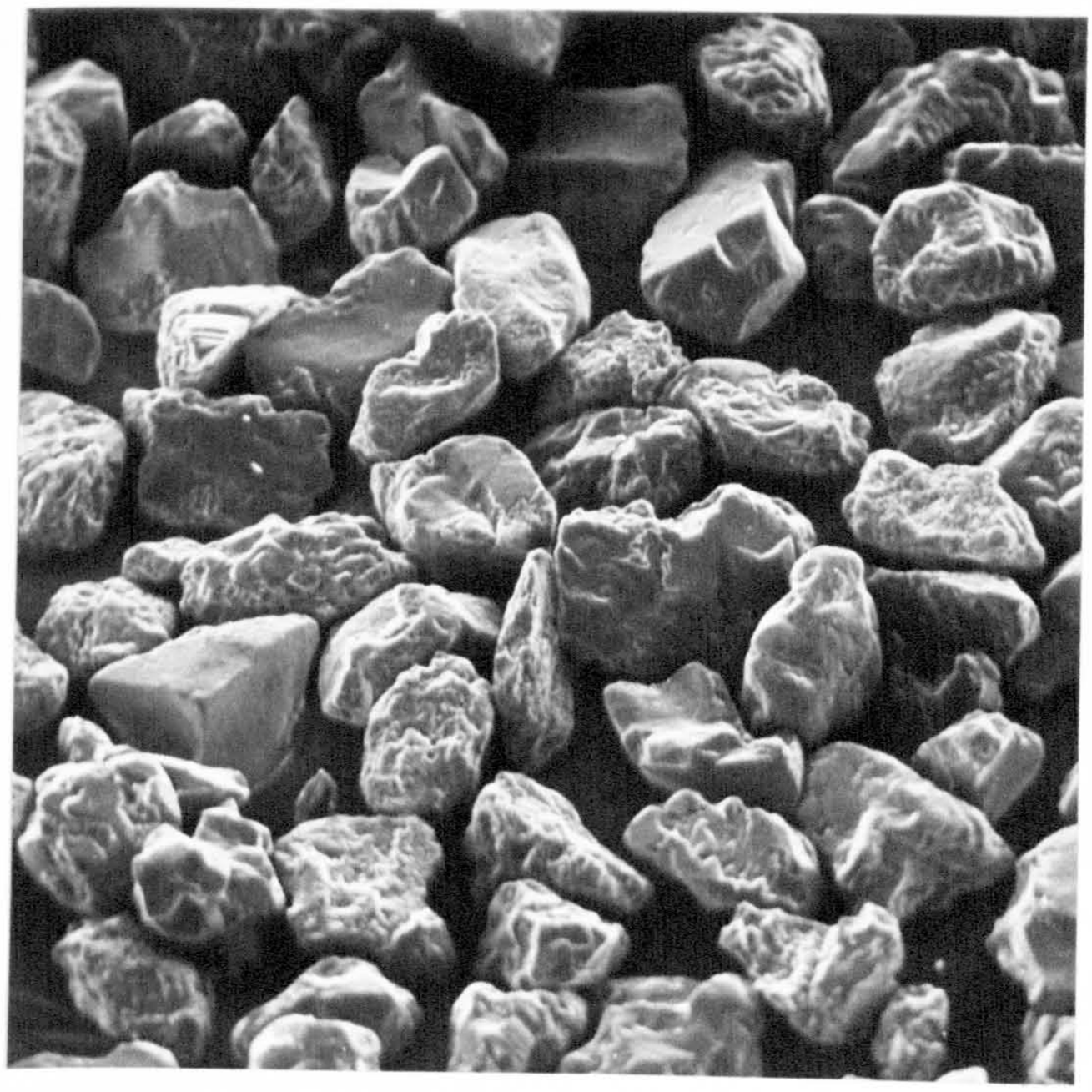

PLATE 3 FINE-GREY SAND (x100)

Glass apparatus was used in order that the homogeneity and total liquid saturation of the sand bed could be visually confirmed. The best method of producing a completely water saturated homogeneous bed was by simultaneously flowing sand and water into the column at a slow, regular rate. At the same time a laboratory vibrating probe was applied to the outside wall of the column. This greatly assisted in compacting the bed and releasing trapped air bubbles. Some fines were inevitably transferred to the liquid phase during the packing process, however their quantity was minimal and they were transported through the bed during the first few minutes of water flow without effect. This method produced homogeneous, fully saturated sandpacks. Porosities and permeabilities in the region of 30% and 5-7 Darcy, respectively, could be reproduced. Figure 9 shows that sandpacks prepared in this above described manner were homogeneous.

4.3.3 Constant Head System

Some preliminary experiments were performed in order to observe the pressure response of sand beds under constant head liquid flow. Figure 11 shows the apparatus constructed for this purpose, consisting of an array of Quickfit glass columns of 2 inch internal diameter. These were fed with flooding fluids from Marriott bottles which provide a constant head flow. One column had side-wall tappings for connection to water manometers. The tappings were plugged with a porous pad of cotton wool to prevent transfer of bed solids and fines. The sand beds were supported on porous glass sinter discs formed into the end fittings. The Redhill 110 sand was used during these tests.

Sandpacks for each experiment were prepared with distilled water as described in Section 4.3.2. The following fluid displacement experiments were conducted:

Run No.	Description
2	1% wt NaCl - distilled water (DW)
3	1% wt $CaCl_2.6H_2O$ - DW
4	1% v/v surfactant - DW
5	0.01 M HCl - DW
6	0.01 M NaOH - DW

All flooding solutions were prepared with AR grade salts made up with distilled deionised water and adjusted to pH 7 in the case of Runs 2-4.

The maximum head available for flow was 0.6m measured to the top of the bed. This produced a flow through a typical sandpack (0.5m depth) of approximately 10 ml/min corresponding to a superficial velocity of 1.5 m/hr. In terms of reservoir flooding velocities (1 m/day) these flow rates were necessarily high to achieve measurable pressure drops and to maintain the ability to detect small changes in the pressure in the column. Each solution was allowed to flow through the bed for one hour, equivalent to more than three pore volumes. The inlet and intra-bed pressures were recorded with water column manometers. The effluent flow rate was also measured and the effluent turbidity was used as a measure of particle release and migration effects in the bed. Turbidity was measured with a Hach Portalab instrument. Changes in the effluent flowrate reflected changes in bed permeability.

From these results it was apparent that a constant rate flowrate flooding system could be a more effective technique for the measurement of permeability changes in sandpacks. Before embarking on this stage however, it was necessary to determine the flocculation

characteristics of clay and fines suspensions. These tests are described in Section 4.7.1.

4.4 Constant Rate System

The investigations of Mungan [34], Jones [18] and Khilar [43,44] reported spontaneous permeability reduction when fresh water displaced brine in sandstone core samples under constant rate flooding. These studies have indicated particle plugging to be the cause of the permeability reduction, however the mechanisms for particle detachment and migration are not fully understood. Particularly, the influence of ionic composition of fluids and factors such as flow rate, fines concentration and pH in the clay-sand grain-fluid environment has not been fully investigated. One of the primary objectives of the experimental work was to determine the causes of particle detachment, migration and plugging effects in sandpacks. A summary of the flooding experiments is tabulated in Table 11. Experiments were divided into two series wherein different experimental parameters were investigated.

4.4.1 Description of Rig

Based on the results of the preliminary experiments, as interpreted in Chapter 5, the constant-rate flooding rig was designed to measure pressure changes in a sand bed under a wide range of simulated water flooding conditions.

Figure 12 is a system flow diagram of the experimental rig for sandpack flooding. The apparatus consisted of a vertically mounted borosilicate glass low pressure liquid chromatography column 400 mm in length and 25 mm inside diameter. The maximum fluid pressure rating of the leak tight column was 5.5 bar absolute. The column was vertically

mounted in a flow system, consisting upstream of the following main elements:

a) feed reservoirs
b) high pressure variable-stroke positive displacement pump (Mono Pumps Ltd)
c) switching valve
d) isolation valve
e) pulse damping air column
f) needle valve (flow rate control)
g) in-line filter (2 micron)
h) pressure gauge

A Philips in-line PW9560 conductivity probe was placed in the bed outlet. This probe was electrically connected to a Philips model 9509 digital conductivity meter. Isolation, needle valves and sample collecting vessels were also utilised at required points in the system. An output signal from the conductivity meter was directed to the multi channel chart recorder.

Of paramount importance was the need to reduce the dead volume of the system. This was achieved using fine-bore flow lines and elements commonly used in the high performance liquid chromatography systems (HPLC). A Plexiglass safety shield was secured in front of the column as shown in the photograph of the system, Plate 5.

Although there was a need for in-bed pressure measurements, tappings could not be made through the sidewalls of the glass column due to safety considerations. Instead stainless steel fine bore tubing less than 2 mm diameter was placed through the upper PTFE end plate of the column. Six tubes were employed in this way such that the in-bed

pressure could be measured at equidistant points in the bed or, where desired. The arrangement of the tubes and the glass column can be seen in Plate 5. Care was taken to ensure that the fluid flow profile and more importantly permeability would not be adversely affected by the presence of the tubes. In tests where a clay dye (methylene blue) was employed, there was evidence of minor channelling effects, however their overall effect on permeability was found to be negligible. Furthermore, since changes in permeability were of interest, this potential problem were reduced. The ends of the pressure microtubes were connected to fine bore plastic tubing using standard leak tight ferrule fittings. An electrically actuated six port solenoid valve block received the polythene pressure lines from the column. This was in turn hydraulically connected to two pressure gauges one of which measured the differential pressure (maximum 1 bar, 15 psi) of any one of six levels in the bed with respect to the fluid inlet pressure. The column inlet pressure relative to atmospheric pressure was also continually monitored by a second pressure transducer (3.5 barg, 50 psig max).

An electrical control module was constructed to control the operation of the pump and solenoid valves and to provide power supply to the pump which would cut out on an overpressure signal from the system pressure measurement transducer. A chart recorder output port was also available on the module.

The sand bed was contained within the two PTFE column end fittings in which were inserted 50 micron glass sinter discs which allowed the passage of fines but prevented sand from entering the flow lines. The seal between the glass lip of the column and end fittings was maintained by using suitably cut rubber washers. The needle valves at

the inlet and outlet of the column allowed the setting and control of flow rate and application of back pressure if operation at higher pressure was desired. In addition, the damping of flow pulsations produced by the metering pump could be enhanced with the inlet needle valve and air column system employed. This was observed when an oscilloscope was connected to the pressure measurement system. It was verified that pulsation amplitude was significantly reduced by using the inlet needle valve. The rig could be controlled automatically or manually. In manual control, the pressure at any of six points in the bed could be displayed. Under steady state conditions, it was also possible to determine the pressure drop across adjacent sections of the sandpack. The control module also displayed a continual reading of the inlet pressure.

4.4.2 Run Procedure

A flooding experiment entailed the packing of a saturated sand bed, flushing through with double distilled water to remove any initially detached fines, followed by constant-rate flooding by the liquids of interest. Two or three feed reservoirs were prepared at the start of the flood to ensure interruption free and pressure pulse free switch-overs.

It was important to obtain a sand bed of as low a porosity as possible in view of real formation porosities in the region of 100-200 md for a reservoir of medium porosity. Secondly, it was of primary importance to remove all air bubbles from the sand bed during the packing process and from all flow lines as these would result in false pressure readings. In order to do this the system was completely purged at the start of each flood and in a particular sequence. With the isolation valve at the column base closed, the fluid inlet and pressure lines to

the transducers were manually filled with packing solution (usually double distilled water) and connected. The transducer measurement ports were cleared of air by syringing with distilled water, capillary pressure preventing water from draining out. The pump was then switched on with the column outlet valve remaining closed. This allowed the in bed pressure microtubes to be purged of air at which point connections to the flow line leading to the solenoid valves could be made. With the purging of the pressure transducers and the solenoid valve manifold all air from the system could be removed at the purge valve, the highest point in the system.

Except for some of the experimental runs where the effect of increased flowrate on migrating fines effects was studied, the flow rate of fluids was set at the pump at a constant 10 ml/min. This was manually checked in addition to the pump calibration runs. The inlet and outlet needles valves were then adjusted to introduce, respectively, pulse damping and the option to operate at higher pressure. Once stable pressure readings were achieved after the air purge, packing solution was pumped through for up to half an hour to ensure steady state operation.

During the run, effluent samples were collected at three minute intervals which was reduced to 30 seconds or less if a fines concentration profile was desired. Effluent conductivity readings were available in the form of digital display and chart recorder trace. Effluent samples collected were analysed for their clay content and particle size distribution.

4.4.3. Experimental I - Ionic and Chemical Factors

4.4.3.1 Brine-water Flood

Separator sand from the North Sea Forties field was used in this experiment (Run 7). The size distribution, and fines analyses of the sand are shown in Figure 8 and Table 7 respectively. The grain size ranged from 50 microns to 150 microns though some grains were observed in optical study to be of > 200 microns diameter. Surface fines content of the sand was 5-6% wt, mainly kaolinite and illite.

A sandpack possessing a porosity of 30.6% was sequentially flooded with distilled deionised water, a 0.5M aqueous sodium chloride solution and finally with water again at a constant flow of 10 ml/min. Flooding liquids were adjusted to pH7. The system inlet pressure was adjusted to stabilise at 1.7 barg (24 psi) by using the needle control valves on the inlet and outlet flow lines. These valves were set at the start of the experiment and not altered subsequently. In-bed pressure readings were recorded at 30 second intervals.

The conductivity of bed effluent was measured and samples were collected at three minute intervals for turbidity and particle analysis. At the end of the run the sandpack was cut into 8 cm sections and each section was then analysed to see if a fines concentration profile had been set up in the sandpack. This was done by washing with a fixed volume of water and turbidimetrically analysing wash liquors. The dry weight of sand in each section was then determined.

4.4.3.2 Rapid Salinity Decrease

During the later waterflooding stages of oil production formation water is often replaced by treated sea water for pressure maintenance, subjecting the reservoir to a salinity contrast. In an attempt to measure the effects of these ionic strength changes, a flood (Run 8) was carried out comprising initially, M NaCl solution (58500 ppm wt), followed with 0.5M NaCl (29250 ppm wt) and finally distilled water, at neutral pH conditions. The flow sequence consisted of five pore volumes (PV) of each of the brine solutions followed by water for at least 20 PV.

4.4.3.3 Gradual Salinity Decrease

Two floods (Runs 15-16) examined the response of sandpacks to slowly decreasing salinity environments, employing the technique of continuous salinity decrease as has already been mentioned [34,43]. Here the flooding brine was fed from a constantly stirred reservoir which was diluted at a rate such that the concentration of brine being pumped to the sandpack decreased exponentially. Varying rates of salinity decrease were obtained in this way. Pressure profiles and the effluent conductivity and turbidity were measured through the run. In Run 15, a 0.17M aqueous sodium chloride was used whilst in Run 16 a 0.1M potassium chloride solution was used.

4.4.3.4 Low Salinity Flood

In Run 9, a 0.17M sodium chloride solution was passed through the column, followed by step change brine floods with concentrations of 0.05M and 0.017M sodium chloride respectively. The objective here was to determine if flocculation-deflocculation processes were operating and their effects on internal bed pressure differentials and effluent solids production. This flood was conducted in conjunction with the

flocculation value tests, described later in this Chapter, which determined the minimum salinity required for coagulation of a clay suspension.

4.4.3.5 Ion Contact Time

A series of floods (Runs 11-14) were performed in which the contact time of the brine flooding solution was varied before water was introduced into the column. In the first of these runs 10 PV of 0.5M aqueous sodium chloride was pumped followed in successive runs by 2.5, 1 and 0.3 PV. Each run was conducted with a freshly packed column of Fine Grey sand. Standard pressure data were recorded, in addition to the effluent conductivity and effluent sampling.

4.4.3.6 Potassium Chloride Treatment

Clays associated with reservoir rocks possess a variety of ionic species attached to their surfaces, one of these being the potassium ion which is often associated with illite clay [22]. It was therefore decided to incorporate potassium chloride as a test ion based on analysis showing that fine grey sand contained some illite.

Run 17 was designed to measure the response of a sandpack to flooding with potassium chloride solutions. An aqueous 0.4M potassium chloride solution adjusted to pH7 flowing for 10 PV was displaced with water. This made the run equivalent to using a 0.5M sodium chloride brine on the basis of conductivity (the mobility of K^+ ions being greater than that of Na^+).

Run 16, described earlier, measured permeability effects due to slowly decreasing potassium chloride salinity.

4.4.3.7 Divalent Ion Treatment

Formation waters and seawater contain a mixture of ionic species, sodium, calcium, and magnesium, being the most abundant. Current oilfield flooding practice often involves dosing of specific chemicals, polymers and ionic species for the stabilisation of clays.

In Run 18, the effect of an aqueous 0.5M calcium chloride solution was evaluated in a sandpack under standard test conditions (pH7, flow rate 10 ml/min). This solution was pumped for 7.5 PV then displaced with water, a sodium chloride brine each for 7.5 PV and finally water again. This run constituted the 'pretreatment' of a sandpack with divalent ions before a monovalent ion was introduced.

Run 20 used a simulated formation water at pH 6.5 (reservoir pH) with a separator sand bed. The composition of the flooding liquids is given in Table 12. The flow sequence simulated the ionic strength change in a reservoir when seawater displaces recirculating formation waters.

In Run 19, a separator sandpack was first flooded with a 0.5M aqueous NaCl brine for approximately 10 PV. This was then displaced with a similar volume of 0.5M calcium chloride solution followed by distilled water. This run modelled the sandpack post-sensitisation treatment situation.

4.4.3.8 Variation of pH

The pH of reservoir fluids can vary depending on the presence of sulphates and chemicals producing weak acids in situ. Formation water pH values vary widely depending primarily on the type of reservoir rock and composition of connate brines. In sour wells the pH may be less than 5 whereas alkaline conditions can exist in limestone reservoirs.

Runs were carried out to determine the effect of pH changes in sandpacks (Runs 21-24). Sandpacks were prepared with distilled deionised water. In Run 21, after flow of the packing fluid (water) for a few pore volume, water adjusted to a pH = 9 (with 0.1M sodium hydroxide solution) was pumped for 10 PV at a flow rate of 10 ml/min. Water was then reintroduced to the bed.

This was followed by a flood (Run 22) under identical initial conditions, with a displacing water pH of 5. This procedure was repeated for Runs 23-24 with 0.5M sodium chloride brine. Analysis of pressure and fluid effluent data was carried out for permeability determination and clay analysis.

4.4.4 Experimental II - Hydrodynamic Factors

Early results with the sandpack flooding experiments which have been interpreted in Chapter 5 indicated the similarity of behaviour of Forties separator and Fine-Grey sands.

Experimental work for the second series of tests was thus confined to the substitute 'Fine-Grey' sand. A number of workers [40-42] have proposed that changes in flow regime are the main cause of clay mobilisation and consequent permeability loss. The following set of floods included experiments to test these theories.

4.4.4.1 Effect of Flow Rate

The effect of displacing fluid flow rate was measured in 'un-sensitised' and 'sensitised' sandpacks. Sensitised sandpacks are those which a monovalent brine has been used as a flood stage. In Run 25, a freshly prepared column was subjected to brine flow rates of 2.5, 5, 10, 15 and 25 ml/min. Each step change on the pumping rate

was followed by a flow of approximately 1 PV to allow pressures to stabilise. In Run 26, a sandpack treated with 0.5M sodium chloride was progressively subjected to higher flowrates of distilled water. The effect of these changes in flow regime on inlet pressure and effluent solids production was observed.

4.4.4.2 Effect of Reverse Flow

In oilfield practice a flow reversal is often proposed when the reservoir experiences pore blocking due to pore-plugging. Usually the effect is beneficial in the short term.

In Run 27, a sensitised sandpack was used in which fines release was already underway through brine-water shock. After approximately 0.5 PV, the water flow was stopped, the bed inverted and the flow of brine (0.5M NaCl) continued in reverse flow.

4.4.4.3 Effect of Gravity

The effect of gravity in sandpacks was determined in Run 28. A sandpack was contacted with 3 PV of distilled water displaced with 2PV of 0.5M sodium chloride and finally with distilled water. Bed pressure data were recorded and samples of effluent were collected from the exit at the top of the column.

4.4.4.4 Clay Filtration Tests

The processes of clay deposition (and release) in sandstones undergoing flooding and of particle capture in deep bed filtration are similar. This analogy was investigated in a number of runs (Run Nos. 29-30).

Very clean sand was required for the experiments. This was obtained by subjecting Fine-Grey sand to sequential two brine-water treatments. This treatment caused the elution of clay fines which were collected. The sand quantity was then mixed with water and ultrasonicated for three minutes. This caused the removal of more fines from the sand grain surfaces. These fines were discarded. The sand produced in this way was dried and used for bed preparation for the filtration tests. The clay suspensions collected from the cleaning procedure were filtered, washed and resuspended in distilled water to form clay concentrations of 1 g/l and 10 g/l respectively.

The clay suspensions, in turn, were pumped through 'clean' sand and naturally contaminated sandbeds at 10 ml/min and pH7. Filtration tests were run with the clay suspended in distilled water and in a 0.01M sodium chloride solution. Pressure changes in the sandpack were recorded and samples of effluent collected for solids analysis.

4.5 PARTICLE DEPOSITION AND REMOVAL EXPERIMENTS

Experimental work using the unconsolidated sandpack in flooding experiments provided a measure of the macroscopic effects due to changes in the ionic or flow conditions of flooding fluids. It was felt that deposition and detachment effects between clay particles and grain surfaces should be analysed on a microscopic level. Two experimental alternatives were considered. These were the Rotating disc, and the more recently developed Flow cell technique which has been described in Section 4.6.

4.5.1 The Rotating Disc

This is the classical method of measuring the deposition of sub-micron and colloidal particles from a surface under defined flow conditions [89]. The apparatus consists of a simple motor-driven vertical shaft on the end of which is fixed the deposition surface using a non- or semi-hardening adhesive. The collector, usually a thin glass or silica disc, is immersed in the suspension from which deposition is to take place. The rate of rotation of the shaft determines the flow conditions on the surface.

In the context of the present investigation, pure silica (Spectrosil 'B') microscope cover slips were used. These were attached to the shaft end with lithium grease.

Suspensions of pure kaolin (English China Clays, Cornwall, UK, non-chemically treated, 75% less than 2 micron) were prepared. After a fixed deposition time period the disc was removed, allowed to dry and examined under the optical microscope. A standard particle counting method was used.

After a few runs, it was apparent that 'clean-room' conditions would be required to operate the rotating disc effectively. Despite precautions, discs were found to be easily contaminated with dirt and fibre during the dismounting, drying and counting stages.

4.6 THE FLOW CELL EXPERIMENTS

After some work with the rotating disc it was decided to continue the kaolinite deposition studies using the Flow cell method. It was felt that the flow cell was better suited, from an experimental point of view, to the study of both particle deposition and removal.

4.6.1 Description of Cell

In this apparatus, particle deposition is obtained by the impingement at an angle of 90^{o}, of a suspension of particles onto a collector surface. A well-defined stagnation flow is formed around the region of impingement. Particle deposition can be observed and measured using a microscope under incident light.

The technique was originally developed for particle deposition studies in paper and pulp manufacture, (Dabros and Van de Ven [97,98]). A version of their apparatus was built for use in this work (Figure 13 and Plate 6).

This was done by grinding down the ball of a Quickfit ball and socket joint to form a flat circular surface. The ball was mounted onto the elongated cone piece of a cone and socket, the outside diameter of the socket being 20 mm. This socket formed the outer body of the cell. The particle collection surface, typically a cover slip 20 mm or more in diameter was placed on top of the socket. Thus, a space between two circular surfaces is formed, with a constant separation distance. Two cells were built with gaps of 1.5 and 2.5 mm. The particle suspension, flowing vertically upwards through the inner body of the cell enters at the centre of the lower surface impinging the underside of the collector disc. From the stagnation point region, fluid flows radially outwards and is routed to a reservoir from the outer body of the cell.

The whole of the apparatus was attached to a micro-manipulator which enabled its placement under the objective lens of a microscope. Particle collection could thus be studied at any radius on the disc surface.

Observations and particle deposition or release measurements could be made in-situ using incident light at magnifications up to 1000X. Another advantage of the technique over the rotating disc was that the collecting surface was stationary during deposition. Also the deposition surface was held in position by the slight sub-atmospheric pressure in the cell rather than with grease (used in the rotating disc) which could contaminate the surface.

4.6.2 Materials

Since the main interest was the interaction between clay particles and silica surfaces, pure materials were chosen for the experiments.

Twice distilled filtered (0.1 micron) water was used to prepare clay suspensions. Its conductivity was in the range 0.8-1 micron S cm^{-1}.

The clay was a pure kaolin from English China Clays, St Austell, Cornwall, England, used as a non-chemically treated reference clay. Its composition is given in Table 13. Clay suspensions were made to a concentration of 5×10^7 particles per cm^3.

Pure 'Spectrosil B' silica 22 mm microscope cover-slip type discs obtained from UQG Ltd, Cambridge, UK, were used as collectors.

4.6.3 Disc Surface Treatment

Clay deposition on silica discs appeared initially to be very low and unpredictable. Cleaning discs with acetone and de-greasing solvents proved unsuccessful. From the literature a number of methods of disc pre-treatment were found. This was found a necessary part of the preparation procedure. The best method was found by particle counting to be that of Dabros [98] who treated discs with concentrated nitric

acid (12 hrs) and hydrochloric acid (1 hr) followed by rinsing with copious quantities of filtered distilled water. Other methods considered involved boiling the discs in detergent (10% in water) and rinsing with water and a sulphuric acid-nitric acid treatment.

Figure 45 shows the coating density of kaolinite on un-treated and acid treated silica discs. Many workers describe the acid soak as a necessary procedure in order to impart a uniform charge to the surface.

4.6.4 Deposition of Kaolinite

Table 14 presents a list of runs carried out with the Flow cell apparatus with the objective of characterising the clay-silica interaction and the clay-clay interactions near silica surfaces. The variables of interest were the salinity of the medium, its pH and flow rate and the concentration of fines in suspension.

4.6.4.1 Salinity

The effect of brine strength on the deposition of kaolinite suspensions on silica was measured. Kaolin suspensions were made in sodium chloride brines of 10^{-3}M, 10^{-2}M and 10^{-1}M. Higher brine concentrations were not used because they were expected to result in very short half-lives of the kaolin suspensions leading to coagulation. The half-life is time taken for the suspension concentration to halve. The Schmolukowski equation (from [27]) was used to determine the concentration of suspension:

$$t_{1/2} = \frac{3\,\mu}{4k\,TC} \qquad (55)$$

where μ = viscosity

k = Boltzmann constant

T = temperature, K

C = suspension concentration, particles/m^3

The kaolin suspensions used had half lives of 5.5 hours, much longer than the duration of an experiment.

4.6.4.2 pH

Runs were carried out at a flow rate of 5 ml/min and suspension pH's of 5 and 9 respectively. The pH of suspensions was adjusted with molar hydrochloric acid and molar sodium hydroxide. The coating density of deposited kaolinite was measured after one hour.

4.6.4.3 Flowrate

Kaolinite particles were deposited onto silica from neutral suspensions Flow rates of 2.5, 5, 10 and 30 ml/min were achieved by altering the level of the constant head feed suspension reservoir. The deposition was measured from clay suspensions in distilled water, and from 0.01M and 0.1M sodium chloride solutions.

4.6.4.4 Clay Concentration

Three suspension concentrations, 1×10^7, 0.5×10^8 and 1×10^8 particles per cm^{-3} were prepared in distilled water and flowed through the cell for one hour at 5 ml/min. The density of deposit was then measured. Experiments were repeated at higher salt concentrations.

4.6.5 Detachment of Kaolinite

Standard deposition conditions were imposed in the flow cell to achieve repeatable, uniform coating densities of kaolinite particles on silica discs. A kaolinite suspension in 0.01M flowing at 5 ml/min for one hour gave a saturation coating density suitable for detachment experiments.

4.6.5.1 Salinity

Water shock experiments were carried out on a particle coated disc which were similar to brine-water shock experiments with the sandpack flooding rig.

A disc with a saturation deposit was prepared. Sodium, potassium and calcium chloride solutions were then run through the cell for 1/2 hr at 5 ml/min. This stage of flow attempted to sensitise the deposited particles.

A particle count was then carried out. Then the flow was switched to enable water to be run through without interruption or surge. After approximately 1/2 hour of water flow, the flow was once again stopped and a particle count conducted.

4.6.5.2 pH

The effect of pH on particle release was determined. An attempt was made to remove deposited particles using water at pH 5 and 9 respectively. Sodium hydroxide and hydrochloric acid solutions of 0.1M concentration were used in pH control.

4.6.5.3 Flow Rate

The effect of flow rate on the detachment of deposited kaolinite particles. Flow rates of 5, 10, 30 and 60 ml/min were tested. These flowrates were achieved by increasing the height of the feed reservoir to predetermined levels.

4.7 ANALYTICAL METHODS

4.7.1 Flocculation Value Tests

Flocculation value tests were carried out with suspensions of fines from separator and Fine Grey sands. The standard method of Van Olphen [27] was used. The flocculation value of a colloidal particle suspension is the minimum salinity required for coagulation.

The peptisation salinity is the salt concentration below which a coagulated suspension disperses. The required amounts of fines from separator and Fine-Grey sands were dispersed to form aqueous suspensions of equal concentrations. A pure kaolin suspension was also prepared in this way.

Taking each fines suspension in turn, aliquots from the stock solutions were placed in each of five large diameter glass test-tubes. Calculated volumes of aqueous ion was added to each test-tube so that a series of mixtures of increasing salt concentration were obtained. After inverting three times the mixtures were allowed to settle. A period of half an hour was usually sufficient to allow the formation of an interface. Repeated tests were performed over narrower salt concentration until the flocculation concentration was defined. For the pH variation tests, molar sodium hydroxide or hydrochloric acid was added from a micro-pipette into stirred solutions until the

desired pH was obtained. The flocculation value tests were conducted at pH values of 5, 7 and 9 in large diameter test-tubes to minimise wall effects.

4.7.2 Clay Analysis

Effluent samples were analysed for suspended solids using a Hach Portalab Model 2000 turbidimeter. This method, though not providing an absolute measure of solids content, did achieve a fairly good measure of consistency. It possessed the advantage that even very small concentrations of fines could be measured.

The instrument was calibrated against suspensions of fines from both Fine-Grey and separator sands. Care was exercised to keep the special optical measurement cell dirt and scratch-free to guarantee the accuracy and comparability of readings. Measurements were available in nephelometric turbidity units (NTU) which were converted to clay concentrations. Concentrated samples were analysed by dilution.

The Malvern Model 2200 Laser Diffractometer, Coulter Model TAII (with 40 micron orifice) and the Micromeritics Sedigraph Model 5000ET Size Analyser were used to determine the particle size distribution of fines.

For fines obtained from Fine-Clay and separator sand the best instrument was found to be the Coulter Counter although the orifice was prone to clogging. This was minimised by ultrasonicating the suspension for a few minutes prior to an analysis.

For dilute suspensions of pure reference clays the laser diffraction apparatus was used because the Coulter method was at the limit of its resolution.

Fines eluted during sandpack floods were separated, dried at 50°C and analysed for mineralogical composition by X-ray diffraction. Clay mineral content was estimated by B.E.T surface area analysis using Krypton adsorption*.

4.7.3 Atomic Absorption Spectroscopy (AAS)

Atomic Absorption Spectroscopy (AAS) identifies ionic species by examining the light emission spectra produced when a sample of liquid is ionised in a flame.

Using this method, the amounts of specific ions in a solution can be determined very accurately and comparisons in the concentration of different ions can be made. For sodium and potassium determinations the method involves the illumination of an air-acetylene flame with a sodium lamp. In the case of calcium, it is necessary to use a nitrous oxide-air mixture to achieve the appropriate ionisation conditions, in conjunction with a calcium lamp. Aluminium determinations also require the latter flame conditions with an aluminium lamp. In the context of this study, sodium, potassium and calcium ions were the principal ions of interest. Pure kaolin and clay materials from Fine-Grey sand were analysed for their ion adsorption characteristics.

4.7.3.1 Procedure

The following steps were involved in the AAS investigation:

1. 100 ml samples of 0.001M and 0.01M strength electrolytes were made up. Electrolytes to be used were sodium, potassium and calcium chloride.

---

* BP Research Centre, Sunbury-on-Thames, Middlesex, UK.

2. 50 ml of each sample was retained for use as the standard in the AAS analysis.

3. A 2000 ppm suspension of clay was prepared using double distilled water.

4. 50 ml samples of clay suspension were mixed with the remaining 50 ml of each electrolyte and shaken vigorously before being allowed to stand for 24 hrs.

5. The kaolin-electrolyte mixtures were then filtered through a 0.025 micron Millipore filter.

6. The last 30 ml of filtrate from each 100 ml sample was collected for the analysis.

7. After each sample was filtered, the pump, piping, and filter unit were flushed through with double distilled water to remove residual ions.

8. Depletion of cation content in the filtrate is determined by comparing against the standards using AAS analysis.

9. Background counts for double distilled water and clay filtrate alone were also taken for comparison.

4.7.4 Microelectrophoresis

A Rank Brothers* apparatus Mark II was used for the determination of the electrophoretic mobility of clay in suspensions. The cylindrical cell was used. The instrument was calibrated and used in accordance with the manufacturers instructions.

4.7.5 Scanning Electron Microscope Study

The morphology of fines released from sandpacks, pure reference kaolinite and sand grain surfaces were examined using a Cambridge Stereoscan MKIIA Scanning Electron Microscope at magnifications up to 20000. Samples were prepared for examination by coating with carbon.

Further, an SEM-EDX (Energy-Dispersive-X-Ray) examination was carried out for a qualitative analysis of the surface ion content of clay particles and sand grains.

EDX is a technique which is used in conjunction with an electron microscope. When electrons of appropriate energy impinge on a material, they cause the emission of X-Rays whose energies and quantity depend on the chemical composition of the sample. Thus every element will emit a unique and characteristic pattern of X-Rays which are roughly proportional in magnitude to the concentration of that element. The X-Ray spectrum emitted by the sample is detected and electronically analysed for examination of its component parts.

In this work, the EDX technique was considered a potentially useful way of locating specific ions on the surfaces of sand grains and clay surfaces.

---

* Rank Brothers, Bottisham, Cambridgeshire, UK

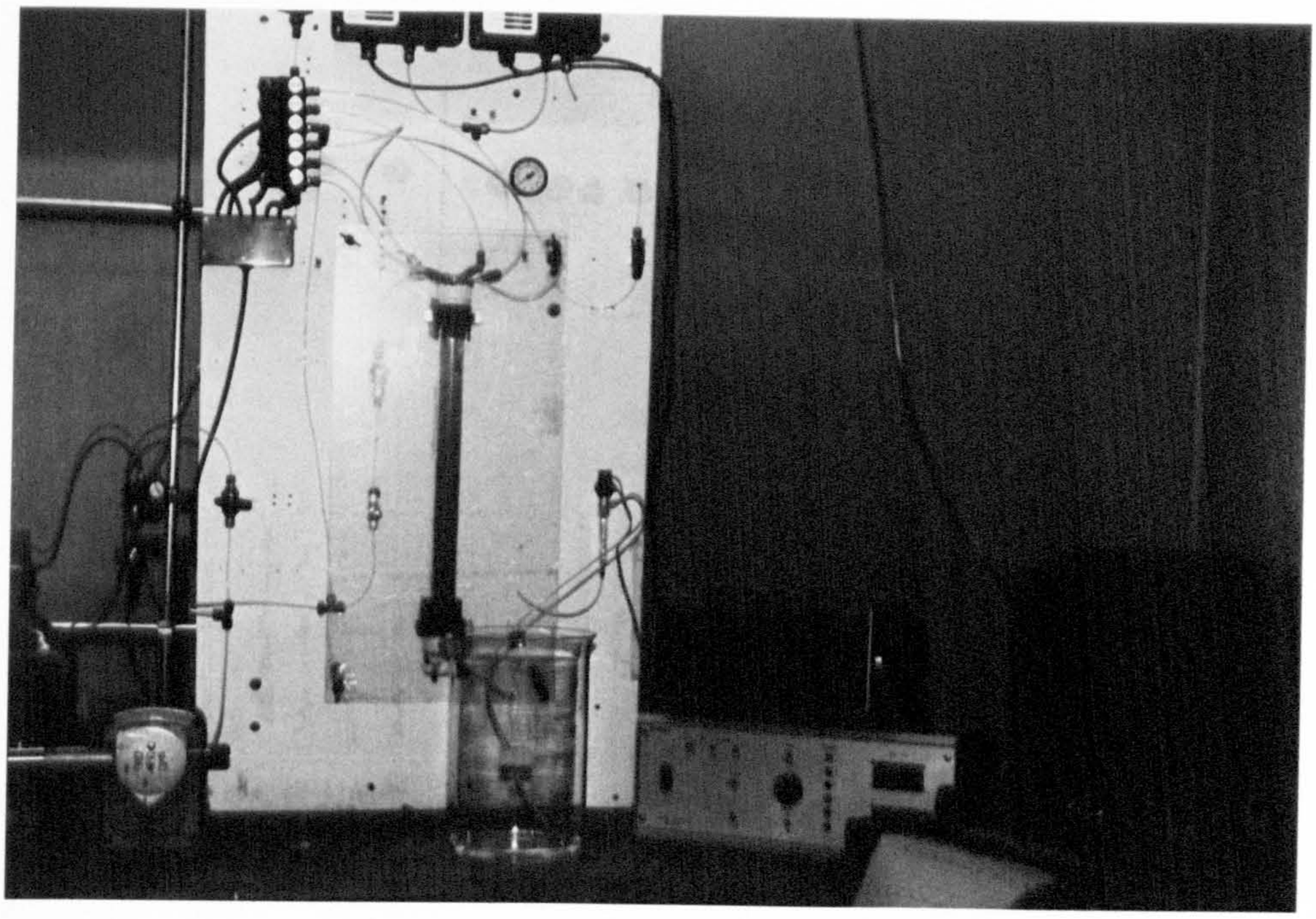

PLATE 4 CONSTANT RATE SANDPACK FLOODING RIG

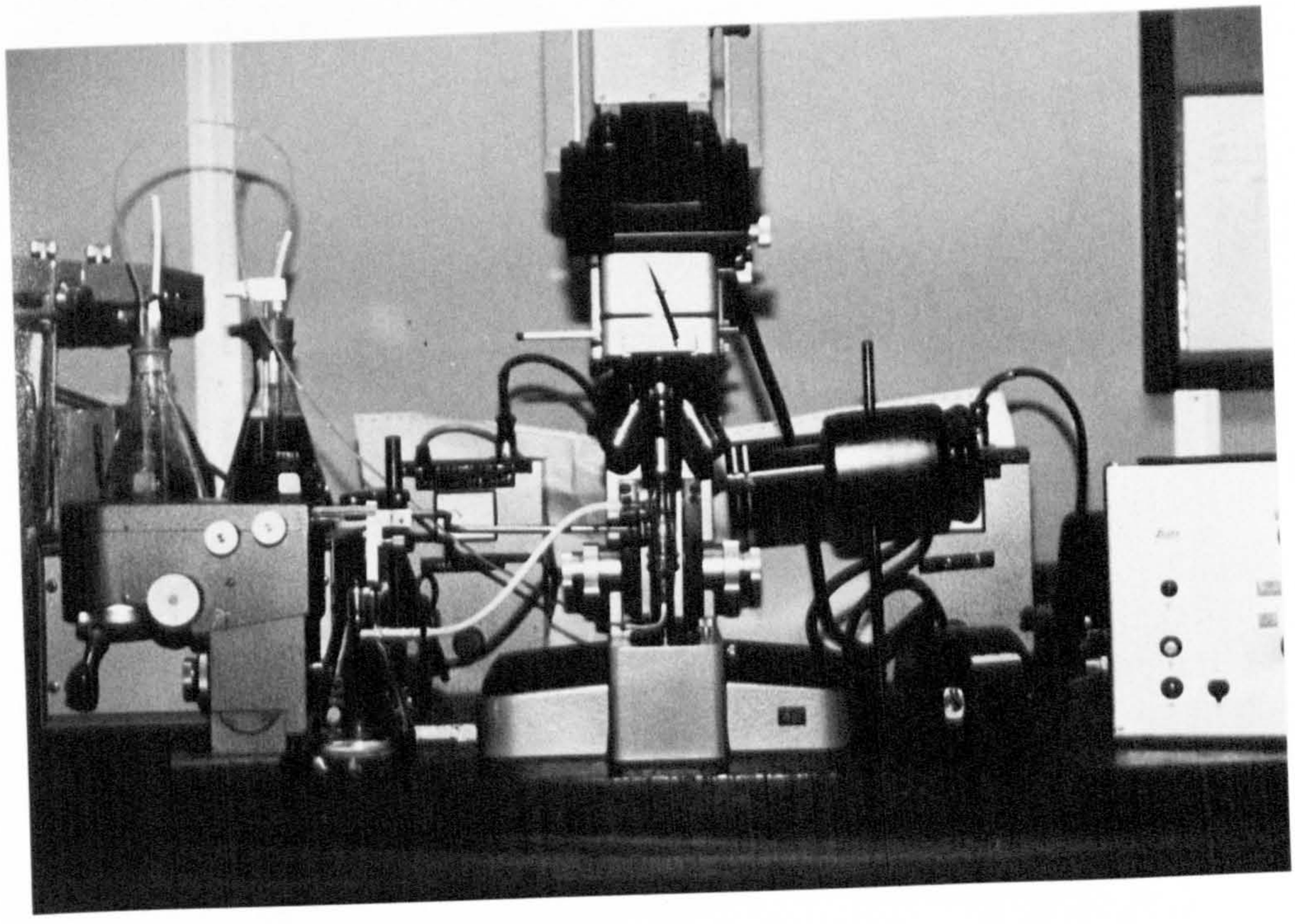

PLATE 5 THE FLOW CELL APPARATUS

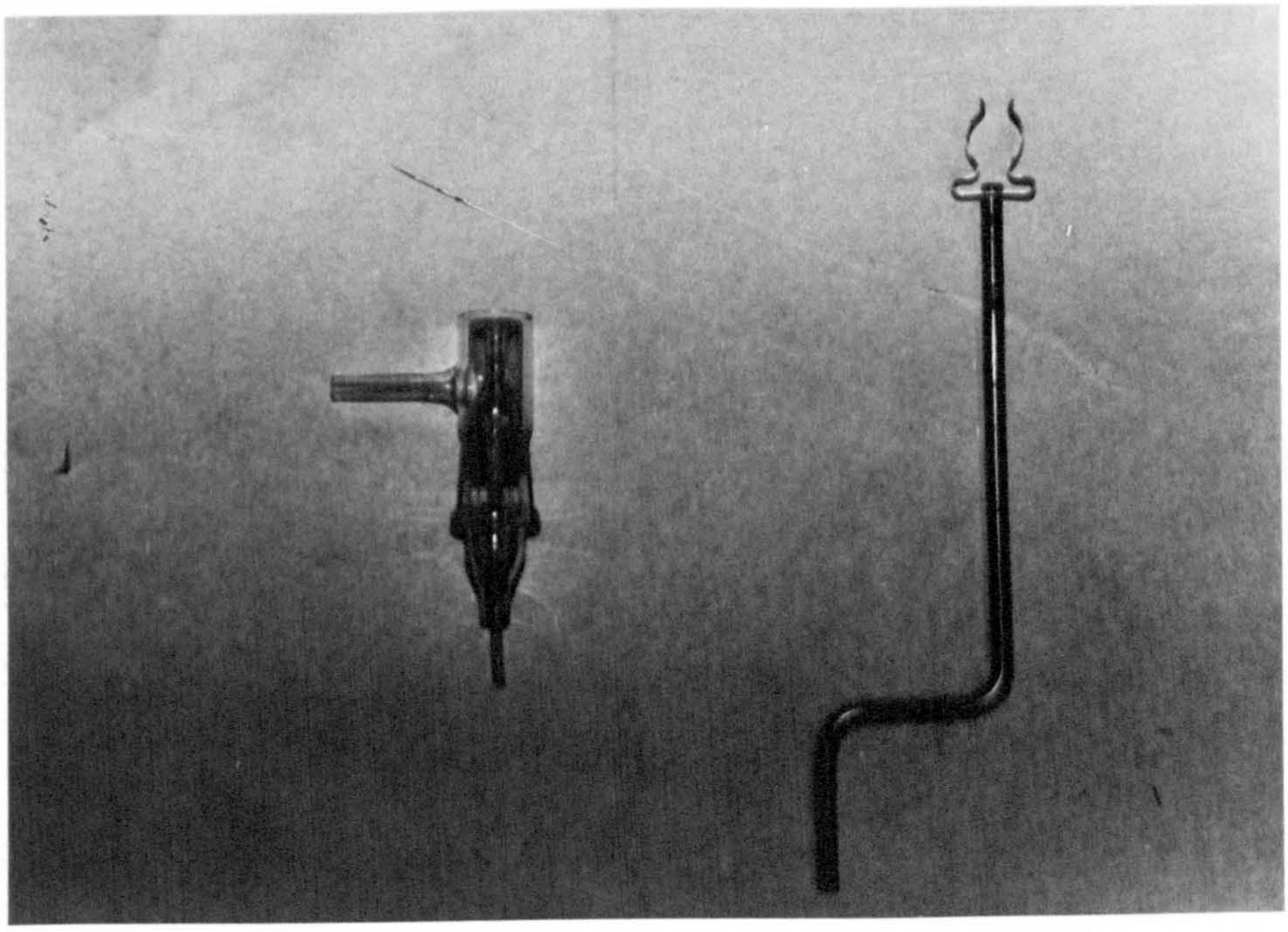

PLATE 6 THE FLOW CELL AND FIXING ARM

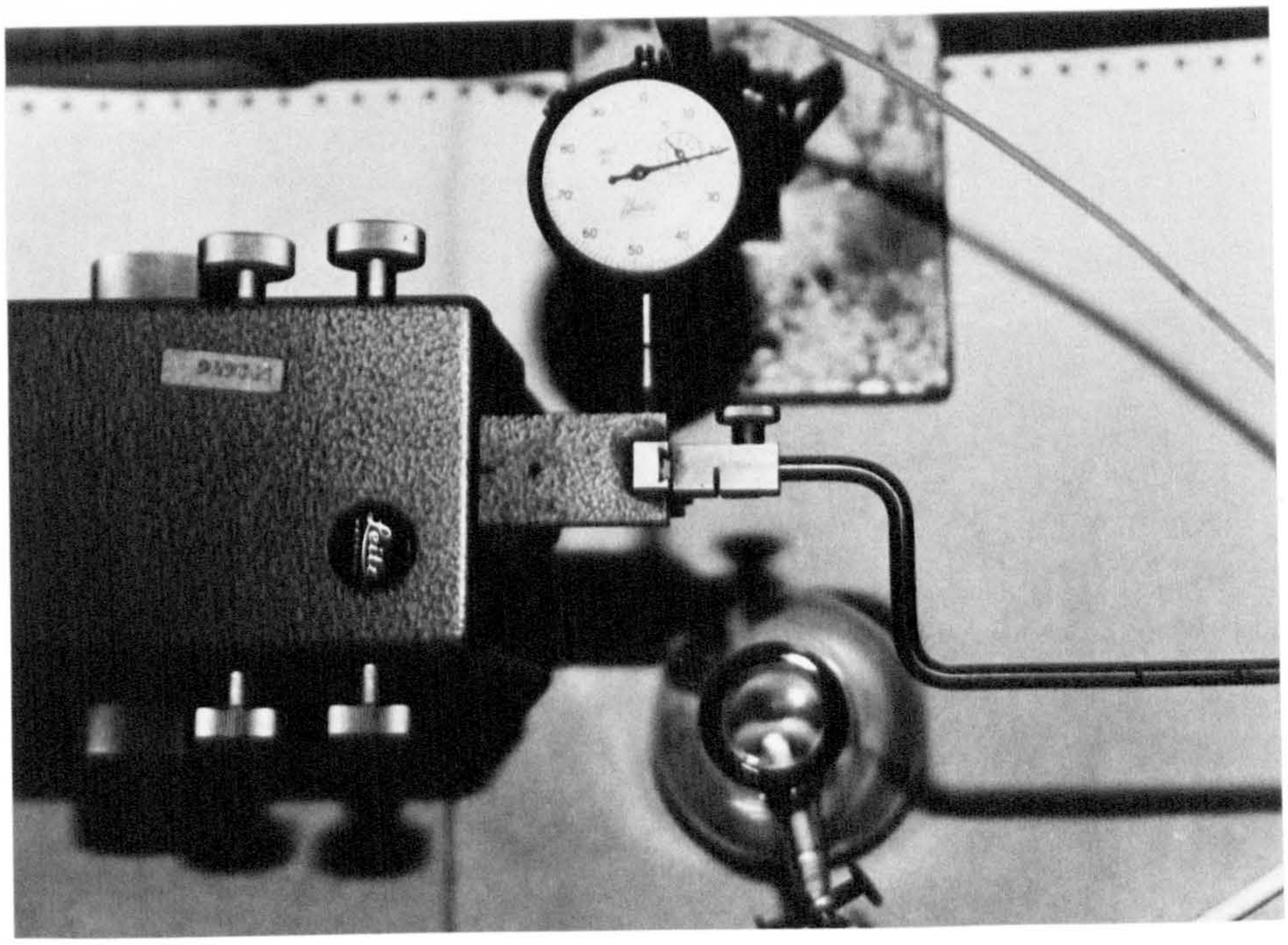

PLATE 7 MICROMANIPULATOR

CHAPTER 5

RESULTS AND INTERPRETATION

5.1 PRELIMINARY WORK

5.1.1 Reservoir Core Flooding

The permeability profile of a 1" x 1" (length x diameter) core from a suspected water sensitive North Sea reservoir is shown in Figure 14. The flood liquids were toluene, methanol, a simulated brine of similar composition to the reservoir brine and distilled deionised water. The test, as outlined in Section 4.2 forms one of the standard formation damage evaluation tests in industry.

The initial brine permeability of the core was 9 millidarcy (md) indicating that its source was a 'tight' formation. Flow of toluene caused oil to be extracted from the core but had little effect on the permeability. Drastic permeability reduction occurred when methanol displaced toluene. Methanol is used as a 'spacer' solvent because it is soluble in both brine and toluene. Permeability fell to less than 5 md, a 45% reduction. There was no release of fine material from the core at this stage. With brine flow, permeability recovered to just under 9 md. With water flow, spontaneous permeability loss to 1.1 md occurred. Core effluent became visibly cloudy, indicating the release of fine particles by the core. Permeability was partially recovered on the first flow reversal. The second reversal resulted in a very small increase in permeability. The final permeability was about 25% of initial value. This pattern of behaviour is typical of fines-plugging related permeability loss. The flood also highlighted problems with solvent treatment of core samples particularly with treatment with methanol which may have hydrated any clays present.

5.1.2 Constant Head Floods

Figures 15(a) and 16(b) present the permeability profiles of sandpacks subjected to constant-head floods using sodium chloride and calcium chloride brines, respectively. These runs confirmed the existence in sandpacks of permeability loss through fines migration, similar to the observed behaviour of reservoir cores under water-shock conditions. By comparing these results with core-flood results in Figure 14 it is apparent that permeability reduction is far more severe in the water shocked cores than in sandpacks. The magnitude of damage appears to be related to the initial permeability level. It is reasonable to expect a lower level of permeability loss in a sandpack flood, since they possess permeability which are roughly an order of magnitude higher than cores. Also, in a core the straining effect is much greater due to finer pores. Figure 15 shows that the permeability was drastically reduced for the sodium chloride flood. Core effluent was very concentrated in its fines content, a marked difference with the core flood where effluent was observed to be cloudy. This is further supporting evidence of the effect of straining in permeability loss in core floods.

Permeability can be seen to have increased marginally in Figure 17 during the flow of a surfactant solution (1% v/v). Fines were eluted from the bed earlier than in the water, in fact, after only one pore volume of flow.

Figures 18 and 19 show the effect of acid and alkaline conditions on a sandpack under constant head flooding conditions. In the acid flood, there was no significant change in permeability. A small increase in eluted fines did appear in the final distilled water phase. A moderate decrease in permeability occurred with flow of 0.01M NaOH solution.

This was coincident with a gradual increase in fines released from the bed. Permeability at the end of run was slightly reduced in the case of the alkaline flood. In the case of the acid flood, permeability was largely unchanged.

The difficulty in the operation of the constant head system necessitated the design and construction of a much more robust system. This constant-rate flooding rig was better equipped to measure the sometimes small pressure changes associated with fines movement in a sand bed.

5.2 CONSTANT-RATE SANDPACK FLOODS

5.2.1 Salinity

In Run 7 a sandpack of Forties separator sand was initially packed in distilled water and flooded with 0.5M aqueous sodium chloride at pH7. Its porosity was 30.6%.

The pressure, permeability, conductivity and effluent turbidity profiles for this flood are shown in Figures 20 (a)-(d). In these and subsequent plots, the labelled PV represents the cumulative volume of liquid pumped through the bed as a ratio of the pore volume. The pore volume for sandpacks in this work was approximately 60ml. Therefore, at a constant flooding rate of 10 ml/min, 1 PV is the equivalent of 6 minutes of flow. The pressure and permeability traces showed small changes when the brine solution displaced the initial water flood. During these stages of flow the effluent remained clear. On switching to fresh (distilled) water flow again, an immediate increase in differential pressures across the bed occurred. The conductivity trace shows that the front of water displacing brine appeared in about

six minutes (or approximately 1PV) and took a further two to three minutes to stabilise to its new value. This suggests some longitudinal mixing which was probably due to the embedded pressure microtubes. The effect of these tubes, and the column wall effect were taken into consideration in the selection of the column diameter. The column to sand grain diameter was 250. Deep bed filtration theory suggests a minimum ratio of 30.

There was an increase in effluent turbidity coincident with the appearance of water at the base of the sandpack. The maximum concentration of fines in the effluent can be seen from Figure 20 (c) to occur at water-brine front reducing sharply further upstream in the water phase. The near-vertical changes in the effluent conductivity profile was conclusive evidence of the plug-flow in the column. The final water flood was continued for approximately 10 PV, the sandpack was dismantled into five sections. Each of these analysed for its 'mobile' fines content by washing with water. The fines concentration profile in the bed is shown in Figure 20 (d). It is apparent that each section of the bed retained roughly similar quantities of fines.

Permeability changes in producing reservoirs can also occur due to changing salinity when displacing formation water to with seawater. This is common practice for maintenance of a reservoir's pressure when insufficient formation water is available. Run 8 attempted to reproduce this effect by using sodium chloride solutions of 1M, 0.5 and 0.17M concentration. In sequence the results shown in Figure 21 show that small increases in permeability occur as the salt concentration is lowered in each flooding stage. The increase in permeability was more marked in going from 1 M NaCl to 0.5M NaCl brine than in the 0.5M-0.17M stage. However there was no evidence of any release of fines during the brine flow stages.

One of the reasons for testing high concentration brine was to determine the magnitude of brine concentration or valency of ions was important in the clay release process. The fact that fines were released in Run 8 showed that high concentrations of monovalent brines did not protect the sandpack from fines release and its detrimental effects if low salinity fluids were contacted with the bed at a later stage.

The results of Coulter particle size analyses on effluent fine materials, presented in Figure 52 showed 97% of the fines to be <1.58 micron diameter on the basis of number concentration (58% wt basis due to probable presence of some large fines clusters or small quartz grains). This fact, and composition analysis of effluent fines (Table 7) leads to the conclusion that it is mainly the small illinite and kaolinite fines which are released. It appears that other fine materials such as quartz, mica and illite are also affected to some degree, although it is probable that these are intermixed with the kaolinite fraction and are dispersed only when the 'binding' clays are released. The probable mechanism of release is fully discussed in Chapter 6.

Run 9 was conducted on the basis of the results of flocculation value tests as interpreted in Section 5.1.3. The results of the flood are presented in Figures 22(a)-(c). Aqueous sodium chloride brines of 0.17M, 0.057M and 0.02M concentrations were prepared and sequentially pumped through a sandpack followed by water. As shown in the permeability profiles, there was no evidence of permeability decline on switching from 0.057M brine to the 0.02M brine. Permeability did not decrease even when water was introduced as observed in earlier runs. However there was a small but quite characteristic increase in

effluent clays when the change between the 0.057M and 0.02M brines was made. This is clearly seen from the logarithm plot of the effluent clay concentration as shown in Figure 22(d). This is an indication that some fines dispersal does occur, although the amount of fines released was sufficiently small not to have an effect on the permeability of the sandpack.

The effect of an intermediate brine strength (0.17M Na Cl) was investigated in Run 10. This brine was displaced with fresh (distilled) water. The resultant permeability and effluent solids profiles are presented in Figures 23(a)-(c). It can be seen from these plots that the permeability of the sandpack decreased temporarily when water was introduced. However the magnitude of the decrease was small. In fact the permeability recovered its initial value in a few pore volumes. Again, as with Run 9, there was some fines release as a result of the brine-water switch.

These experiments showed that it was likely that a critical minimum salinity was required to keep fines in their natural flocculated states. The observed response of the sandpack in Runs 9 and 10 led to experiments in which the effect of continuously decreasing salinity on permeability was investigated. Figures 28(a)-(c) show the effect of a flood where salinity is decreased at very high (half-life = 5 minutes) and comparatively low (half-life = 20 min) rates, respectively. In both cases the permeability was found to decrease when the salinity (NaCl) fell below 0.08M. At the higher rate of salinity decrease the final end of run permeability was slightly lower. This indicates that the rate of decrease in salinity across the critical salinity is an important factor in determining the magnitude of shock damage. A similar experiment with a Fine-Grey sand bed showed the critical salinity level was in the region of 0.1M (Figures 28(d)-(e)).

Runs 11-14 examined the effect of the length of time that a brine remained in contact with the sandpack on the severity of a fresh water shock. Figures 24-27 show the results obtained for contact times from 60 minutes (10 PV) to 2 minutes (0.3 PV). In each case a 0.5M aqueous sodium chloride brine at pH = 7.0 was used as the brine stage.

In these experiments the maximum permeability reduction was in the region of 30% in all cases except for the case where the brine flood was shortest (0.3 PV). In this case the peak permeability reduction was about 20% although permanent damage, as measured by end of run permeability, was comparatively higher. Permanent damage amounted to 10-12%. The amount of fines mobilised increased with contact time of the brine although Figures 26-27 provide evidence that a threshold turbidity value exists. Thus it is apparent that the length of time that a monovalent 'sensitising' brine is in contact with the sandpack materials does not affect the severity of the permeability damage occurring on subsequent fresh water contact. Even very short contact times can have severe effects on permeability.

5.2.2 Effect of Potassium Chloride

Figures 30(a)-(c) show the effect of a water shock experiment conducted with a 0.4M potassium chloride sensitising brine. Permeability and the effluent turbidity profiles display the characteristic spontaneous permeability reduction coincident with the appearance of fines in the effluent. Analysis of the particulate material produced confirmed the presence of both kaolinite and illite clays in the produced effluent, (Table 7). The level of permeability reduction was of similar magnitude to that obtained with the sodium chloride sensitisation runs, though the amount of fines was noticeably smaller than in the shock experiments using sodium chloride.

Figure 29 shows the average bed permeability profile for a decreasing salinity flood with an initial 0.1M potassium chloride solution. Permeability damage is prevented until the inlet salinity falls below 0.05M KCl. This compares with the 0.11M minimum level of salinity required with a sodium chloride brine. This is an indication that a lower concentration of potassium chloride may be required for shock prevention, compared with sodium chloride.

5.2.3 Effect of Ion Valency

5.2.3.1 Pretreatment with Divalent Ions

Figure 31(a)-(c) illustrates the effect of pretreating a sandpack with a calcium chloride solution before introducing a sensitising sodium chloride brine.

The profile shows that permeability during the flow of calcium chloride decreased slightly compared to the initial distilled water flow. In the final stage of the flood when water flow was expected to reduce bed permeability only very small changes were observed. Some fines were produced but their low concentration indicated that mobilisation had been significantly reduced.

Analysis of produced fines by the SEM-EDX ion-mapping technique and Atomic Absorption Spectroscopy described later in this Chapter indicated that calcium ions remained on the clay particle surfaces (Plates 17 and 18).

5.2.3.2 Post-treatment with a Divalent Ion Solution

The permeability response of an already 'sensitised' sandpack to treatment with calcium chloride solution and distilled water is shown in Figure 32. Minor permeability damage was noted during the final

stage of water flow, the level of which was slightly greater than in the pre-treatment experiment. On the basis of these observations, pretreatment would appear to be a more effective practice at permeability damage prevention since the fines sensitisation process is prevented.

5.2.3.3 Treatment with Mixed-ion Solution

Simulated formation waters contain mixtures of ionic species in prescribed quantities. The composition of the simulated brine used is given in Table 12. The flood represented in Figure 33 consisted of the flow of mixed brines of 10% and 3% equivalent NaCl concentration, respectively, preceded and completed by stages of distilled water flow. Permeability increased slightly on flow of the lower concentration brine. The flow of water in the final stage had little effect on permeability with a virtually fines-free effluent being produced.

5.2.4 Effect of pH

The profiles of sandpack permeability and effluent fines concentration presented in Figure 34-37 show the effect of experiments where the pH of flooding liquids was varied. Separate runs were carried out using firstly, distilled water as flood liquid and secondly 0.5M NaCl in order to determine the combined effect of pH and salinity on the response of the sandpack. The pH of these fluids was adjusted with careful addition of molar sodium hydroxide and hydrochloric acids.

On reduction to pH = 5 a small increase of permeability occurred (Figure 34(a)-(b). A small amount of fine material was observed in the effluent when neutral water was re-introduced. Some difference in the fines profile was noted with that obtained during water shock

tests which increased rapidly after a brine-water flow switch was made. The return to neutral pH brought a further small decrease in permeability coincident with an increased concentration of effluent fines. The final permeability was about 95% of the initial water permeability.

A step increase to pH=9 (Figures 35(a)-(b) reduced permeability gradually. This was co-incident with a rise in produced fines. After 5 PV under high pH conditions the bed permeability stabilised at a lower steady state. The re-introduction of water caused the production of further fines in the effluent and a small decrease in permeability.

In Run 23, water was displaced by a 0.5M sodium chloride brine at pH 5. Run 24 repeated the same flood but with brine at pH 9. In both runs, water was re-introduced to the pack after approximately 5 PV of brine flow. The sandpack permeability and effluent fines profiles are shown in Figures 36-37. Figure 36a shows that permeability damage due to monovalent brine at neutral pH is moderated when brine at low pH is used. Damage due to brine at pH 9 (Figure 37a) is also less severe than expected although a significant amount of fines were produced (Figure 37b)

5.2.5 Effect of Clay Concentration

Figures 42-43 show the effect of injecting sandpacks with clay suspensions of increasing concentrations according to the procedures described in Chapter 4. Figures 42(a)-(b) show the effect on bed permeability of the filtration of clay suspensions of 1g/l and 10g/l concentration, respectively.

The filtration of low concentrations (1 g/l) of clay suspension had an insignificant effect whilst with 10g/l suspensions of measurable drop in permeability was observed. The deposition of clay from 0.01M sodium chloride suspensions resulted in greater permeability loss. Figures 43 (a)-(b) show that in natural sandpacks (i.e. one where fines had not been artificially removed) permeability decrease was higher than in the 'cleaned-sand' beds.

5.2.6 Effect of Flowrate

Figure 38 shows the effect of step increases in flowrate of distilled water on the pressure differential in a freshly packed sand bed. The regimes of laminar and turbulent flow can be observed in the pressure drop-flowrate characteristic. The constant permeability laminar flow regime was used in all floods so that the D'Arcy equation for porous media flow could be applied. High flowrates did not bring about spontaneous fines release in sandpacks.

This was evidence in support of the 'chemical' model of formation damage theories which propose that some chemical interaction between fluids and reservoir rock materials is necessary for clay mobilisation to occur.

Figure 39 displays the effect of a range of flowrates on beds in which fines mobilisation was induced. Higher flowrates caused severe plugging in the bed, activating the pump trip switch set at 3 barg inlet pressure. The permeability profiles show that once fines have been mobilised, the extent of damage caused is directly related to the flowrate of the flooding water. Flowrates of distilled water lower than the flowrate of sensitising brine are beneficial to the recovery of permeability.

5.2.7 Effect of Reverse Flow

In Run 27, a bed in which fines were mobilised was inverted and original brine flow continued in the reverse direction in an attempt to limit the effects of the migrating fines front on the permeability.

Figure 40 shows the resultant permeability profile. It is clear from this profile that the decline in permeability is arrested. On introduction of brine permeability increased fell initially until the fines concentration in the bed effluent had peaked again. At this point, bed permeability recovered. However the final permeability was still lower than the initial water permeability. The interpretation which may be put forward here is that in the reverse flow stage where a brine flood is displacing a distilled water phase, fines mobilised by the water 'shock' were redeposited in the bed. This is probably due to the flocculation of mobilised fines at the brine-water front. It should be pointed out here that the design of the column and the bed paving process ensured that no rearrangement of the bed had occurred during the bed inversion in the middle of the experiment.

5.2.8 Effect of Gravity

In Figure 41 the response of a sandpack to a water sensitivity test in the upflow mode is shown. Comparing the permeability profile with that obtained in earlier runs conducted in the downflow mode reveals some marked differences in sandpack behaviour.

Permeability loss was found to be lower than with water sensitivity tests at the same conditions for downflow experiments. However fines eluted from the top of the bed were at a much lower concentration than in the downflow case. This leads to the conclusion that, either fewer fines are released in upflow floods or that more fines are retained in

the bed. The latter explanation is the more likely. Analysis of the suspended solids in downflow runs showed that only about 20-30% of fines mobilised by water shock were eluted from the base of the bed. The rest were retained within the bed by straining or deposition effects. It appears likely that in upward flow water shock tests, more particles are retained by the bed after they have been mobilised. This is reflected in the higher permeability loss observed. Increased deposition in upward flow through filters has been observed by Ison and Ives [117]. They found that a larger number of particles deposited on the downstream surfaces of glass spheres, in packed bed experiments. Thus the gravity effect does contribute significantly to the deposition process could be expected to be significantly reduced.

5.3 THE FLOW CELL

5.3.1 Deposition of Latex

Spherical polystyrene latex particles 0.8 micron in diameter were deposited onto treated silica discs from distilled water and weak electrolyte suspensions. Latex was used as a preliminary material to observe the hydrodynamics of the cell and the capabilities of the optical microscope for counting of deposited particles. Figure 44 shows the latex particle deposit in the stagnation point region and radially across the disc surface. The deposition from distilled water suspensions was extremely low, increasing markedly as the ionic concentration of the suspension was increased.

The amount of deposition varied from 2 particles per 10^4 sq. microns when deposition was carried out in distilled water to over 10 particles/10^4 sq. microns when deposition was carried out in 0.1 molar sodium chloride. The region of constant deposition extended a minimum of 0.2 mm on either side of the stagnation point. Progressing radially outwards deposition was observed to decrease gradually. The runs with latex confirmed that the cell could be used for the study of particle deposition phenomena. However, latex is unsuitable as a material for use in clay deposition studies as it does not possess the irregular particle shape and surface charge properties of clay particles. In order to accurately model the clay-silica interaction it was important to use actual clay materials.

The pattern of deposition on the collector surface, the silica coverslip, was characteristic for all deposition experiments. At the stagnation point the coating density was generally constant. Consistent with theoretical predictions [98], this was a circular

region on the deposition surface with a radius of 20-25% of the feed suspension inlet tube radius. This was the region in which deposition under laminar flow and true stagnation point conditions was measured. Progressing radially outwards from the stagnation point deposition was generally slightly lower. At high Reynolds numbers (>20) deposition on the stagnation point region was extremely high and irregular, with the formation of large particle clusters or dendrites. This is in line with theoretical predictions which show the origin of inertial forces as the Reynolds Number rises to 30. The thickness of the hydrodynamic boundary layer, constant under laminar flow (Re < 20), is reduced, with a consequently increased rate of mass transfer. The Reynolds Number was calculated on the basis of the dimensions of the suspension feed inlet tube.

The silica collector discs were treated with acid in the way described in Section 4.6.2.3. This treatment produced measurable levels of deposition.

5.3.2 Effect of Disc Pre-treatment

Figures 45(a)-(b) illustrates the problems with achieving a measurable particle number deposit. The deposition of kaolin onto a non-acid treated clean, degreased silica disc was attempted. Coating densities of the order of 5 particles per 10^4 sq. microns were obtained using 0.01M sodium chloride suspensions as deposition mediums. Deposit levels increased when the silica disc was treated with the acid 'soak' method (Section 4.6.2.3). Coating densities of 30-50 particles per 10^4 sq microns could be achieved after one hour of suspension flow at a Reynolds Number of 8.8. Higher deposits in the region of 80-100 particles per 10^4 sq microns were obtained when depositing kaolinite from suspensions make up in 0.1M sodium chloride.

5.3.3 Deposition of Kaolinite

5.3.3.1 Effect of Salinity

The effect of salt concentration on the deposition rate of kaolinite can be seen from Figure 46. Sodium chloride concentrations from 10^{-3}M -10^{-1}M were used as depositing suspensions under neutral pH conditions. The deposition rate was observed to be a function of the salt concentration but independent of the time of suspension flow, except at high deposit levels (>80 particles/10^4 sq microns). At these levels, a reduction in the deposition rate was observed. It has been suggested [97,98] that this is due to 'blocking and masking' of the collector surface by already deposited particles. An alternative explanation may be that charge deficiencies on the clay-silica surfaces may be satisfied by deposited particles such that a saturation coating density is reached.

5.3.3.2 Effect of pH

Figure 47 presents the measured coating densities of kaolinite particles on silica from dilute kaolin suspensions at pH values of 5, 7 and 9 and with electrolyte (NaCl) concentrations varying from 10^{-3}M to 10^{-1}M. Laminar flow (Re = 8.8) was maintained for all runs.

Significant deposition (>50 particles/10^4 microns) occurred at pH5 for all ionic concentrations, the highest rate occurring at 0.1M NaCl. At this concentration secondary and multiple deposition occurred distorting the particle count. At 0.01M NaCl deposition was markedly reduced compared to the 0.1M NaCl deposit. Low deposition rates also occurred at electrolyte concentrations of 0.001M NaCl.

At pH7 and pH9 deposition was lower at all brine concentrations indicating that pH exerted a controlling influence over the deposition of kaolinite.

5.3.3.3 Deposition Flow Rate

The deposition characteristic of kaolinite particles on silica surfaces from distilled water and sodium chloride is shown in Figure 48. It can be seen that at very low Reynolds Numbers (<5), deposition is minimal for distilled water deposition. Increase in Reynolds Number resulted in a gradual increase in deposition. At a salinity level of 0.01M sodium chloride deposition was slightly higher than the distilled water case. Under the high salinity and Reynolds Numbers deposition was heavy and non-uniform. Heavy deposition can be seen in Plate 11 with the tendency towards the formation of dendrites and multiple deposits ("clusters") clearly illustrated under these conditions.

5.3.3.4 Effect of Suspension Concentration

Figure 49 shows the effect of clay concentration on coating density. Kaolin-distilled water suspensions of 10^7, 5×10^7 and 10^8 particles per cm^3 were passed through the cell for 1 hour at pH7. It can be seen that higher clay concentrations increase deposit density, particularly at 0.1M salt concentrations. At 10^{-3}M and 10^{-2}M salt strengths, surface coverage was considerably lower.

5.3.4 Detachment of Kaolinite

The conditions under which deposited kaolinite particles could be removed were determined. Detachment was measured by a comparison of the particle coating densities after a removal experiment, with the initial deposit. A uniform initial particle deposit of approximately

50 particles per 10^4 micron was obtained with a 100 ppm kaolin suspension in 10^{-2}M NaCl, at pH7 and at a Reynolds Number = 8.8 (5 ml/min).

5.3.4.1 Effect of Salinity

Figures 50(a)-(b) show the results of detachment experiments with different brine solutions used in attempts to simulate sandpack flooding experiments. The plots show that particles could be removed by displacing a solution of brine (sodium, potassium and a mixed brine sodium/calcium chloride were used) with distilled water. Plates 12 and 13 illustrate a water-shock experiment conducted with a very high initial deposit, necessary to show the water shock effect clearly.

However, it may be observed that the silica surface was not completely stripped of all deposited kaolinite particles. This is also true in the case of sandpack water-shock floods where analysis showed that only a small proportion of the fine material was eluted from the bed. In the latter case, straining and particle recapture are likely reasons for such behaviour. In the case of the flow cell the strength of adhesion between particles and collector is probably the determining factor in preventing re-entrainment.

5.3.4.2 Effect of pH

In Figure 51 the effect of acid and alkaline conditions on detachment is seen. Water at pH = 5 did not bring about any significant reduction in the particle deposit. At pH = 9 detachment of kaolinite was obtained. This behaviour is similar to the observed response of sandpacks under the same flooding conditions. The presence of hydrogen ions in the acid flood condition further compresses the ionic double layer around deposited kaolinite particles thus in fact

increasing the adhesion force. The dispersing action of sodium hydroxide was also observed. Higher pH experiments were not attempted due to possible problems of silica dissolution through sodium hydroxide attack.

5.3.4.3 Effect of Flowrate

Figures 50-51 show that particles deposited from distilled water suspensions were much more tightly held on the silica surface. These particles could not be dislodged even at high flowrates (Re >50).

However, if the deposit was made from suspensions of monovalent or mixed-ion brines, particles could be removed at much lower flowrates of water. This is an illustration of the water shock effect in the flow cell system.

5.4 RESULTS OF ANALYTICAL WORK

5.4.1 Flocculation Value Tests

Table 10 presents the flocculation concentrations of natural and pure suspensions.

Trends apparent from examination of the results are the greatly decreased flocculation concentration as the valency of the ion increases. This effect is consistent with the empirical Schulze-Hardy rule which predicts the effect of counter-ion charge on suspension stability. This law states that the flocculation concentration decreases with an increase in the valency of ions in the suspension. The size of an ion can also influence flocculation values due to its direct effect on the charge density of the ion.

In Table 10 the results of flocculation salinity tests have been presented on both naturally-occurring and pure clay suspensions. The tests were conducted at pH values of 5, 7 and 9 and sodium, potassium and calcium chloride brines were used as the flocculation electrolytes. The critical sodium chloride concentration for flocculation of a dilute mixed fines suspension from Forties separator sand was in the region of 0.5M (0.3% wt) The flocculation value of the pure kaolin suspension, is much lower than in the case of natural clay suspensions. The broad size distribution of suspended material and contamination by quartz and other fines in natural clays is the probable cause of these differences.

5.4.2 Clay Analyses

The particle size distribution of fines released in water shock experiments with separator and Fine-Grey sands is presented in Figures 52-53 respectively. Figure 52 shows that virtually all the fines released were of the one micron size class. In this figure the difference between the two curves is probably due to some larger fines distorting the analysis because of their higher weight. The mineralogical composition of these fines (Table 7) shows kaolinite to be the major component.

Figure 53 shows the size difference between those fines which could be removed by ultrasonicating a sample of sand in water and those obtained by a brine-water displacement experiment in a sand pack. These fines were termed 'loose' and 'attached' fines respectively. The loose fines can be seen to possess a much wider size distribution.

The particle size distribution across a front of migrating fines is presented in Figure 54. These fines were produced from Run 11. The graph shows that smaller particles are found at the head of the front.

5.4.3 Atomic Absorption Spectroscopy

The results of ion adsorption tests are given in Table 15. In these tests, described in Section 4.7.3, clay suspensions were contacted with electrolyte solutions of various strengths. The depletion in the cation content of the electrolyte solutions was measured using this technique.

Pure kaolin was found to absorb both sodium and potassium ions in amounts which varied with the strength of the electrolyte contact. The data shows that 15 times more sodium ions were adsorbed for 0.01M sodium chloride than with a 0.001M solution. Similarly, the potassium ion adsorption was 7 times greater over the same concentration range of potassium chloride. Calcium chloride adsorption was approximately 4 fold greater. Small concentrations of sodium ions were found to exist naturally with kaolin clay. However, potassium and calcium ions were absent. These results show that kaolin has a greater affinity for potassium ions than for sodium or calcium ions.

Clays washed from Fine-Grey sand had much higher adsorption capacities than for kaolin. The affinity for sodium ions was greater than that for potassium ions, in contrast to the results for pure kaolin. Also, calcium ion adsorption was greater in the natural clay although this did not increase with electrolyte strength.

5.4.4 Electron Microscope Study

The morphology of clays and fine materials on sand grain surfaces was studied using scanning electron microscopy. Plates 1-2 show the surface of separator sand grains. Plate 3 looks at Fine-grey sand at low magnification. Clay material separated from separator and Fine-grey sands are examined in Plates 14-15 respectively. The typical hexagonal-shaped form of kaolinite platelets was found in relative abundance in the reservoir clays. Plate 16 shows evidence of a more disordered kaolinite in clay from Fine-grey sand.

The SEM-EDX(Energy Dispersive X-Ray) technique for detecting the presence of surface ions on clay surfaces provided evidence of the existence of trace quantities of potassium and calcium ions on clays from separator and Fine-grey sands. Plates 17 and 18 represent a calcium ion map of fines from a Fine-grey sand sample which was contacted with calcium chloride before being thoroughly washed with distilled water and dried for examination. A comparison of these micrographs shows that a concentration of calcium ions remains on the clay surfaces.

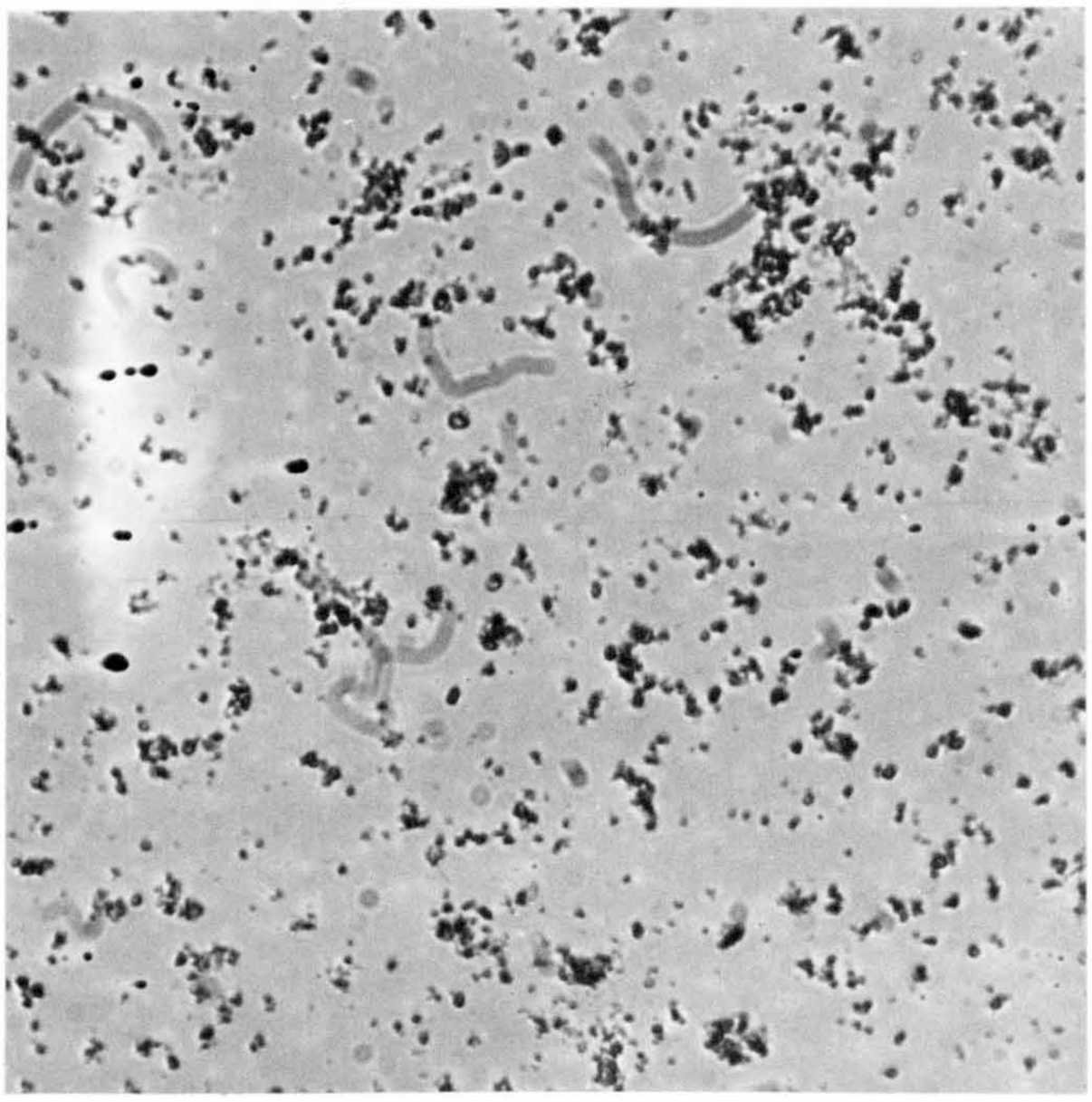

PLATE 8 DISPERSED CLAY SUSPENSION (x100)

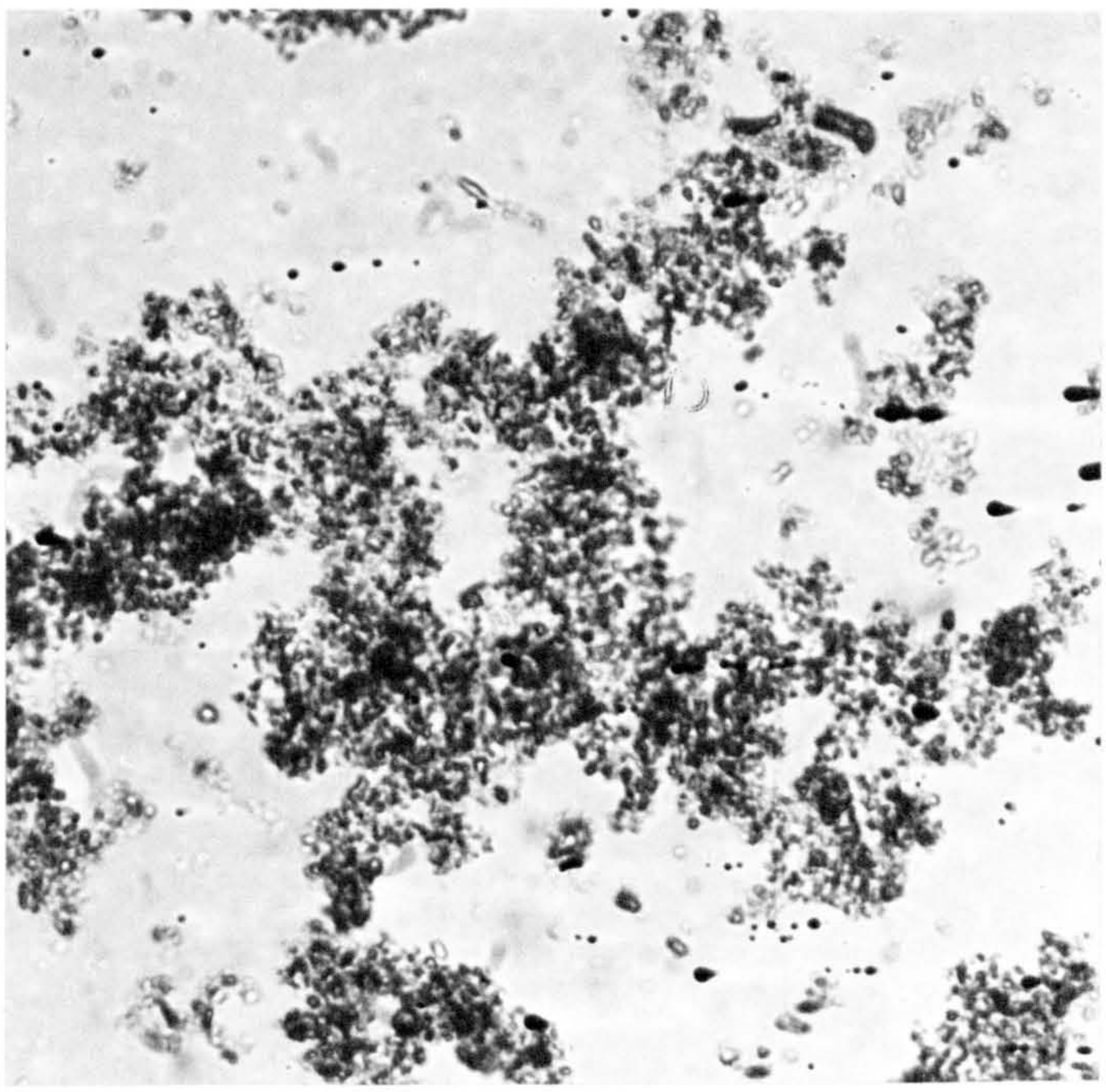

PLATE 9 FLOCCULATED CLAY SUSPENSION (x100)

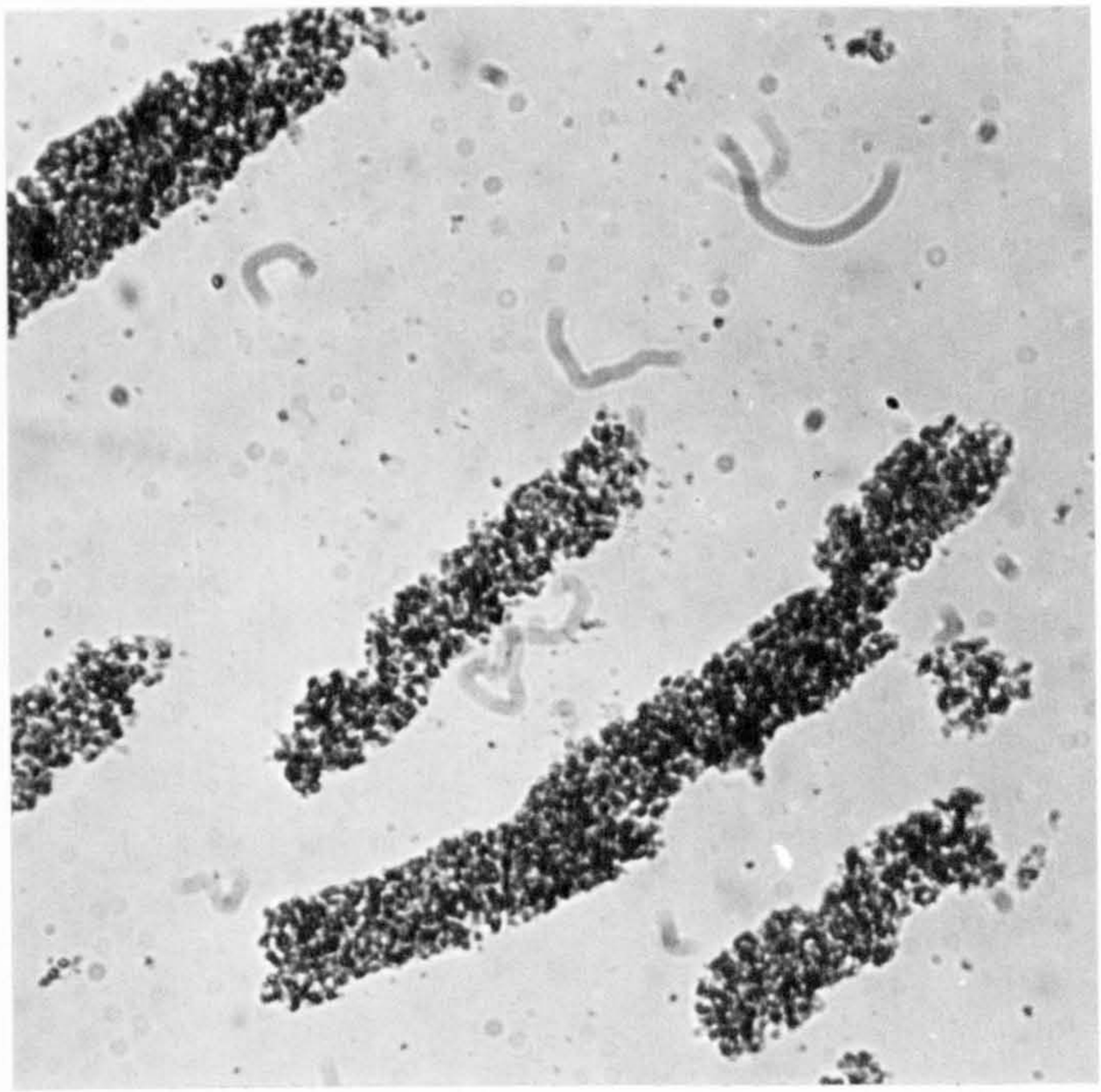

PLATE 10 CLAY FLOC STRUCTURE UNDER SHEAR (x100)

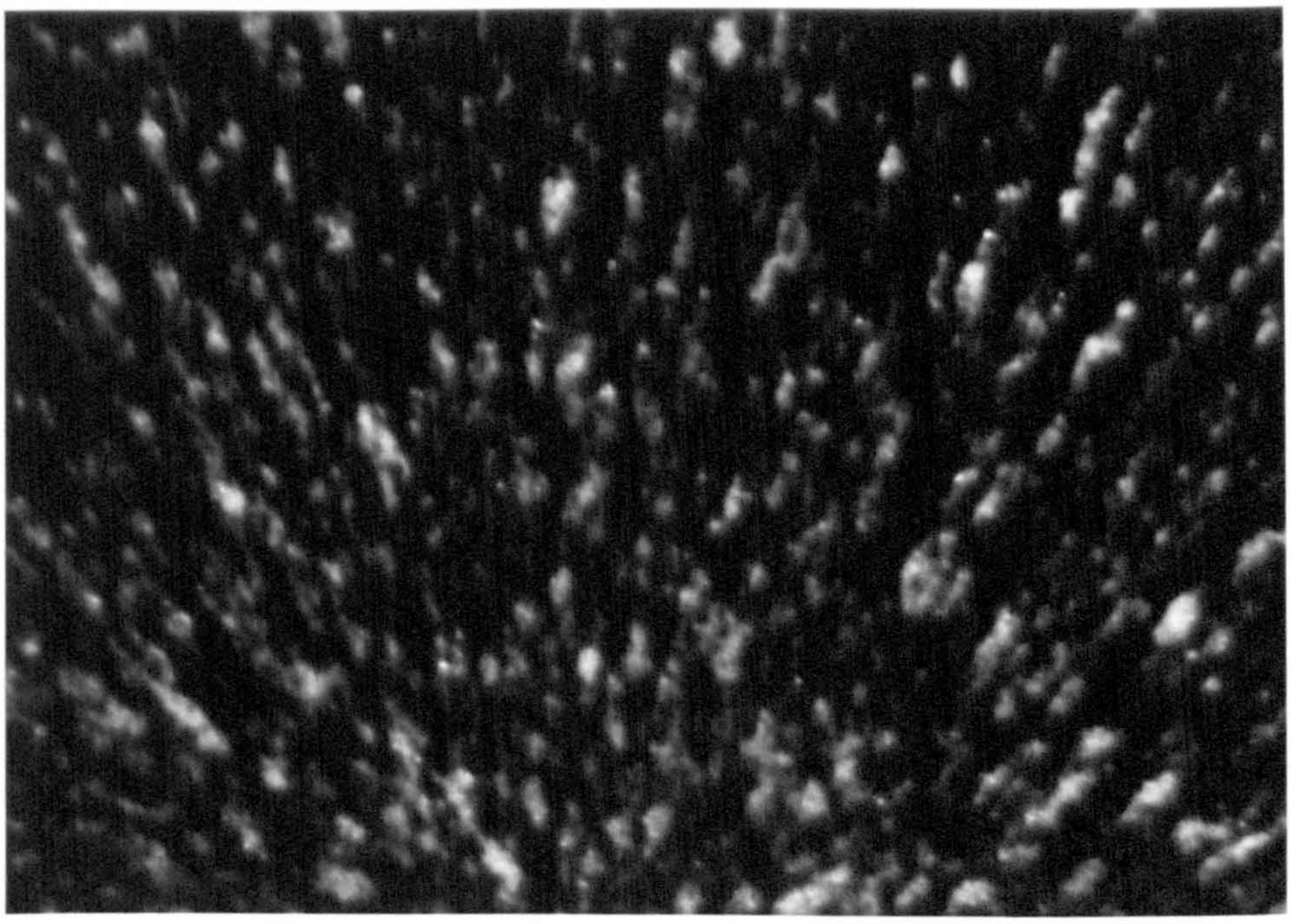

PLATE 11 TYPICAL PATTERN OF HEAVY DEPOSITION
IN FLOW CELL (x64)

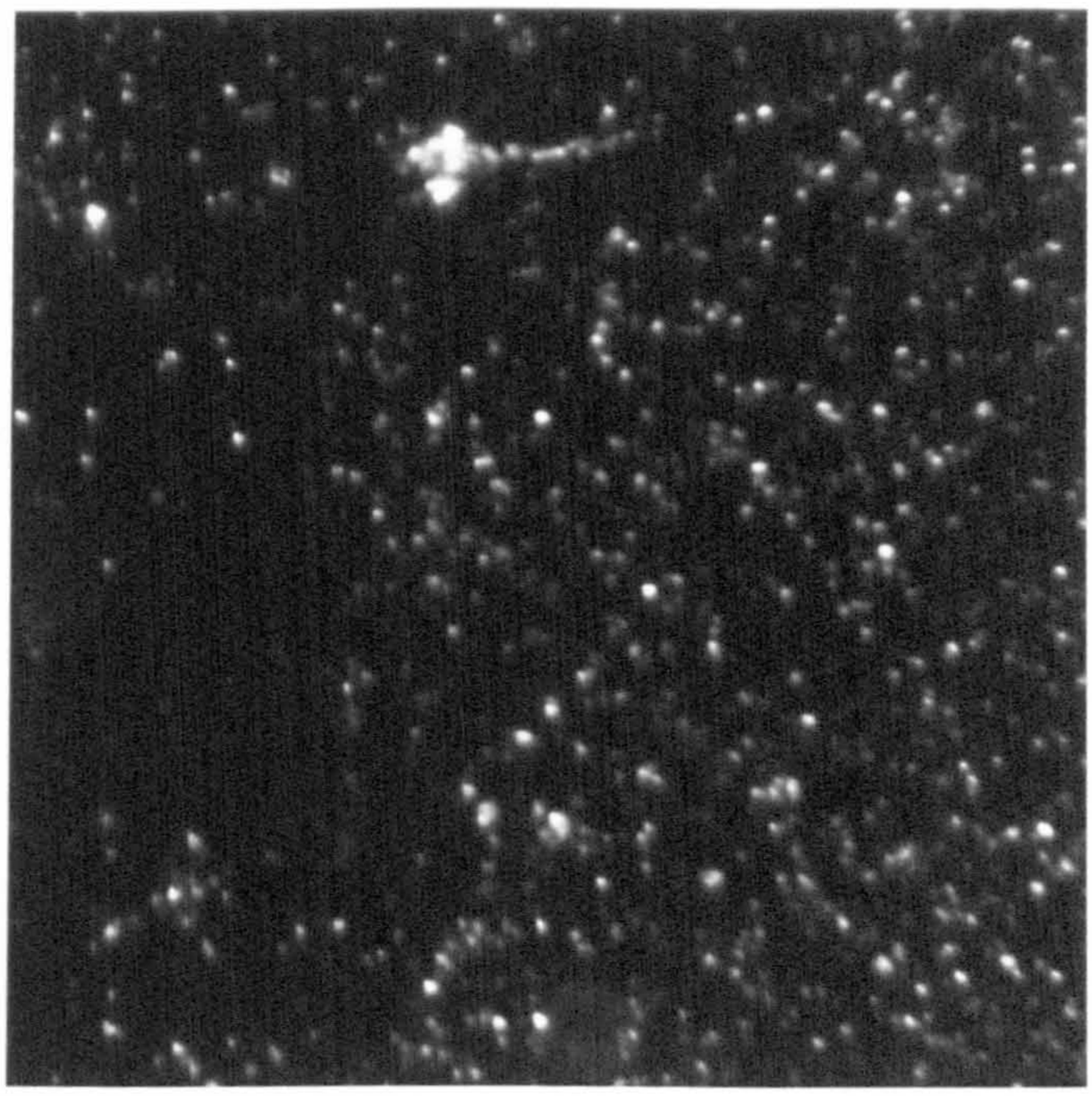

PLATE 12 KAOLINITE DEPOSIT ON SILICA BEFORE WATER SHOCK (x100)

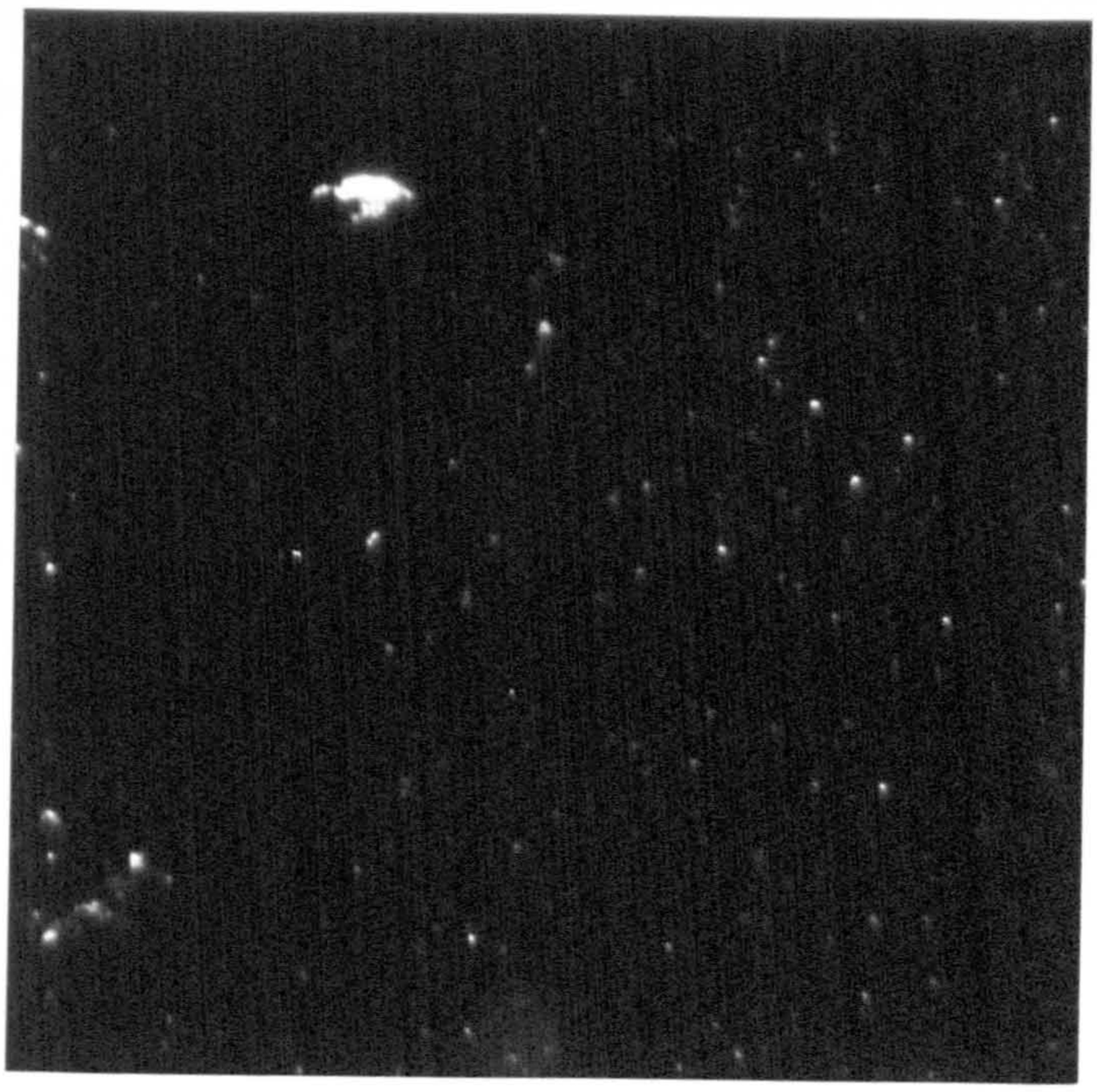

PLATE 13 KAOLINITE DEPOSIT ON SILICA AFTER WATER SHOCK (x100)

CHAPTER 6

DISCUSSION

6.1 MECHANISMS OF FORMATION DAMAGE

The permeability of a reservoir can be permanently reduced by the action of incompatible fluids and plugging solids in the well-bore region. Drilling, cementing, well completion, stimulation and production operations may cause damage due to a number of effects. These include:

a) The invasion of the well-bore by solid particles in drilling fluids.
b) The precipitation of salts and insoluble products of acid-base type reactions (e.g. iron sulphide, barium sulphate).
c) The formation of hydrates.
d) Bacterial activity(e.g. of sulphate reducing bacteria (SRB).

Formation damage may also be caused by specific fluid-clay interactions, investigated in this work. These effects can cause damage both near the production and injection wells but also deeper within a reservoir. This type of reservoir damage is evidenced by a gradual or in some cases rapid decline in permeability, and is very difficult to prevent. As reservoirs progress through maturity to depletion, water/oil ratios increase. The compatibility of flooding brines and reservoir clay takes on greater significance under these conditions. The interaction of clays and flooding liquids has been considered, with some uncertainty, to be a potential cause of the problem. Although the effects of clay damage are often reported, the

causes have been less well investigated. The effects of this type of damage are significant in terms of the amount of recoverable oil lost to production. There are, in principle, three proposed mechanisms of clay related damage as follows:-

e) The effect of swelling clay in reducing the available pore space.

f) The dispersion of adventitious particles of clay minerals and quartz resulting in plugging of the pore constrictions.

g) A combination of swelling and dispersion since both mechanisms result in an increased, or potentially increased mobility of fines.

Colloidal clays are found intermixed with quartz and other fine particulate matter in the pore spaces of reservoir rock. The forces holding these clays to the pore walls in their agglomerated state largely depend on the depositional history of the reservoir. Both mechanical and electrochemical forces contribute to the equilibrium which exists between clays, the pore surfaces and connate fluids. Clays may exist as well-impacted materials in the pore constrictions and voids or as a loosely distributed agglomerated mass in the pore space.

The experimental work has shown that for single phase experiments with sandpacks, hydrodynamic forces are unable to entrain the intergranular materials. This has also been shown for two phase core flooding tests [41] where the wettability of fines is a factor. Average flood velocities in a reservoir are of the order of a few metres per day. In producing oil reservoirs the region around the well-bore may however be susceptible to damage by solids deposition and pore-plugging through the action of the high fluid velocities. High velocities lead

to the formation of low permeability cake-type deposits. In experiments in this work, flood velocities in the range from 7-75 m/day were unable to bring about any release of already adhered particles. A second exception to the general rule that fluid forces do not play a major role in the mobile fines problem is when the fines in a formation may already exist in a semi-stable or 'sensitised' state. This condition may be difficult to detect from a study of field data. In this state any change in the hydrodynamic conditions in the reservoir is likely to affect the state of equilibrium which exists.

Formation damage can also be caused by clay swelling as opposed to clay migration effects. However there are characteristic differences in the way in which permeability changes occur in each mechanism. In the case of swelling of clays, permeability decreases when the salinity of pore fluids drops below some critical value or if fresh water is introduced. An indirect result of the swelling process is that fine material may yet become dispersed. This gives rise to combined swelling-pore plugging. Swelling clay has not been considered to be a major problem in the Forties North Sea sandstone. Consequently, the investigation was designed to preclude its effects. Both separator and Fine-grey sands, used in the the experimental work contained insignificantly small amounts of the swelling clays. Permeability loss caused by the release, migration and pore-plugging action of fines occurs initially at a faster rate. Secondly, in core-floods, a reversal of flood direction results in a temporary increase in permeability before the rapid decrease typical of pore plugging behaviour occurs (Figure 14). This has also been shown, in this work, to hold true for conditions in sandpacks (Figure 40).

6.2 EFFECT OF SALINITY CHANGE

Spontaneous permeability loss effects have been observed when fresh water displaces monovalent brines in sandpacks. The permeability reduction is coincident with the release of large quantities of clay from grain surfaces. Analysis showed that kaolinite formed approximately ninety percent of these fines. Typical permeability profiles, Figures 20 and 24 show that there are two aspects to the observed effects. On water flow, an immediate effect on bed permeability occurred, with a decrease to approximately 60-70% of brine permeability. There followed a period of recovery which occurred at the same time as the fine clay material was eluted from the bed. The final permeability was about 70-90% of initial. It is evident that fines advancing through the bed in a highly concentrated zone located at the brine-water interface have a marked though temporary effect on permeability. The more permanent reduction occurs due to the recapture of fines within the bed. These fines remain as pore-surface type deposits, decreasing the available cross-sectional area for flow. This reflected in the permanent permeability loss. The experiments with the separator and Fine-grey sands showed that these materials behaved in essentially the same way, with respect to permeability and clay mineralogy, when flooded under identical conditions.

Permeability reduction effects were minimised in experiments where flood salinity was continuously reduced. Two rates of decrease in salinity were tested. At the lower rate of salinity decrease (half life t1/2 = 3PV, measured as the time taken for the salinity to decrease by 50%), there was a small but noticeable decrease in the permeability of the sandpack when the inlet salt concentration had

fallen to less than 0.11M, for a sodium chloride flood. This was combined with a sharp increase in effluent fines production. With a higher salinity decrease rate of 1 PV the sandpack displayed similar behaviour but with a higher permeability loss caused by a much higher concentration of fines in the effluent. In both runs, the permeability loss was far less severe than earlier experiments in which the sandpack was subjected to fresh water flow after being sensitised with sodium chloride brine. An interesting observation was that flow of fresh water at the end of the slowly decreasing salinity runs did not have further drastic effect on permeability. Decreasing salinity floods with an initial potassium chloride brine showed a similar critical salinity level for permeability reduction and clay release.

The results of continuous salinity decrease tests points to the existence of a critical level of salinity of about 0.11M sodium chloride at neutral pH conditions for Fine-grey-sand packed beds. Flocculation value tests (Table 10) indicated a clay suspension flocculation concentration at about 0.057M sodium chloride for fine-grey sand clays.

With an abundance of sodium ions at the start of run conditions the naturally occurring divalent and other clay-compatible ions which 'bond' clay particles together and enable attachment to grain surfaces are largely removed from their preferred sites. The extent to which the binding ions are removed depends on the concentration of the salt solution in intimate contact with clay masses present. Most binding ions can be said to have been removed from particle surfaces when a 0.5M sodium chloride brine is contacted with a fine-grey sand bed. Reservoir core clays possess a different level of monovalent brine

salinity for this process to occur. The ion exchange properties of the clays present have a direct effect on the critical salinity level.

As the sodium ion concentration falls in the reducing salinity floods, repulsive double layer forces increase and counteract existing Van der Waals forces. A change in the total interaction potential energy of the system is effected such that the clay materials are 'partially' sensitised from a state of strong adhesion to a weaker condition. It is probable that, in electrochemical terms, clays previously in a primary energy minimum have reached an equilibrium secondary minimum condition. Studies on the mode of aggregation of clay particles have proposed that changes occur in the mode of clay-clay and clay-grain surface condition. It is well known that, for example, kaolinite platelets, adopt very specific face-face and edge-face interactions under conditions of varying ionic strength [78,80-81,85]. It is probable that the mode of flocculation and grain attachment of kaolinite and illite undergoes some change. Such changes have been difficult to observe physically in sandpack or core studies, though electron microscope studies show the existence of a number of attachment states [14]. Experimental work done in this study showed some variation in clay flocculation structure when clay suspensions were in contact with different brines. Clay flocs in contact with divalent brines were observed to possess seemingly smaller bulk volumes than those with monovalent salts. This is most likely due to stronger binding forces between clay particles when divalent ions are present.

Clays most susceptible to dispersal can be assumed to be those most accessible to the changing salinity patterns of pore fluids. These would be the discrete particles, small flocs and the outermost

particles of larger flocculated masses. It is proposed that the partial expansion of the double-layer in the continuously reducing salinity floods brings about the release of such clays which are exposed to the sensitising action of sodium ions. Residual divalent ions present in the clay mass prevent complete dispersion of all clays unless the rate of salinity decrease is infinitely high(as in fresh water displacements) when even these ions are extracted from tightly bound clays.

The reducing salinity technique appears to result in a semi-stable, transition state as regards clay water sensitivity. Increases in flow rate adversely affected permeability under these conditions. The method may offer, if properly implemented, an alternative to fresh-water injection in on-shore reservoirs. However, complete investigation of salinity and flow regimes using accurate and reliable laboratory data is essential before employing reducing salinity waterflooding.

It is proposed that during a flood, <u>both</u> the critical minimum salinity and the rate of decrease of salinity are the determining parameters for clay particle release. Either factor alone is insufficient to cause mobilisation even though clays may exist in a sensitised state. Evidence for this can be found in the results of runs where an initial 0.5M NaCl brine was replaced by a 0.17M NaCl brine in a step change. Even though the rate of salinity decrease was very high, no fines mobilisation or permeability reduction effects were observed. In floods where 0.5M NaCl and 0.17M NaCl brines were displaced with fresh water, spontaneous fines release and permeability reduction occurred. This was because in the latter runs, the salinity fell below the critical minimum level required to maintain fines in a flocculated

state. Thus even though a 0.5-0.17M NaCl step change represents a high rate of salinity decrease, permeability did not decrease. In fact permeability under flow of 0.17M NaCl was slightly higher than that under 0.5M NaCl flow. This increase in permeability is probably a result of the phenomenon of electro-osmosis [27]. This is the effect where an electrolyte or suspension of charged particles flowing through an electric field experiences a drag which is related to the concentration of the electrolyte and magnitude of the electric field.

6.3 EFFECT OF pH

The pH of flooding liquids is an important factor in the clay mobilisation process. Extreme conditions of pH are also known to cause matrix dissolution effects [8,34]. Because of their plate-like structure and high surface sensitivity, clays in oil reservoirs play a significant role in all stages of production.

As can be seen in Plates 14-15, kaolinite particles are hexagonal shaped plates from sub-micron to a few microns in their major dimensions. The thickness of each plate is usually less than 0.1 micron [26,78]. A kaolinite card-pack may be composed of tens of plates held together by strong Van der Waals forces operating when the electrolyte concentration and pH are high. Under neutral pH conditions kaolinite particles and clays in general are negatively charged. Low pH conditions favour the binding of potential determining hydrogen ions at the edges. This imparts a net positive charge to some clay particles causing edge-face attraction. Loosely associated high permeability card-house structures are formed in this manner. The transition between negative and positively charged kaolinite particles occurs between pH4 and pH5. Under alkaline and low electrolyte

conditions, kaolinite particles deflocculate into discrete particles or small groups of platelets in face-face association.

In alkaline water floods, clays previously in equilibrium with formation water undergo cation exchange in which hydrogen, calcium and magnesium ions are lost to the displacing fluids with resultant loss of alkalinity. In surfactant flooding, cation exchange results in ion transfer from the clays to the surfactant solution causing their precipitation. Surfactant and polymer solution floods are also adversely affected by their adsorption by clay surfaces.

The consumption of caustic by clays is a function of the amount and type of clay minerals, the concentration of caustic, salinity of water, temperature and contact time of the flood. The concentration of a caustic flooding solution can be significantly reduced when clays exchange binding hydrogen or calcium ions for sodium ions, thus great care should be taken in designing caustic flooding operations.

Sandpacks were damaged to varying degrees when treated with acid and alkaline solutions [34]. In this work, sandpacks suffered minor permeability reduction when treated with dilute acid and alkali liquids. It is likely that the observed permeability reduction was caused by a combination of dissolution effects and rearrangement of the clay in the sandpack. Low pH conditions favour both face-face and edge-face association. In sands containing calcite, dissolution of basic calcite materials is observed, and is a mechanism of damage when acidic conditions prevail [49].

With alkaline solutions (0.01M NaOH), significant quantities of quartz were found in the effluent. Permeability loss was more severe. These results indicate the dissolution of amorphous quartz which is usually found as intergranular cementing material. Hydroxyl ions also attacked the clay-clay agglomeration forces, causing large clay masses to break up and disperse when distilled water was introduced.

Fine grey sand exhibited hydroxide retention properties. This was observed in high pH sandpack flooding tests with a 0.5M NaCl brine adjusted to pH 9 with sodium hydroxide. Figure 35b shows the effluent pH profile. On introduction of the high pH brine, the effluent pH response was dampened for 3 PV before attaining the pH level of the influent. It appears that during this period, clays in the sandpack were actively adsorbing hydroxyl ions. Other workers have observed similar behaviour with core flooding tests although the processes of ion exchange have not been well understood [15].

It appears that when sodium ions are present, hydroxyl ions form a large part of the diffuse double layer around clay particles. They are prevented from attacking the 'acidic' silica surfaces by the already established double layer. In the case when no sodium ions are present, dissolution of the acidic parts of the sandpack matrix occurs with resulting particle dispersal.

6.4 CONTRIBUTION OF ION EXCHANGE

Ion exchange leading to weakening of interparticle and particle-surface forces is the likeliest cause of particle dispersal. Under natural reservoir conditions, clays exist as flocculated materials which are sedimented in the pore space. Flocs are held to the pore

surfaces by a combination of mechanical interaction, largely determined by the geological conditions, and the presence of a range of ions occupying specific positions on the clay surfaces. Calcium, magnesium, potassium and sodium salts are all present in appreciable quantities in connate waters and on clay surfaces in their natural state.

It is proposed that changes in the double layer around clay particles are preceded by ion exchange processes between clays and flooding fluids. The extent and nature of these processes determine the extent of double layer expansion or contraction. Calcium, magnesium and other high valence are preferentially adsorbed by kaolinite clay when they are present in mixtures of monovalent and divalent brines. Similarly potassium has been found to be associated with illite clay. These 'preferential' ions may however be removed from clay surfaces if a displacing flood medium has high concentrations of monovalent ions.

As already mentioned fine materials exist as well-impacted floc clusters due to their pressure-temperature influenced deposition history. Thus it is likely that only the outermost and therefore most accessible particles of a flocculated mass of clay are attacked by monovalent brines. Ion exchange occurs rapidly at these locations.

There is also the question as to whether it is the clay-clay forces or the clay-silica forces which are affected before the onset of dispersal. Flow cell studies showed that clay-silica forces are fairly strong compared to the clay-clay forces (Section 5.3). It is unlikely that individual clay particles are dispersed but that the forces holding flocculated clays together are disturbed. In the case of kaolinite, this means the break-up of forces holding the card-pack

aggregates. These structures then travel through the pore under fluid flow. Individual particles of kaolinite may then break off the aggregates through the action of fluid shear, particularly near the pore constrictions where high local velocity gradients exist.

The mechanism of ion exchange appears to be concentration and pH driven. The pH of flooding liquids appears to be a governing factor in the inhibition of ion exchange processes between clays and surrounding fluids. Low pH has the effect of preventing the loss of divalent ions originally on clay surfaces when monovalent ions would be expected to replace them. This is primarily due to the interaction of clay particles with hydrogen and hydroxyl ions. In the case of kaolinite, these ions are strongly adsorbed onto the edges of clay plates. This has a marked effect on the clay zeta-potentials which dictate double layer effects.

This work has shown that the critical sodium chloride concentration for ion exchange exists at a higher level than the minimum threshold salinity reported to prevent permeability reduction [34,43]. There is a critical minimum salinity for each ion type. Above this the fines remain flocculated. However there is also the fact that if monovalent ions are present they will replace any stronger ions on the clays. This explains why in Run 9 fewer fines were produced (NB: 0.3% Na = 0.056M NaCl). Simple flocculation tests (Table 10) showed the range of flocculation salinity for various fines to lie in this region.

It is conceivable and reasonable to suppose that fines which are easily accessible in the pore space would be influenced by a low sodium chloride concentration on the basis of deflocculation. This was witnessed in Run 9 when a change from 0.05M to 0.02M brine caused a

small fines release. These were the easily accessible fines responding to a decrease in salinity by their flocculation-deflocculation behaviour. Comparatively fewer fines were produced in Run 9 when compared with earlier fresh water shock floods when fines concentrations were in the region of 150 g/l. This suggests that deflocculation is not the primary cause of mobilisation although a small expansion of the double layer(evidenced by minor particle release) does in fact take place.

Results show that for reservoir separator sand the concentration of sodium ions should be at least 0.11M for ion exchange to take place. Calcium ions or divalent ions have much higher charge densities than dictated by their increased valence compared to monovalent ion. This is due to the fact that there is little difference in ionic sizes in the alkali metal ions. For example, calcium has an ionic radius almost equal to that of sodium and smaller than that of potassium (Table 2).

Thus, in order to remove a calcium ion from a clay particle complexation or preferential adsorption site, five or six times as many monovalent ions are needed in close proximity. Further the divalent ion may be of such a size that it is tightly held on an adsorption site on the particle surface or in the structure. This would explain why sodium chloride concentrations higher than the flocculation concentration would be required to remove such ions. These ions may be termed 'binding' ions as their location on clay surfaces determines the adhesion between clay particles (flocculation) or the adhesion between clays and grain surfaces. Thus the sodium ion concentration would need to be high before ion exchange can take place as proposed here.

Atomic Absorption Spectroscopy provided a means of measuring the levels of various ionic species associated with sandpack clays. The results of work done using this technique provide further evidence of the concentration dependence of ion exchange processes. Table 15 shows that the cation adsorption capacities of pure and natural kaolin materials are a strong function of the electrolyte concentration. This dependence was measured in the case of sodium, potassium and calcium chloride brines. The presence of calcium ions on clay surfaces was confirmed in SEM-EDX analysis as already described in Chapter 4. Plate 18 is a calcium ion map of agglomerated clay material as shown in Plate 17 which were obtained from Fine-grey sand.

6.5 HYDRODYNAMIC FORCES

A waterflood may advance through a formation at a rate of a few metres a day. Invariably the Reynolds number based on the superficial velocity will be very low, in the region of 0.001. In sandpack experiments in this work the Reynolds number was 0.3. Fluid shear forces are likely to be most important since values of Reynolds number less one are sufficiently low so that inertial effects are small [106,109]. However, the pore velocities will vary widely. The distribution of pore velocities will be influenced mainly by the pore size distribution. The pore velocity is an arguably better criterion for fluid force calculations especially where rock heterogeneity is known to exist.

The reservoir heterogeneity and the morphology of deposits in the pore space will affect the fluid forces experienced by their effects on the interstitial velocity. Clays in reservoir sandstone cores exist in one or a mixture of modes of association. They may be found as discrete

particles lining the pores, or as a flocculated mass in the pore space and blocking the pore throats. The clay deposits may be loosely associated 'card-house' type structures, 'card-pack' platelets weakly attached to pore walls or as rigid 'cake-type' deposits. Each of these modes and mixtures of these modes are a result of a specific ionic-chemical equilibrium between clay and the surrounding fluid. The size distribution of fines also affects the type of deposit and the rheological properties of pore fluids when mobilisation occurs. Large particles are easily trapped at pore constrictions where they increase the capture of smaller colloidal fines.

Figure 55(a) shows the hydrodynamic forces acting on a deposited particle or an assemblage of particles, assuming spherical geometry of particles and grains. A deposited particle will experience a shear force due to frictional drag from the flowing fluid.

The hydrodynamic force calculated using equation (26) is in the range 0.5-2 N/m^2 for a sandpack porosity of 0.3, an average grain size of 100 microns and typical reservoir flood velocities (approximately 1 m/day). These forces are negligible when compared with colloidal double layer and Van der Waals forces as calculated in Section 6.6.

In freshly packed water-saturated sandpacks of fine-grey sand there was virtually no increase in entrained fines in response to increases in flow rate of distilled water. After the initial peak in eluted fines, produced by the packing process, the fines concentration profile decreased to a constantly low level. Step variations in water injection flow rates in the range 2.5-25 ml/min corresponding to superficial velocities of 7-70 m/day produced very small surges of fines in the bed effluent. These surges were insignificant when

compared to the amount of fines produced in a water-shock test. Further, the lack of any measurable decline in permeability leads towards the premise that in their naturally adhered condition, in the case of fine-grey sand, clays are not mobilised by increasing the flood velocity. Investigation of wetting phenomena and oil-water interfacial effects would be required to prove conclusively that flood velocity was not a factor in 'real' reservoir floods [41].

Flooding velocity was determined to be an important factor in permeability reduction when the mobilisation of fines in the sandpack was already underway in brine-water shock floods. In this condition, permeability reduction was dependent on flood velocity. Typical results for sandpacks undergoing water-shock showed that permeability decreased abruptly when the flowrate was increased during the experiment. Severe permeability reduction was observed. The resistance to flow due to the increased viscosity of the mobilised zone of fines was the primary reason for the observed effect. The rheological properties of concentrated clay suspensions are well-known for their irregular response to fluid shear.

6.5.1 Critical Flood Velocity

The experimental work has shown that in sandpack flooding, clay particles are not mobilised by increasing the flooding velocity alone. Gabriel and Inamdar [47] found that in flow tests with Berea sandstone cores(permeabilities of about 150 md), saturated with a 2% potassium chloride solution a critical maximum superficial velocity of 0.007 cm/s (6 m/day) existed, above which particle mobilisation occurred with any chemically-compatible wetting fluid. No critical velocity criterion was found for the flow of a chemically compatible non-wetting fluid (e.g. oil) at connate water. This was attributed to the confinement of particles in the water film.

The absence of fine materials in the effluent from sandpacks is not necessarily in conflict with the above work. Unconsolidated sandpacks have much higher permeabilities than reservoir core media. This means much higher tortuosity of flow paths in core media, resulting in higher lift and drag forces on adhered fines. Secondly the extraction of cores with solvents prior to flooding experiments could leave these cores in a sensitised state as occurred with core flooding experiments in this work.

Core materials have pore diameters which are a few tens of microns at maximum [12]. Thus the interstitial velocity in the smaller pores is likely to be much higher than the superficial velocity and adhered particles would be literally 'sheared' off from their deposition sites. These shear and inertial 'lift' forces are much lower in sandpacks.

The mechanism of release of clay particles from grain and pore surfaces is very much a chemical-ionic controlled process with fluid velocity playing a part only after the desensitisation process has occurred.

6.6 ELECTROCHEMICAL FORCES

Suspensions of colloidal particles are subject to electrochemical forces as a result of their interaction with surfaces or other similar particles. If two particles are a long way apart, their motion is completely independent of the location of the other particle. However, if they pass sufficiently close to each other, Van Der Waals forces will cause them to attract one another. If the particles are electrically neutral the two particles will continue to be attracted

until they reach the equilibrium separation, corresponding to a minimum in the mutual potential energy curve.

If however, a double layer system exists, as with charged particles, the particles will move towards each other until the diffuse layers start to overlap. When this occurs some ions will leave the overlap area (due to the concentration gradient), and consequently the surface charges will no longer be adequately screened. This causes a repulsive force between the particles, and the particles move apart. The combination of attractive forces and repulsive forces determines the overall potential energy of the system. A series of curves can be obtained which characterise the interaction force under the ionic and chemical conditions of interest.

Thus for low ionic strengths (low value of K, the Debye-Huckel reciprocal double layer thickness parameter), the double layer repulsion effect dominates, and the particles are repelled, except at distances near to the equilibrium position. Even if the equilibrium position is adopted, the particles will separate much more easily than if no double layer existed, as the potential well is small. So the presence of large numbers of ions would be expected to improve the adhesion of particles to one another, and small numbers of ions decrease the adhesion.

In Chapter 2 the double layer repulsion forces, F_R and the attractive Van der Waals forces, F_A have been studied. A summation of these forces will result in a total force, F_T, to which the colloidal particles are subjected. Double layer and Van der Waals forces were calculated using equations (23) and (9) respectively. The zeta-potential of kaolinite and silica surfaces have been extracted from

the literature [78,79,36]. The sum colloidal forces for face and edge association of kaolinite are shown for various pH conditions and sodium chloride concentrations in Figures 56-57. It can be seen that the total colloidal interaction force in a kaolinite-silica system is in the range -100 to 100 kN/m^2 and thus many orders of magnitude higher than the hydrodynamic shear force. This is not to say that the hydrodynamic force does not contribute to the clay mobilisation process. Colloidal forces fall rapidly to zero as the particle to grain separation increases. Hydrodynamic forces then begin to be strong enough to bring about particle detachment and re-entrainment processes.

6.6.1 Clay Face Association

In their natural state, reservoir clays exist as well flocculated materials which are strongly attached to pore surfaces. The normally high salinity conditions maintain the strength of Van der Waals interparticle and particle-grain attraction forces over weak double layer forces caused by depressed double layers. Secondly, the Van der Waals attachment forces between flocculated clays and grain surface are thought to be greater than those between an equivalent mass of non-flocculated clay and surface. Strong Van der Waals forces are responsible for the 'plate-stack' condition which is usually encountered with well-crystallised kaolinite in reservoir core materials. These card-pack structures are attached to pore surfaces by a combination of Van der Waals and double layer forces.

Figures 56 to 57 show the force balance for these interactions between a model clay card-pack faces and a flat silica surface. The calculations have been based on the zeta-potentials under the range of pH and salinity conditions as given in Tables 3 and 4. Equations (9)

and (23) were used to estimate the Van der Waals and double layer force components respectively.

At neutral pH conditions, Figure 56b, the transition between attractive and repulsive forces is theoretically predicted when the salinity, based on sodium chloride, falls to below 0.08M NaCl. This figure, which is for pure kaolinite, is within satisfactory agreement with the critical salinity of 0.11M observed in this study, bearing in mind that natural clay fines contain a wide variety of mineral species which have different and specific zeta potentials.

At lower pH values, Figure 56(a), the critical salinity level for particle detachment decreases further. As mentioned in Section 6.3, hydrogen ions function as effective ion exchange inhibitors. This implies that the salinity of a low pH flood could decrease further than with a neutral pH flood. At higher pH, the critical salinity level for detachment increases. The dispersing action of the hydroxyl ion in this case means that higher salinity levels are required to keep clays flocculated and immobile in the high pH floods.

It can be seen that the pH of fluids in contact with clay exerts a controlling influence on the dispersive behaviour of the flocculated clays. Thus, at higher pH conditions, in general, clay dispersal is promoted even with high electrolyte concentrations. At pH conditions below neutral, face-face attraction forces predominate and the electrolyte strength for particle dispersal is reduced.

6.6.2 Clay Edge Association

The edges of clay particles offer highly active ion exchange sites due to the presence of a high surface density of broken bonds. These occur both in the alumina (negative) and in the silica layers (positive). The response of edges to changes in pH and electrolyte strength are difficult to accurately predict for this reason. Although the edge area is physically a fraction of the total surface of a clay particle, the edge surface potentials under specific pH conditions are comparable in strength to those on the basal surfaces.

Edge zeta potentials for kaolinite (Table 3) become increasingly more positive as the pH of the suspension containing the clay decreases. Above a critical pH level, negative double layers (i.e. negative zeta-potentials) prevail, although they do, characteristically, become increasingly positive with any increase in the electrolyte concentration.

At all low pH levels below 7.5 clay particle edge-silica grain surface forces are attractive and keep particles deposited or in a mode of flocculation. This is because the hydrogen ions act effectively as divalent ions and are strongly adsorbed onto clay surfaces, depressing double layers. Attractive forces prevail at all electrolyte concentrations under low pH strengths.

However, at pH = 9, clay particle edge to silica grain forces become slightly repulsive if the electrolyte strength decreases below about 0.1M sodium chloride.

6.7 A MODEL FOR CLAY MOBILISATION

The phenomena of spontaneous mobilisation of clays in sand beds, as has been reported in this work, is a response to specific changes in the ionic environment to which the bed is subjected. Depending on ionic conditions after mobilisation, the fines suspension in the pores may either progress through the bed with increasing or decreasing concentration. The permeability reduction due to clay mobilisation and consequent plugging effects can only be modelled if account is made of the ion exchange processes which occur. The work has shown that there are clearly many ways in which the clays associated with sand surfaces can respond to changes in the fluid environment.

It is proposed that the process of clay mobilisation and subsequent permeability loss is the result of the occurrence of a number of processes which act rapidly and in sequence. Figure 59 is a schematic representation of the proposed model for mobilisation.

6.7.1 Sensitisation

Sensitisation represents a change in the electrical potential energy level of the clay system from a state in which forces of attraction predominate (between charged surfaces) to one where inter-particle and particle-surface repulsion becomes stronger. This change in the energy level is accompanied by small, imperceptible increases in the clay-clay and clay-substrate attachment distances which are of the order of a few nanometres. As yet, such changes have not been measured. However, it appears that the process of sensitisation elevates clays previously trapped in a deep primary energy minimum to a shallow secondary minimum or some transition state. A further expansion of the double layer from the secondary minimum position, as with water shock,

invariably results in mobilisation. A combination of double layer and hydrodynamic forces then causes the spontaneous particle dispersal and permeability loss.

Sensitisation is brought about by changes in the pH and salinity of fluids. They determine the extent of ion exchange processes involving the loss of divalent ions from the clay surfaces and their replacement by monovalent or other divalent ions of suitable size. Under a given flooding environment, these factors may either reinforce or reduce the beneficial effects of one another. Naturally occurring clays possess a mixture of monovalent and divalent ions adsorbed onto their surface. The ion exchange arises because of the inherent charge deficiency of the clay mineral atomic structure. This is due to substitutions of one atom for another, or preferential ion adsorption where specific ions are strongly attracted to the clay surface or incorporated in the structure. Broken bonds, particularly at the edges of clay particles also increase the ion exchange capacity of clays. Broken bonds increase with decreasing particle size and crystallinity. Kaolinite from Fine-grey clay was found to be of low crystallinity.

The state of sensitisation of a clay in a reservoir undergoing waterflooding is difficult to detect. This is because the sensitisation process does not result in any noticeable effects.

6.7.2 Entrainment

There has been widespread debate about the role of mechanical forces in formation damage in the literature. Many workers [40-42,47] have found that a critical flooding velocity exists above which damage occurs, whilst others have reported that damage is independent of such physical factors. This work has shown that ionic-chemical mechanisms

are needed to explain the process of sensitisation whilst entrainment is very much governed by the flooding velocity. Since it is entrainment which controls the amount of fines which will migrate, and possibly plug the formation, the flooding velocity is of great importance in determining the level of damage. However, without the initial stage of sensitisation which is entirely an ionically governed process, clays would not mobilise even under very high flooding rates. Once a clay mass is sensitised, even very small flooding velocities will cause entrainment. The effects of high flooding velocities appear to be significant not on the entrainment step but in the migration and subsequent depositional behaviour of clays in suspension. In microcell studies clay deposition on silica surfaces was found to be directly proportional to the suspension velocity under favourable ionic conditions of deposition.

6.7.3 Migration and Pore Plugging

Once chemical or ionic changes in the fluid bring about the release of fines, a concentrated zone of fines quickly develops between displaced and displacing fluid. This occurs because the low salinity fluid causes significant double layer expansion which is sufficient to cause fines entrainment. Released fines accumulate at the interface between the low and high salinity fluid. The fines concentration in the front reaches a maximum equilibrium, value which depends on the fines content of the sandpack and the flowrate. A lower flowrate results in a higher front concentration in a zone of narrower width. In addition, permeability is less severely affected at lower flowrates after mobilisation has taken place.

The experimental work done in this study has shown that the rate of particle plugging at constrictions is proportional to the fines concentration in the fluid and at the plugging site and also to the flood velocity. Plugs formed at high velocities are less likely to be broken by techniques such as reverse flow which dislodges weaker bridges. This is because of the degree of impaction of particle plugs and the penetration of pore constrictions achieved by a deposit. Thus, increases in flow rate designed to increase production in the field may have detrimental effects unless fluid compatibility is first determined.

6.7.4 Permeability Reduction

Most models of permeability reduction refer to the pore-plugging action of mobile fines.

Simple straining of fines at pore throats accounts for some of the fines retention properties of sandpacks. Reservoir core material with its finer pore dimensions can be severely plugged by the mobilisation of even small quantities of fines. Large fines become trapped and act as deposition sites for smaller colloidal-sized materials. This leads to the formation of cake type deposits.

In this work, permeability reduction has also been caused by the increased viscosity of pore fluids due to their high clay content. Though temporary, the permeability loss caused by the increased resistance to flow was significant. Clay concentrations approaching 150 g/l were measured in the mobile fines zone.

Permanent loss occurs due to re-deposition effects. High clay concentrations ensure that some linkage of clays persists after mobilisation. It is unlikely that complete de-flocculation takes place. Large flocs previously in their natural states have been broken down into smaller units through the action of double layer and entrainment forces. These units can link together under low shear steady flow in a pore channel. This linkage is a contributing factor to permeability decrease. At the walls of the pore, continuous deposition takes place from a layer of slowly moving suspension. Thus, effectively the deposition of a layer of clay suspension occurs on the pore channel wall. This layer reduces the effective pore cross-section that is available to flow. This is evidenced as reduced permeability. The clays in this stagnant or slowly moving layer interact with one another to form a 'network' type structure which is sufficiently resistant to break-up. The thickness of this layer continues to increase until the pore diameter equals the diameter of the pore constriction downstream. Further deposition in this pore would probably lead to complete plugging. The effects observed in experiments with sandpacks in this work are consistent with this hypothesis.

At the pore throats, plugging occurs with severe effects on permeability. Individual particles and small multiple particle units break off from larger flocs under the action of the high shear forces. These particles are able to progress through the pore throats until they are eventually captured or produced.

Suspension stability effects become significant when dealing with mobilised clays. The term stability is used here as in classical colloid theory whereby if the double layers are expanded then the

suspension exists in a 'stable', disperse or de-flocculated state. An unstable suspension is one undergoing coagulation. The term 'clay stabilisation' is also used in oil production terminology where the clays in a reservoir are prevented from becoming dispersed or entrained in the fluid flow. Clay stabilising agents may be considered as any agents which by adsorption into the clays or by their compressing effect on the double layer prevent or minimise the mobilisation of reservoir clays. Most of the alkali metal salts, some heavy metal salts, and cationic polymers have been and continue to be used as stabilising agents during secondary and tertiary flooding.

Water flooding practices are directly affected by the ionic composition of reservoir and well fluids. Previous work has concluded that at least ten percent of flooding water should be in the form of calcium, magnesium or other compatible divalent salts. Most formation waters contain far greater concentrations of these ions. Formations with connate water containing sodium salts would be likely to have clays in their sodium base form. Fresh injection waters containing calcium and magnesium salts would lose their divalent ions to the clays and pick up sodium ions. It is conceivable that the sodium ion concentration of displacing waters could rise to levels which could be harmful to parts of the reservoir further downstream.

CHAPTER 7

CONCLUSIONS

1. Kaolinite and illite are the predominant clay minerals among the fines adhered to grain surfaces of cleaned separator sand from the Forties North Sea reservoir. These clay types are also found in association with the Fine-Grey sand which has been successfully used as a test sand in this work.

2. The mobilisation of clay particles is caused by a weakening of the adhesion force between the particles and grain surfaces. The break up of flocculated clays also contributes to the magnitude of dispersal. Kaolinite and illite have been found to spontaneously detach from grain surfaces when sandpacks are flooded with high salinity brines followed by fresh water or low salinity fluids. This mobilisation results in the build-up of a highly concentrated zone of clay which migrates through the sandpack. Clay suspension concentrations greater than 100 g/l have been recorded under the experimental conditions of this work. Small particles of quartz are also found in the migrating fines fraction.

3. Ion exchange processes between clay and solution environment are responsible for the weakening of the adhesion force.

4. Kaolinite, illite and clay minerals in general, have cation-specific ion exchange and adsorption characteristics. Each clay type possesses its own 'blue print' which determines the nature and extent of its ion exchange capacity. Kaolinite and illite exhibit strong ion exchange when in contact with sodium and potassium chlorides.

5. The rate of ion exchange is dependent on the concentration of electrolyte and pH of the fluid environment in contact with the clay.

6. The critical strength of aqueous sodium chloride which initiates spontaneous clay dispersal in sandpacks is in the region of 0.1M at neutral pH. Potassium chloride brine exhibits a similar critical concentration.

7. The pH of fluid environment is a controlling parameter for ion exchange between clays and fluids.

8. Low pH conditions (pH values less than 6) minimise particle dispersal by inhibiting the exchange of those ions originally on clay surfaces with monovalent ions from the bulk solution. It is likely that the hydrogen ion interacts with clay surface charges to prevent exchange processes.

9. High pH conditions (pH values greater than 8) promote particle dispersal and deflocculation processes. The hydroxide ion interacts with clay surfaces causing expansion of the double layer.

10. Fluid shear forces alone at typical reservoir flooding velocities are not sufficiently strong to initiate the detachment of an adhered particle. A weakening of the colloidal adhesion force is a precursor for clay dispersal. This weakening allows double layer expansion to take place when fresh water or low salinity fluids come into contact with clays. The fluid shear force then becomes strong enough to bring about dispersal.

11. There are two mechanisms of permeability reduction in sandpacks where clay mobilisation has taken place. Firstly, there is increased resistance to flow due to the increased viscosity of the migrating zone of clay material. This permeability reduction, which is temporary was about forty percent in sandpack floods. The second more permanent form of damage is due to pore-plugging in the sandpack. The permeability reduction due to this mechanism has been found to be in the region of ten to twenty percent.

12. The treatment of sandpacks with divalent cations or mixtures of monovalent and divalent ions prevents clay dispersal. However, these ions may be removed from the clay particle surfaces by any subsequent flow of sufficiently concentrated monovalent brine.

13. As oil reservoirs progress through maturity to depletion, the water-oil ratio of produced fluids increases and the compatibility of fluids with reservoir materials becomes a more important factor.

7.1 SUGGESTIONS FOR FURTHER WORK

The investigations carried out during the course of this research have suggested a probable mechanism of clay mobilisation. The results obtained have also identified specific areas where more information is required.

Further work on the electrochemical properties of individual clay species and quartz silica would enable better characterisation of colloidal particle behaviour. The interactions between, for example, kaolinite and quartz fines could then be better understood. Ion exchange properties should also be studied in greater detail with particular emphasis on the effect of non-crystallinity of clays.

The understanding of flow effects in porous media could be greatly enhanced by further study of the rheological properties of kaolinite suspensions. Interactions in systems of mixed fines suspensions containing kaolinite should also be studied within this subject area.

APPENDIX

Experimental Errors

This appendix discusses the sources and magnitudes of the errors occurring during the experimental work. In order to minimise errors procedures were standardised and instruments carefully calibrated. However, some error is inevitable. The possible sources of experimental error were the measurement of sandpack pressure differentials, pH and estimate of the clay content of liquids eluted from the sand columns. An unknown in most experiments of this type is the homogeneity and isotropy of the sand pack. The method of filling devised using sedimentation was devised to minimise errors due to these causes. It was thought that the more usual procedure of compaction would be more likely to lead to anisotropy, particle fracture and banding.

The particle counting methods used in the flow cell studies of clay deposition are also subject to errors but these are more statistical errors which can be minimised by taking a sufficiently large number of replicate particle counts.

Preliminary flooding experiments were carried out with the constant head sandpack system, using water manometers for pressure measurement. At the low differential pressures found the manometer reading error was about 5% but for the lowest pressures (approx 10 mm water head) this error was thought to be as high as 20%.

The use of the constant flow rate flooding rig reduced this error significantly. Accurately calibrated high precision pressure transducers (Thorn-EMI Datatech Ltd type SE 21/C/1.02 bar ΔP) were used, reducing the measured differential pressures errors to <1%. For this system, as described in the body of the thesis, a design of inset pressure tappings coming up from the base of the column was used to prevent:

(a) baseline errors due to static head differences
(b) errors due to local homogeneity of the packing around the tapping, and
(c) minimum disturbance to the packing procedure by the tapping

The errors in the measurement of bed dimensions and liquid flowrate required for the calculation of bed permeability were estimated to be 2% in the worst case. Thus any error in the calculated permeability could be as much as 5%. However actual errors in most cases were much lower and the objective of the experiments was to study changes in factors leading to changes in permeability rather than absolute values. Bed dimensions were identical from one run to another.

Furthermore, since pressure differentials associated with clay migration in sandpack floods were much higher than the maximum possible instrument error, it can be concluded that the effects of instrument error on the permeability values and their interpretation was small.

REFERENCES

1. NELSON R.C.
   Chemically Enhanced Oil Recovery: The State of the Art.
   Chem. Eng. Prog., 51-57, March (1989).

2. SHAH D.O. and SCHECHTER R.S.
   Improved Oil Recovery.
   Academic Press, New York, (1977).

3. McMILLEN T.J.
   Overview of Enhanced Oil Recovery: A Chemical Engineers Point of View.
   Energy Progress, 4, 1, 45, (1984).

4. GOGARTY W.B.
   Enhanced Oil Recovery Through the Use of Chemicals, Parts I and II.
   J. Pet. Tech., 1581-90, Sept (1983).

5. BURLEY R.W. et al.
   Studies of Fluid Displacement by Foam in Porous Media.
   Chem. Eng. Res. and Des, 62, 92. (1984).

7. FAIRBANKS H.V. and CHEN W.I.
   Ultrasonic Acceleration of Liquid Flow Through Porous Media.
   Sonochemical Engineering in Chemical Engineering Progress Symposium Series, 67, 108-116 (1969).

8. SOMERTON, W.H. et al.
   Screening Tests to Evaluate Formation Damage in EOR Operations.
   SPE Paper 12500, 257-264 (1984).

9. BORCHARDT J.K. and BROWN D.L.
Clay Stabilisers Improve EOR Injection Rates.
Oil & Gas J., p150, Sept 10, (1984).

10. DARCY H.P.G.
"Les Fontaines Publiques de la Ville de Dijon".
Victor Dalmont, Paris, (1856).

11. HOBSON G.D. and TIRATSOO E.N.
Introduction to Petroleum Geology.
Scientific Press, New York, (1975).

12. MUSKAT M.
Physical Principles of Oil Production.
McGraw-Hill (1949).

13. GRAY D.H. and REX, R.W.
Formation Damage in Sandstones Caused by Clay Dispersion & Migration.
Proceedings 14th Conf. Clays and Clay Minerals, Pergamon, (1966).

14. PORTER K.E.
An Overview of Formation Damage.
J. Pet. Tech., 780, Aug (1989).

15. SOMERTON W.H. and RADKE W.
Role of Clays in Enhanced Recovery of Petroleum.
DOE Report Contract No. W-7405-ENG-48, (1982).

16. LEVER A. and DAWE R.A.
Water Sensitivity & Migration of Fines in the Hopeman Sandstone.
J. Pet. Geol. 7, 1, 97, (1984).

17. NEASHAM J.W.
Morphology of Dispersed Clay in Sandstone Reservoirs.
SPE Paper 6858, (1977).

18. JONES F.O.
Influence of Chemical Composition of Water on Clay Blocking.
J. Pet. Tech., 441, Apr (1964).

19. DODD C.G. et al.
Clay Minerals in Petroleum Reservoir Sands and Water Sensitivity Effects.
NAS-NRC 3rd Natl. Conf. Clays and Clay Minerals, 221 (1965).

20. HEWITT C.H.
Analytical Techniques for Recognising Water Sensitive Rocks.
J. Pet. Tech., 813, Aug (1963).

21. LAND C.S. and BAPTIST O.C.
Effect of Hydration of Montmorillonite on Permeability to Gas of Water-Sensitive Reservoir Rocks.
J. Pet. Tech., 1213, Oct (1965).

22. MOORE J.E.
Clay Mineralogy Problems in Oil Recovery.
Petroleum Engineer, B40, February (1960).

23. MORRIS et al.
Clay in Petroleum Reservoir Rocks.
US Bureau of Mines, Rept. 5425 (1959).

24. BRINDLEY G.W.
The Kaolin Minerals, X-ray Identification and Structure of Clay Minerals.
Mineralogical Society of Gt Britain, London, Monograph, Chap. 2 (1951).

25. ROSS C.S. and KERR P.F.
The Kaolin Minerals.
US Geol. Surv. Prof. Paper, Part 165E, 151-75 (1931).

26. GRIM R.E.
Clay Mineralogy.
McGraw Hill, 2nd Ed. (1968).

27. VAN OLPHEN H.
Introduction to Clay Colloid Chemistry.
Wiley (Interscience), New York (1977).

28. REX R.W.
Authigenic Kaolinite and Mica as Evidence for Phase Equilibria at Low Temperatures.
13th Natl. Conf. on Clays and Clay Minerals, p95 (1966).

29. WIKLANDER L.
Cation and Anion Exchange Phenomena, Chemistry of Soils
Chap. 4, 163, American Chemical Society Monograph (1964).

30. SCHOFIELD R.K. and SAMSON H.R.
The Deflocculation of Kaolinite Suspensions and the Accompanying Change Over from Positive to Negative Chloride Adsorption.
Clay Minerals Bulletin, 2,9, 45, (1953).

31. WEISS A. and RUSSOW J.
Proc. Intern. Clay Conf., Stockholm, 1, 203, (1963).

32. VAN OLPHEN H. AND FRIPIAT J.J.
Data Handbook for Clay Materials and Other Non-Metallic Minerals.
Pergamon (1979).

33. SPOSITO G.
The Surface Chemistry of Soils.
Oxford, (1984).

34. ILER R.K.
The Chemistry of Silica: Solubility, Polymerization, Colloid and Surface Properties, and Biochemistry.
Wiley, New York, (1979).

35. ILER R.K.
Effect of Adsorbed Alumina on the Solubility of Amorphous Silica in Water.
J. Colloid and Interface Sci, 43, 2, 399, (1973).

36. GAUDIN A.M. and FUERSTENAW D.W.
Quartz Flotation with Anionic Collectors
Trans. A.I.M.E., 202, 66, (1955).

37. PORTER J.T.
Electron Microscopy of Sand Surface Texture
J. Sedimentary Petrology, 32, 1, 124, (1962).

38. YATES D. and HEALY T.W.
The Structure of the Silica/Electrolyte Interface.
J. Colloid & Interface Sci., 55, 1, 9 (1976)

39. MUNGAN N.
Permeability Reduction Through Changes in pH and Salinity.
J. Pet. Tech., 1449, Dec (1965).

40. DONALDSON E.C. and BAKER B.A.
Particle Transport in Sandstones.
SPE Paper 6905, (1977).

41. MUECKE T.W.
Formation Fines & Factors Controlling their Movement in Porous Media.
J. Pet. Tech., 144, Feb (1979).

42. GRUESBECK C. and COLLINS R.E.
Entrainment and Deposition of Fine Particles in Porous Media.
J. Soc. Pet. Eng.,847,Dec(1982).

43. KHILAR K.C.
Sandstone Water Sensitivity: Existence of a Critical Rate of Salinity Decrease for Particle Capture.
Chem. Eng. Sci. 38,5, (1983).

44. KHILAR K. C.
PhD Thesis, Univ. of Michigan, 1981.

45. SCHEUERMAN R.F. and BERGERSEN B.M.
Injection Water Salinity, Formation Pretreatment and Well-operations Fluid-selection Guidelines.
J. Pet. Tech., 836, July (1990).

46. SHARMA M. M. et al.
Release and Deposition of Clays in Sandstones.
SPE Paper 13562, (1985).

47. GABRIEL G.A. and INAMDAR G.R.
An Experimental Investigation of Fines Migration in Porous Media.
SPE Paper 12168, (1983).

48. GRUESBECK C. and COLLINS R.E.
Particle Transport Through Perforations.
J. Soc. Pet. Eng.,857,Dec(1982).

49. KIA S.F. et al.
Effect of pH on Colloidally Induced Fines Migration.
J. Colloid and Interface Sci. 118, 1, (1987).

50. DIETZEL H.J. and KLEINITZ W.
Required Quality of Water for Injection in Secondary Projects
Oil Gas European Magazine, 24, 3, (1989).

51. BARKMAN J.H. and DAVIDSON D.H.
Measuring Water Quality and Predicting Well-Impairment.
J. Pet. Tech., 865, Jul (1972).

52. LAUZON R.V.
Colloid Science Resolves Shale, Formation Damage Problems.
J. Oil and Gas, 175, July 30 (1984).

53. VAN OLPHEN H. and FRIPIAT J. J.
Data Handbook for Clay Minerals and Other Non-Metallic Minerals.
Pergamon, (1979).

54. REED M.G.
Formation Permeability Damage by Mica Alteration and Carbonate Dissolution.
J. Pet. Tech., 1056, Sept (1977).

55. PUERTO M.C. and REED R.L.
A Three Parameter Representation of Surfactant/Oil/Brine Interaction.
J. Soc. Pet. Eng., 669, Aug (1983).

56. McCOOL C.S. et al.
Interpretation of Differential Pressure in Laboratory Surfactant/Polymer Displacements.
J. Soc. Pet. Eng., 791, Oct (1983).

57. PALLATT N. et al.
Insights into the Relationship Between Permeability and the Morphology of Diagenetic Illite in Reservoir Rocks.
Internal Report, BP Research Centre, Sunbury-on-Thames, Middlesex, (1984).

58. SMITH F.W.
Ion Exchange Conditioning of Sandstone for Chemical Flooding.
J. Pet. Tech., 959 Jun (1978).

59. POPE G. A. et al.
Cation Exchange and Chemical Flooding - Basic Theory without Dispersion.
J. Soc. Pet. Eng., 418, Dec (1978).

60. NELSON R.C.
The Salinity-Requirement Diagram - A Useful Tool in Chemical Flooding Research and Development.
J. Soc. Pet. Eng., 259, Apr (1982).

61. LAKE L.W. and HELFERRICH F.
Cation Exchange in Chemical Flooding: Part 2 - The Effect of Dispersion, Cation Exchange and Polymer/Surfactant Adsorption on Chemical Flood Environment.
J. Soc. Pet. Eng. 18, 435-44, (1978).

62. VISSER J.
Colloid and Other Forces in Particle Adhesion and Particle Removal.
Symposium on "Deposition and Filtration of Particles from Liquids and Gases", Loughborough University, Sept 6-8th, (1978).

63. GREGORY J.
Approximate Expressions for Retarded Van der Waals Interaction.
J. Colloid and Interface Sci., 83, 138, (1981).

64. SHAW, D.J.
An Introduction to Colloid and Surface Chemistry.
Butterworths, (1978).

65. STERN, as cited in Van Olphen
Introduction to Clay Colloid Chemistry, Wiley, (1977).

66. DERJAGUIN B.V and LANDAU L.D.
Acta. Phys. Chim. USSR, 14, 633, (1941).

67. VERWEY J.W. and OVERBEEK J.Th.G.
Theory of the Stability of Lyophobic Colloids.
Elsevier, Amsterdam, (1948).

68. HOGG R. et al.
Mutual Coagulation of Colloidal Dispersions
Trans. Faraday. Soc. 62, 1638, (1966).

69. GREGORY J.
Interaction of Unequal Double Layers at Constant Charge
J. Colloid and Interface Sci. 51, 44, (1975).

70. VISSER J.
Measurement of the Force of Adhesion Between Submicron Carbon Black Particles and a Cellulose Film in Aqueous Solution.
J. Colloid Sci. 34, 26, (1970).

71. VISSER J.
The Adhesion of Colloidal Polystyrene Particles to Cellophane as a Function of pH and Ionic Strength.
J. Colloid and Interface Sci., 55, 3, 664, (1976).

72. AMELINA A.E. et al.
Adhesion of Unlike Particles in Air and in Liquid
Translated from Kolloidnyi Zhurnal 44, 4, Jul-Aug (1982),
Plenum Publishing Corp.

73. REVUT B.I. and US'YAROV O.G.
Adhesion of Colloidal Particles to Flat Surfaces in Electrolyte Solutions.
Translated from Kolloidnyi Zhurnal 44, 1, 149-54, Jan-Feb (1982), Plenum Publishing Corp.

74. OVERBEEK J. Th. G.
In "Colloid Science", H.R. Kruyt ed., Vol I, Elsevier, Amsterdam (1952).

75. LOW P.F.
The Clay-Water Interface.
Proceedings Int. Clay Conf., Denver, (1985), The Clay Minerals Society, Bloomington, Indiana, 247-56 (1987)

76. BOLT G.H.
Cation Adsorption in Aqueous Clay Systems: An Introductory Review.
Proceedings of Intl. Clay Conf., Denver 1985, The Clay Minerals Society, Bloomington, Indiana, 301-4 (1987)

77. SMOLUCHOWSKI as cited by HUNTER R.J.
J. Colloid Sci., 16, 190, (1961).

78. JAMES A.E. and WILLIAMS D.J.A.
Particle Interactions and Rheological Effects in Kaolinite Suspensions.
Adv. Colloid and Interface Sci., 17, 219-32, (1982).

79. WILLIAMS D.J.A. and WILLIAMS K.P.
Electrophoresis and Zeta-potential of Kaolinite.
J. Colloid and Interface Sci., 65, 1, 79, (1978).

80. FERRIS A.P. and JEPSON W.B.
The Exchange Capacities of Kaolinite and the Preparation of Homoionic Clays.
J. Colloid and Interface Sci. 51, 2, 245, (1975).

81. LOCKHART N.C.
Electrical Properties and the Surface Characteristics and Structure of Clays II. Kaolinite - A Non Swelling Clay.
J. Colloid and Interface Sci., 74, 2, 520, (1980).

82. HUNTER R.J. and ALEXANDER A.E.
Surface Properties and Flow Behaviour of Kaolinite, Part I: Electrophoretic Mobility and Stability of Kaolinite Sols.
J. Colloid Sci., 18, 820-32, (1963).

83. HUNTER R.J. and ALEXANDER A.E.
Surface Properties and Flow Behaviour of Kaolinite II. Electrophoretic Studies of Anion Adsorption.
J. Colloid Sci. 18, 833 (1963).

84. HUNTER R.J. and ALEXANDER A.E.
Surface Properties and Flow Behaviour of Kaolinite Part III: Flow of Kaolinite Sols through a Silica Column.
J. Colloid Science, 18, 846-62, (1963).

85. RAND B. and MELTON I.E.
Particle Interactions in Aqueous Kaolinite Suspensions - I. Effect of pH and Electrolyte on the Mode of Particle Interaction in Homoionic Sodium Kaolinite Suspensions.
J. Colloid and Interface Sci., 60, 2, 308 (1977).

86. OMENYI, S.N. et al.
Comparative Isosteric Ion Adsorption for Minerals
J. Colloid and Interface Sci. 110, 1, 130, (1986).

87. THIESSEN P.A.
Z. Elektrochem., 48, 675, (1942).

88. ISRAELACHVILI J.N. and ADAMS G.E.
Measurement of Forces Between Two Mica Surfaces in Aqueous Electrolyte Solutions in the Range 0 - 100 nm.
J. Chem Soc. Faraday Trans I, 74, 975, (1978).

89. LEVICH V.G.
Physicochemical Hydrodynamics
Prentice-Hall, (1962).

90. FITZPATRICK J.A.
Mechanisms of Particle Capture in Water Filtration.
PhD Thesis, Harvard University, Cambridge, Mass., (1972).

91. SPIELMAN L.A. and CUKOR P.M.
Deposition of Non-Brownian Particles Under Colloidal Forces.
J. Colloid and Interface Sci., 43, 1, 51, (1973).

92. SPIELMAN L.A. and GOREN S.L.
Capture of Small Particles by London Forces from Low-speed Liquid Flows.
Env. Sci. Tech. 4, 2, 135, (1970).

93. WNEK W.J. et al.
The Deposition of Colloidal Particles onto the Surface of a Rotating Disk.
J. Colloid and Interface Sci., 59, 1, 1, (1977).

94. CLINT G.E. et al.
Deposition of Latex Particles on to a Planar Surface.
J. Colloid and Interface Sci., 44, 1, 121, (1973).

95. HULL M. and KITCHENER J.A.
Interaction of Spherical Colloidal Particles with Planar Surfaces.
Trans. Faraday Soc., 65, 3093, (1969).

96. FITZPATRICK J.A. and HARPER J.W.
Particle Deposition from Aqueous Suspension onto a Rotating Disk.
Paper Presented at Session on Fundamental Research in Interfacial Phenomena, 81st National A.I.Ch.E. Meeting, Kansas City, April 11-14 (1976).

97. DABROS T. and van de VAN T.G.M.
Kinetics of Coating by Colloidal Particles.
J. Colloid and Interface Sci., 89, 1, 232, (1982).

98. DABROS T. and van de VEN T.G.M.
A Direct Method for Studying Particle Deposition onto Solid Surfaces.
Colloid and Polymer Science, 261, 694-707, (1983).

99. MARPLE V.A. and LIU B.Y.H.
Characteristics of Laminar Jet Impactors.
Environmental Sci. and Tech., 8, 7, 649, (1974).

100. MARPLE V.A. and LIU B.Y.H.
On Fluid Flow and Aerosol Impaction in Inertial Impactors.
J. Colloid and Interface Sci. 53, 1, (1975).

101. FISSAN H. and BARTZ H.
Inertial Impactors.
Internal Report, University of Duisburg, (1984).

102. GLAUERT M.B.
J. Fluid Mech. 1, 625, (1956).

103. HAPPEL J.
Viscous Flow in Multiparticle Systems: Slow Motion of Fluids Relative to Beds of Spherical Particles.
J. A.I.Chem.E. 4, 2, 197, (1958).

104. KUWABARA S.
The Forces Experienced by Randomly Distributed Parallel Circular Cylinders or Spheres in a Viscous Flow at Small Reynolds Numbers.
J. Physics Soc. Japan, 14, 4, 427, (1959).

105. COLLINS R.E.
Flow of Fluids Through Porous Materials.
Reinhold, (1961).

106. DULLIEN F.A.L.
Porous Media, Fluid Transport and Pore Structure.
Academic Press, (1979).

107. MUSKAT M.
The Flow of Homogeneous Fluids Through Porous Media.
Edwards, (1946).

108. BEAR J.
Fundamentals of Transport Phenomena in Porous Media.
Nijhoff, (1984).

109. SCHEIDEGGER A.E.
The Physics of Flow Through Porous Media.
3rd Ed., Univ. of Toronto Press, Toronto, (1974).

110. HAPPEL J. and BRENNER H.
Low Reynolds Number Hydrodynamics.
Prentice-Hall, (1965).

111. PAYATAKES A.C.
A New Model for Granular Porous Media - Application to Filtration Through Packed Beds.
PhD Thesis, Syracuse Univ., New York, (1981).

112. PAYATAKES A.C. et al.
A New Model for Granular Porous Media - Part I & II
J. A.I.Ch.E., 19, 1, 58, (1973).

113. RAJAGOPALAN R. and TIEN C.
Trajectory Analysis of Deep-Bed Filtration with the Sphere-in-Cell Porous Media Model
J. A.I.Ch.E., 22, 523, (1976)

114. IWASAKI T.
Some Notes on Sand Filtration.
J. A.W.W.A. 29, 10, 1591-7, (1937).

115. LANGMUIR I.
Report on Smokes and Filters.
US Office of Scientific Research and Development Sect 1. 865:IV (1941).

116. YAO K.M. et al.
Water and Waste-water Filtration: Concepts and Applications.
Env. Sci. and Tech. 5, 11, 1105, (1971).

117. ISON C.R. and IVES K.J.
Removal Mechanisms in Deep Bed Filtration.
Chem. Eng. Sci. 24, 717-29, (1969).

118. GIMBEL R. and SONTHEIMER H.
Recent Results on Particle Deposition in Sand Filters.
Symposium "Deposition and Filtration of Particles from Gases and Liquids", Loughborough University, 6-8 Sept (1978).

119. TIEN C. et al.
Simulation of the Dynamic Behaviour of Deep Bed Filters.
A.I.Ch.E., National Meeting, Atlanta, Ga., (1978).

120. PENDSE H. et al.
Drag Force Measurement of Single Spherical Collectors with Deposited Particles
J. A.I.Ch.E., 27, 3, 364, (1981).

121. CHIANG H.W. and TIEN C.
Transient Behaviour of Deep Bed Filters.
Proceedings of International Symposium on "Solid-Liquid Separation", Univ. College, London, 19-21 Sept., (1983).

122. O'MELIA C.R. and ALI W.
The Role of Retained Particles in Deep Bed Filtration.
Prog. Water Tech. 10, 5/6, 167-82, (1978).

123. PENDSE H. et al.
Dispersion Measurement in Clogged Filter Beds : A Diagnostic Study on the Morphology of Particle Deposits.
J. A.I.Ch.E., 24, 3, 473, (1978).

124. TIEN C. et al.
Chainlike Formation of Particle Deposits in Fluid - Particle Separation.
Science, 196, 983, (1977).

125. LEITZELEMENT M. et al.
Deep Bed Filtration in a Network of Random Tubes.
Proceedings of International Symposium on "Solid-Liquid Separation", Univ. College, London, 19-21 Sept., (1983).

126. IVES K.J.
Advances on Deep Bed Filtration.
Trans. I.Chem.E. 48, T94-T100, (1970).

127. FITZPATRICK J.A. and SPIELMAN L.A.
Filtration of Aqueous Latex Suspensions through Beds of Glass Spheres.
J. Colloid and Interface Sci. 43, 2, 350, (1973).

128. VREEKEN C. et al.
Effect of Particle Coagulation on the Performance of Filter Beds.
Symposium Proceedings "Deposition and Filtration of Particles from Gases and Liquids", Loughborough University 6-8 Sept, (1978).

129. WYLLIE M.R.J. and GREGORY A.R.
Fluid Flow Through Unconsolidated Porous Aggregates - Effect of Porosity and Particle Shape on Kozeny-Carman Constants.
Ind. and Eng. Chem., 1379, (1955).

130. BO M.K. et al.
The Effect of Particle Size Distribution on the Permeability of Filter Cakes.
Trans. Inst. Chem. Eng., 43, T228, (1965).

131. HERZIG J.P. et al.
Flow of Suspensions through Porous Media - Application to Deep Bed Filtration.
Ind. Eng. Chem. 62, 5, p.8, (1970).

132. SWARTZENDRUBER D. and UEBLER R.L.
Flow of Kaolinite and Sewage Suspensions in Sand and Sand-silt I. Accumulation of Suspension Particles.
J. Soil Sci. Am. 46, 239-44, (1982).

133. CLEAVER J.W. and YATES B.
The Effect of Re-Entrainment on Particle Deposition
Chem. Eng. Sci. 31, 147, (1976).

134. SAFFMAN P.G.
The Lift on a Small Sphere in Slow Shear Flow.
J. Fluid Mech., 22, 385, (1965).

135. PAULING L.
The Nature of the Chemical Bond.
Cornell Univ. Press (1960).

136. O'NEILL M.E.
A Sphere in Contact With a Plane Wall in a Slow Linear Shear Flow.
Chem. Eng. Sci. 23, 1293, (1968).

137. GOREN S.L. and O'NEILL M.E.
On the Hydrodynamic Resistance to a Particle of a Dilute Suspension When in the Neighbourhood of a Large Obstacle.
Chem. Eng. Sci. 26, 325, (1971).

138. SPIELMAN, L.A. and FITZPATRICK, J.A.
Theory for Particle Collection Under London and Gravity Forces.
J. Colloid and Interface Sci., 42, 3, (1973).

139. GOLDMAN, A.J. et al.
Slow Viscous Motion of a Sphere Parallel to a Plane Wall II - Couette Flow.
Chem. Eng. Sci., 22, 653 (1967).

TABLES

TABLE 1: CATION EXCHANGE CAPACITIES (CEC) OF CLAY MINERALS [26]

Clay/Mineral	CEC in meq/100g
Illite	20 - 40
Kaolinite	1 - 10
Montmorillonite	80 - 100
Chlorite	10 - 40
Allophane	25 - 50
Mica	20 - 50

TABLE 2: THE SIZE OF COMMON EXCHANGE IONS [135]

Ion	Radius (nm)
Li^+	0.06
Na^+	0.095
Mg^{2+}	0.065
Al^{3+}	0.05
Si^{4+}	0.041
Cl^-	0.181
K^+	0.133
Ca^{2+}	0.099
OH^-	0.130

TABLE 3: ZETA-POTENTIALS FOR KAOLINITE (in mV, from [78,79])

NaCl concn	Edge				Face
	pH 3	6	7	9	pH 6-9
10^{-1}M	3	4	1	-13	-26
10^{-2}M	17	7	2	-19	-40
10^{-3}M	24	9	3	-24	-43

TABLE 4: ZETA-POTENTIALS OF SILICA (in mV, from [36])

NaCl concn	pH 3	6	7	9
10^{-1}M	7	-9	-15	-20
10^{-2}M	10	-25	-32	-47
10^{-3}M	16	-47	-65	-80

TABLE 5: DRY SIEVE ANALYSIS AND DENSITIES OF SEPARATOR AND FINE-GREY SANDS

Size (μm)	% Greater than	
	Separator	Fine-Grey
30	100.0	100.0
50	99.0	99.0
70	97.0	97.0
90	87.0	85.0
110	72.0	43.0
130	45.0	12.5
150	14.5	2.0
Density (g/cm^3)	2.61	2.56

TABLE 6: DRY SIEVE ANALYSIS AND DENSITIES OF REDHILL AND CHELFORD SANDS

Size (μm)	% Greater than	
	Redhill 110	Chelford 95
63	97.2	98.8
90	83.9	88.4
125	55.4	54.5
180	11.5	14.9
250	4.9	3.0
355	1.5	0.4
Density (g/cm^3)	2.65	2.78

TABLE 7: BET SURFACE AREA AND X-RAY ANALYSES OF SEPARATOR AND FINE-GREY SANDS

Analysis	Separator	Fine-Grey
Surface Area m^2/g	1.2	0.6
% Kaolinite	2-5	1-2
% Kaolinite in <5 μm fines fraction	90	85

TABLE 8: BET SURFACE AREA AND X-RAY ANALYSES OF REDHILL AND CHELFORD SANDS

Analysis	Redhill	Chelford
Surface Area m^2/g	0.22	1.08
% Kaolinite	Trace	None

TABLE 9: SEQUENCE OF FLOODING LIQUIDS FOR CORE WATER-SENSITIVITY TEST (RUN 1)

Fluid	No of Pore Volumes
Formation Water	150
Solvents (Methanol and Toluene)	90
Formation Water	330
Distilled-Deionised Water	110
Formation Water	40

TABLE 10: RESULTS OF FLOCCULATION VALUE TESTS

Flocculation Concentration (ppm wt)	pH	Separator Sand Clays	Fine-Grey Sand Clays	Pure Kaolin Clay
NaCl	5	1850	1500	800
	7	3000	2500	1500
	9	3500	3800	1900
KCl	5	1550	1600	300
	7	2600	2200	1200
	9	3600	2700	1800
$CaCl_2$	5	90	85	10
	7	100	100	40
	9	280	350	150

TABLE 11: TABULATED SUMMARY OF FLOODING EXPERIMENTS

Run No	Description	Results in Fig No
1	Core Flood	14
2	Constant head flood - NaCl	15
3	Constant head flood - $CaCl_2$	16
4	Constant head flood - Surfactant	17
5	Constant head flood - HCl	18
6	Constant head flood - NaOH	19
	Constant Rate Floods	
7	NaCl 0.51M - water	20
8	NaCl 1M-0.51M-0.17M - water	21
9	NaCl 0.17M-0.05M-0.02M - water	22
10	NaCl 0.17M - water	23
11-14	NaCl contact time dependence	24-27
15	NaCl continuous salinity decrease	28
16	KCl continuous salinity decrease	29
17	KCl 0.4M - water	30
18	$CaCl_2$ Pre-water shock treatment	31
19	$CaCl_2$ Post-water shock treatment	32
20	Simulated formation water flood	33
21-24	Effect of pH variation	34-37
25	Effect of flowrate	38
26	Effect of flowrate in a sensitised bed	39
27	Effect of reverse flow	40
28	Effect of gravity	41
29	Filtration of clay suspension - clean bed	42
30	Filtration of clay suspension - natural bed	43

TABLE 12: COMPOSITION OF SIMULATED FORMATION WATER

Component	Quantity g/l
NaCl	79.7
$MgCl_2$	31.6
$CaCl_2.6H_2O$	6.6
KCl	2.2

TABLE 13: COMPOSITION OF NON-CHEMICALLY TREATED REFERENCE KAOLIN

Kaolinite	88%
Mica	10%
Quartz	1%
Feldspar	1%

TABLE 14: TABULATED SUMMARY OF PARTICLE DEPOSITION AND DETACHMENT EXPERIMENTS

Run No		Fig No
FC1	Deposition of latex	44
FC2	Effect of surface treatment	45
	<u>Deposition of Kaolinite</u>	
FC3	Variation of salinity	46
FC4	Variation of pH	47
FC5	Variation of flowrate	48
FC6	Variation of suspension concentration	49
	<u>Detachment of Kaolinite</u>	
FC7	Variation of salinity	50
FC8	Variation of pH	51
FC9	Variation of flowrate	50

TABLE 15: CATION ADSORPTION CAPACITIES OF CLAY SUSPENSIONS

Ion	Adsorption Capacity (micromoles/g clay)	
	Pure Kaolin	Fine-Grey Sand Clay
$NaCl\ 10^{-3}M$	85	180
$NaCl\ 10^{-2}M$	1300	3400
$KCl\ 10^{-3}M$	340	650
$KCl\ 10^{-2}M$	2300	3700
$CaCl_2 10^{-3}M$	35	70
$CaCl_2 10^{-2}M$	120	320

FIGURES

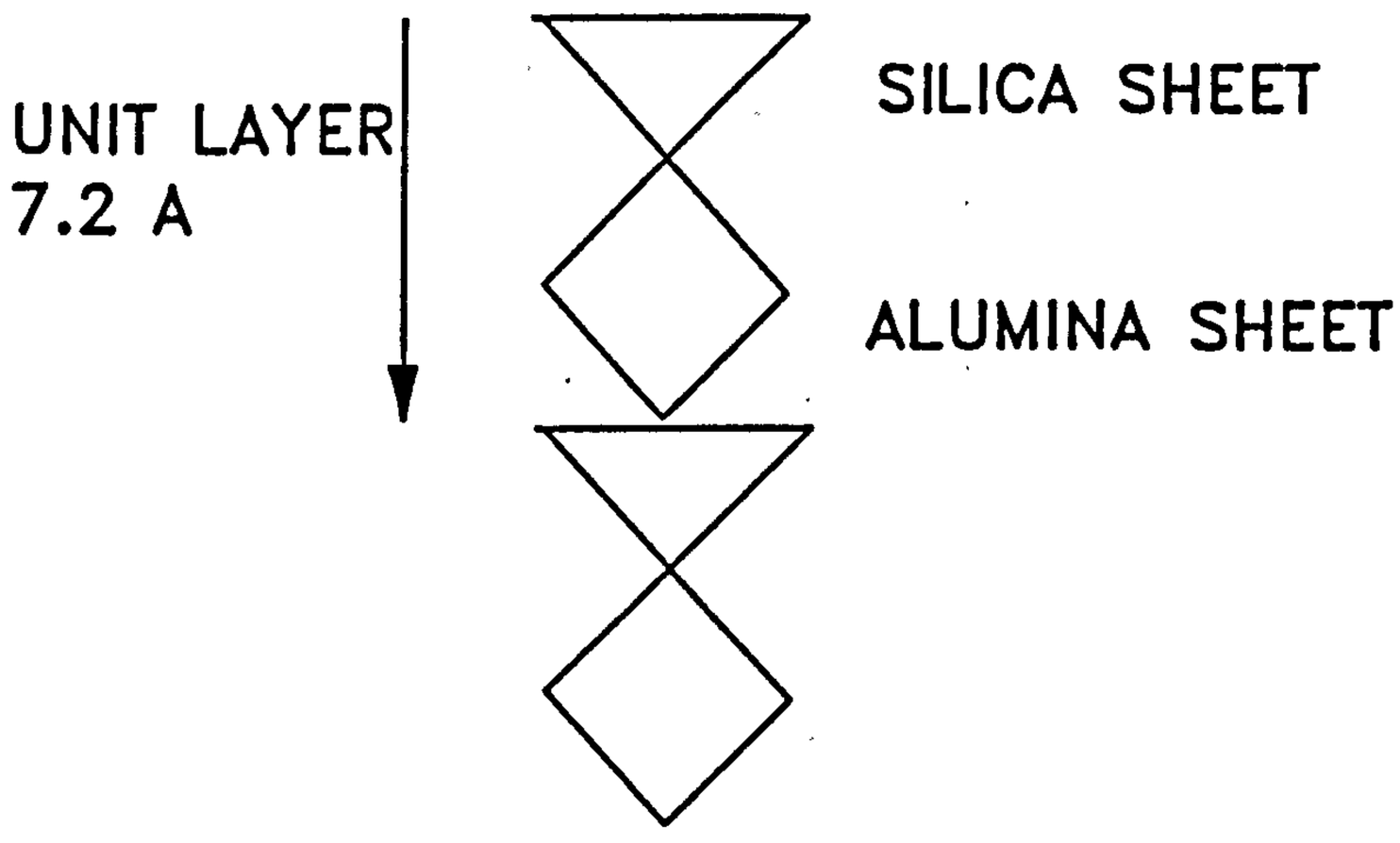

FIG. 1 SCHEMATIC CRYSTAL STRUCTURE OF KAOLINITE

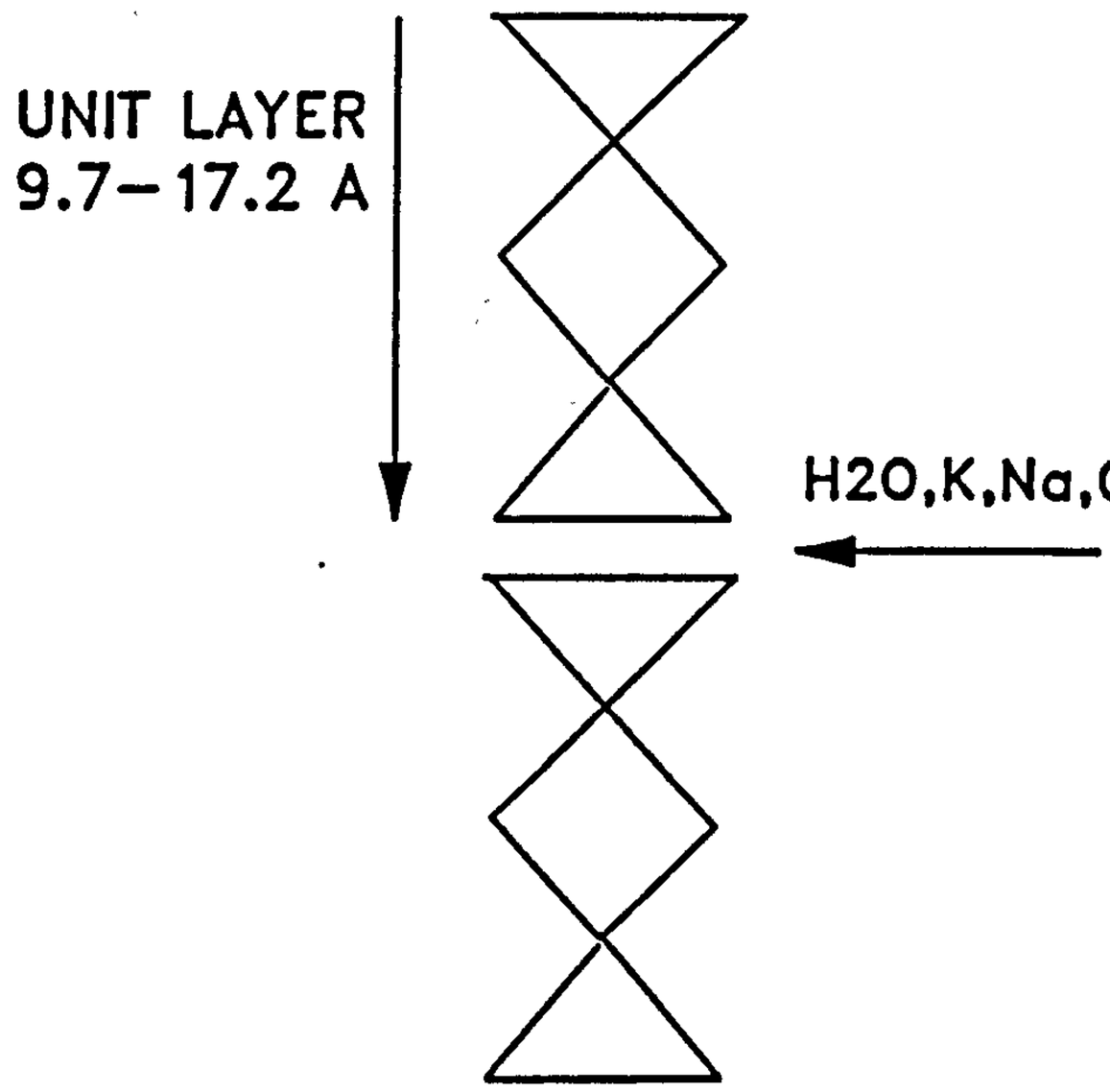

FIG. 2 SCHEMATIC CRYSTAL STRUCTURE OF MONTMORILLONITE

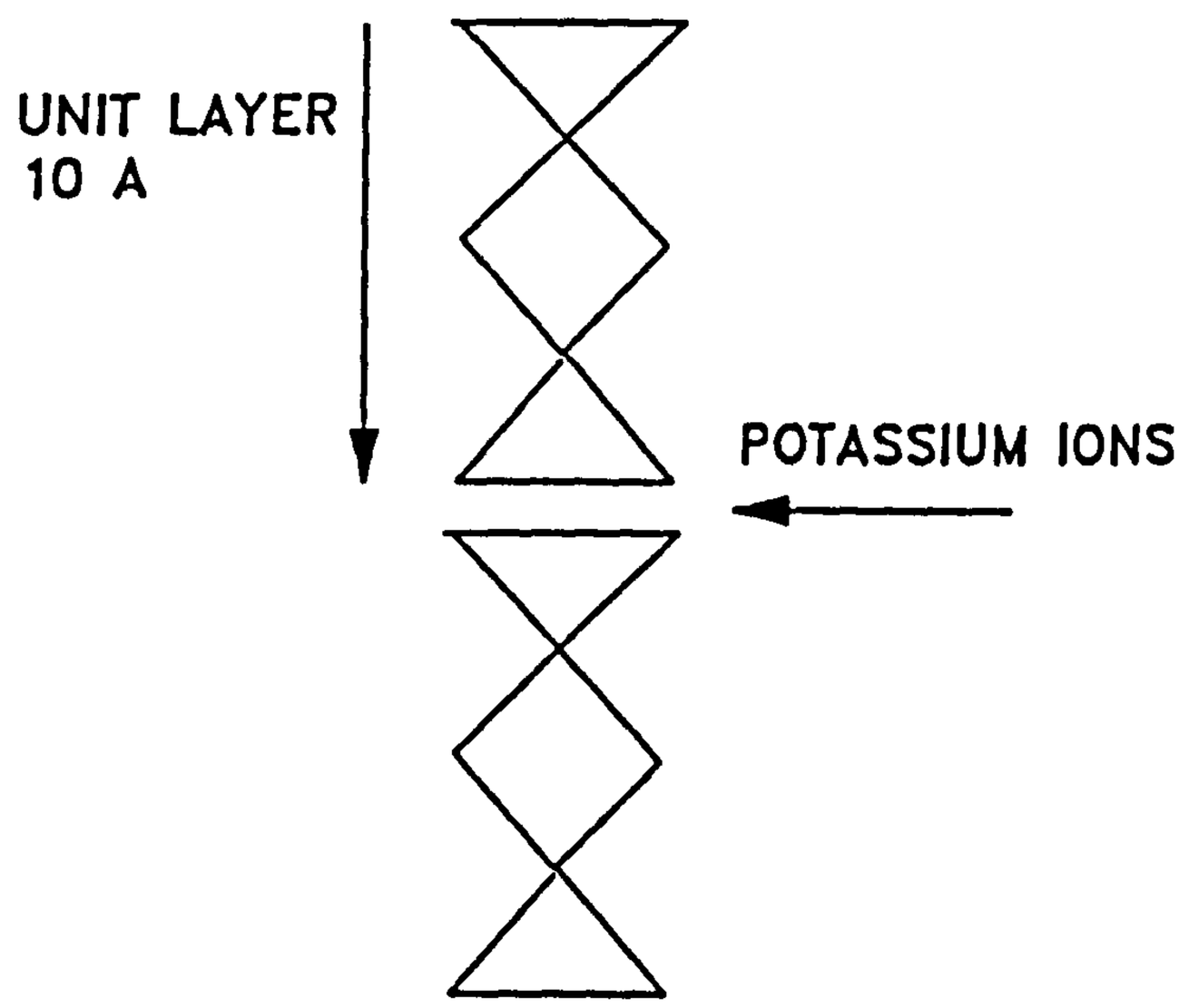

FIG. 3 SCHEMATIC CRYSTAL STRUCTURE OF ILLITE

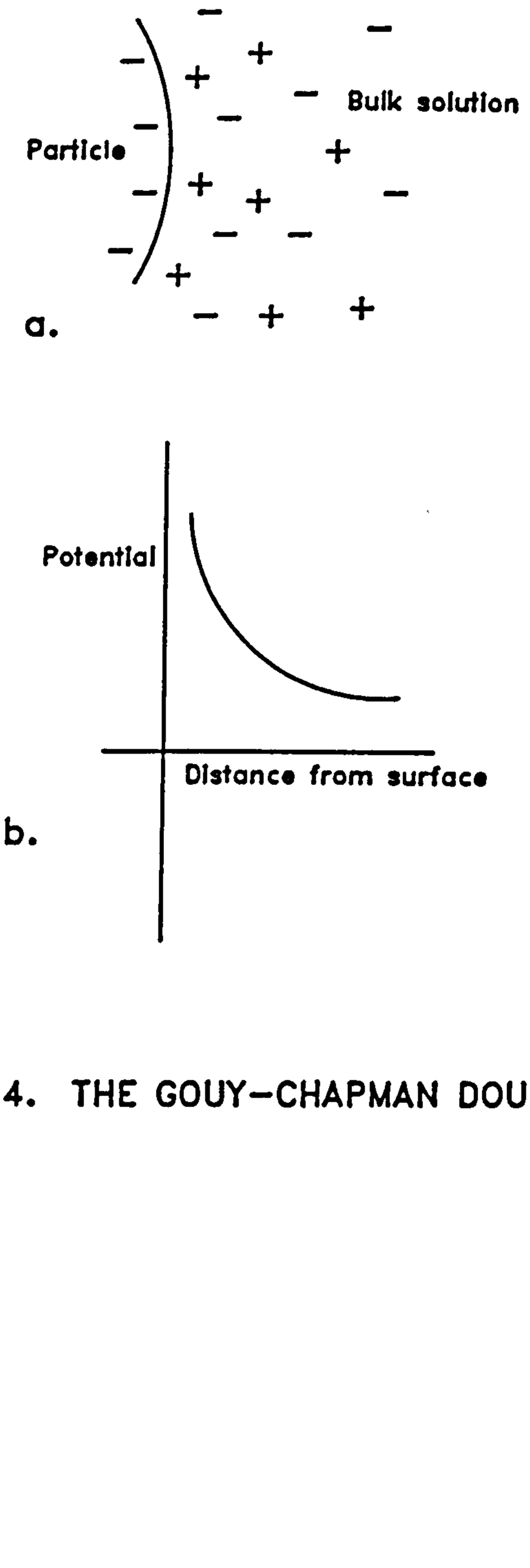

FIG 4. THE GOUY–CHAPMAN DOUBLE LAYER MODEL

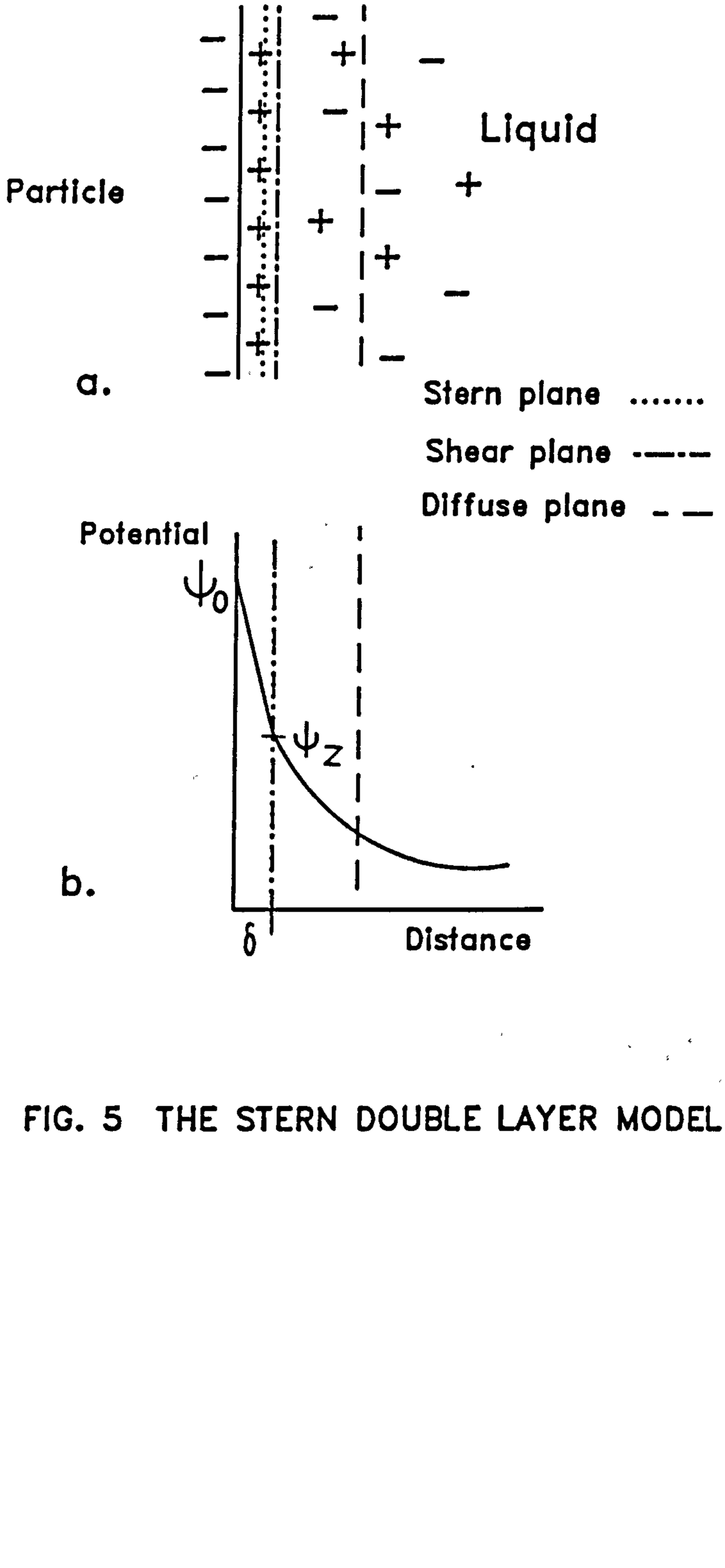

FIG. 5 THE STERN DOUBLE LAYER MODEL

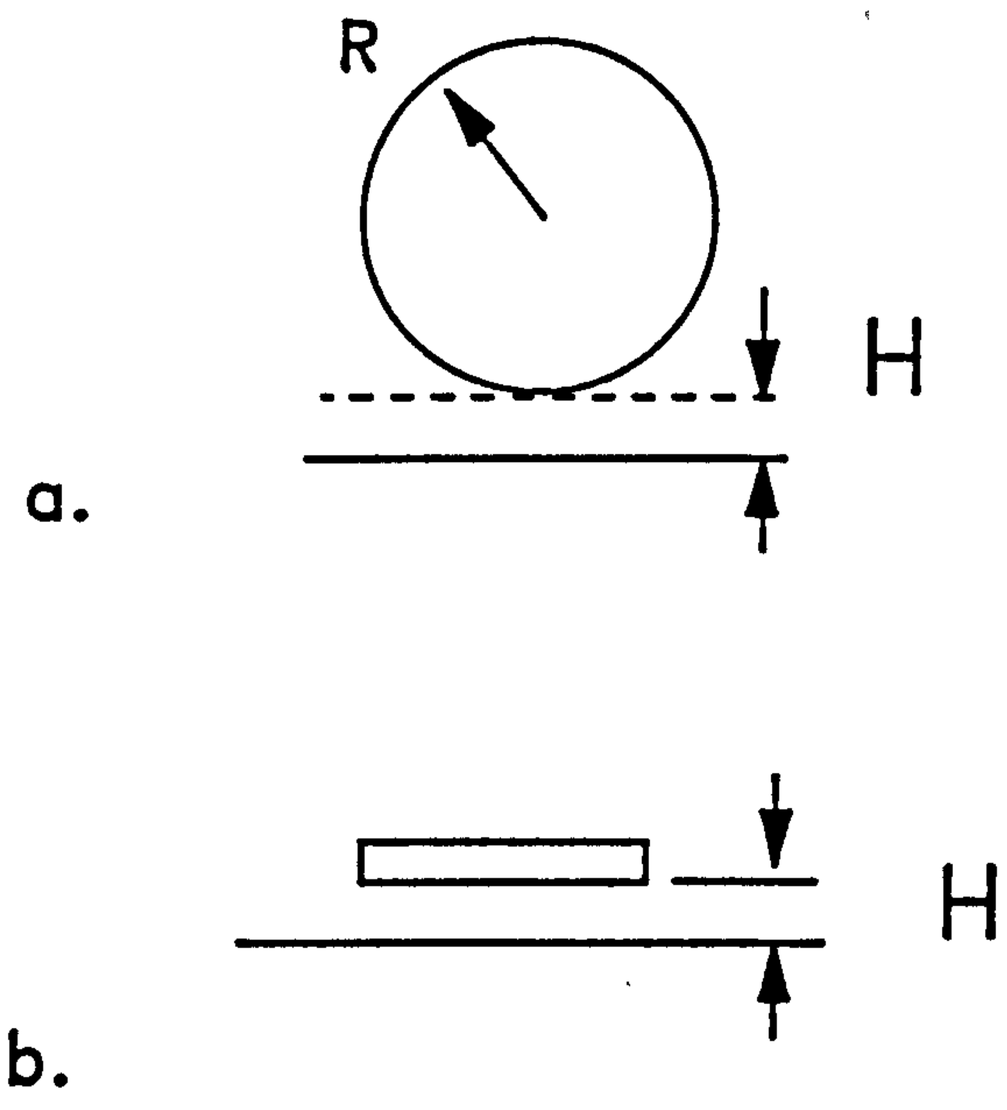

FIG. 6 SPHERE–PLATE AND PLATE–PLATE
MODELS OF VAN DER WAALS INTERACTION

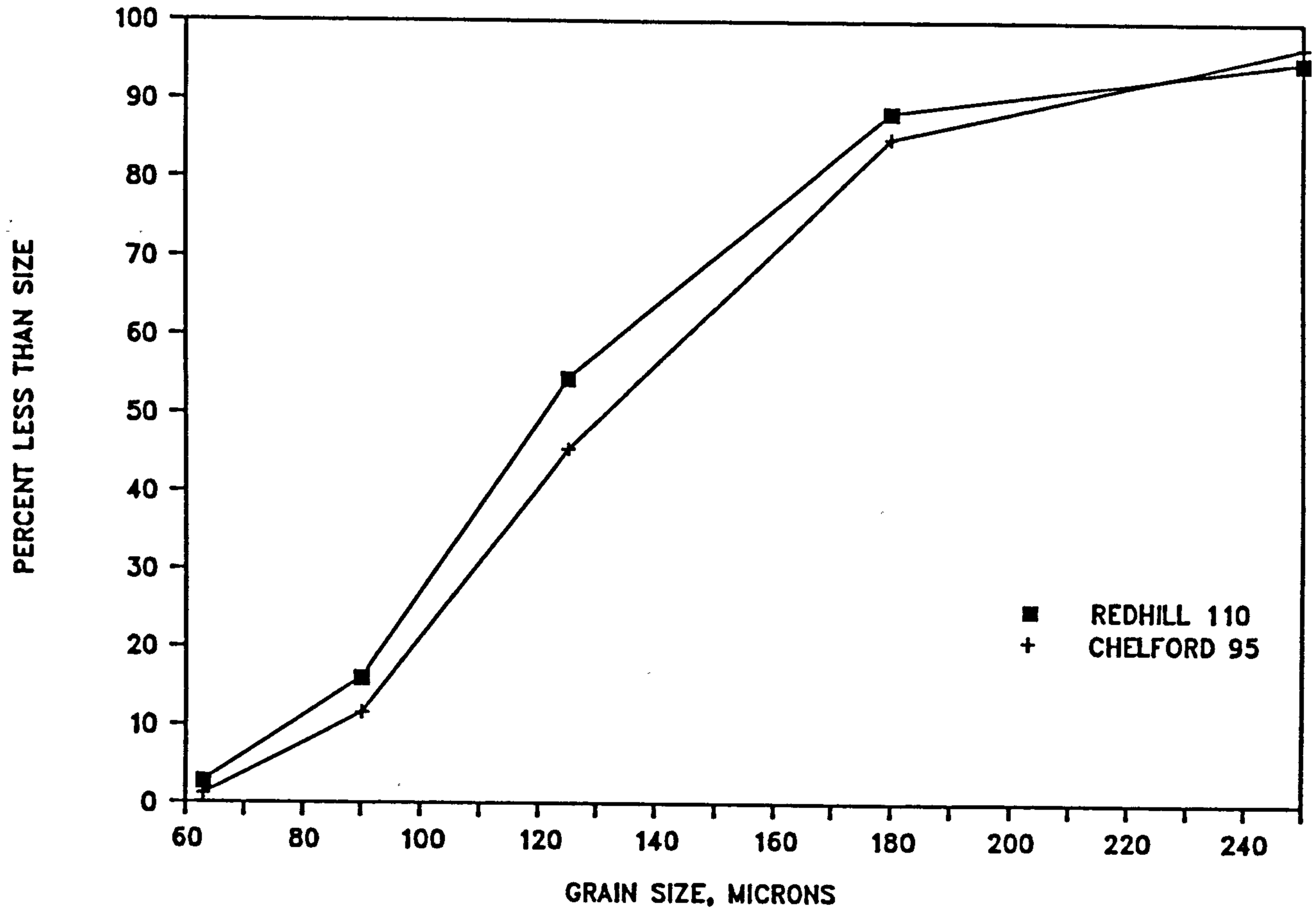

FIG. 7 Grain Size Distribution of Redhill 110 and Chelford 95 Sands

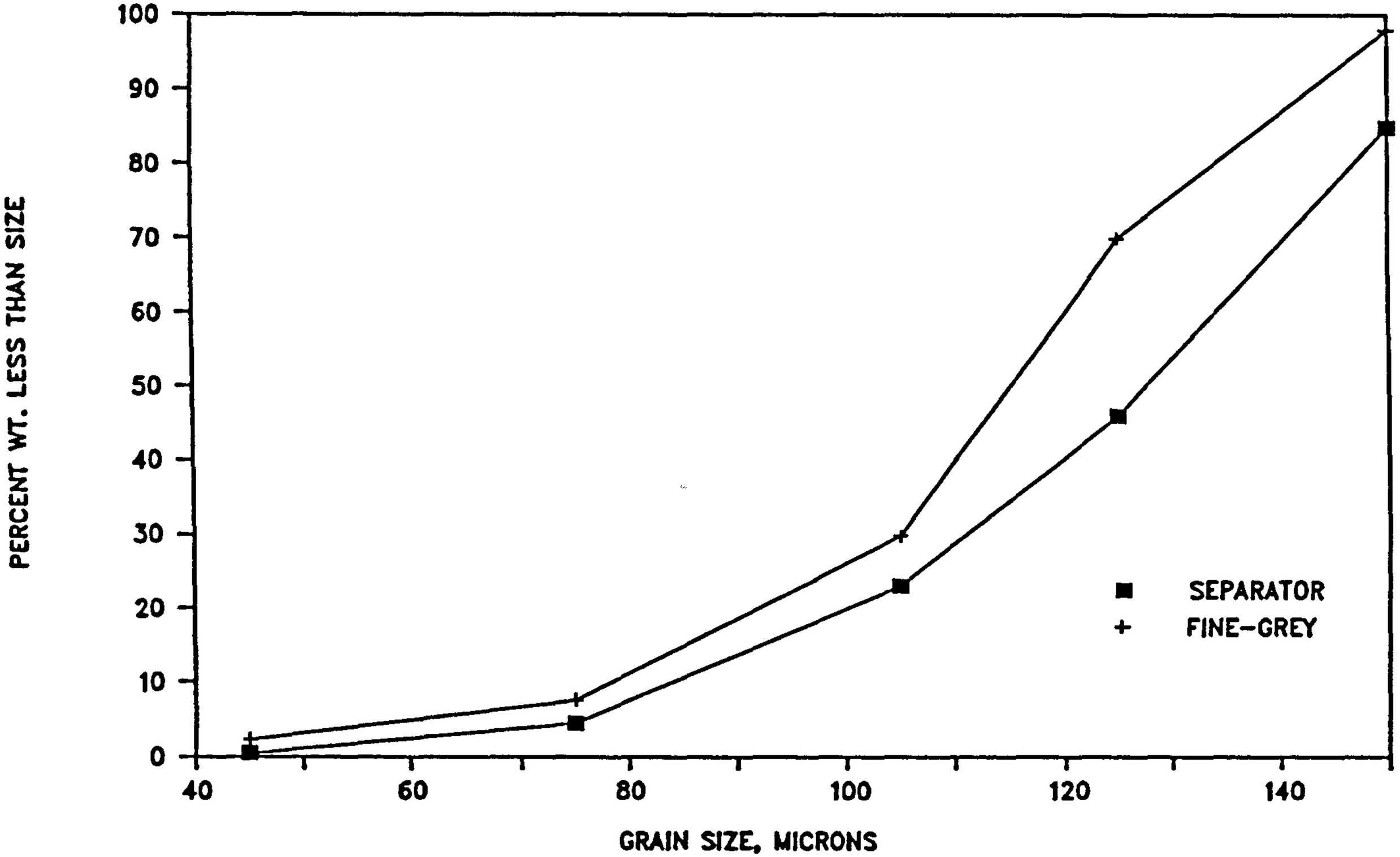

FIG. 8 Grain Size Distribution of Reservoir Separator and Fine-Grey Sands

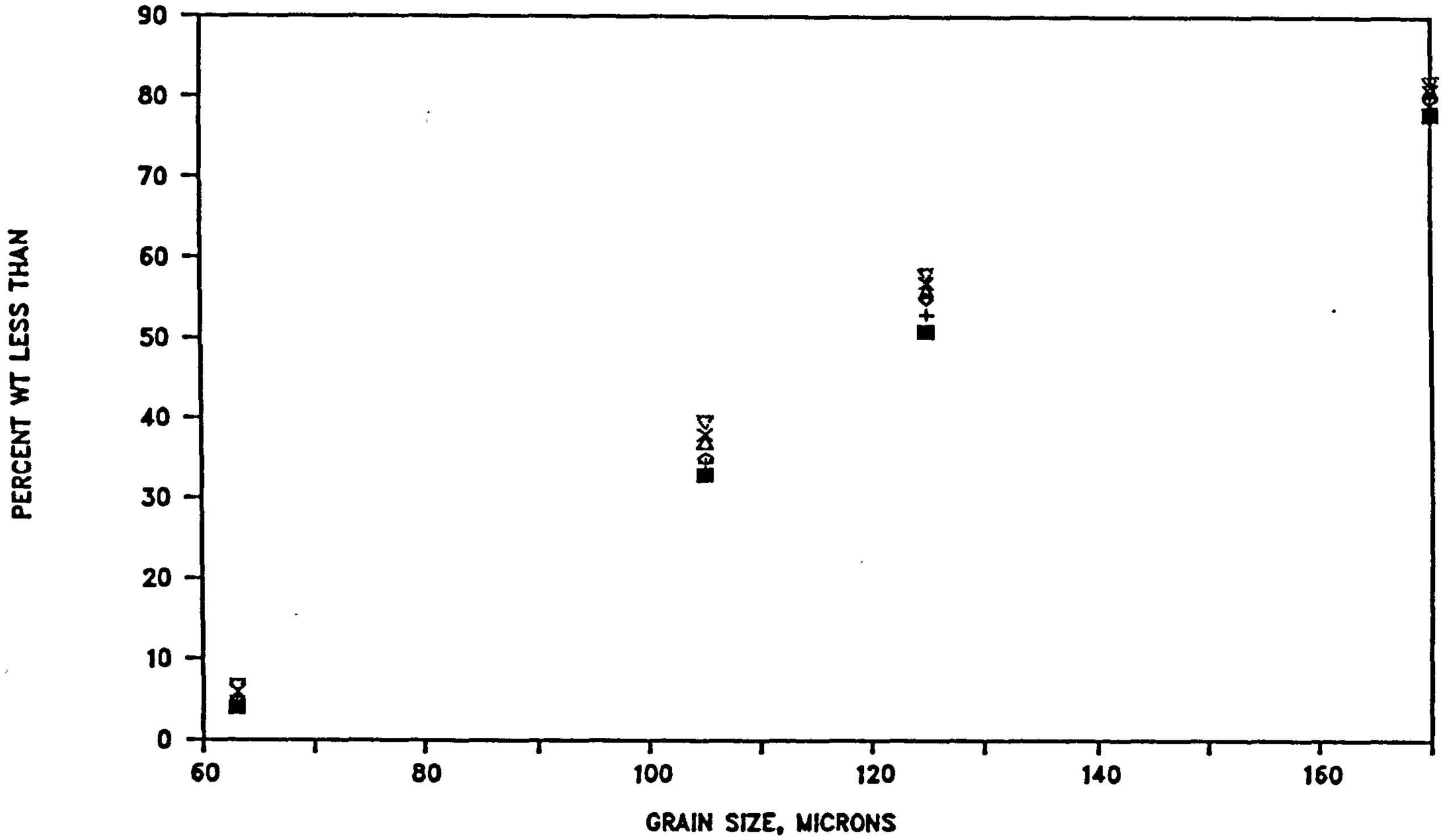

FIG. 9 Sieve Analysis of Sandpack Sections for Confirmation of Homogeneity

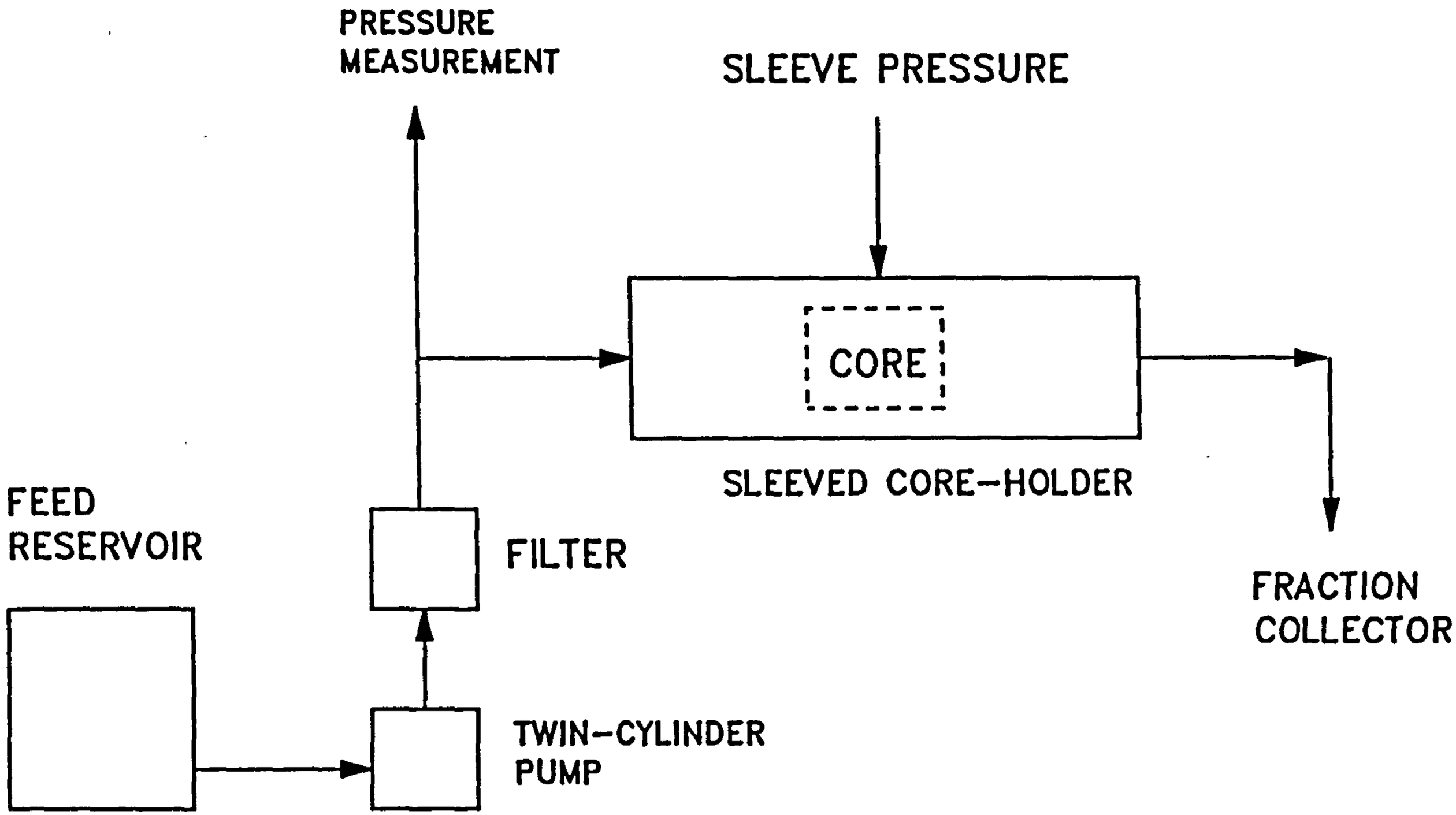

FIG. 10 Flow Scheme of the Core-Flooding System

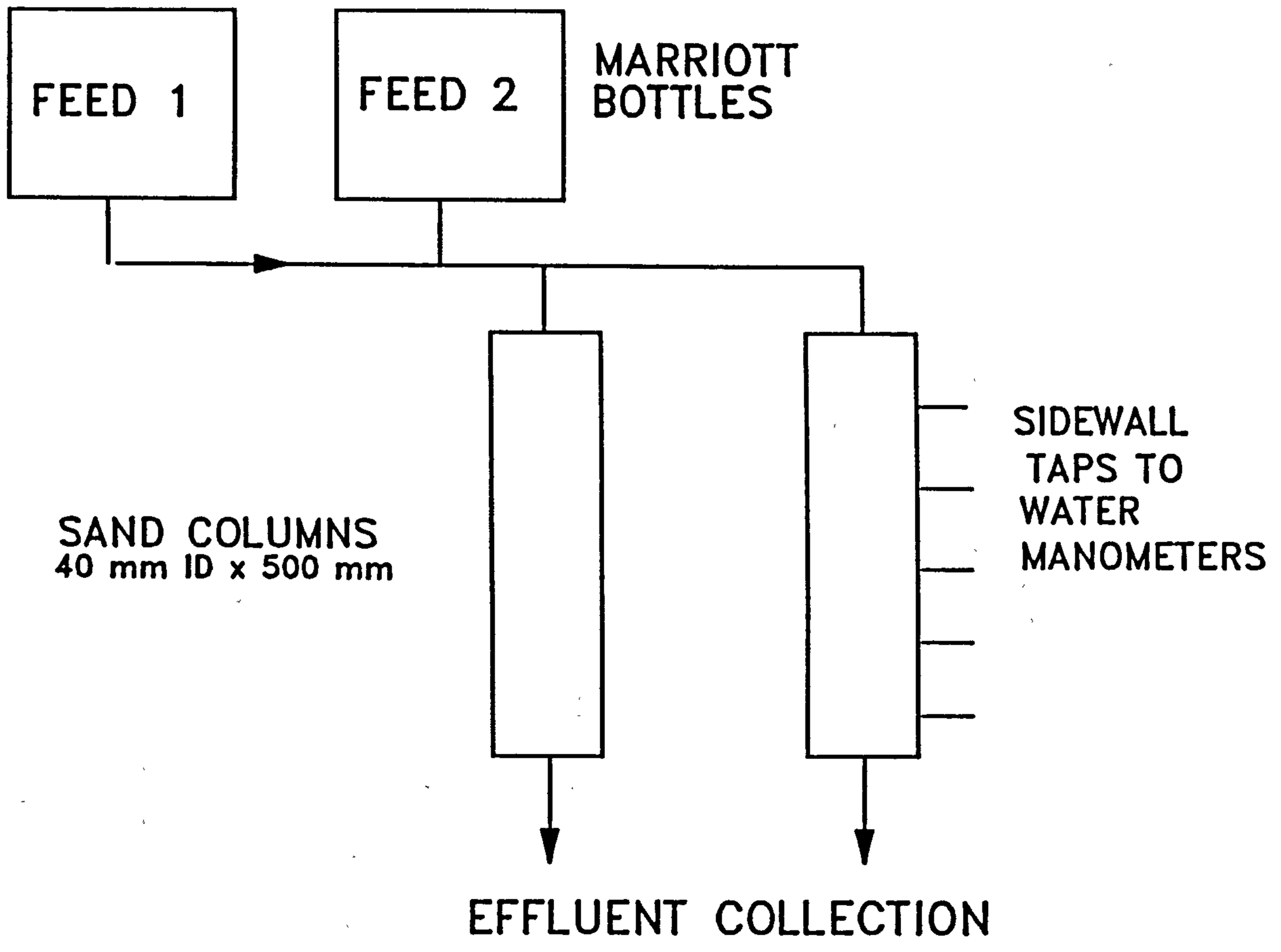

FIG. 11 The Constant-Head Sandpack Flooding System

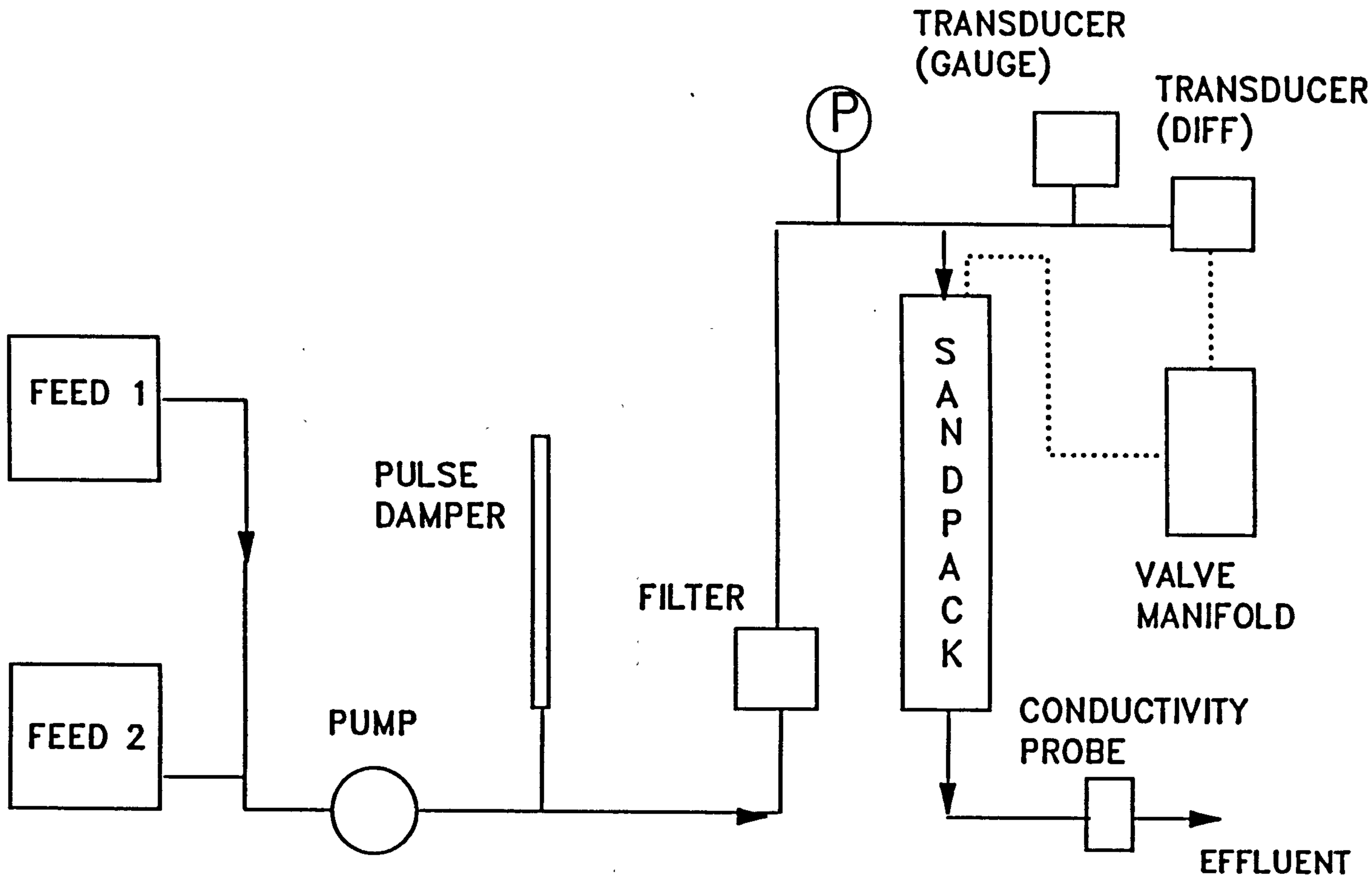

FIG. 12 The Constant-Rate Sandpack Flooding Rig

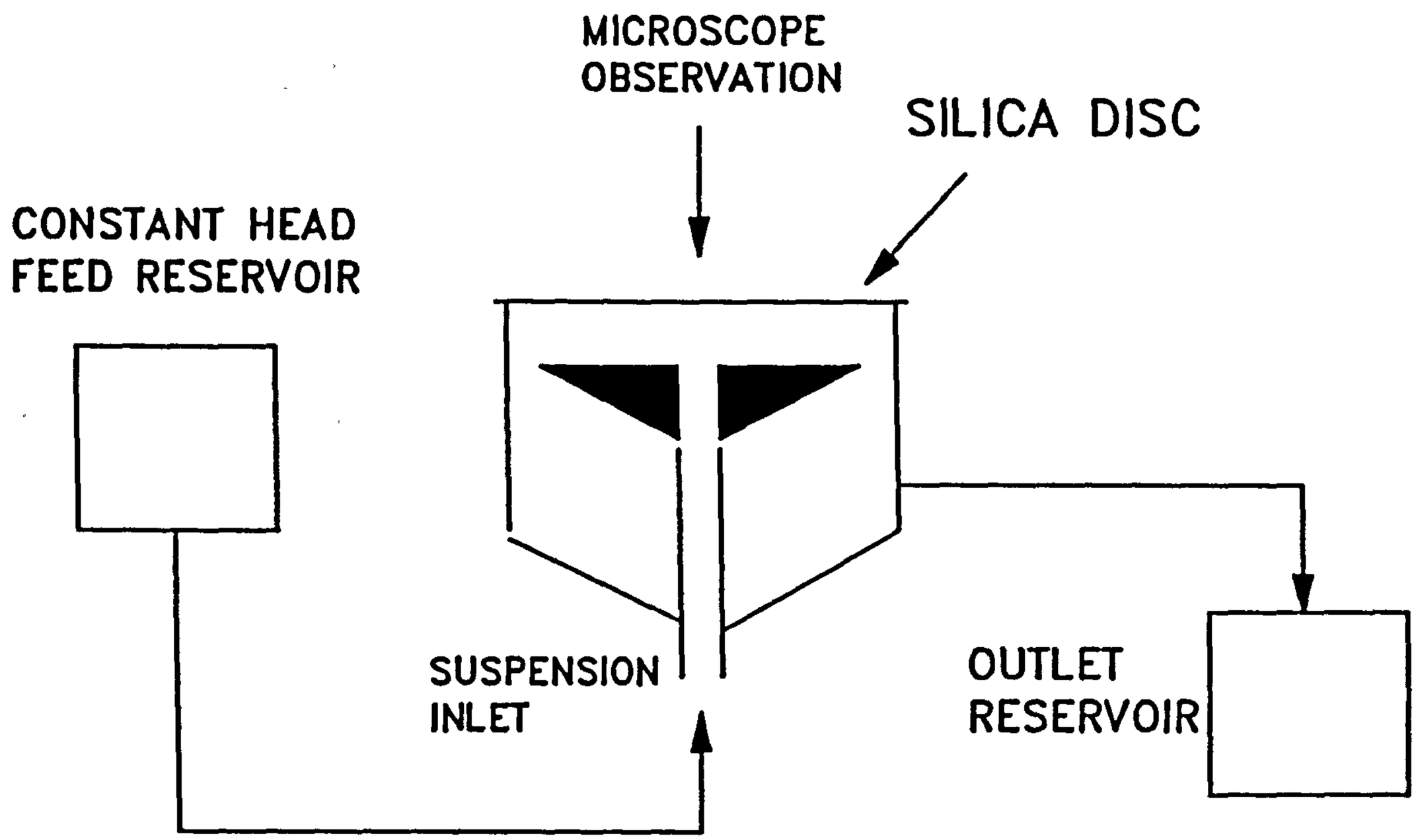

FIG. 13 DIAGRAM OF THE FLOW CELL SYSTEM

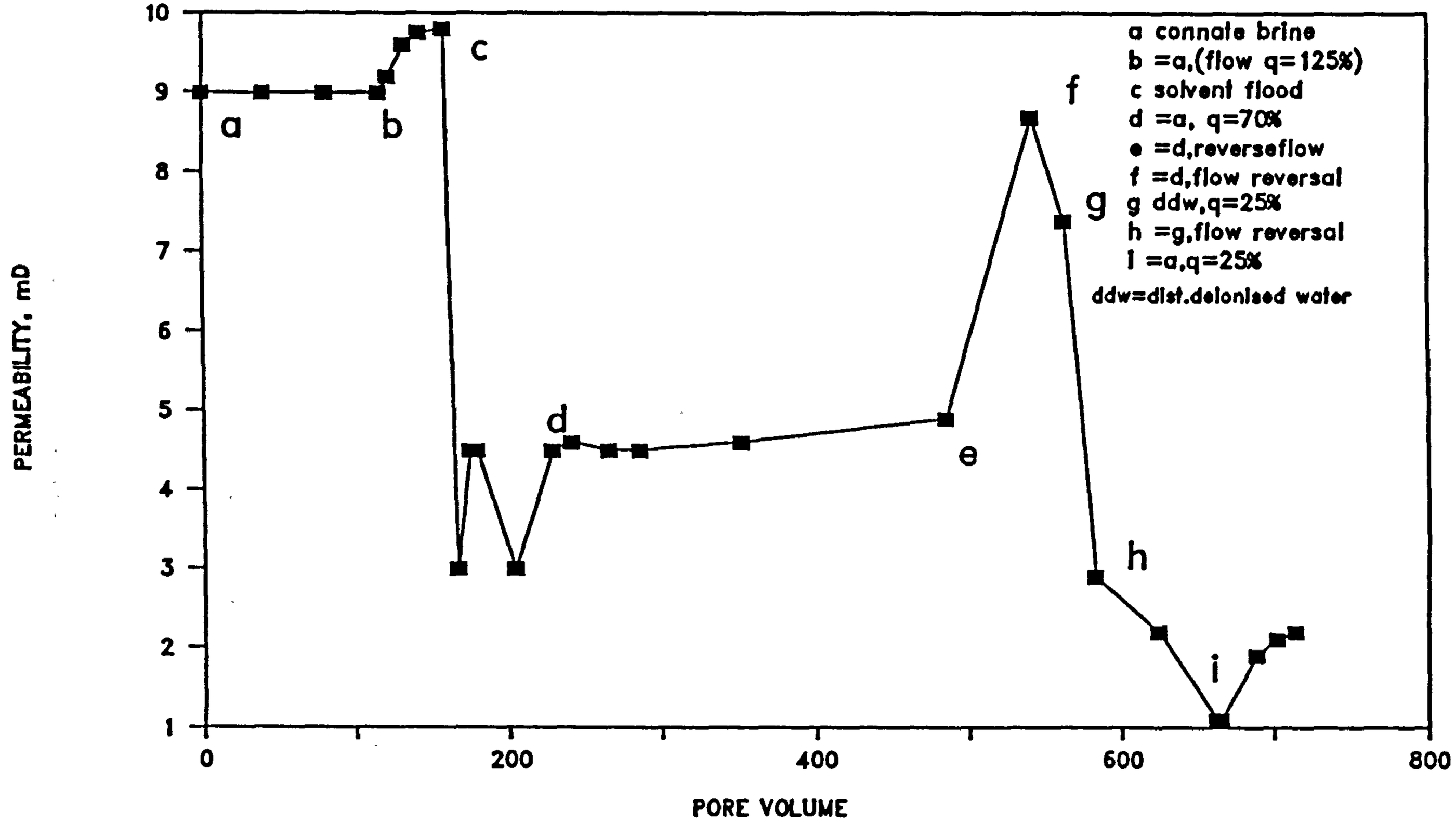

FIG. 14 Flooding of a Suspected Water–Sensitive Core from a North Sea Reservoir Sandstone

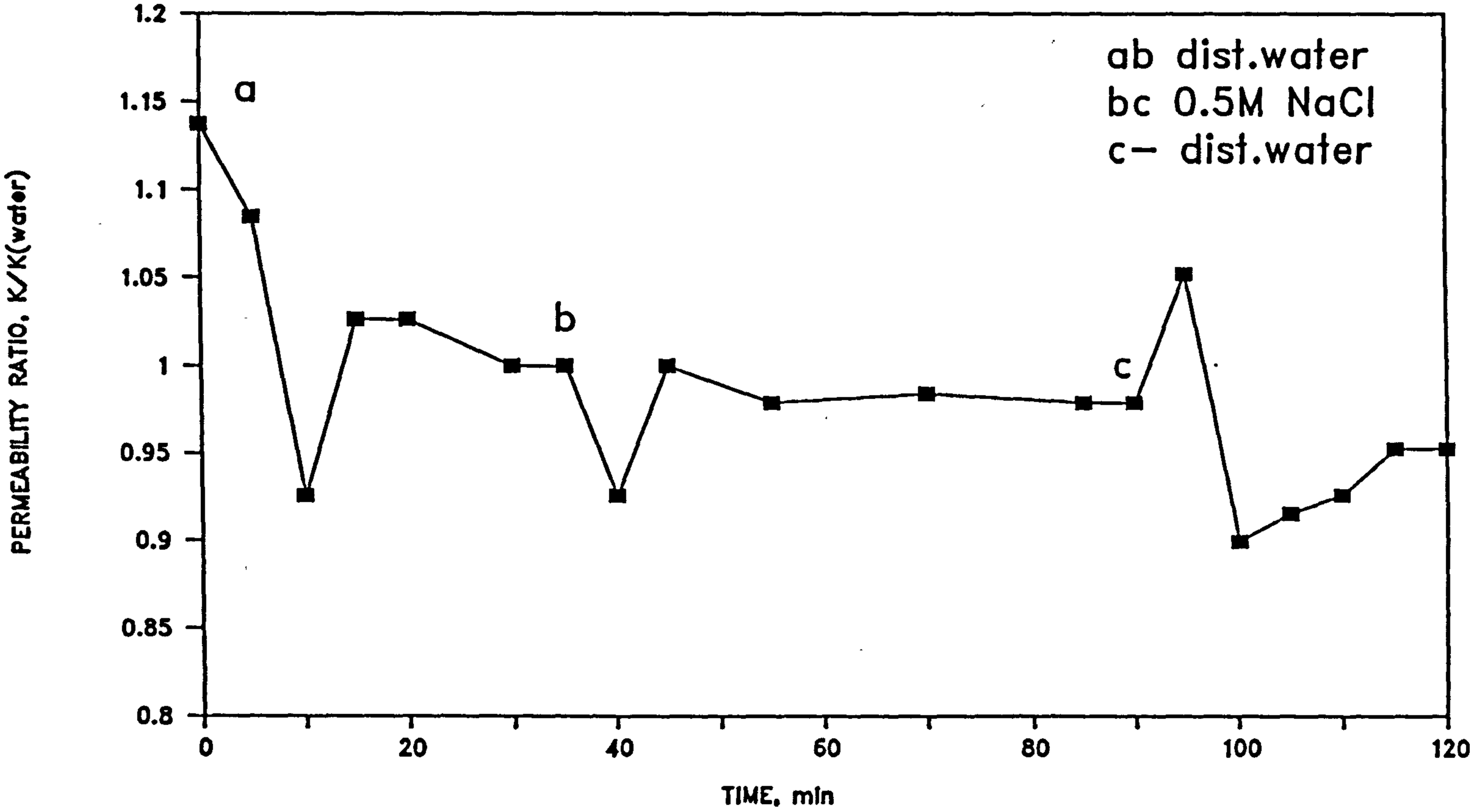

FIG. 15 Constant Head Sandpack Flood
Effect of NaCl Brine on Permeability

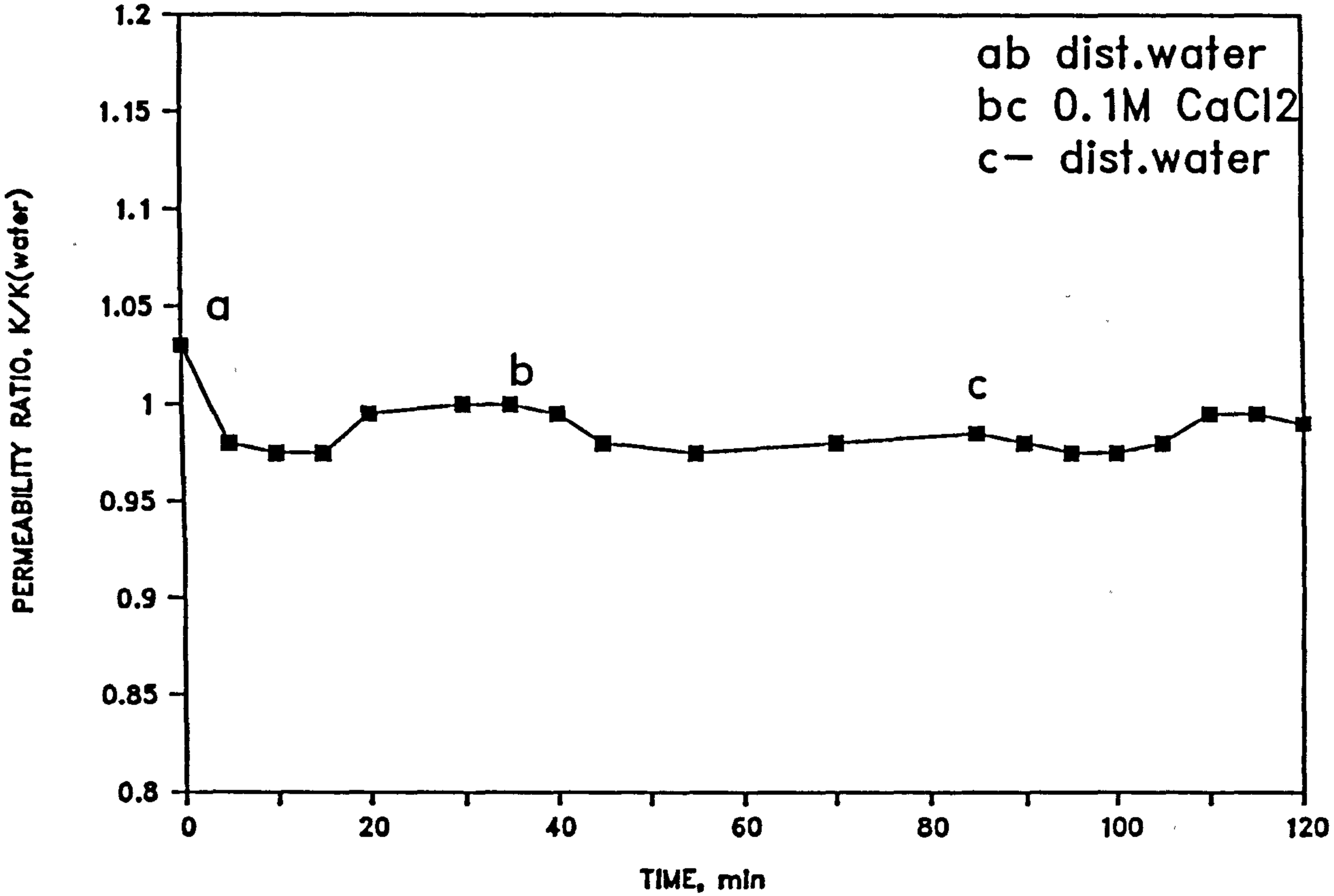

FIG. 16 Constant Head Sandpack Flood
Effect of $CaCl_2$ Brine on Permeability

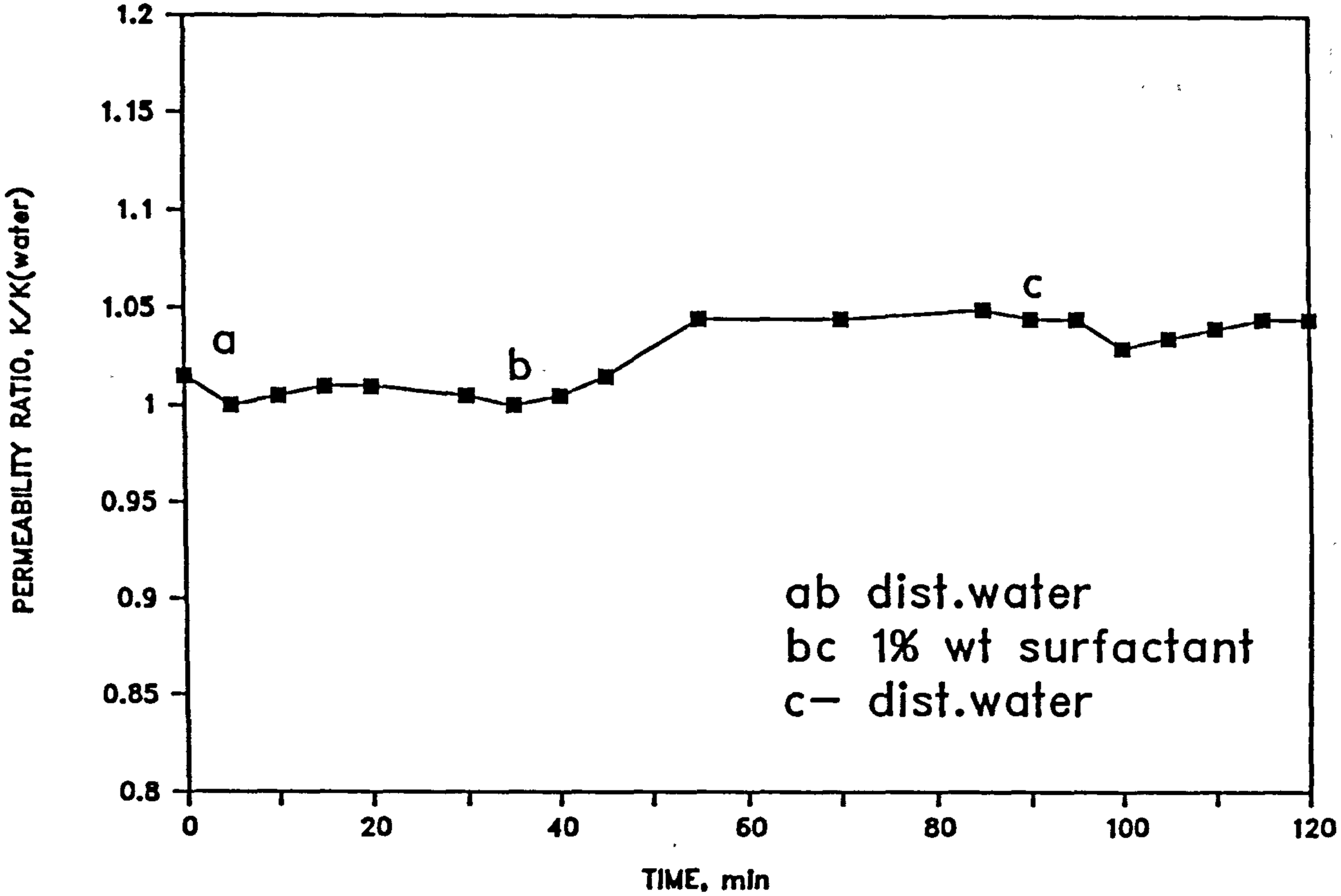

FIG. 17 Constant Head Sandpack Flood
Effect of Surfactant on Permeability

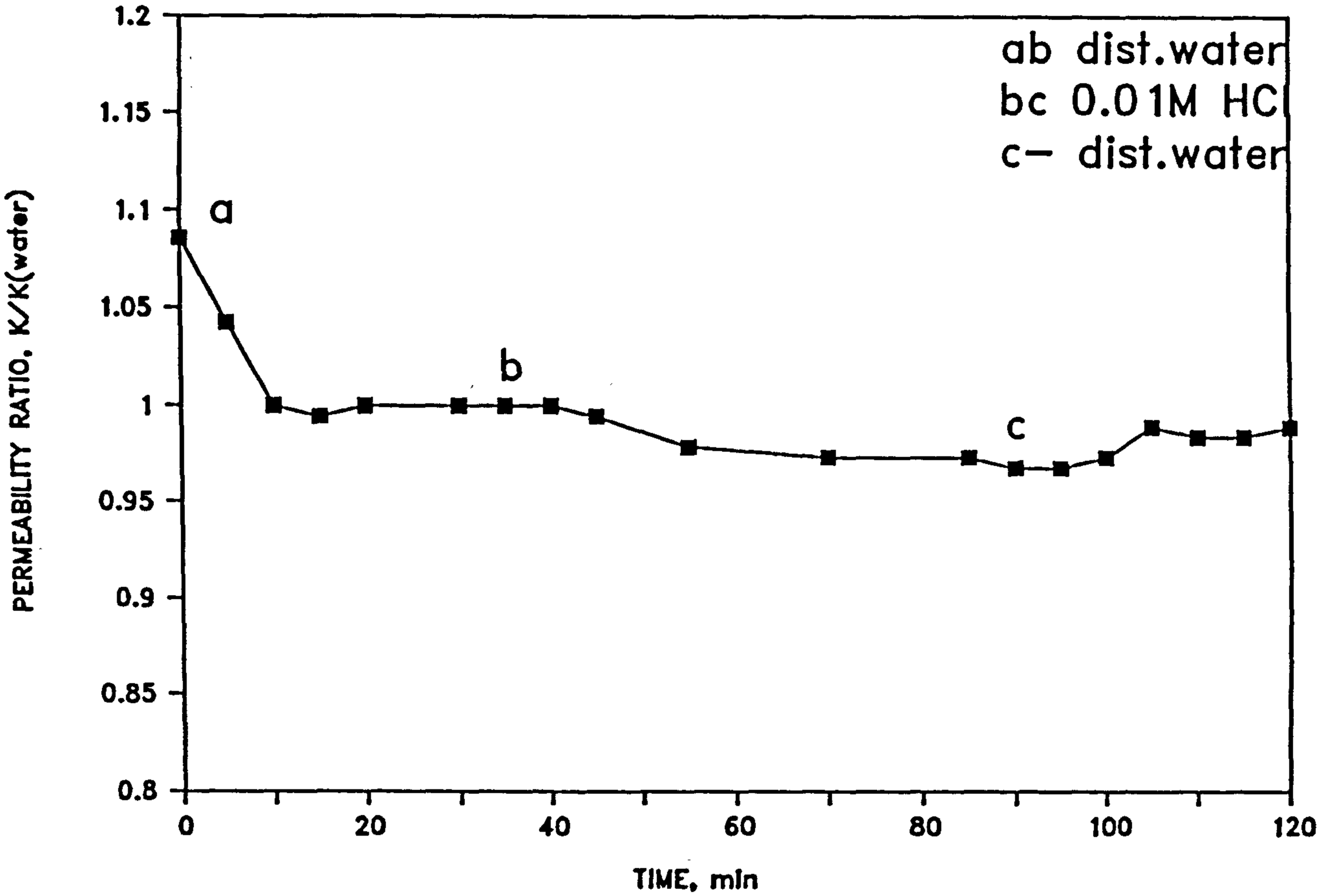

FIG. 18 Constant Head Sandpack Flood
Effect of Acidic Conditions

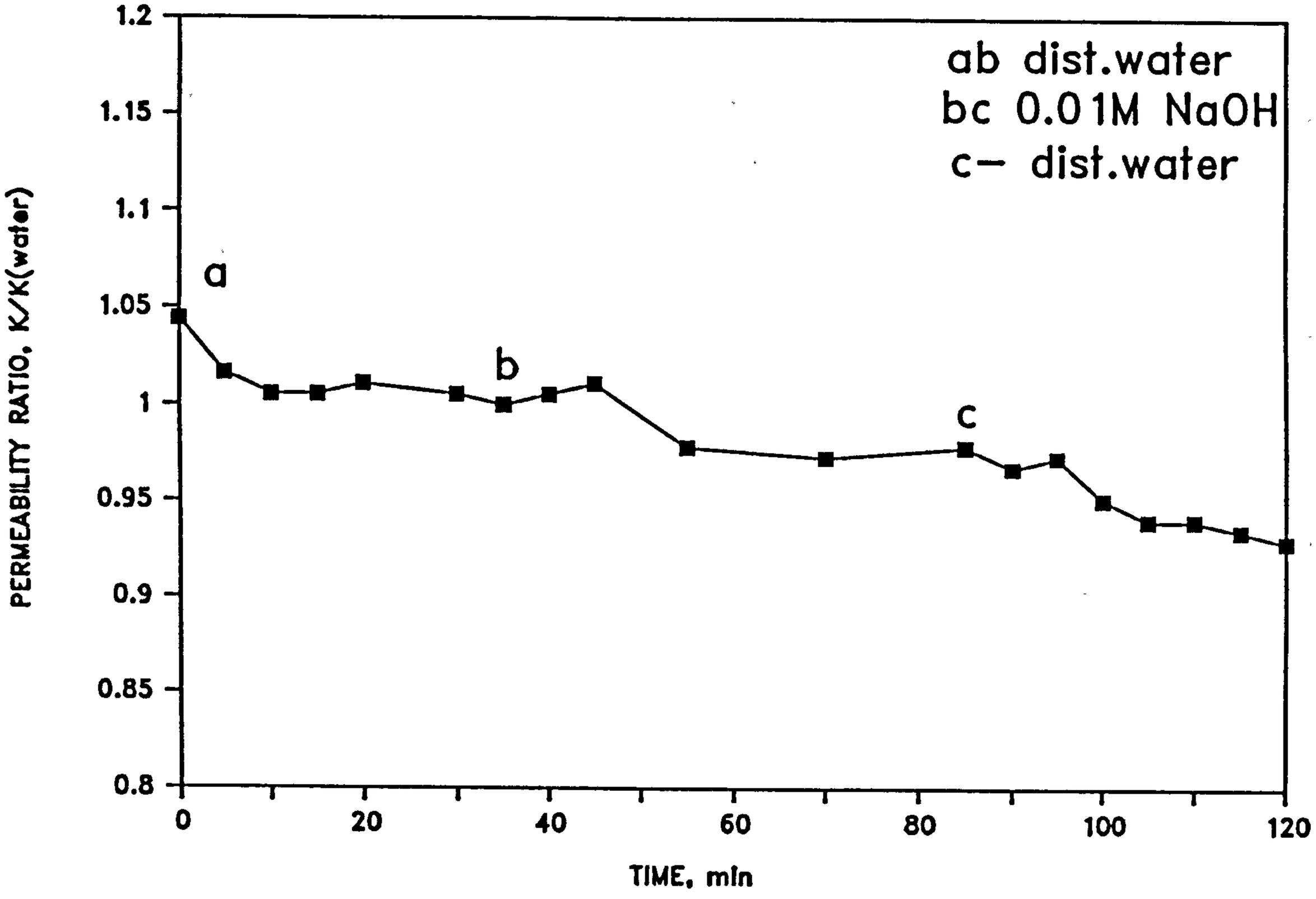

FIG. 19a Constant Head Sandpack Flood
Effect of Alkaline Conditions

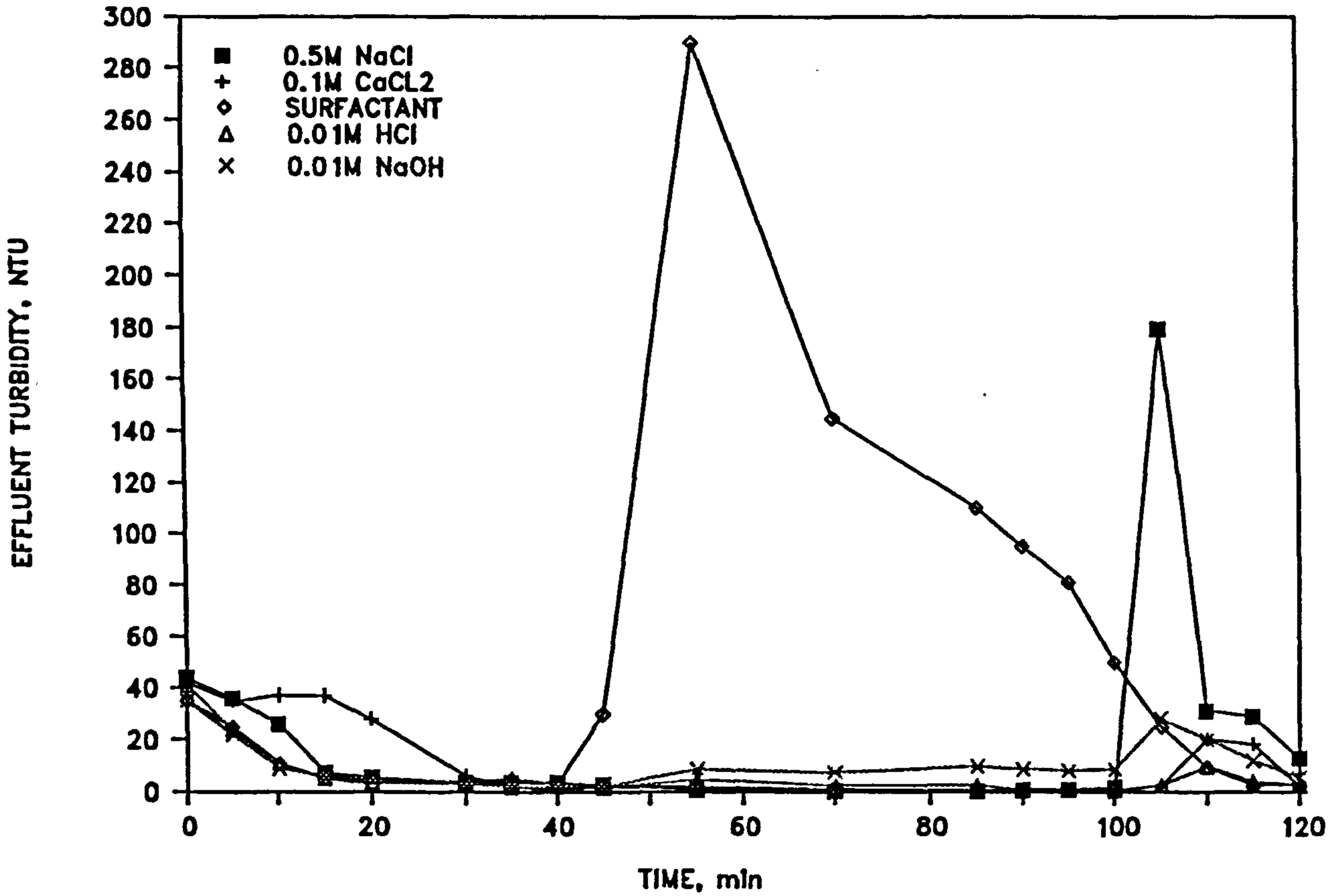

FIG. 19b Effluent Turbidity Profiles for the Constant Head Floods

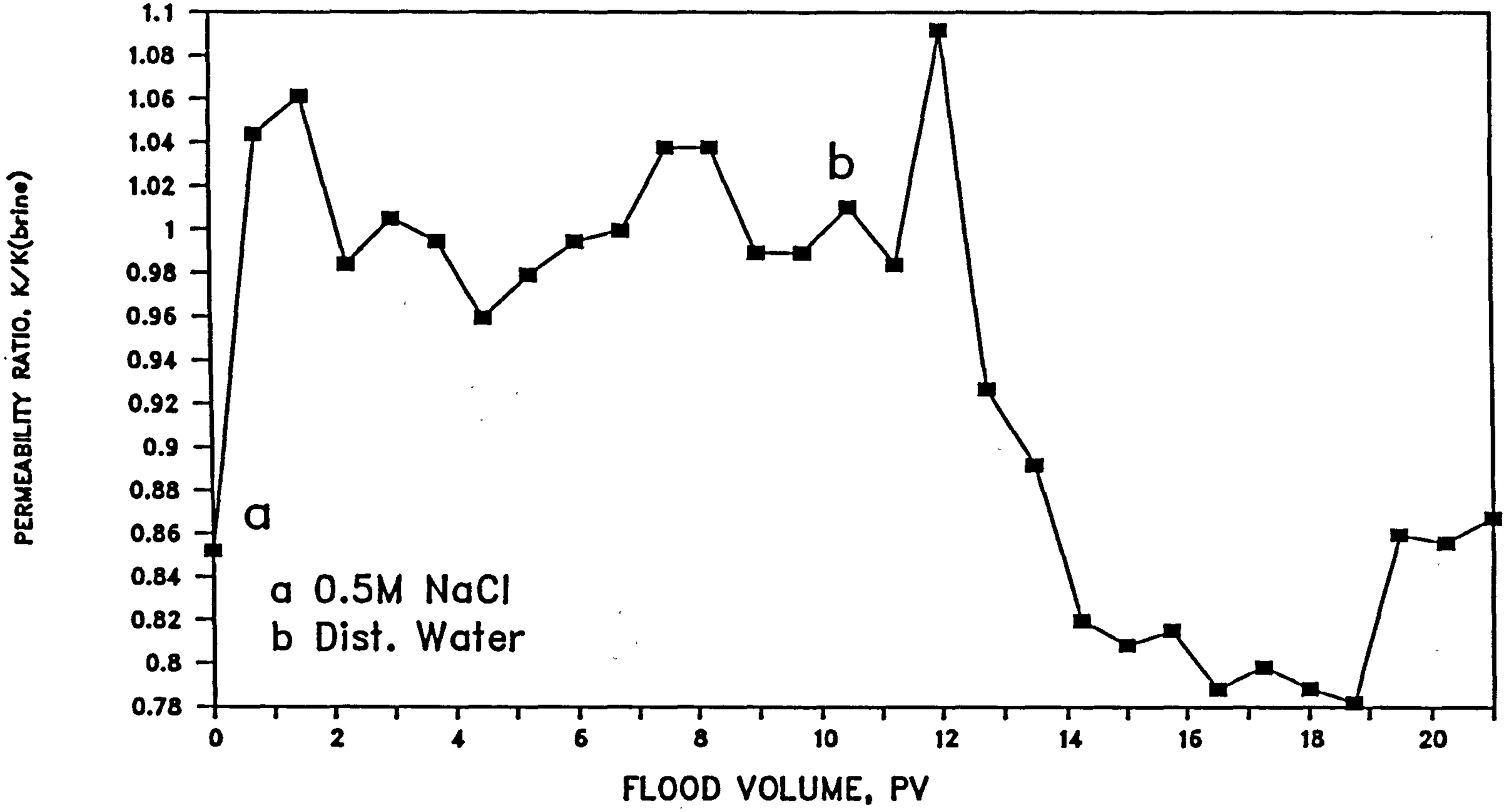

FIG. 20a Sandpack Permeability Ratio Profile
Reservoir Separator Sand, Run 7

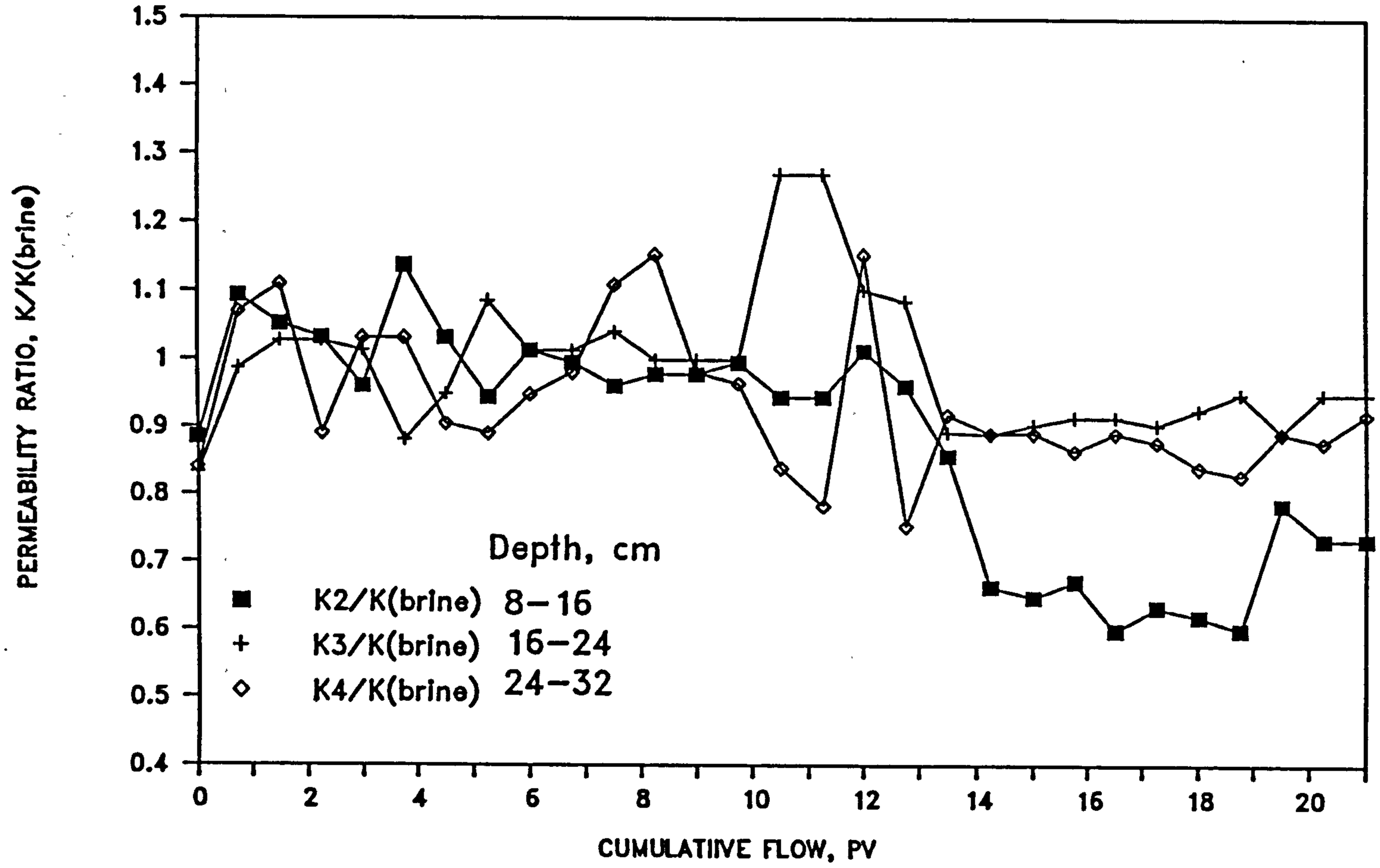

FIG. 20b Intra–Bed Permeability Ratio's, Run 7

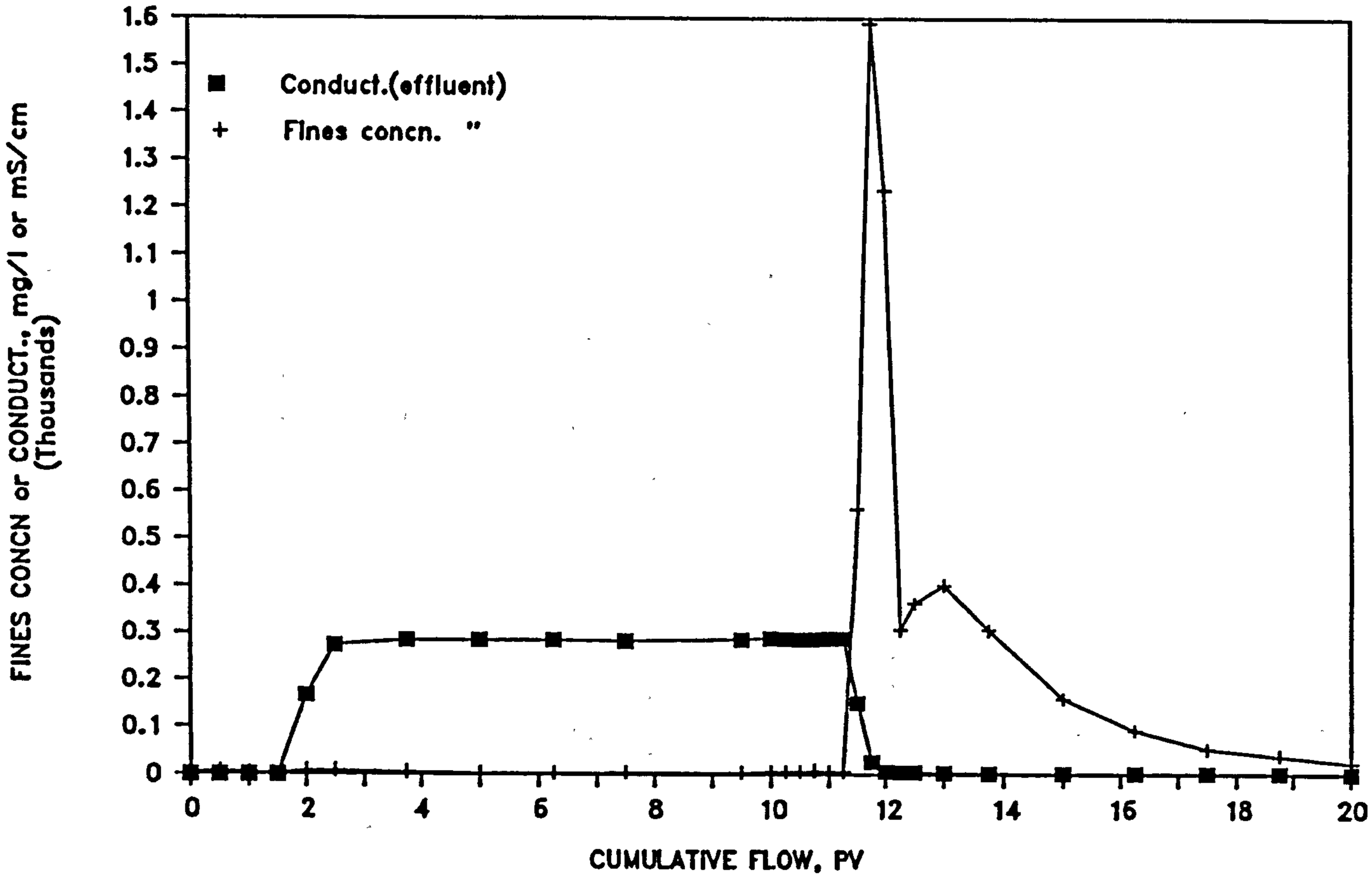

FIG. 20c Sandpack Effluent Conductivity and Fines Content, Run 7

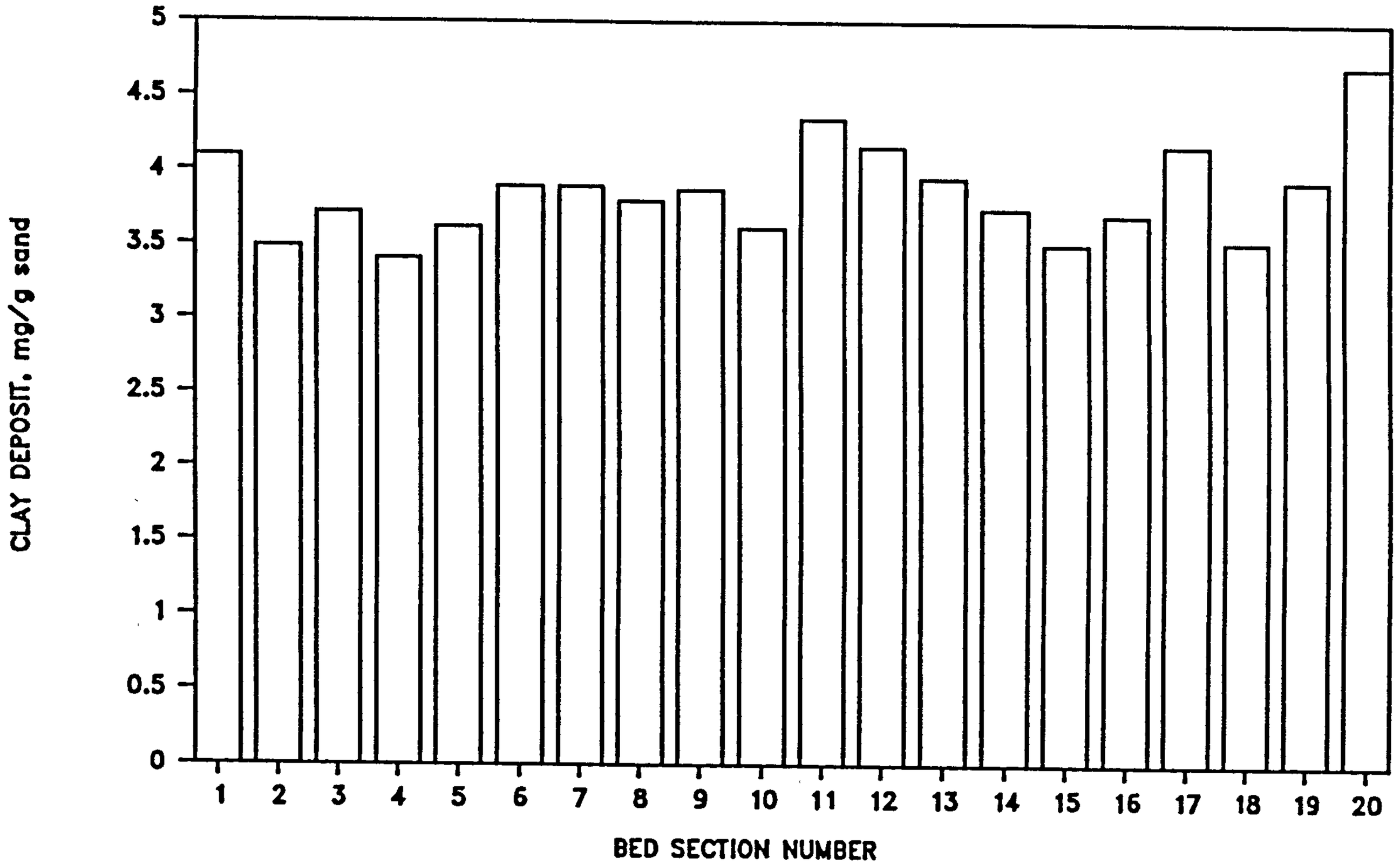

FIG. 20d Intra-Bed Clay Deposit at End of Run 7

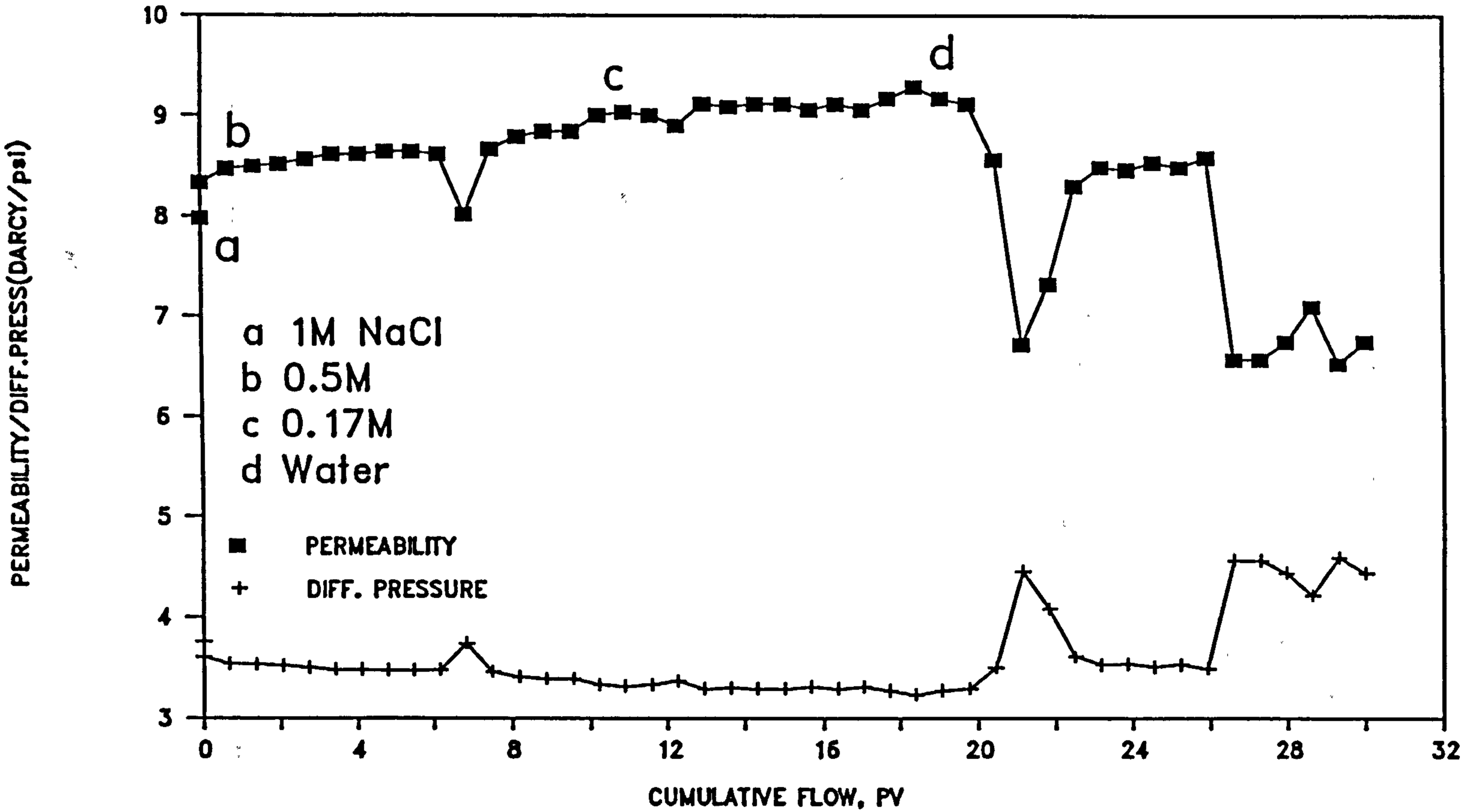

FIG. 21a Sandpack Differential Pressure and Permeability Profile, Run 8

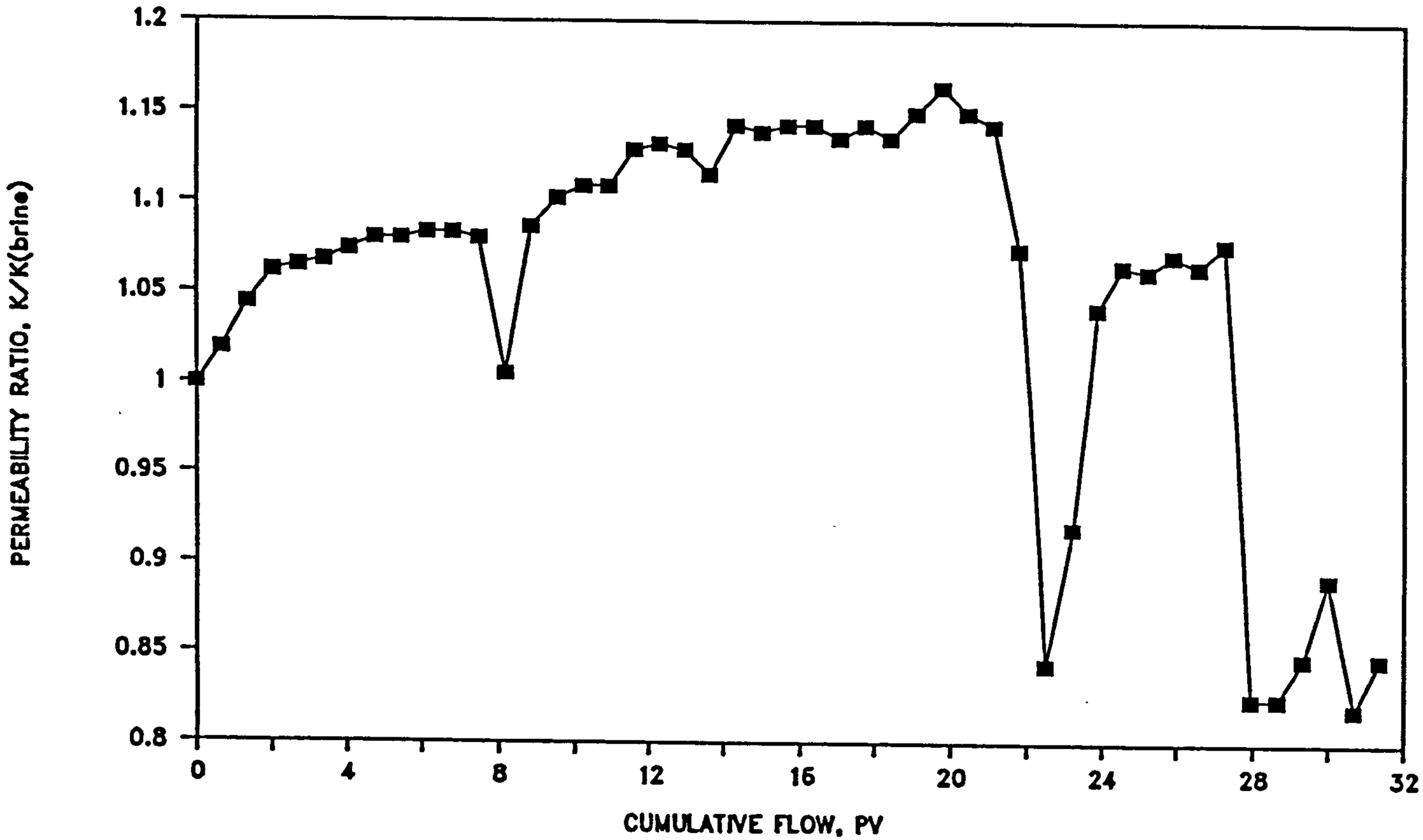

FIG. 21b Sandpack Permeability Ratio, Run 8

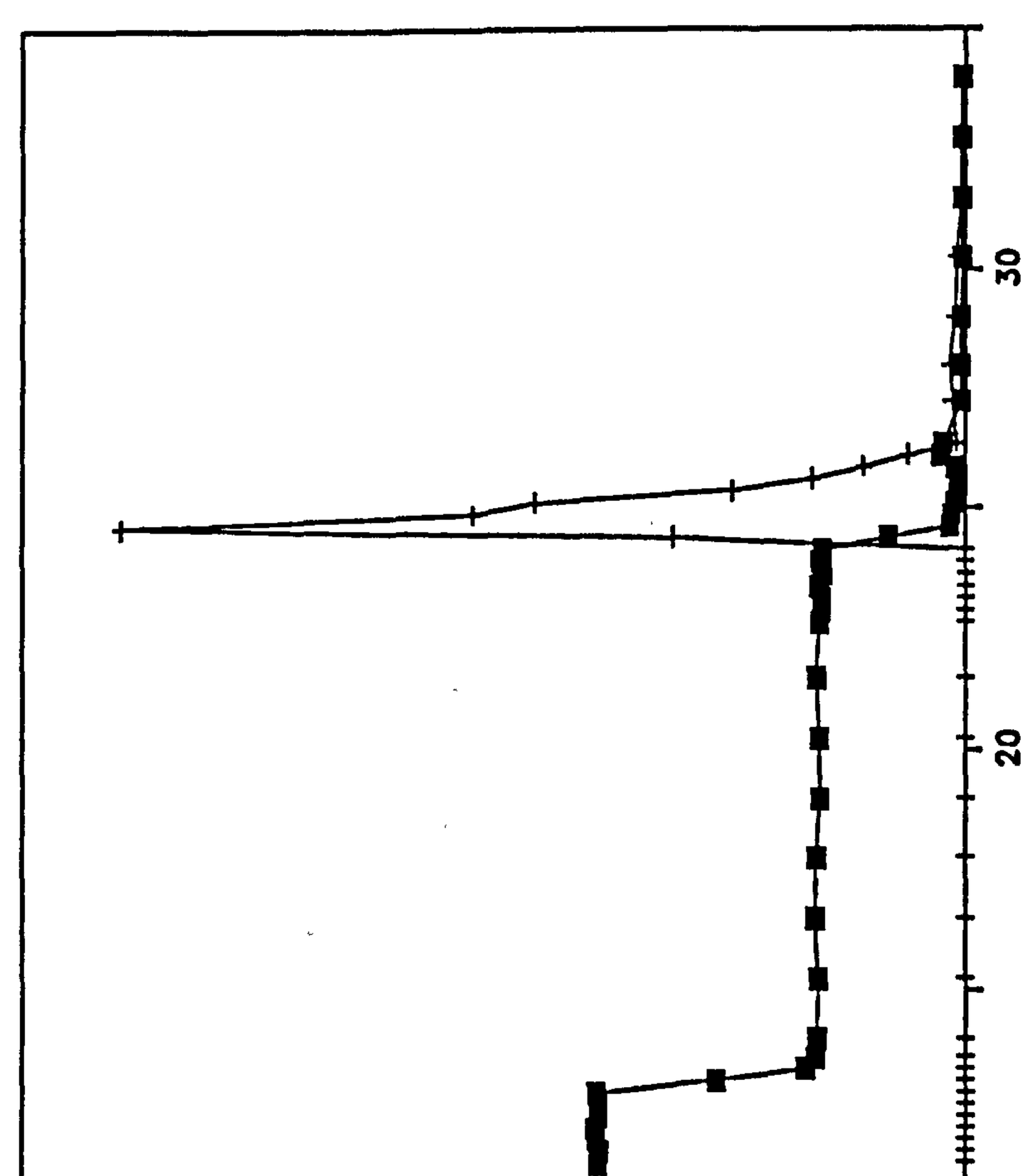
Sandpack Effluent Conductivity and
Clay Concentration, Run 8
Conduct. mS/cm • 0.1
Fines concn. g/l
CUMULATIVE FLOW, PV
CONDUCTIVITY or FINES CONCENTRATION
0
10
20
30
0
1
2
3
4
5
6

FIG. 21c

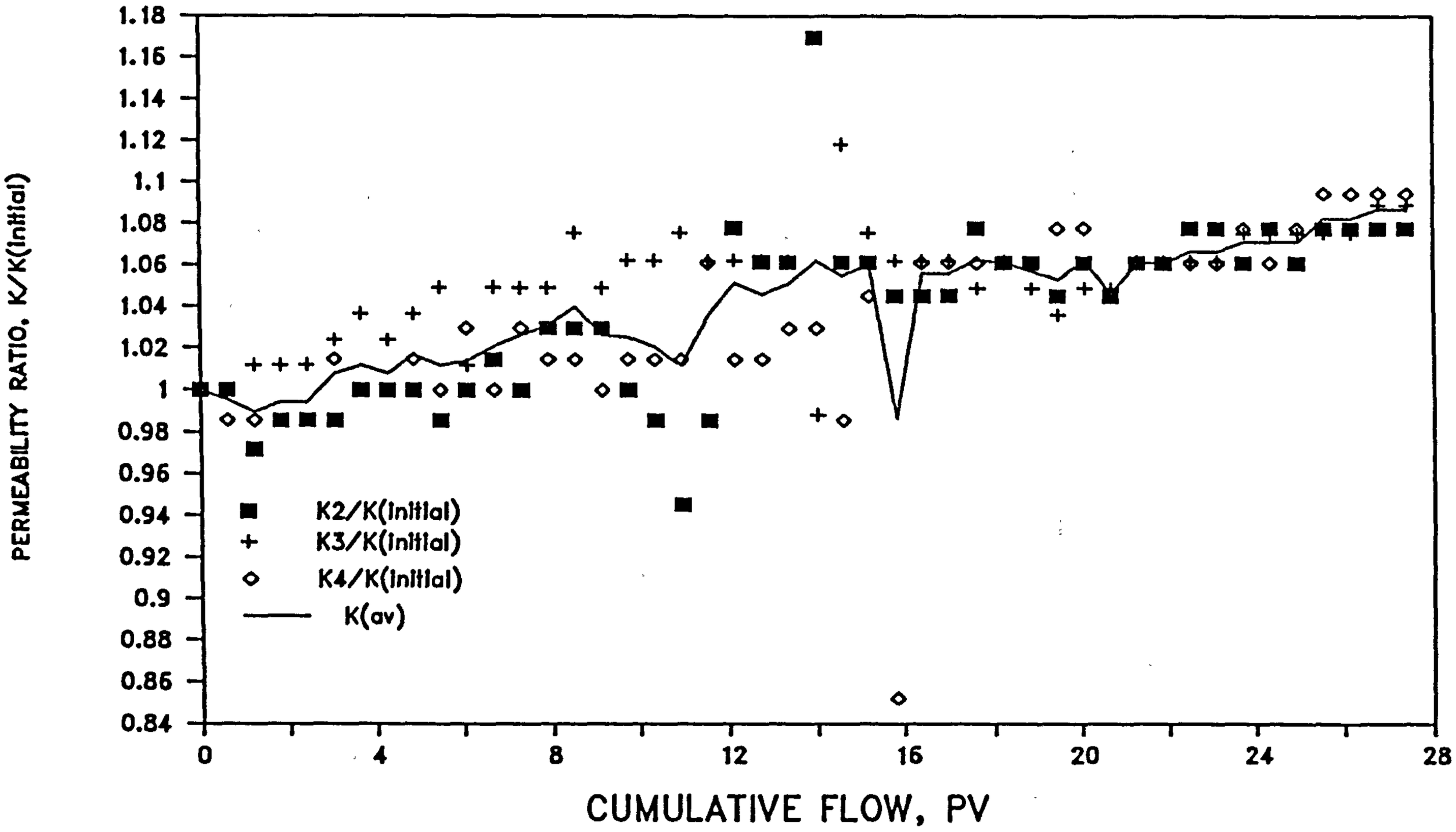

FIG. 22a Mean Sandpack Permeability Ratio
Low Salinity Flood, Run 9

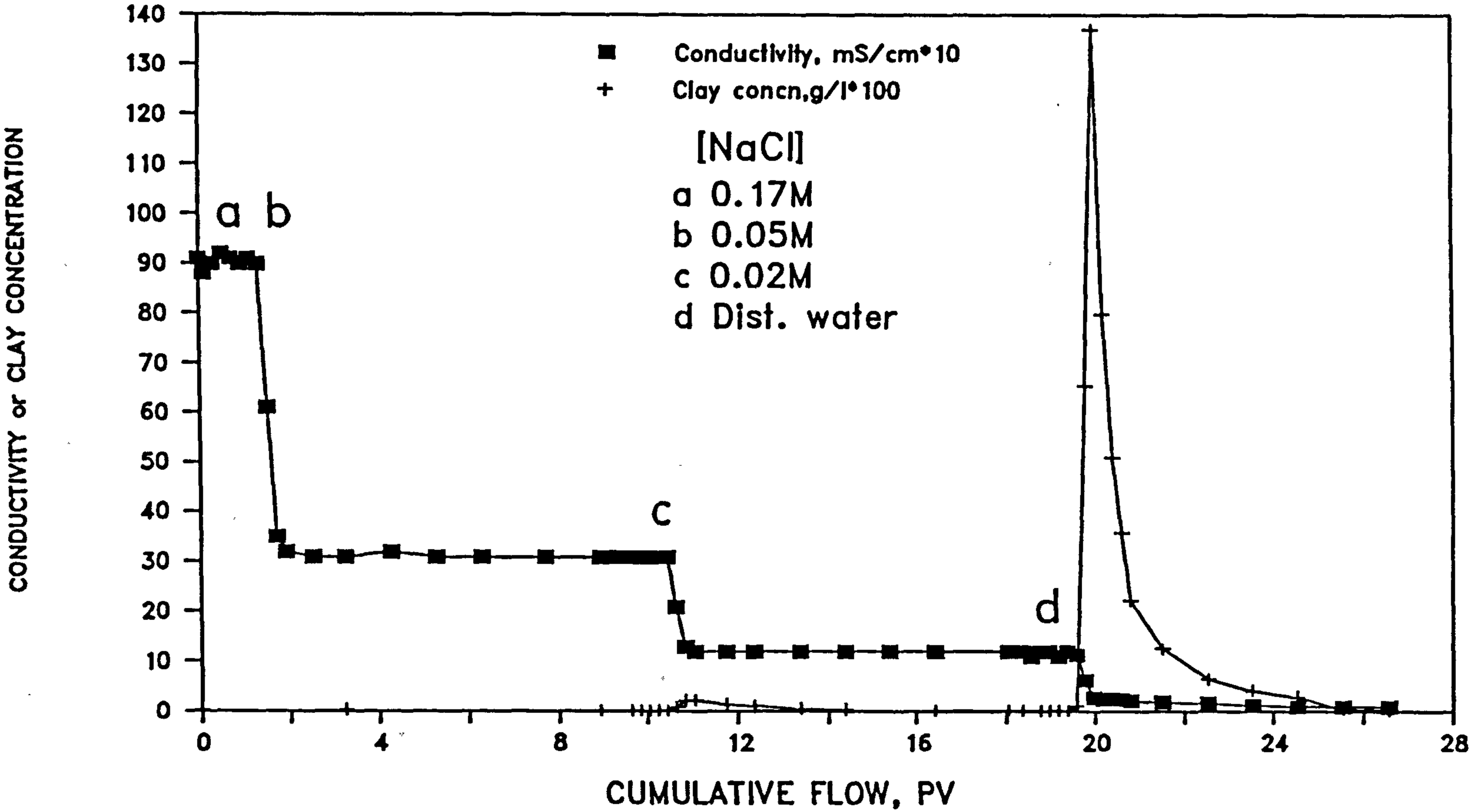

FIG. 22b Sandpack Effluent Conductivity and Clay Content, Run 9

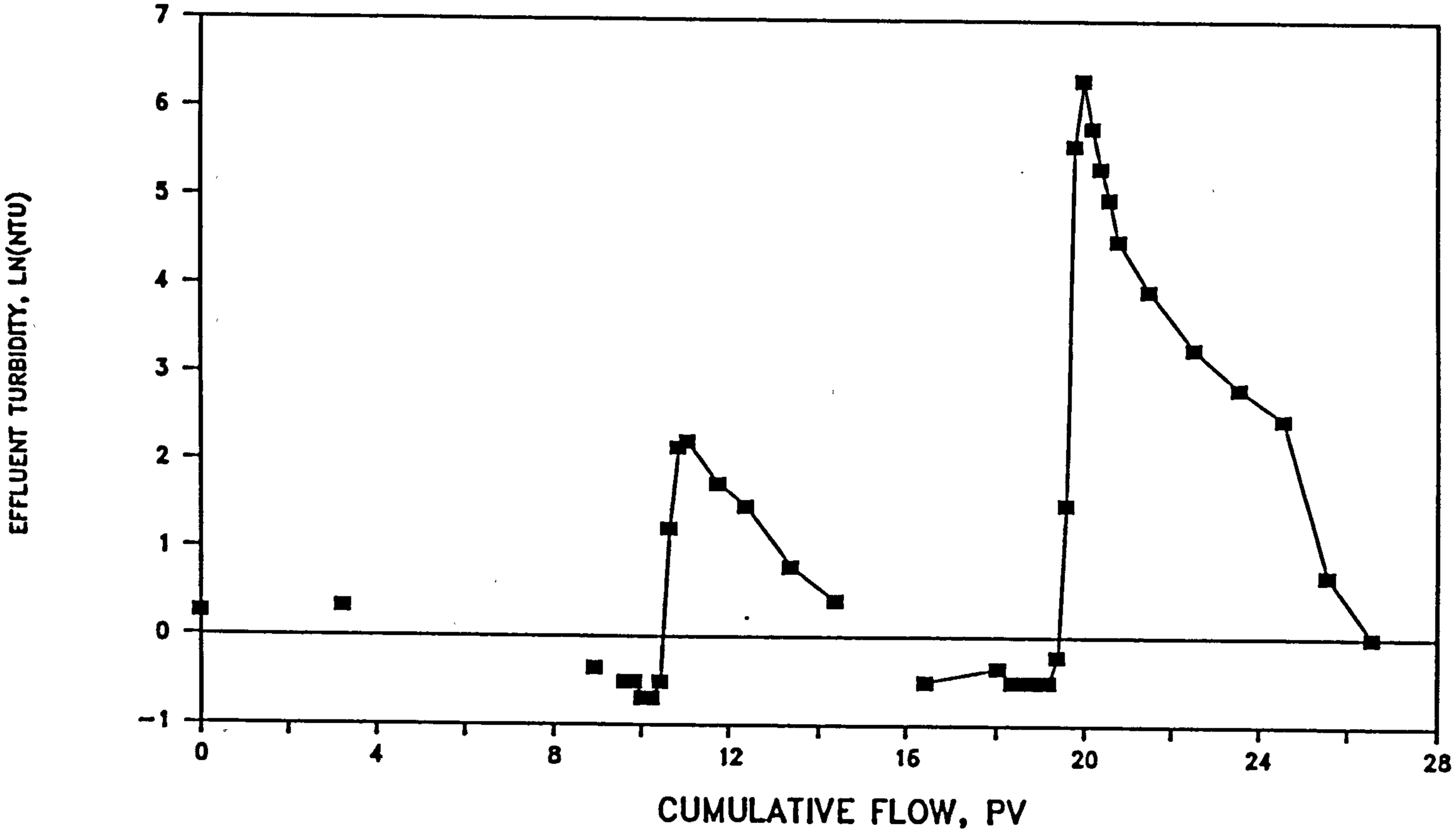

FIG. 22c Effluent Clay Profile, Run 9

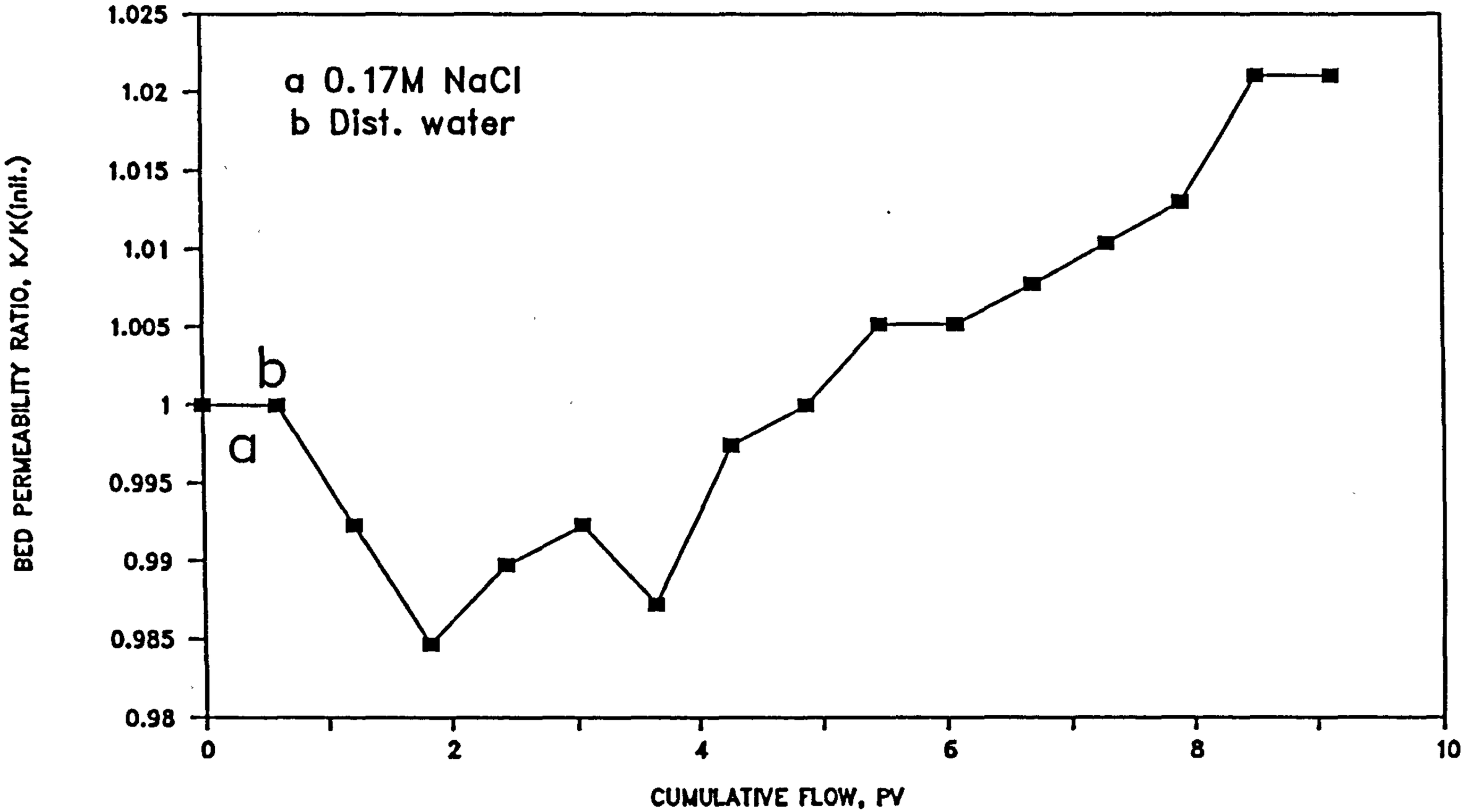

FIG. 23a Sandpack Permeability Ratio for a 0.17M NaCl Flood, Run 10

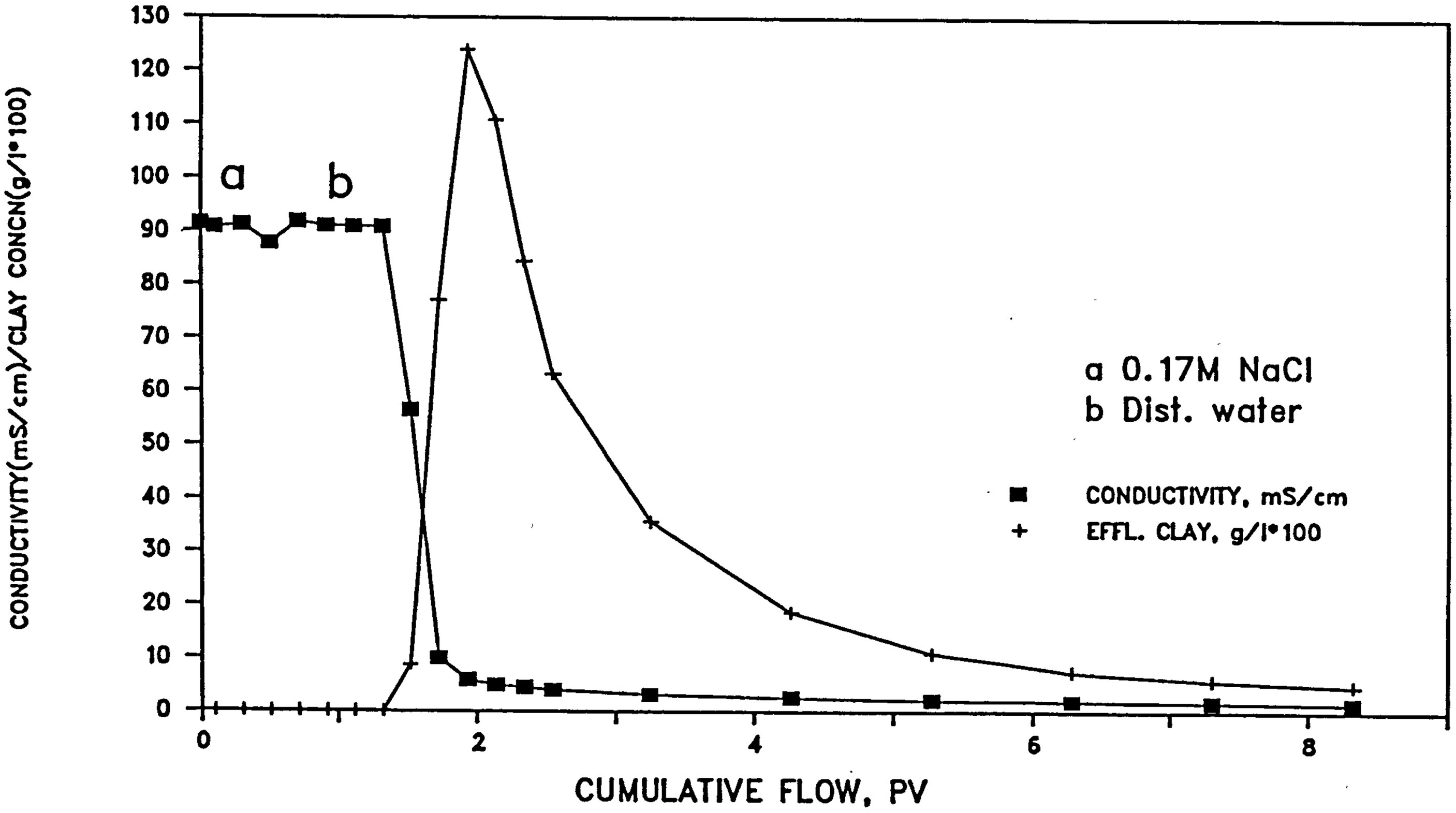

FIG. 23b Effluent Conductivity and Clay Profiles for Run 10

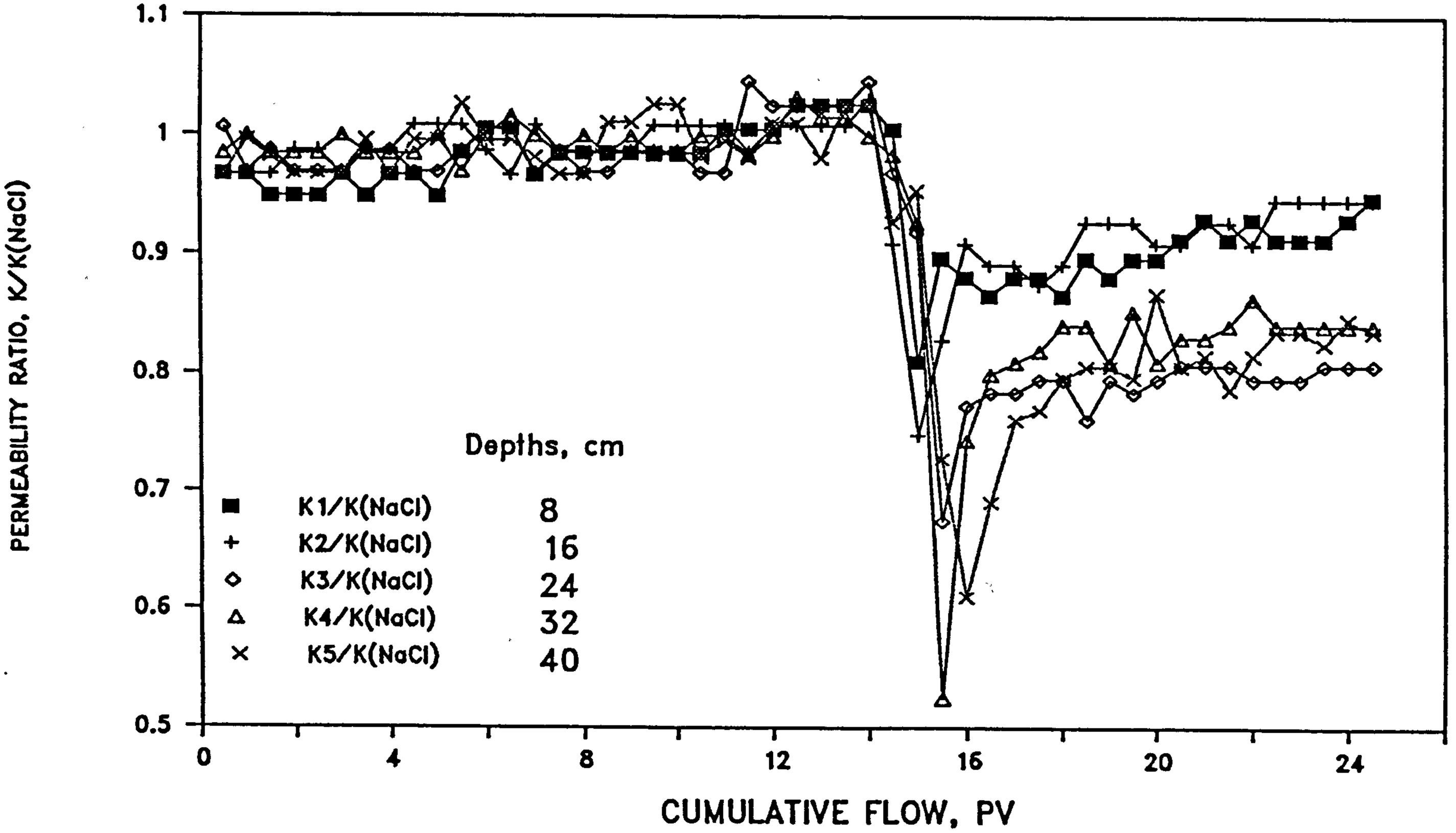

FIG. 24a Sandpack Section Permeability Ratio's Effect of 10 PV NaCl Brine Flood

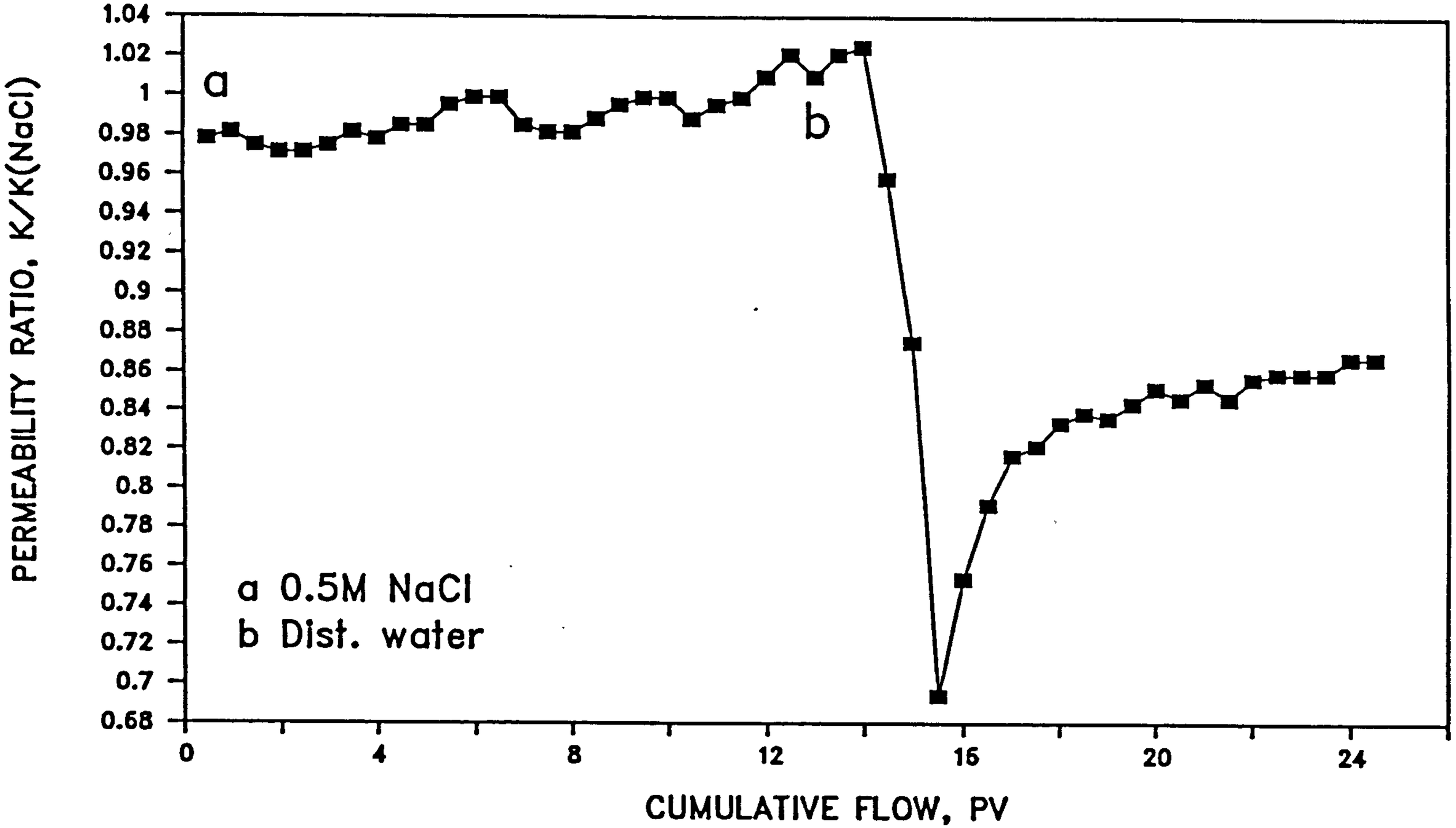

FIG. 24b Mean Sandpack Permeability Ratio
10 PV NaCl Brine Flood

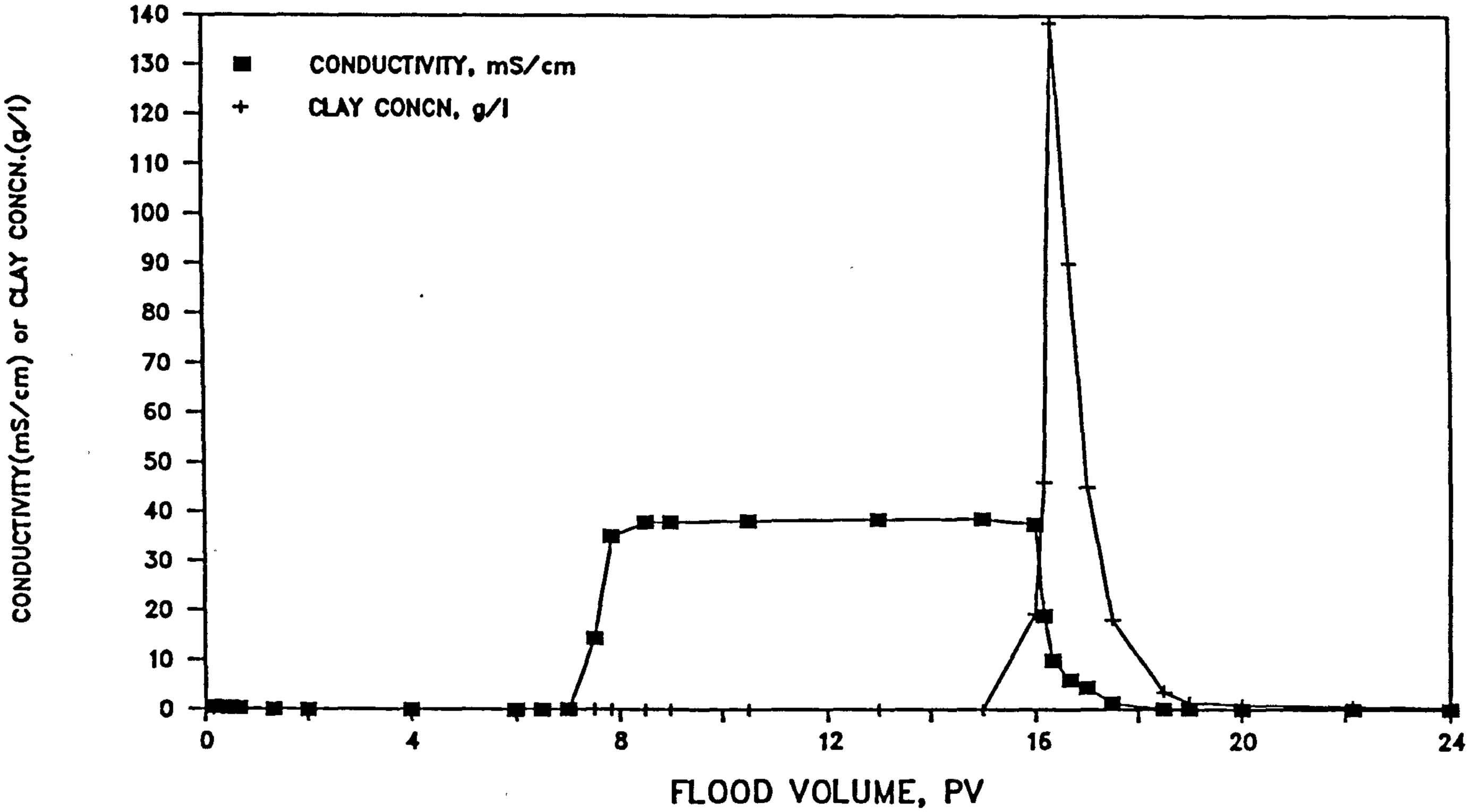

FIG. 24c Effluent Conductivity and Clay Content for 10 PV NaCl Brine Flood

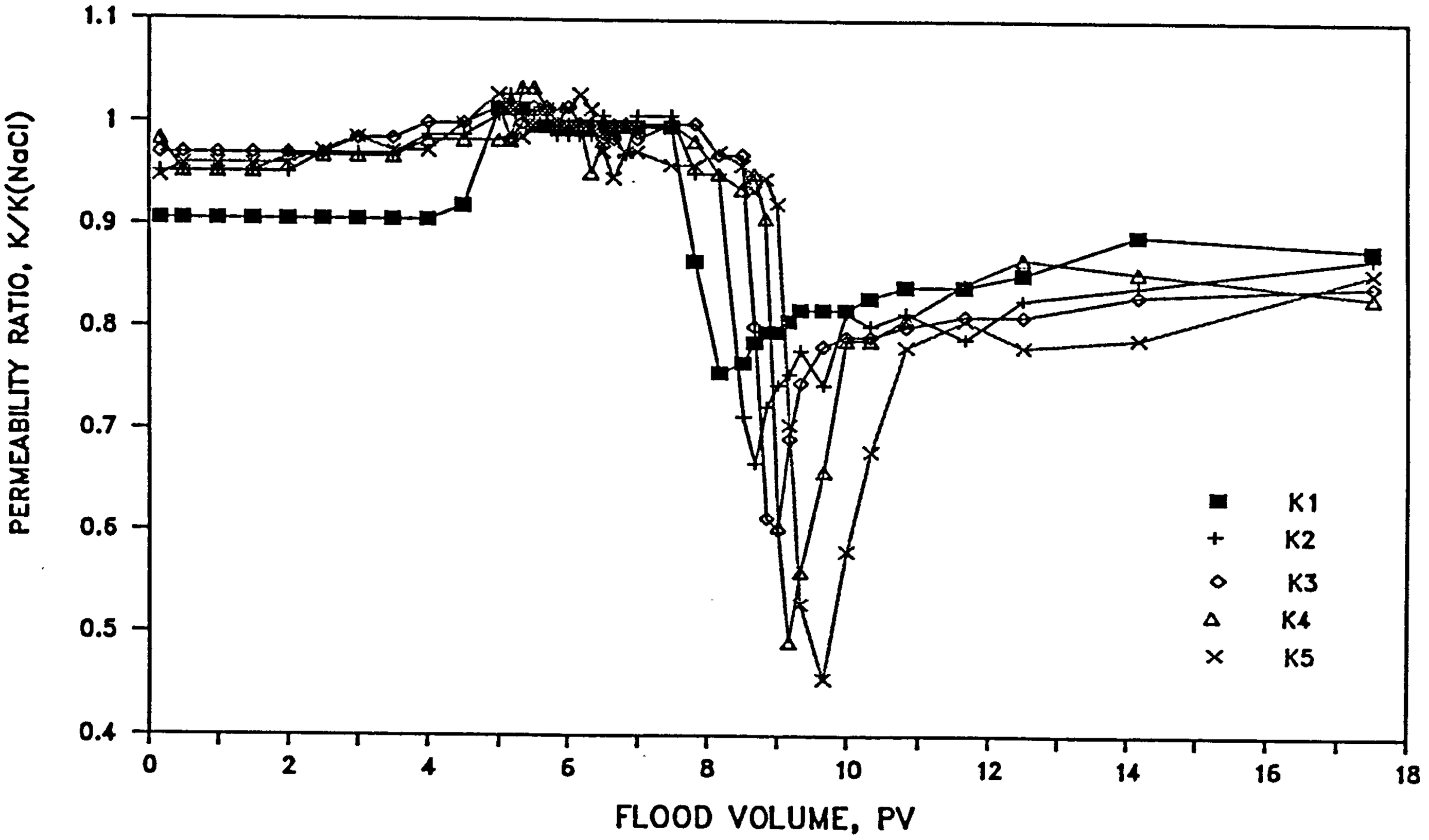

FIG. 25a Sandpack Section Permeability Profiles for 2.5 PV NaCl Flood

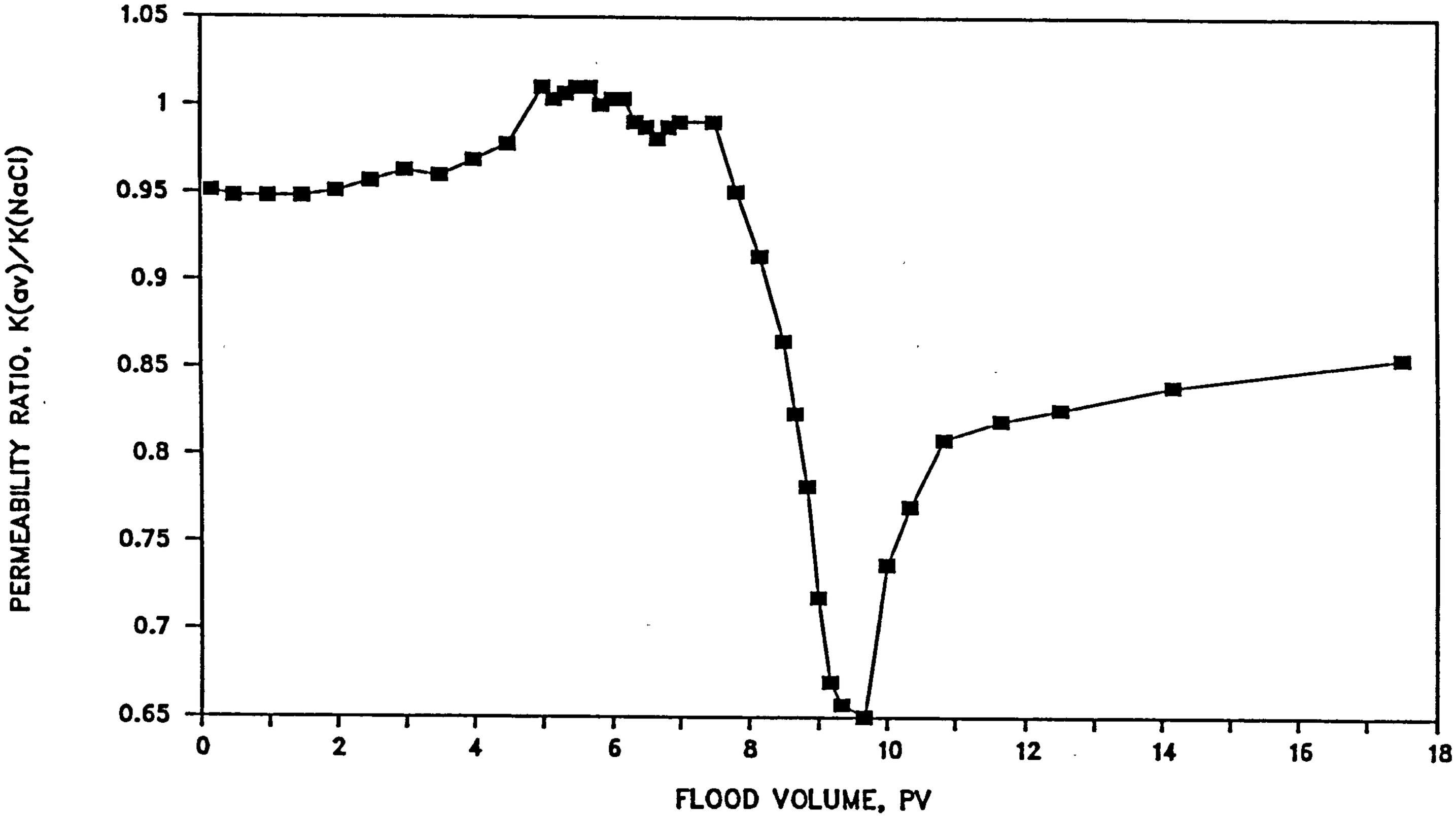

FIG. 25b Mean Sandpack Permeability Ratio for 2.5 PV Flood

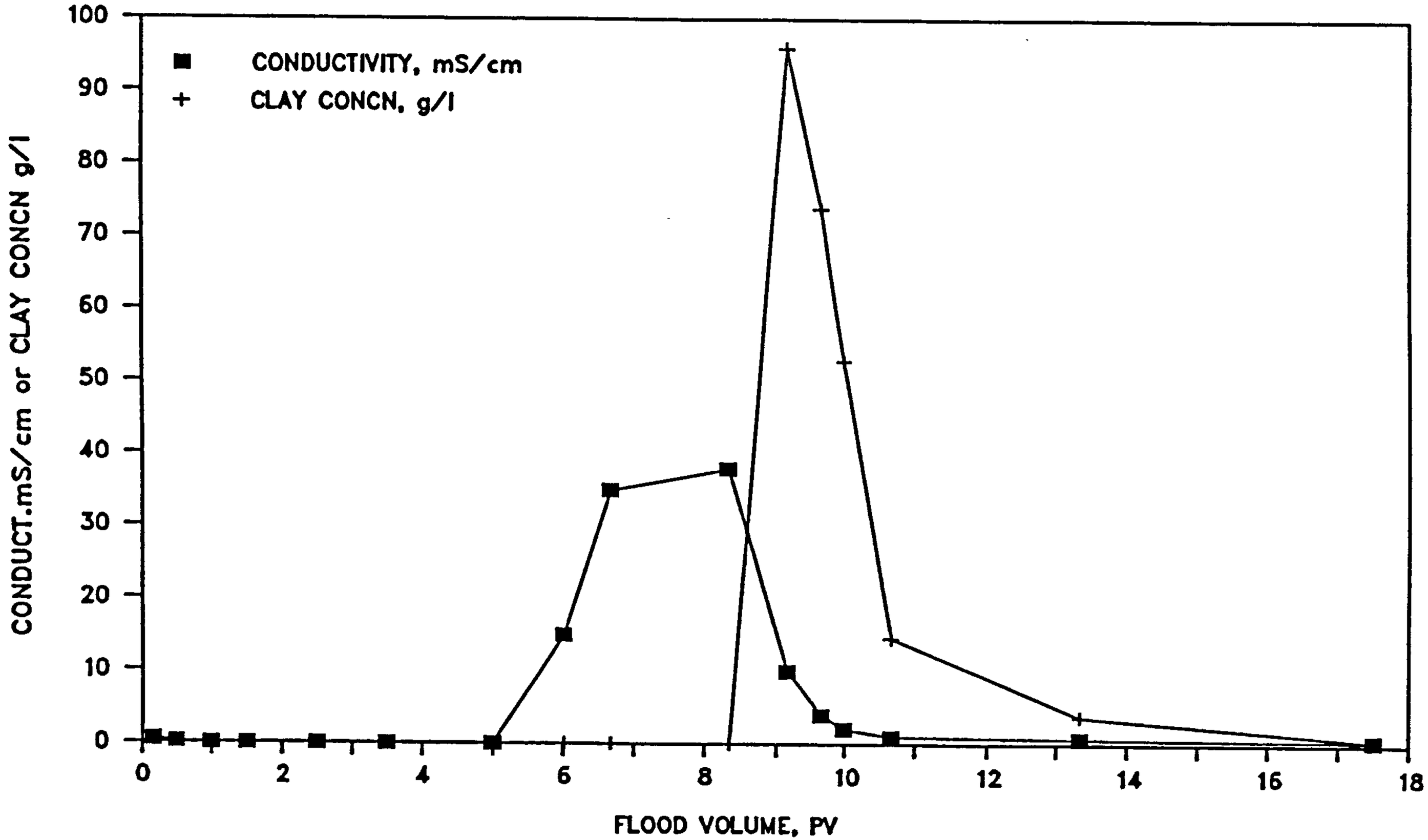

FIG. 25c Effluent Conductivity and Clay Profile for 2.5 PV Flood

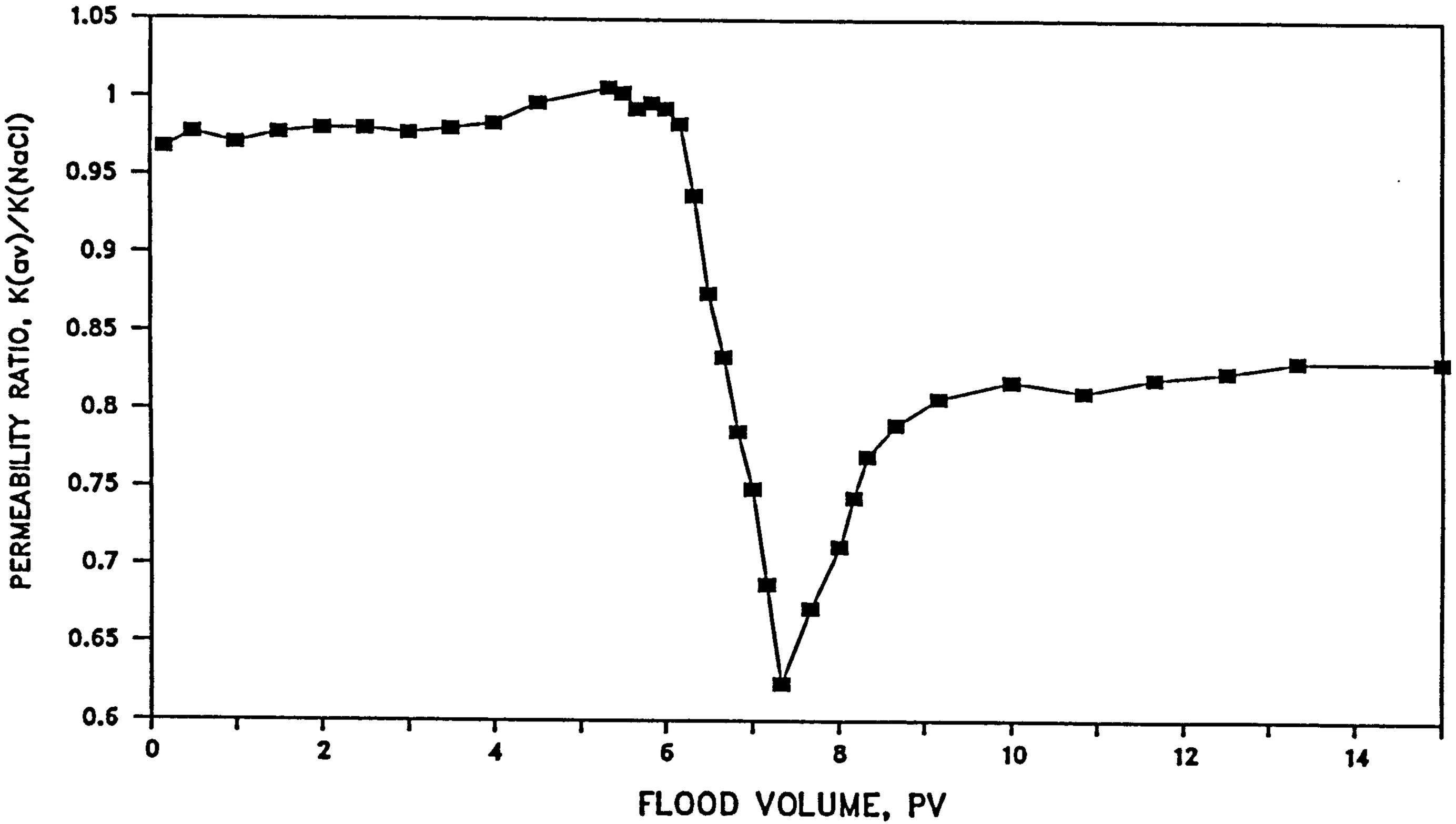

FIG. 26a Mean Sandpack Permeability Ratio for 1 PV Flood

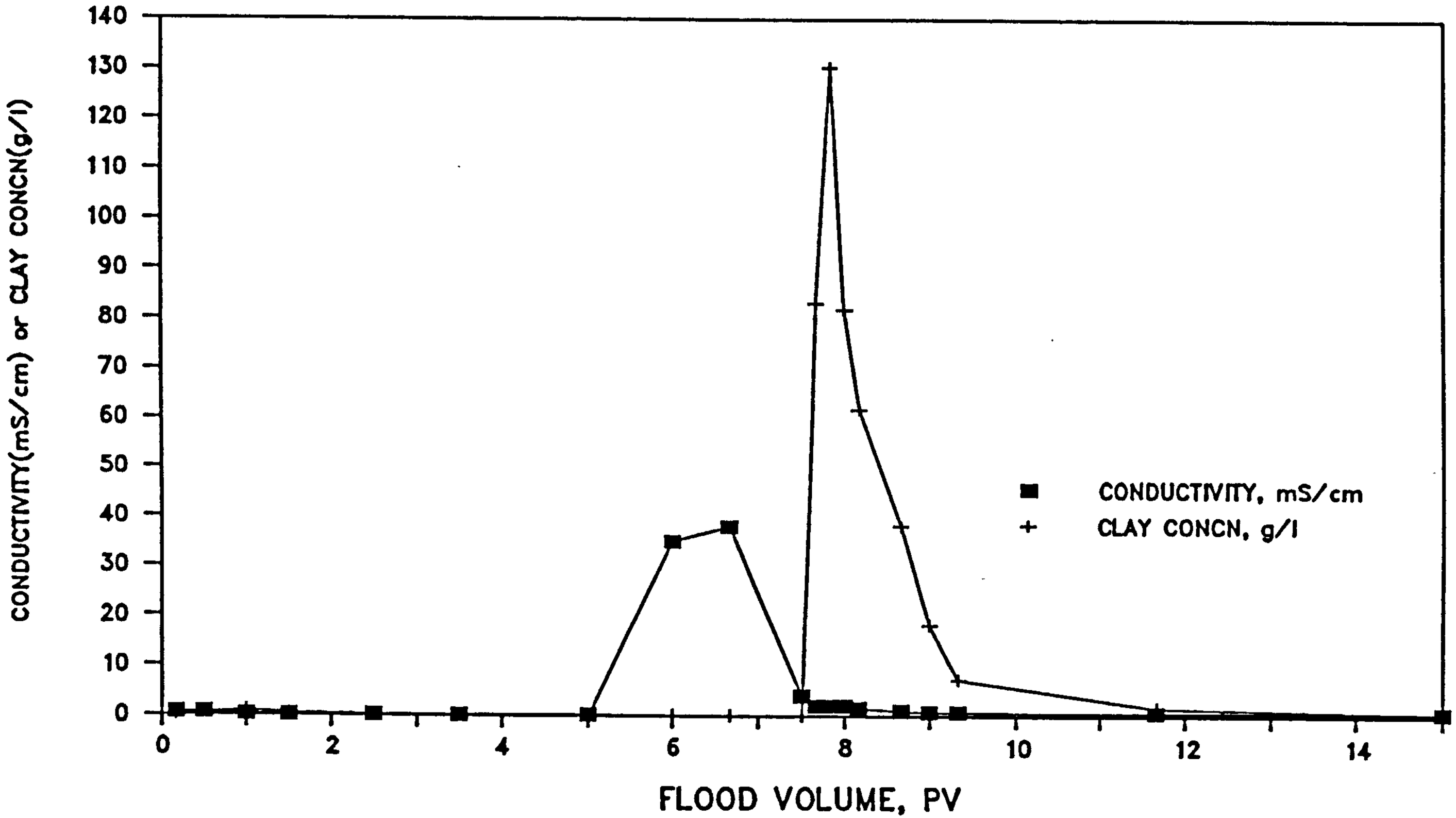

FIG. 26b Effluent Conductivity and Clay Profiles for 1 PV Flood

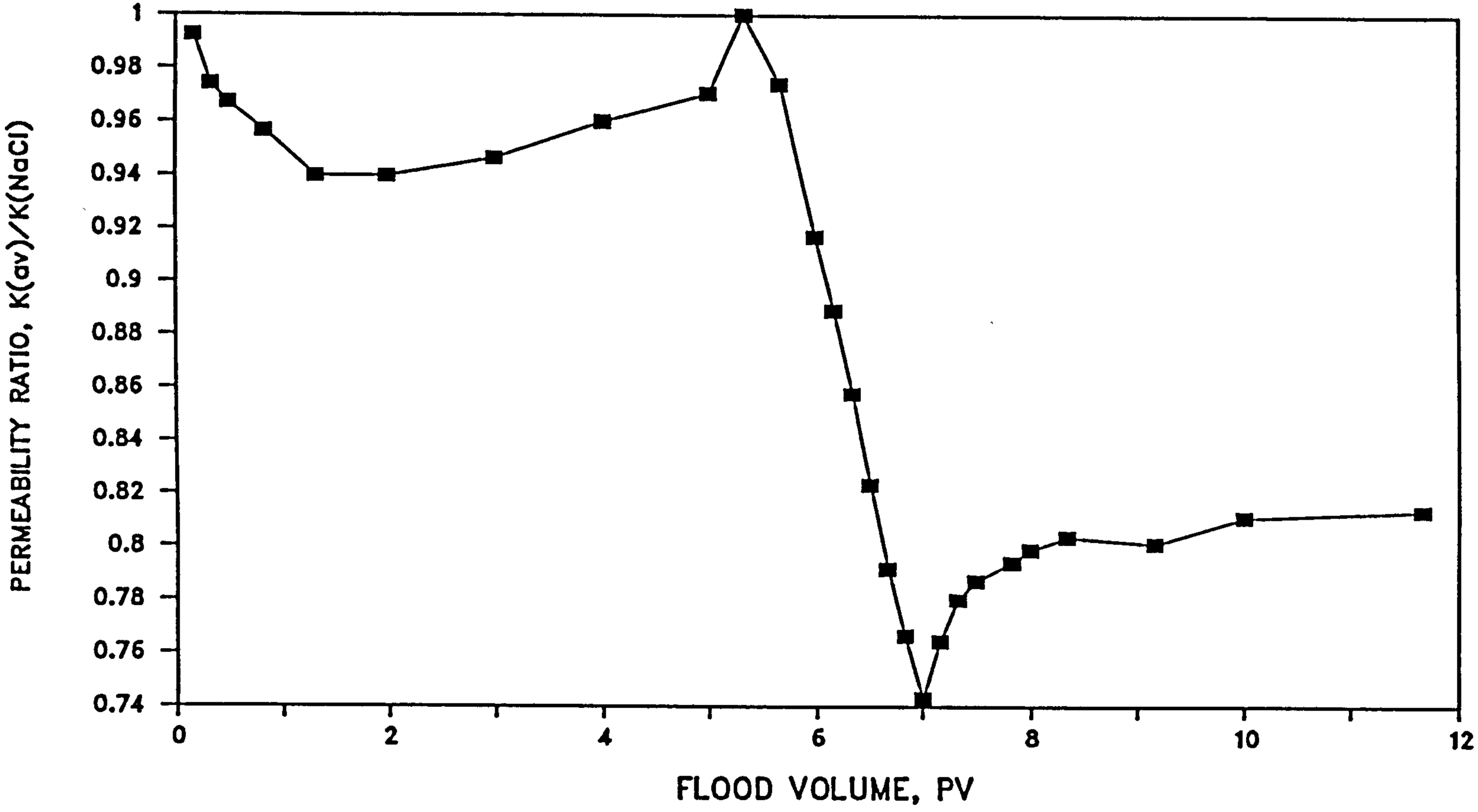

FIG. 27a Mean Sandpack Permeability Ratio for 0.3 PV Flood

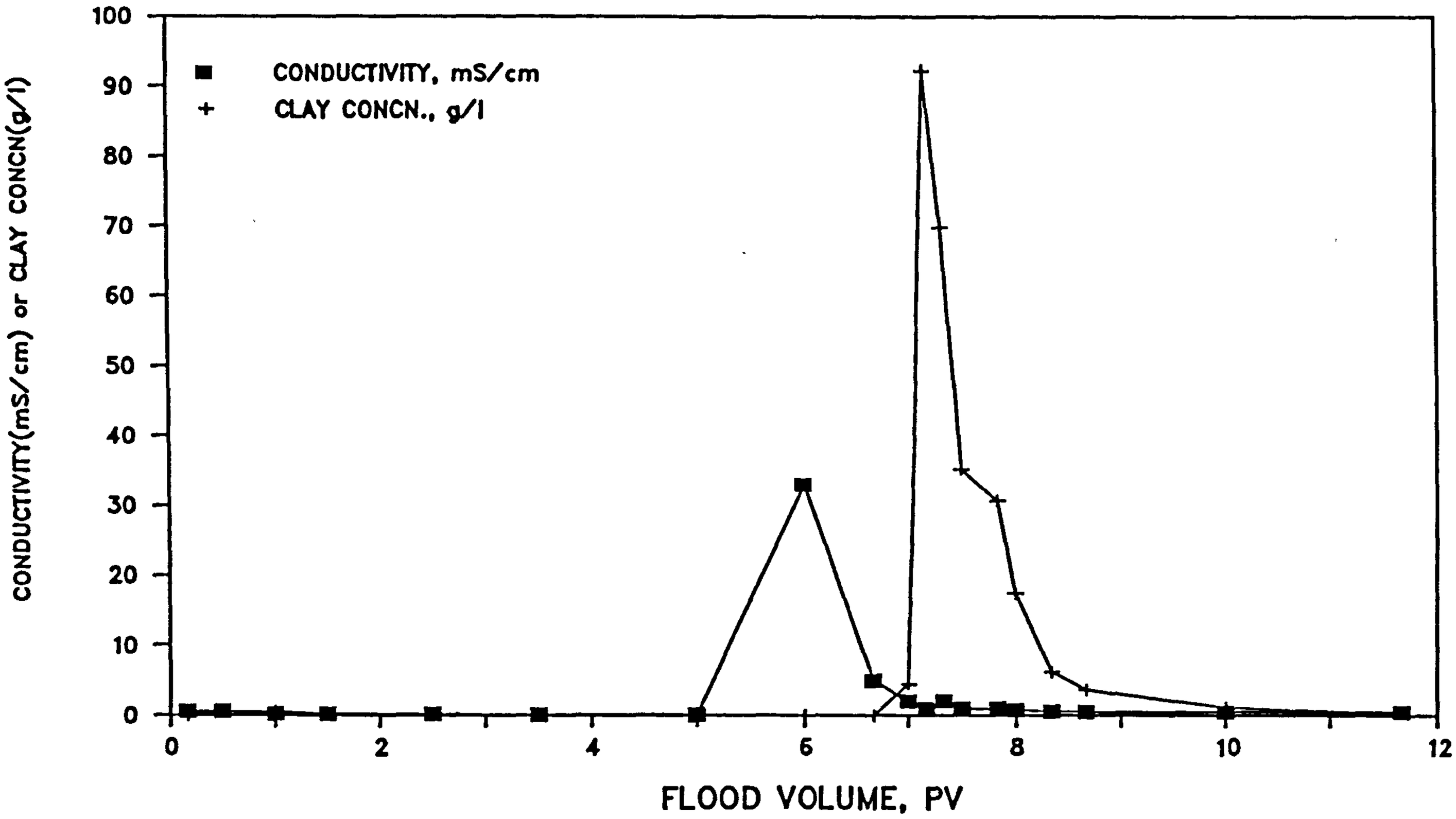

FIG. 27b Effluent Conductivity and Clay Profile for 0.3 PV Flood

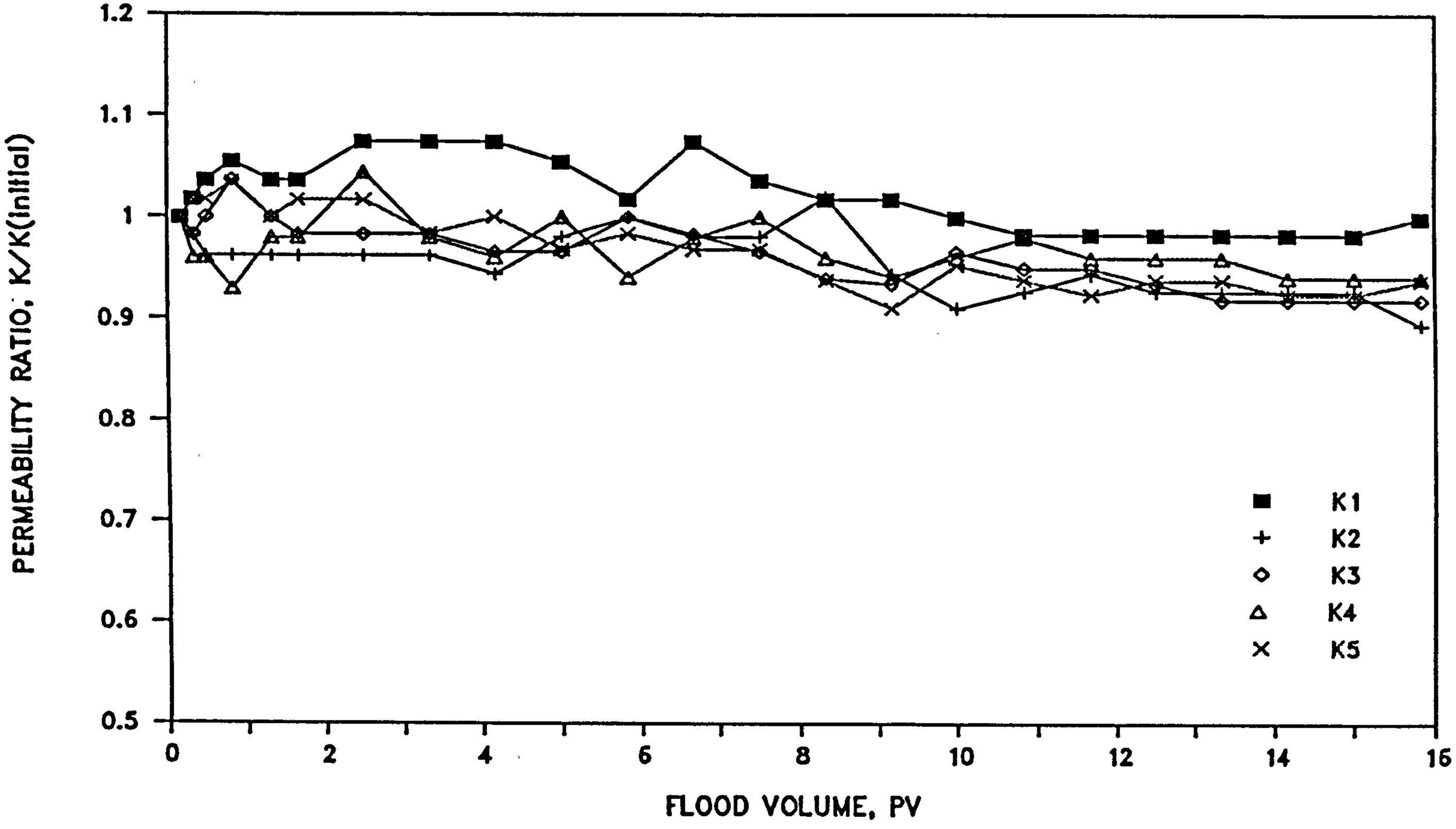

FIG. 28a Sandpack Section Permeability Profiles for Decreasing Salinity Flood($t_{1/2}$= 3 PV)

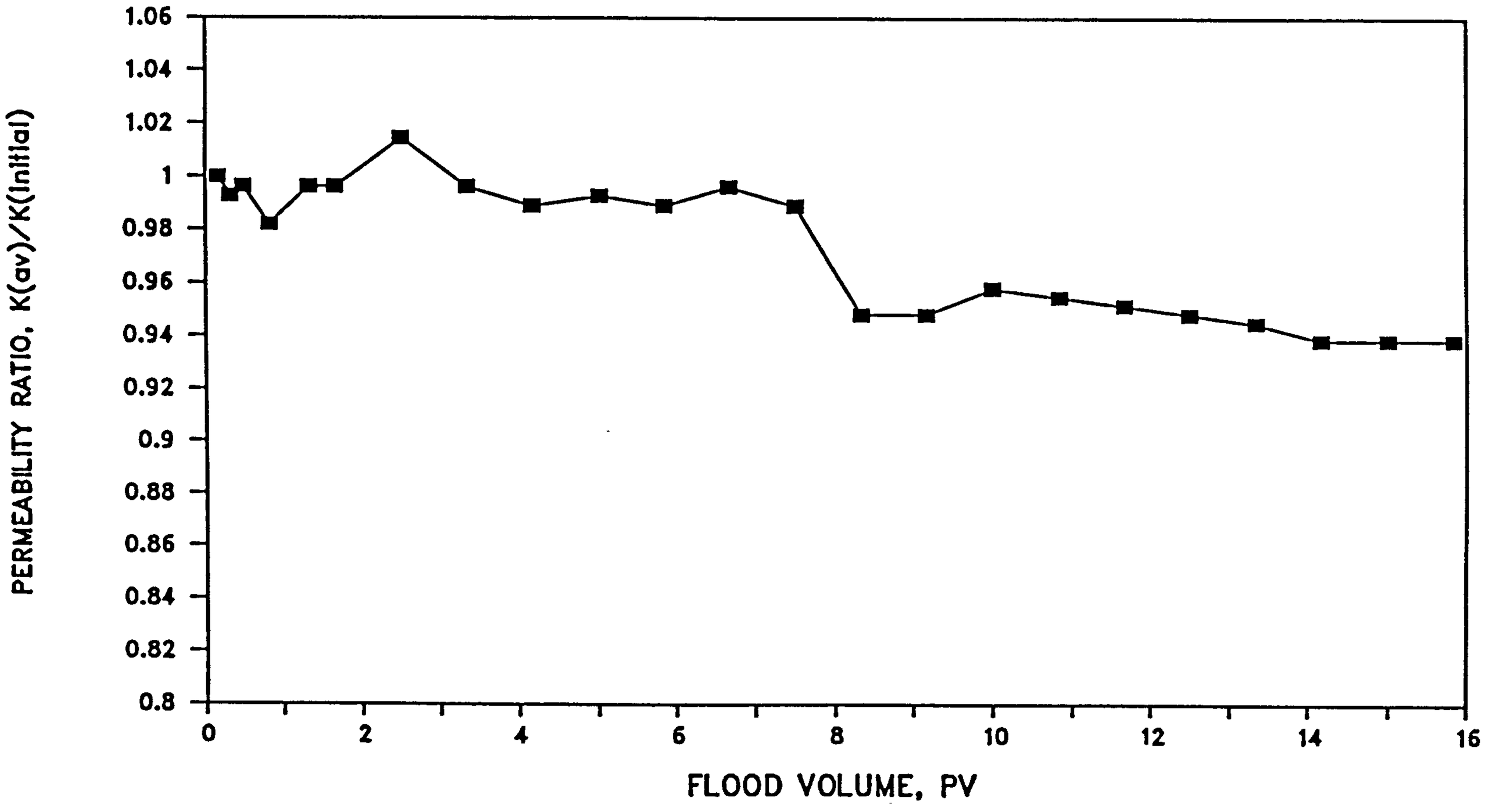

FIG. 28b Mean Permeability Ratio Profile
Decreasing Salinity, t1/2= 3 PV

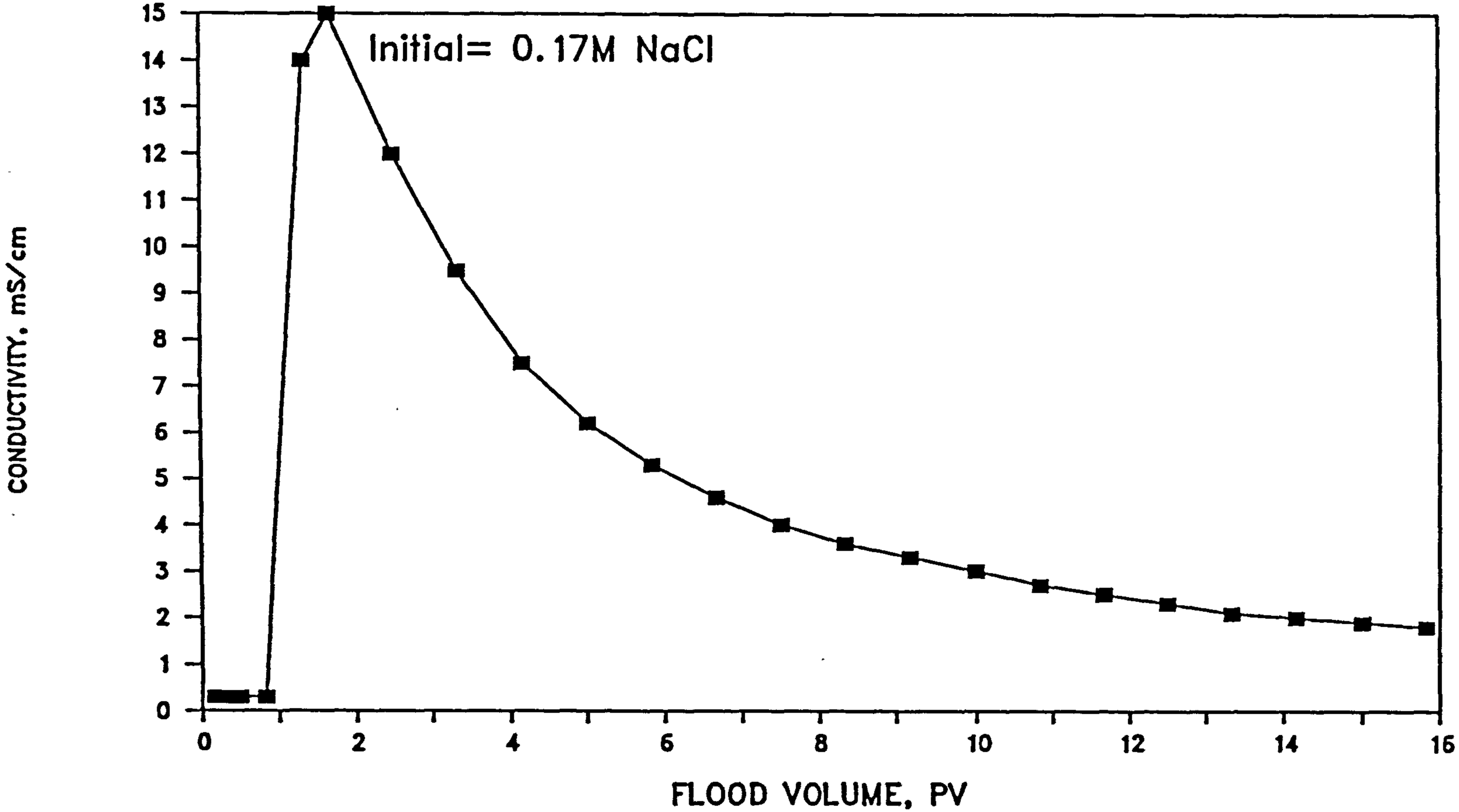

FIG. 28c Effluent Conductivity Profile for Decreasing Salinity Flood, t1/2= 3 PV

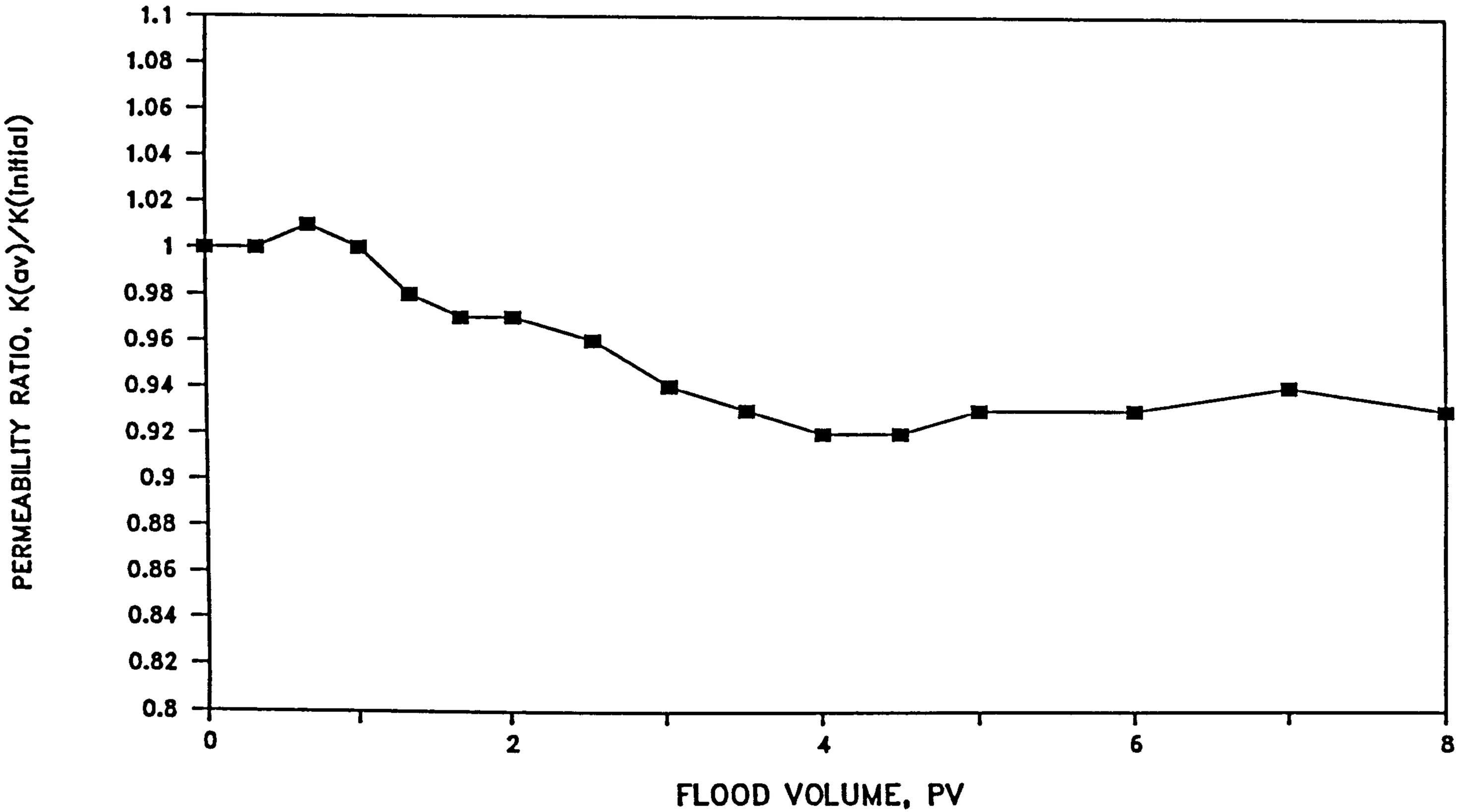

FIG. 29 Mean Sandpack Permeability Ratio Decreasing Salinity Flood from 0.1M KCl Brine

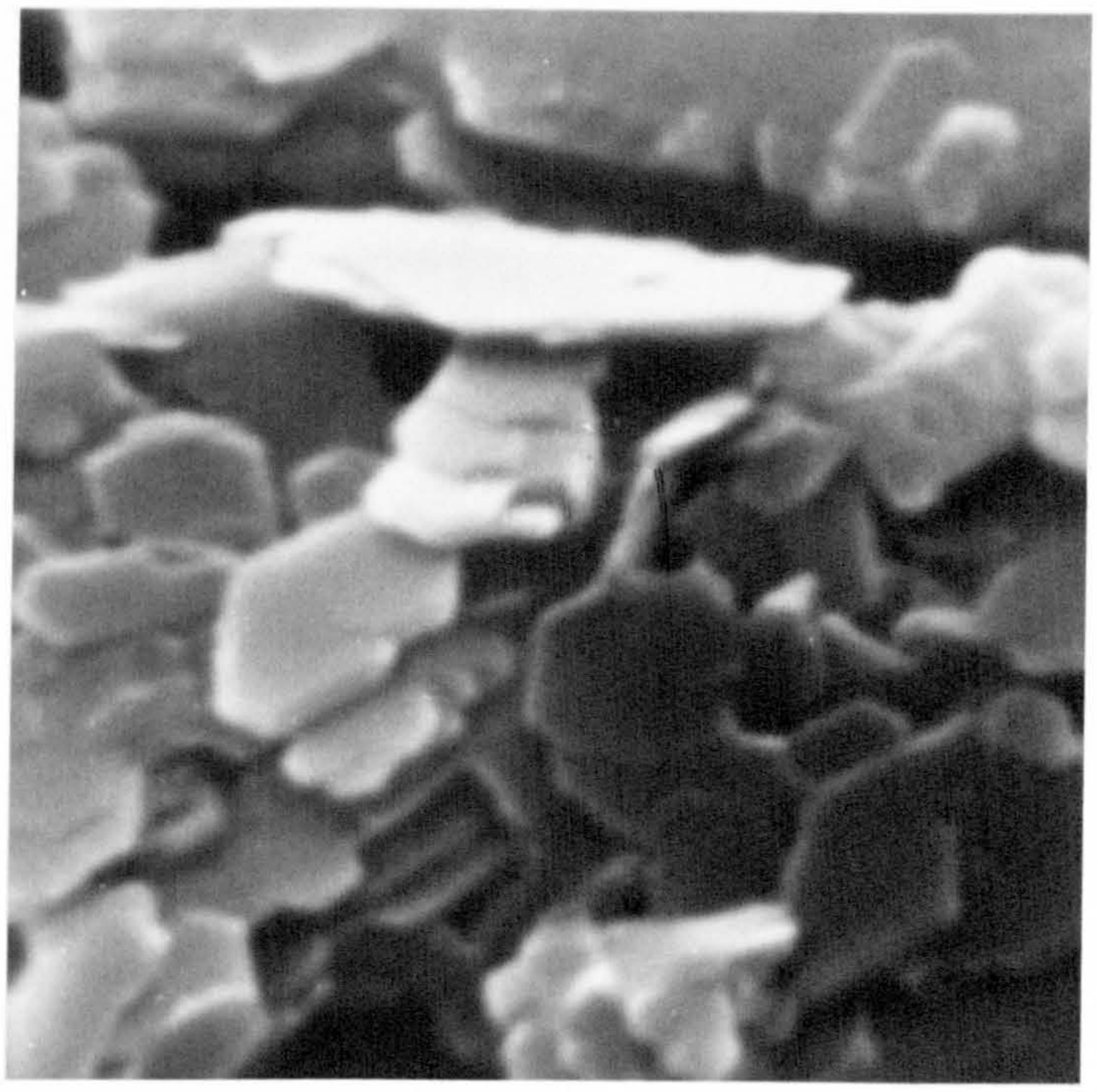

PLATE 14 KAOLINITE PLATELETS IN SEPARATOR SAND CLAYS (x20000)

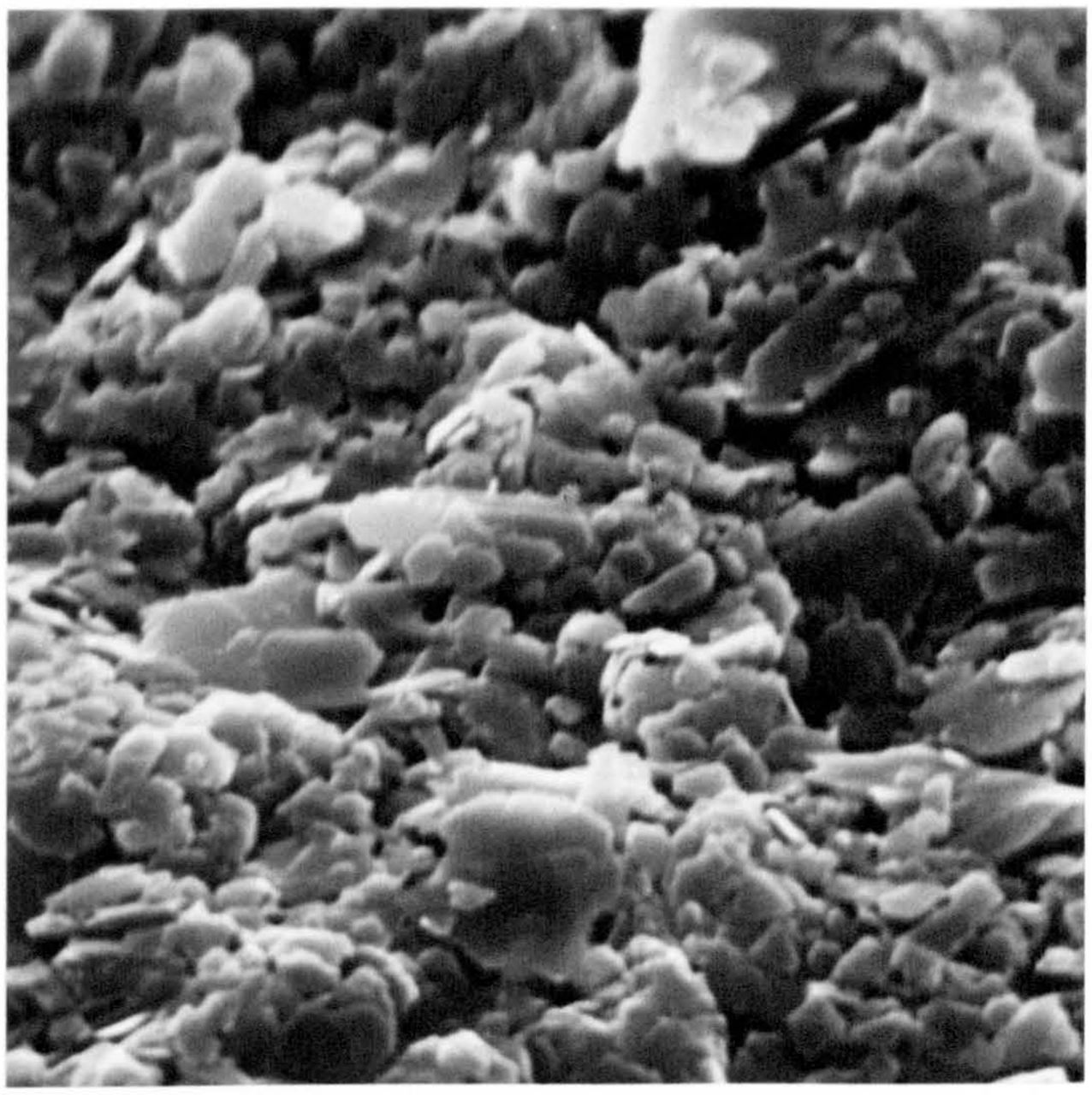

PLATE 15 CLAY FRACTION FROM FINE-GREY SAND (x5000)

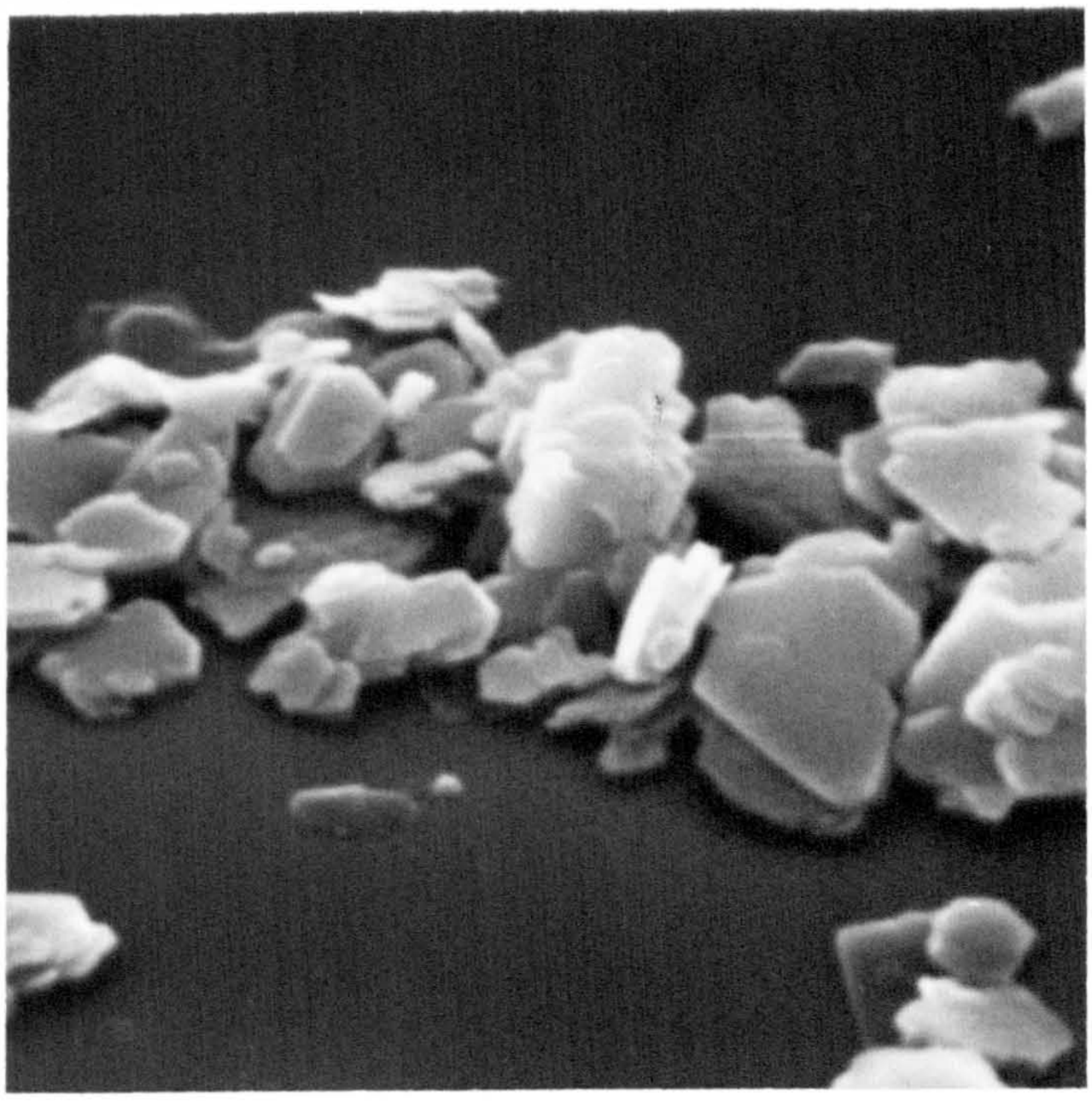

PLATE 16 DISORDERED KAOLINITE IN FINE-GREY SAND CLAYS (x10000)

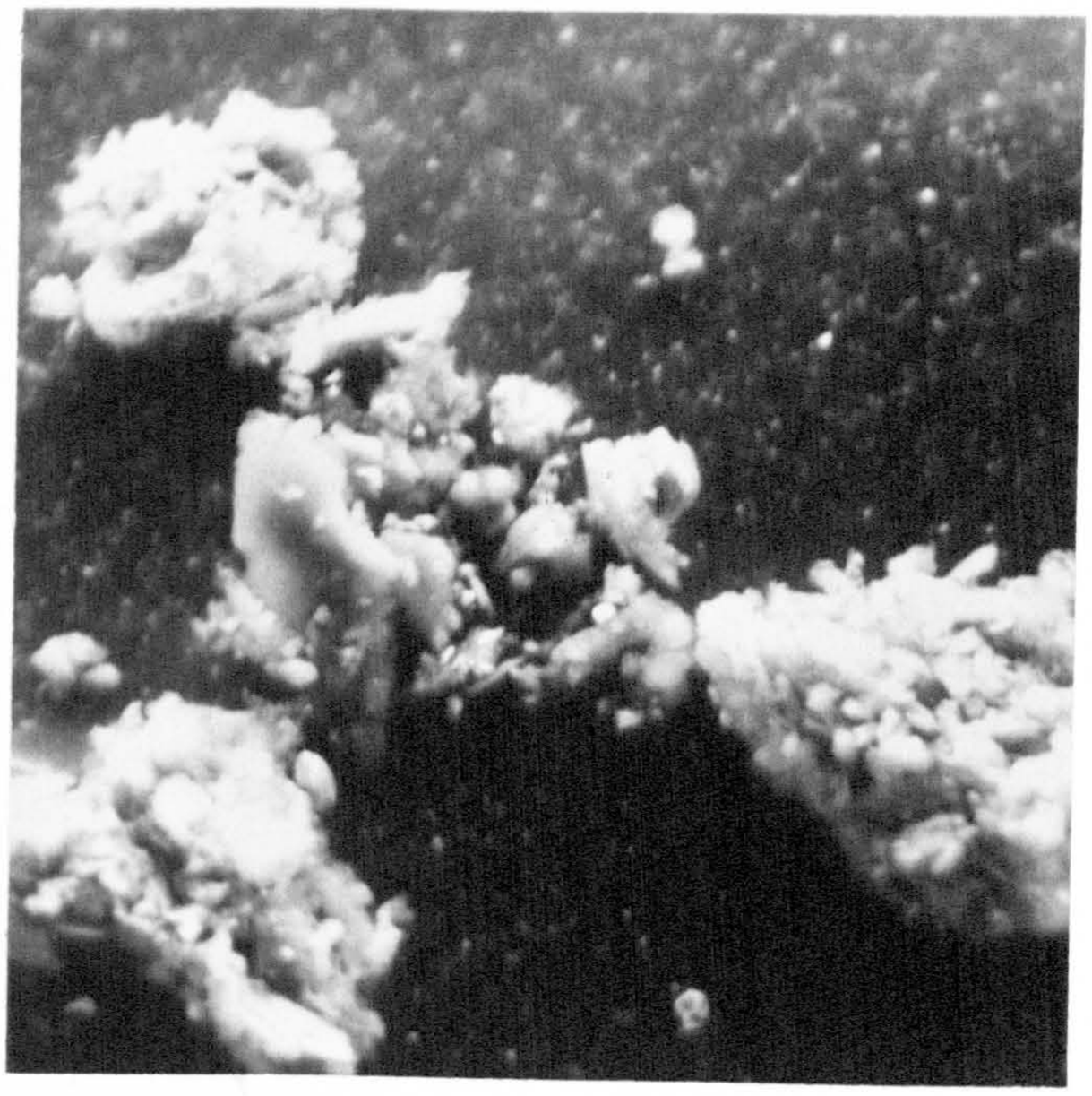

PLATE 17 CLAY MATERIALS ISOLATED FROM FINE-GREY SAND FOR CALCIUM ION ANALYSIS (×1000)

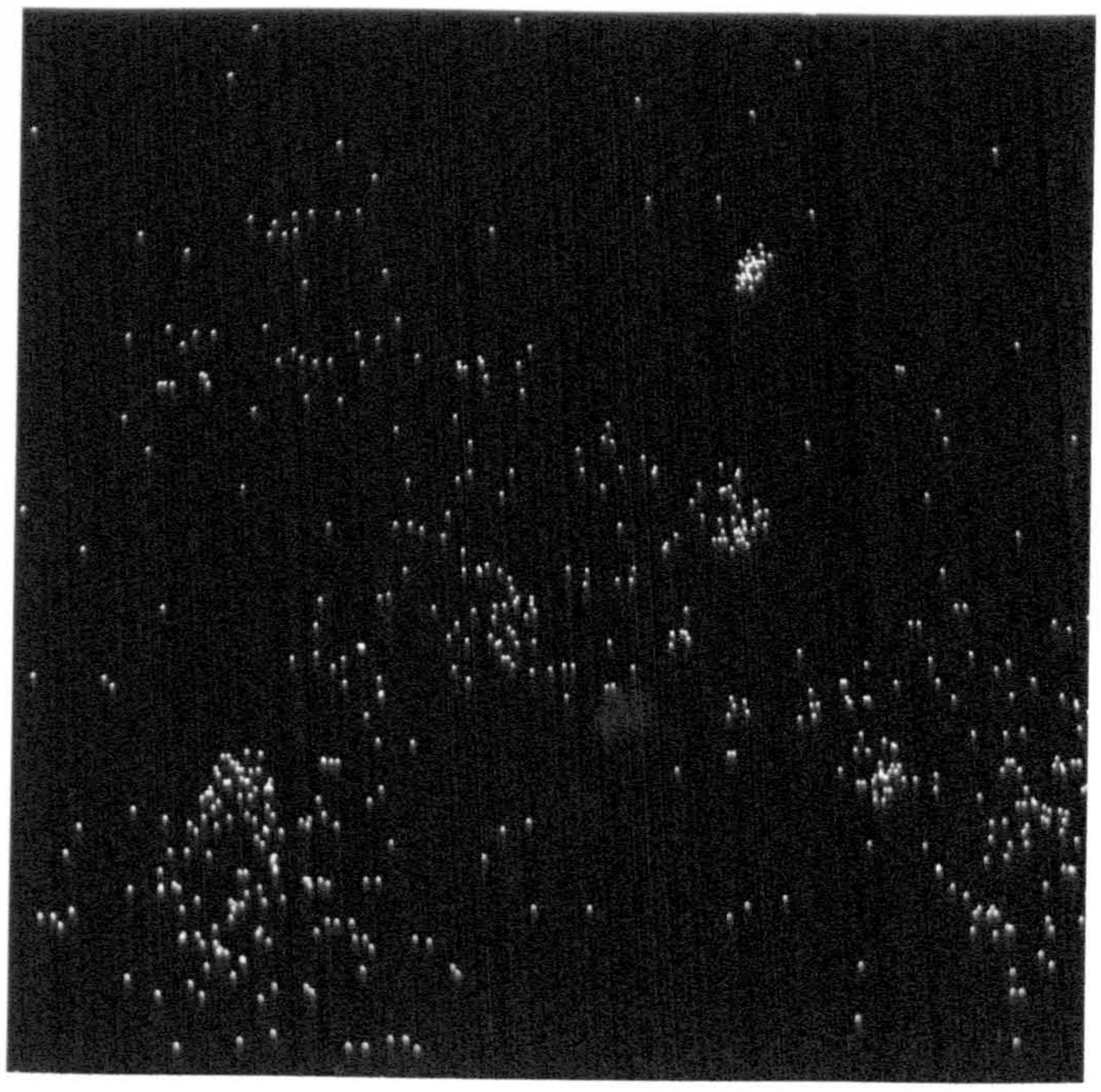

PLATE 18 CALCIUM ION MAP OF CLAYS IN PLATE 17

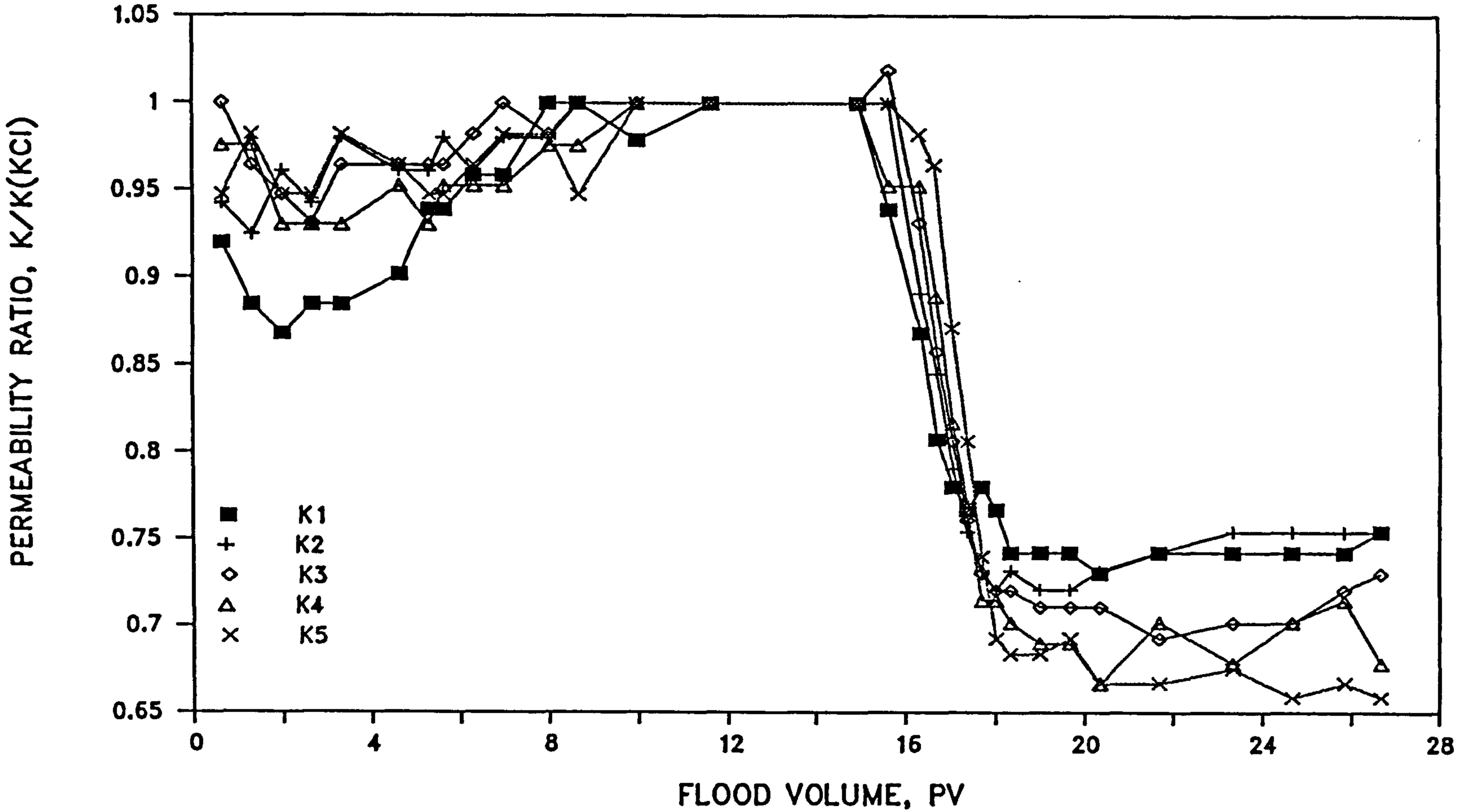

FIG. 30a Sandpack Section Permeability Ratios
Potassium Chloride–Water Flood

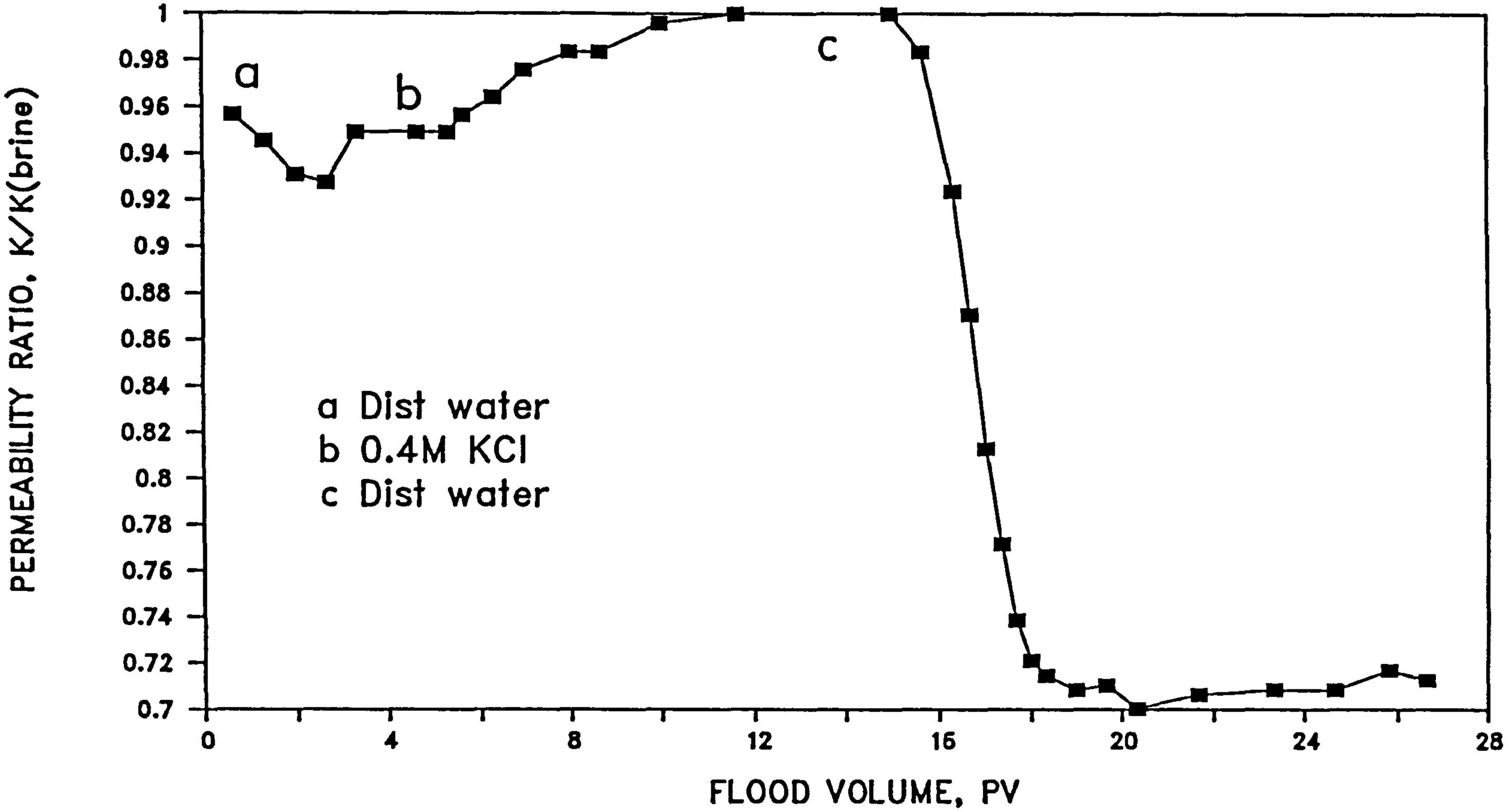

FIG. 30b Mean Sandpack Permeability For 0.4M Potassium Chloride Flood

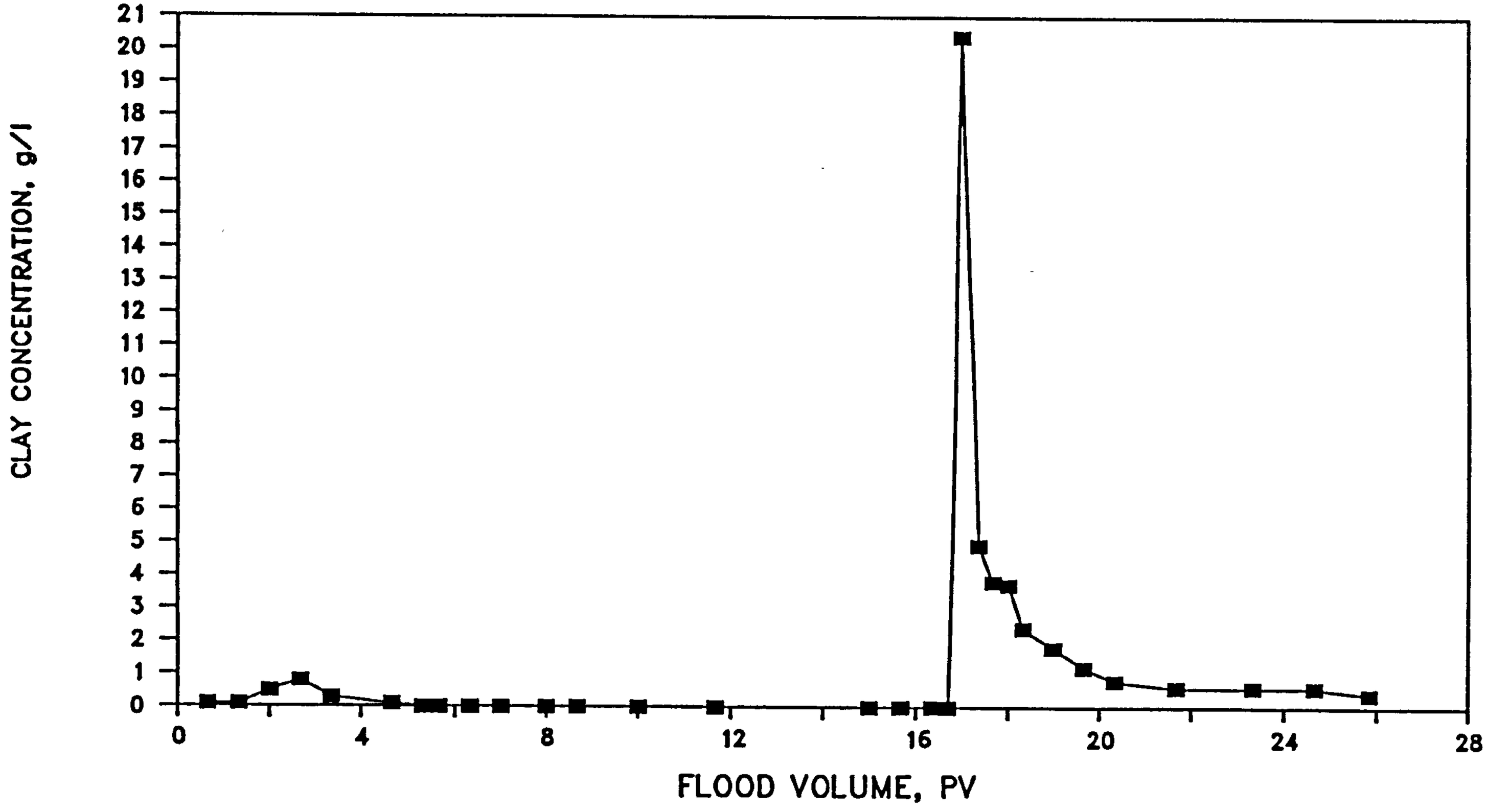

FIG. 30c Effluent Clay Concentration
Potassium Chloride Flood

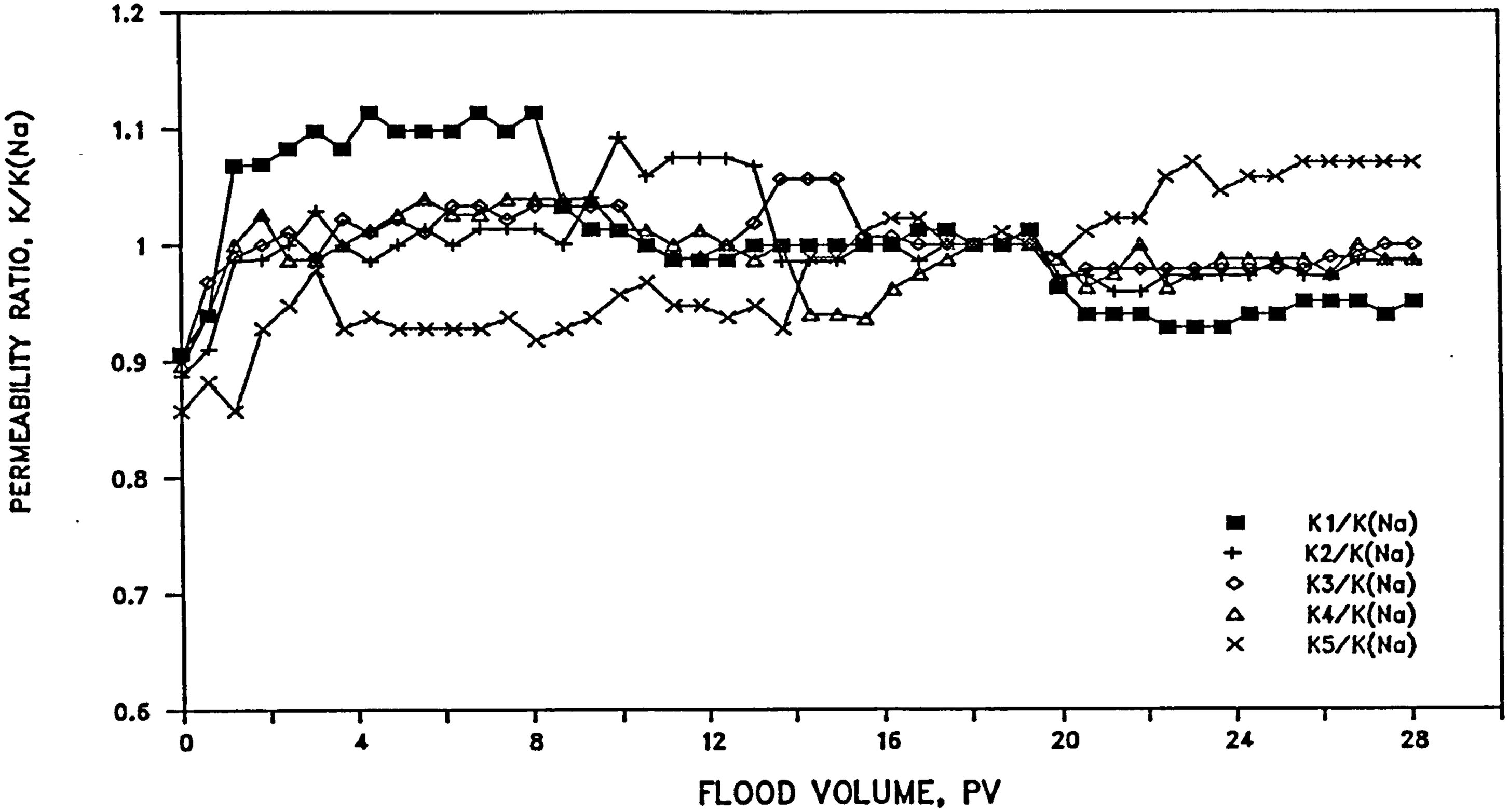

FIG. 31a Sandpack Section Permeability Ratio's
Calcium Chloride Pre-treatment

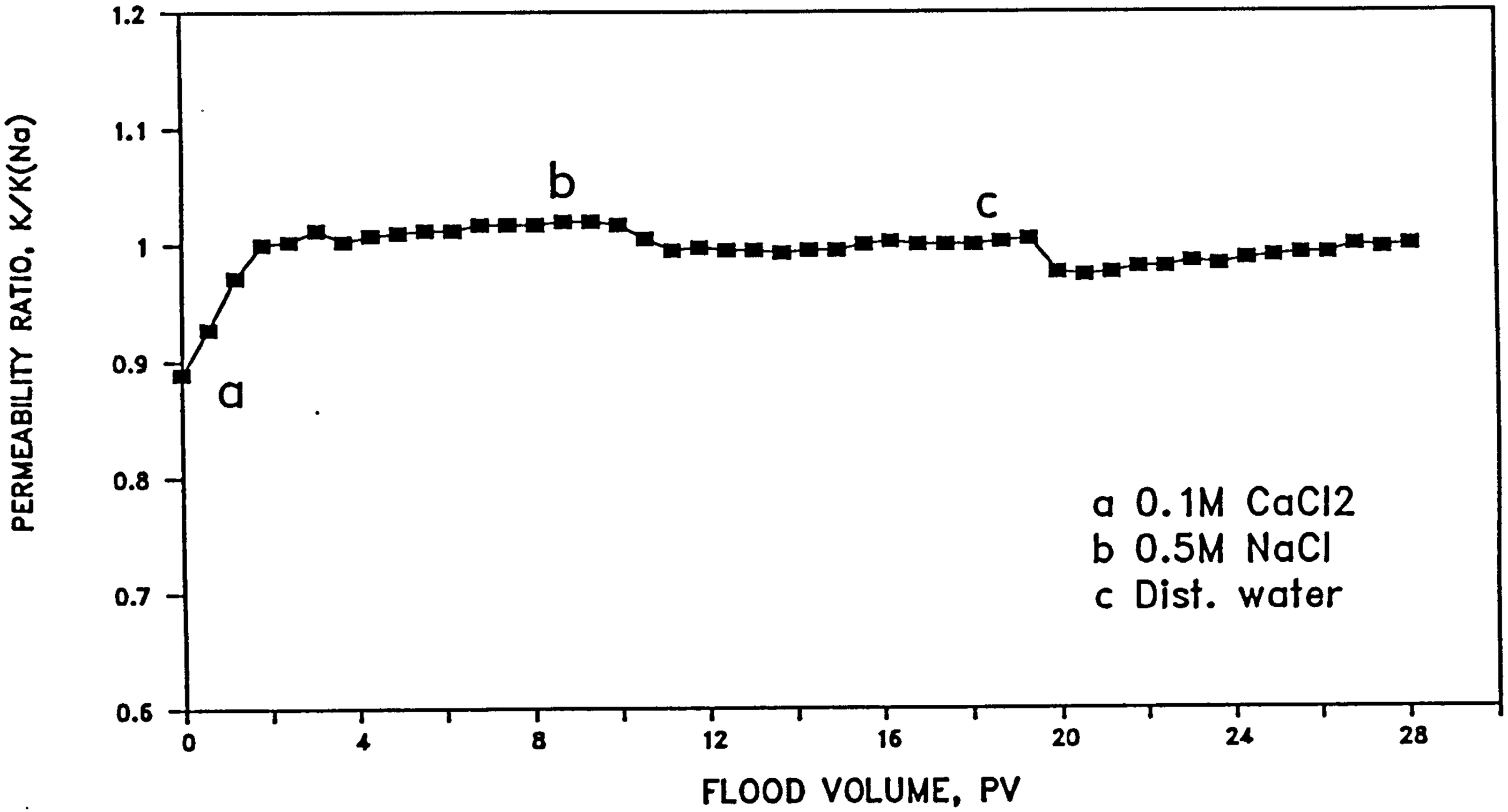

FIG. 31b Mean Sandpack Permeability Ratio
Effect of Calcium Chloride Pre-treatment

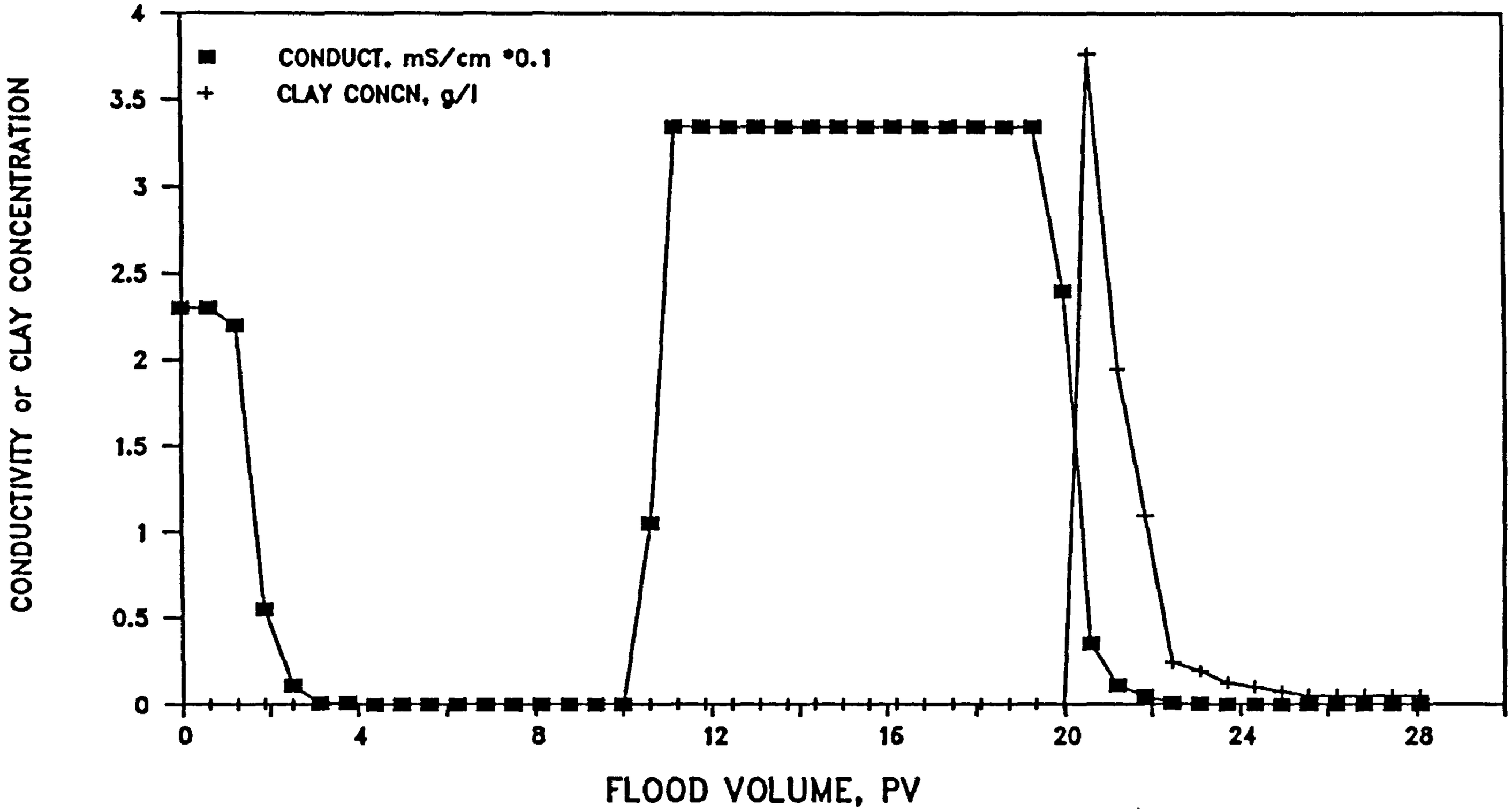

FIG. 31c Effluent Conductivity and Clay Content
Calcium Chloride Pre-treatment

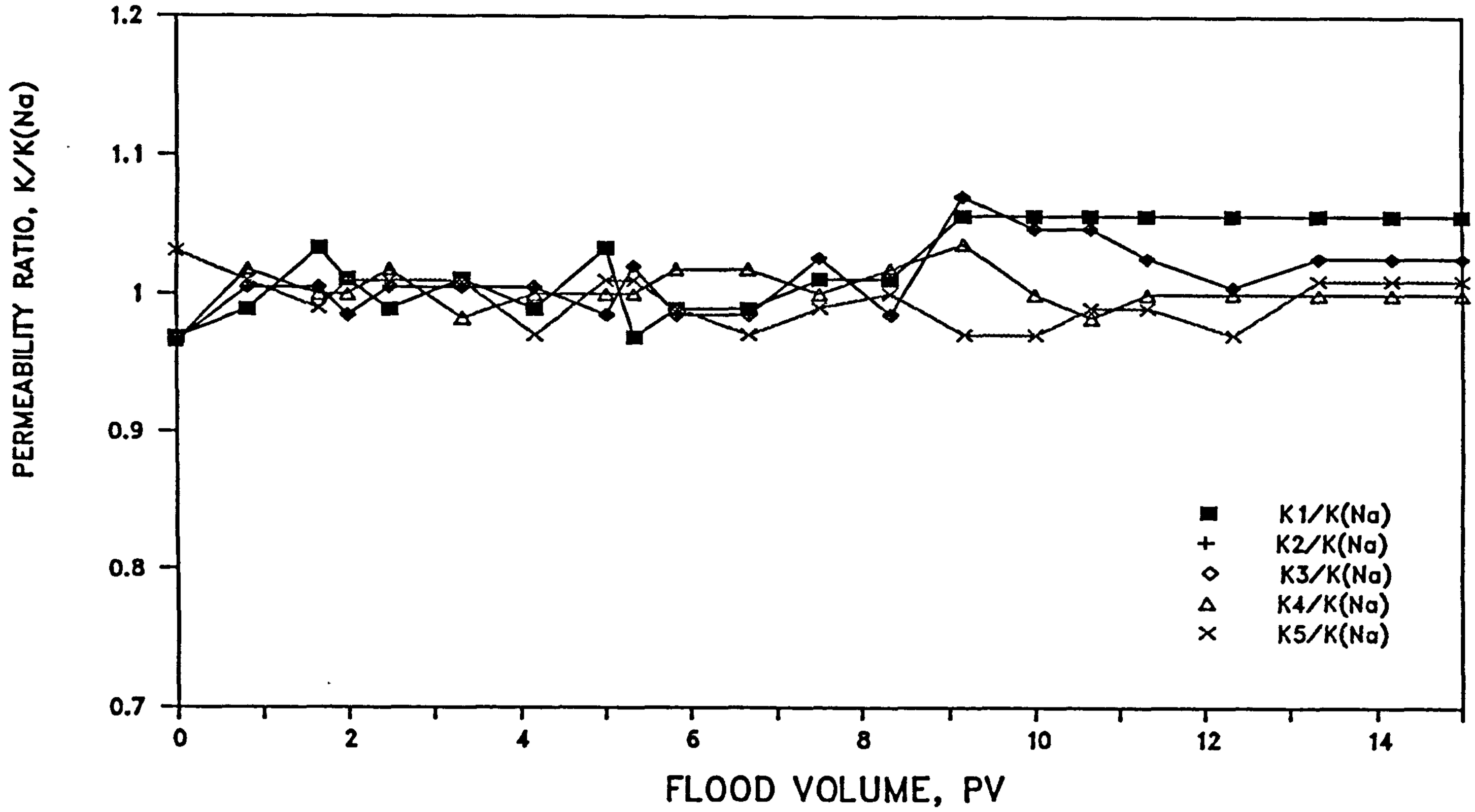

FIG. 32a Sandpack Section Permeabilities
Calcium Chloride Post-treatment

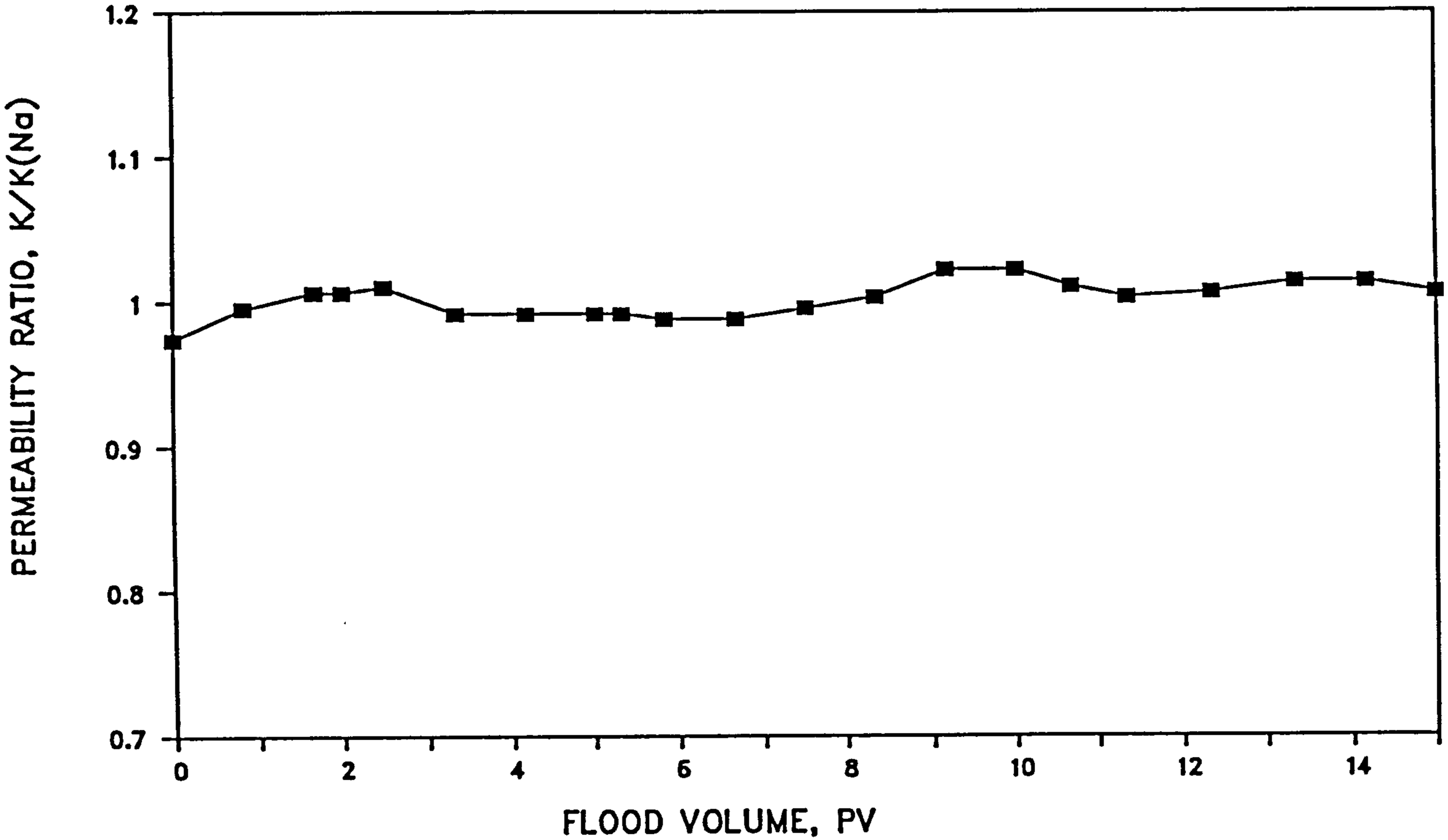

FIG. 32b Mean Sandpack Permeability for Calcium Chloride Post-treatment

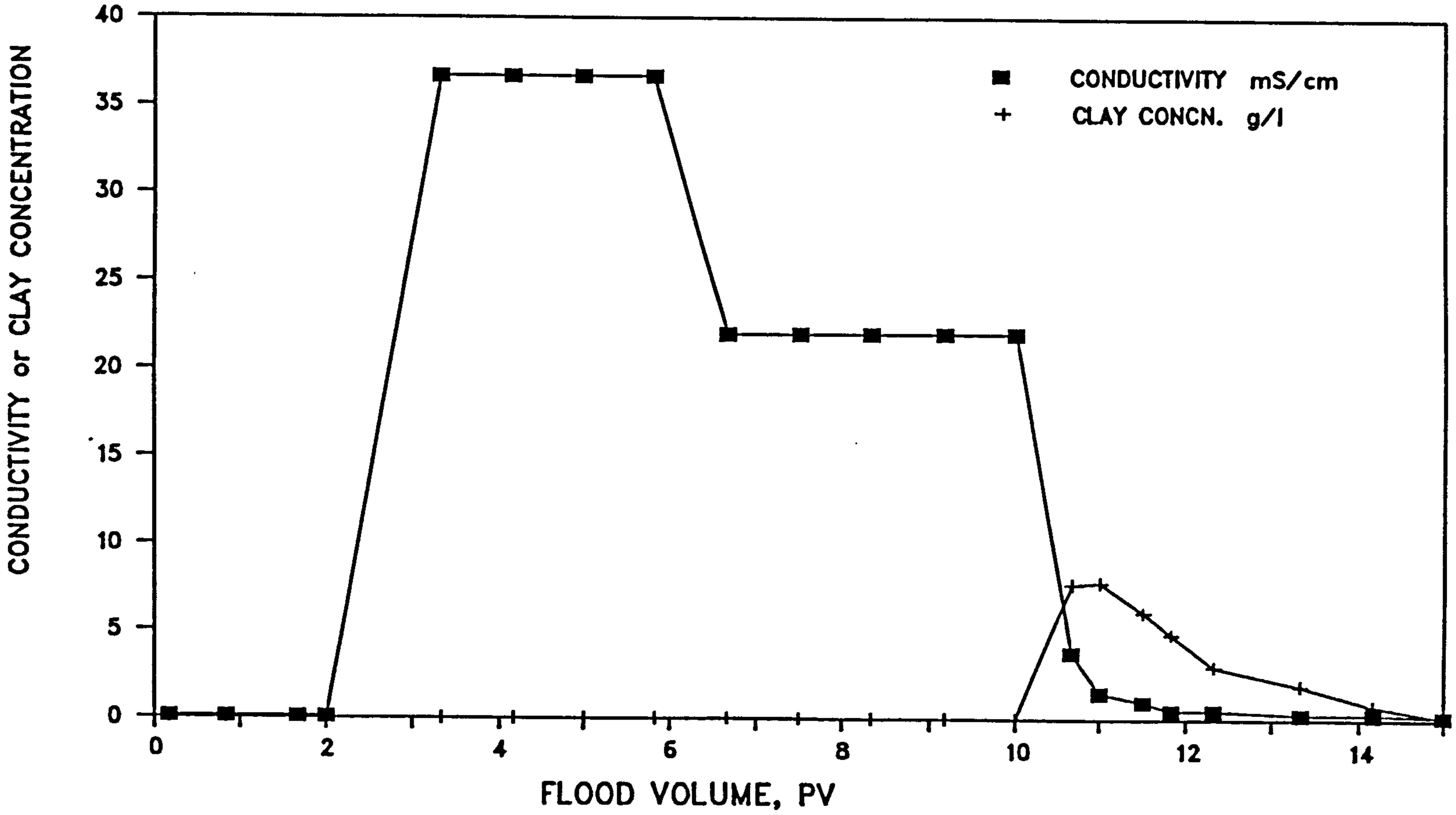

FIG. 32c Effluent Conductivity and Clay Content Calcium Chloride Post-treatment

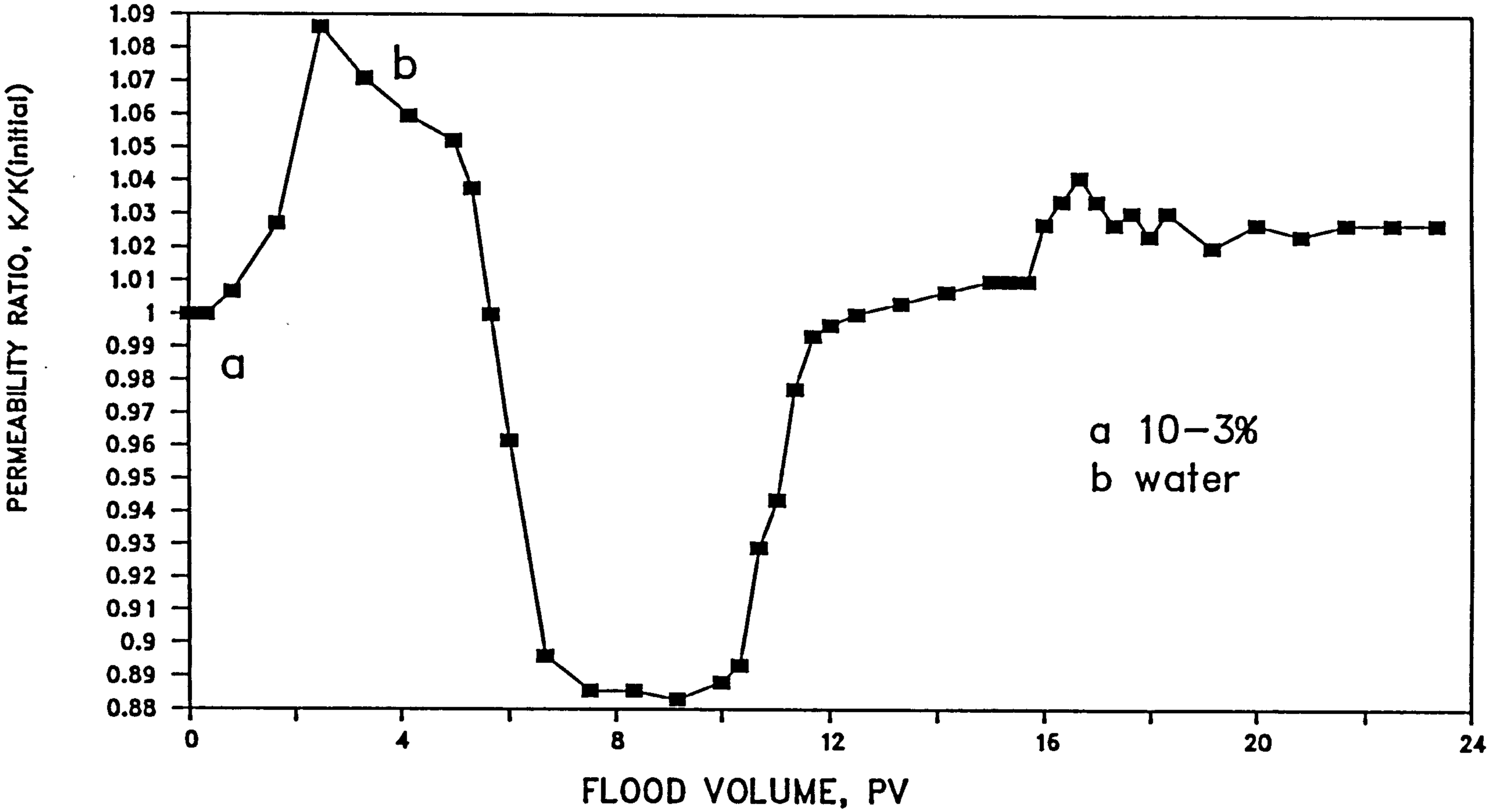

FIG. 33 Mean Sandpack Permeability Ratio
Simulated Formation Brine Flood

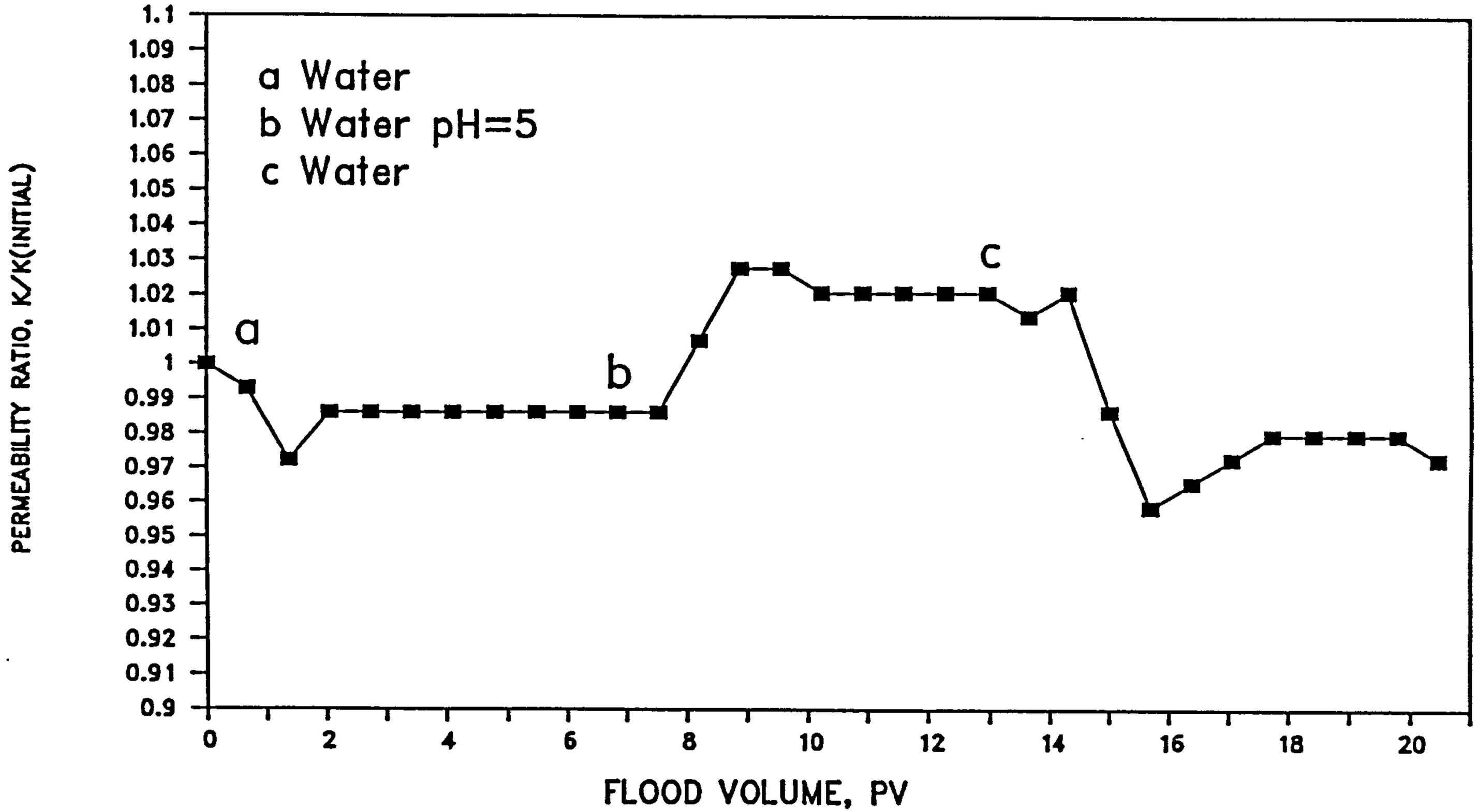

FIG. 34a Sandpack Permeability Ratio
Low pH Distilled Water Flood

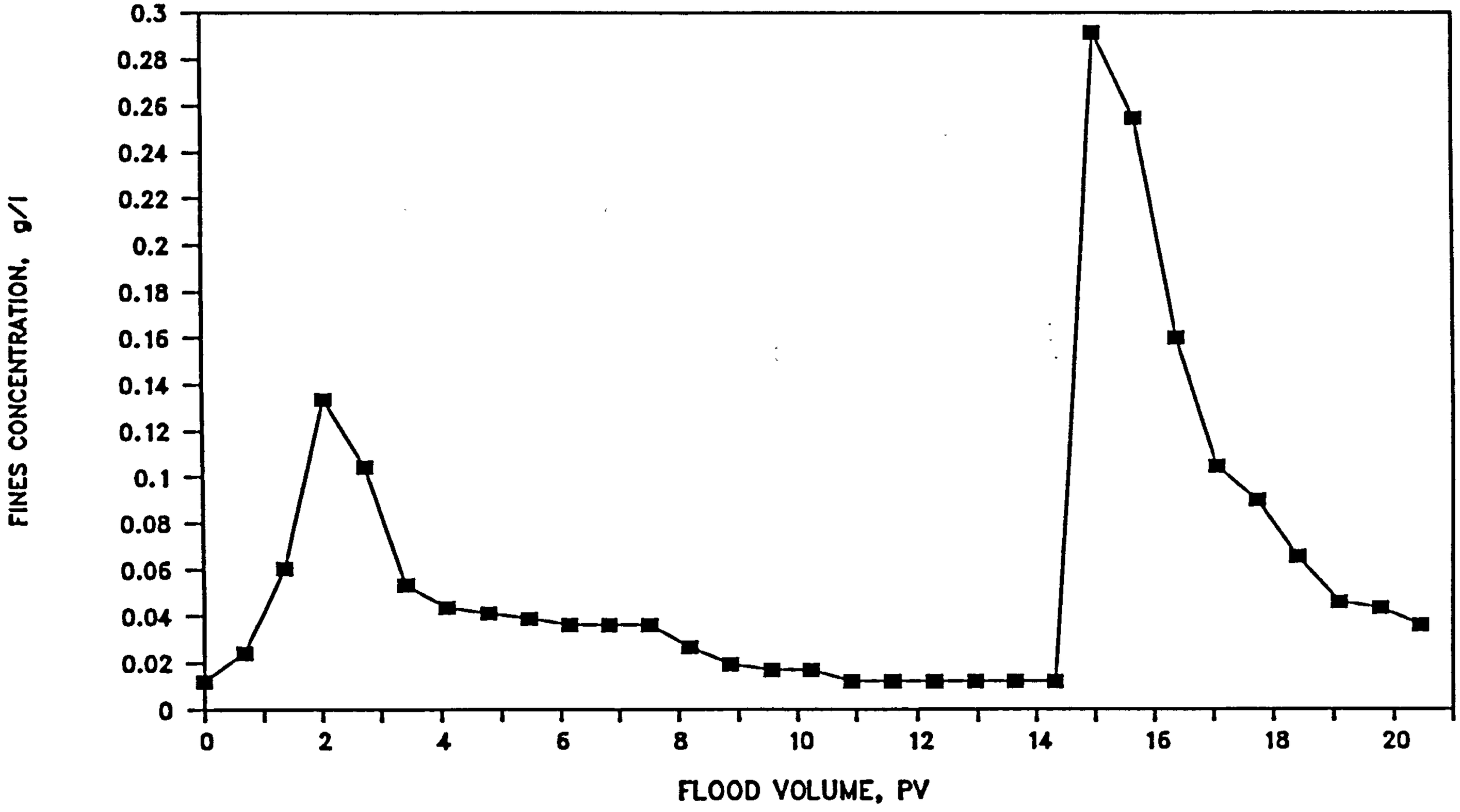

FIG. 34b Sandpack Effluent Fines Content for Low pH Distilled Water Flood

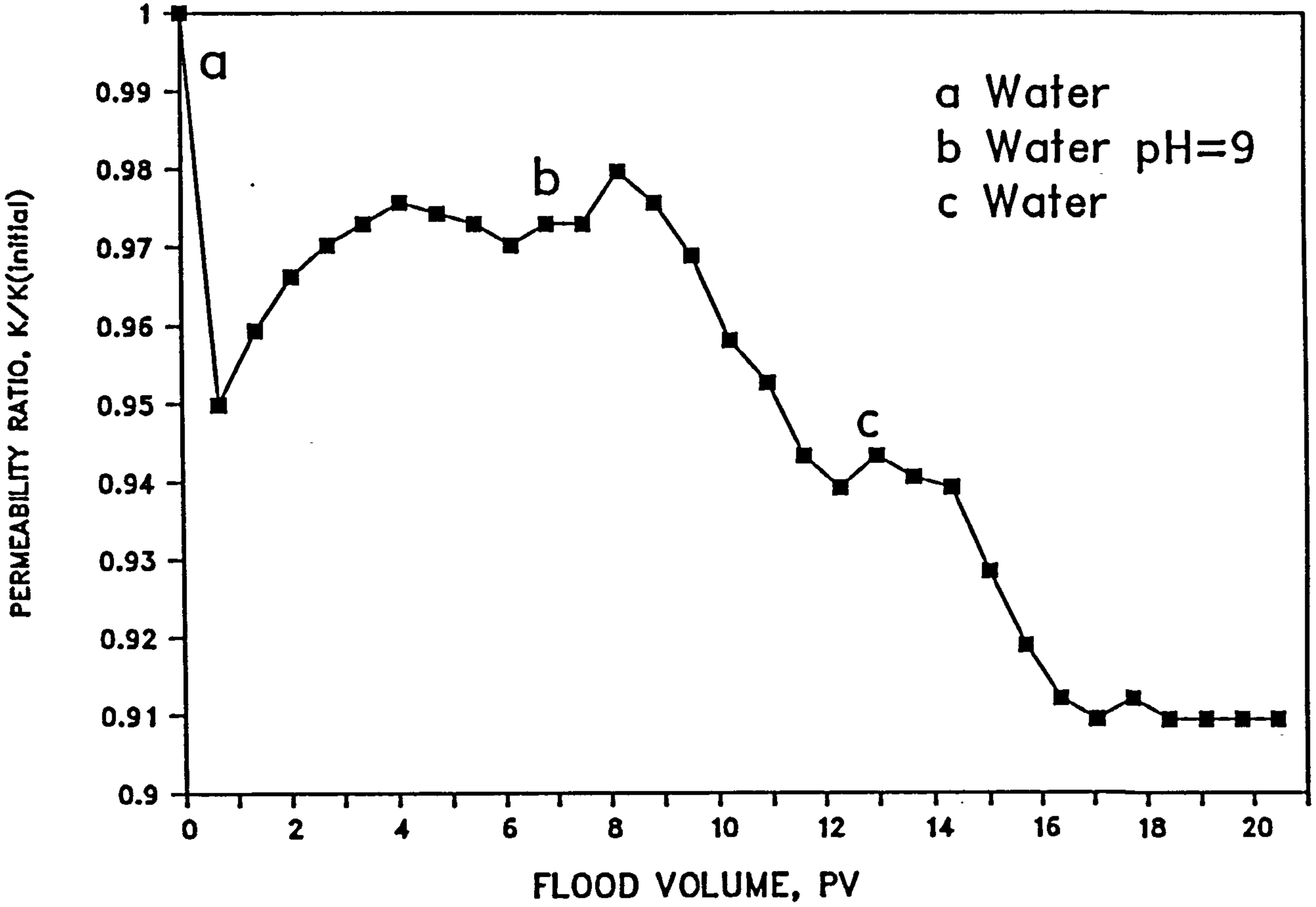

FIG. 35a Sandpack Permeability Ratio for High pH Distilled Water Flood

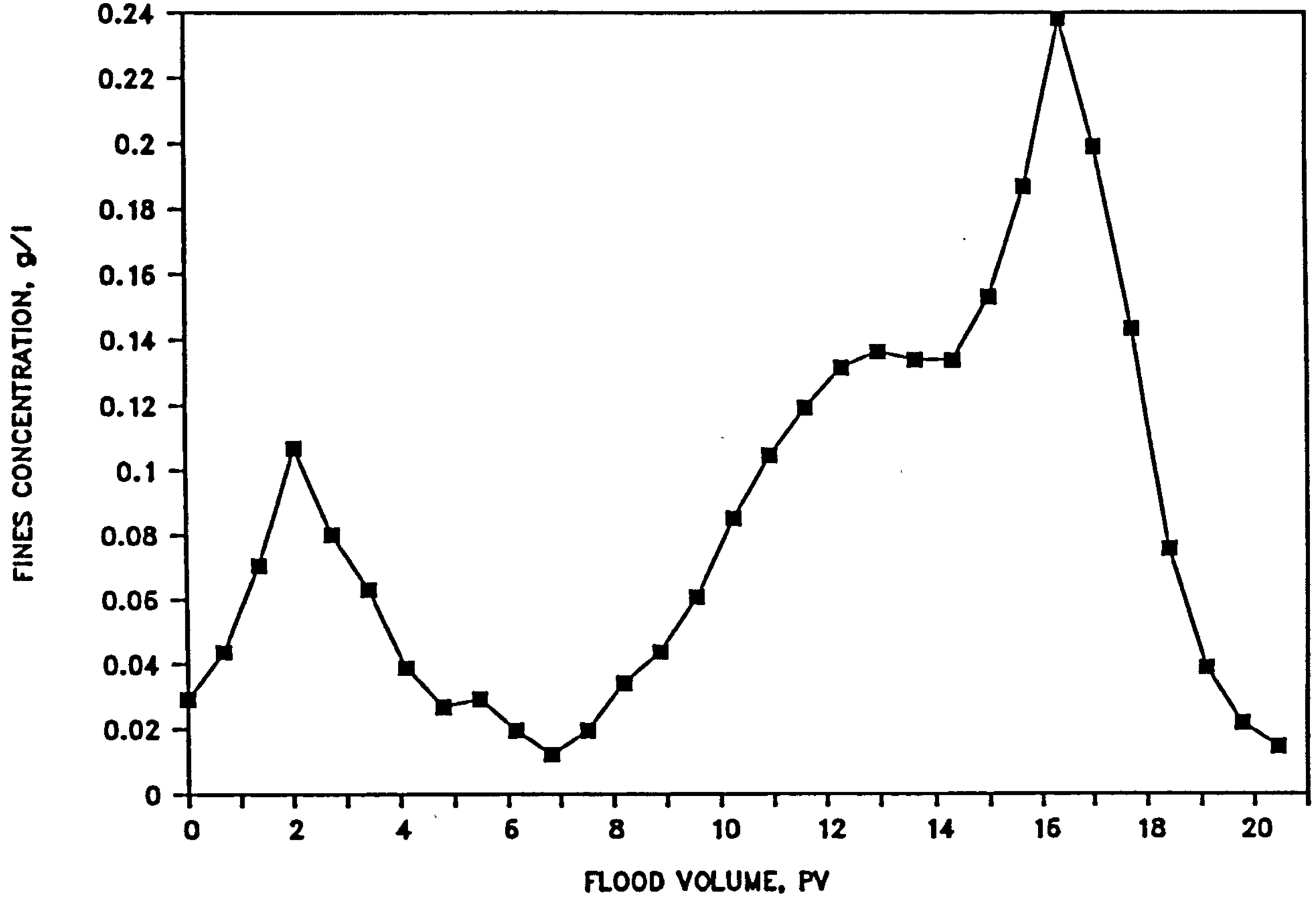

FIG. 35b Sandpack Effluent Fines Content for High pH Distilled Water Flood

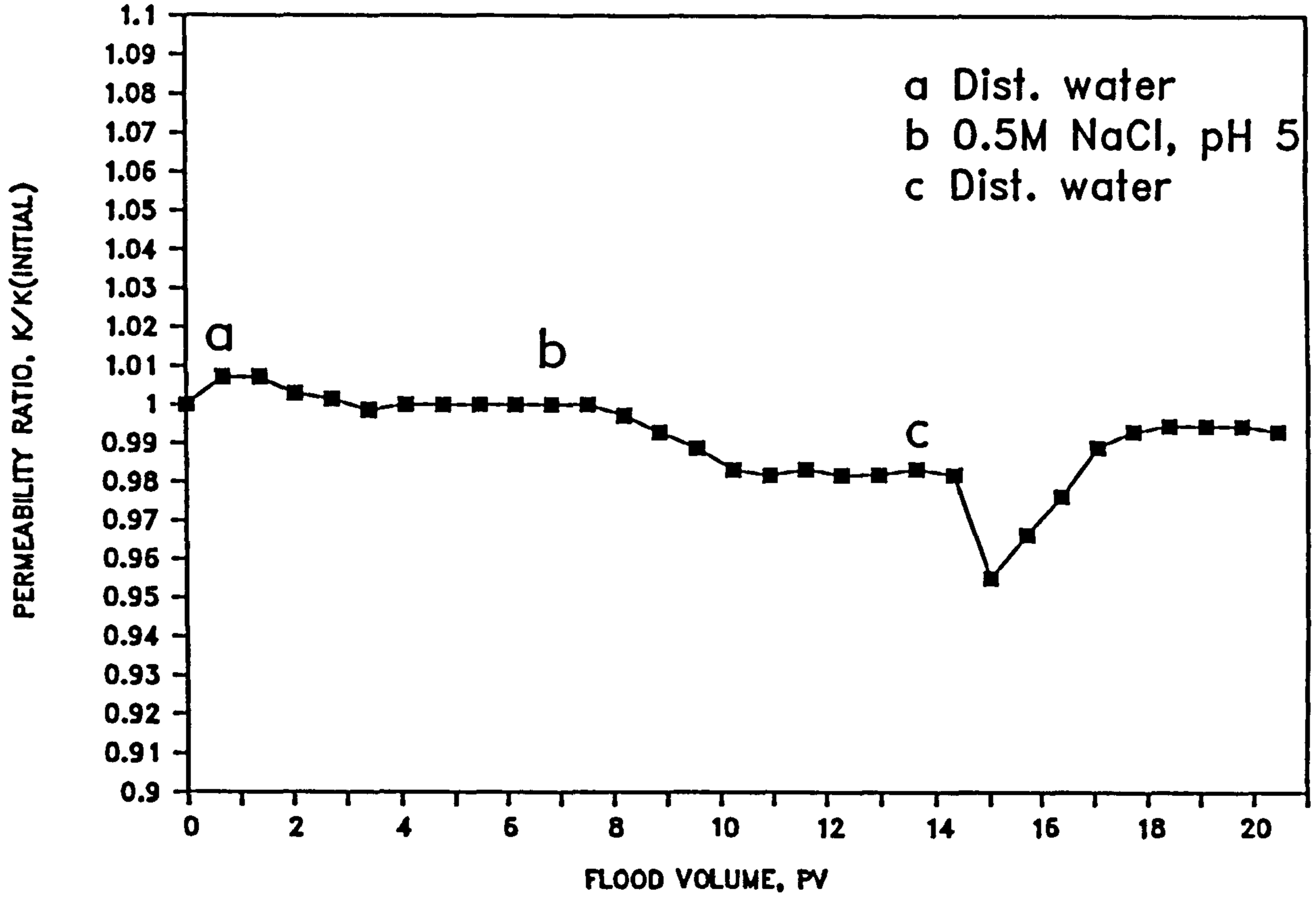

FIG. 36a Sandpack Permeability Profile for Low pH Brine Flood

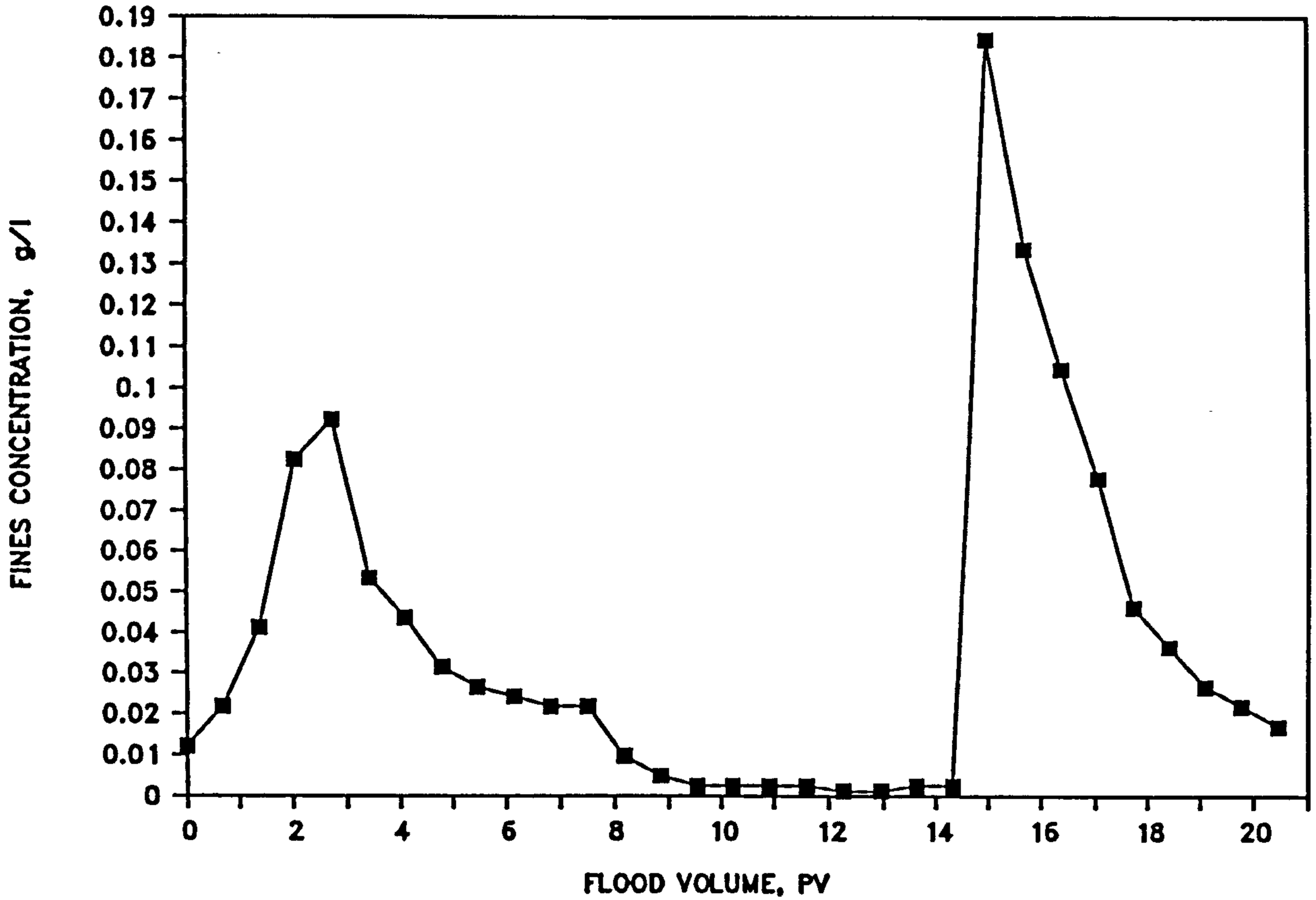

FIG. 36b Sandpack Effluent Fines Content for Low pH Brine Flood

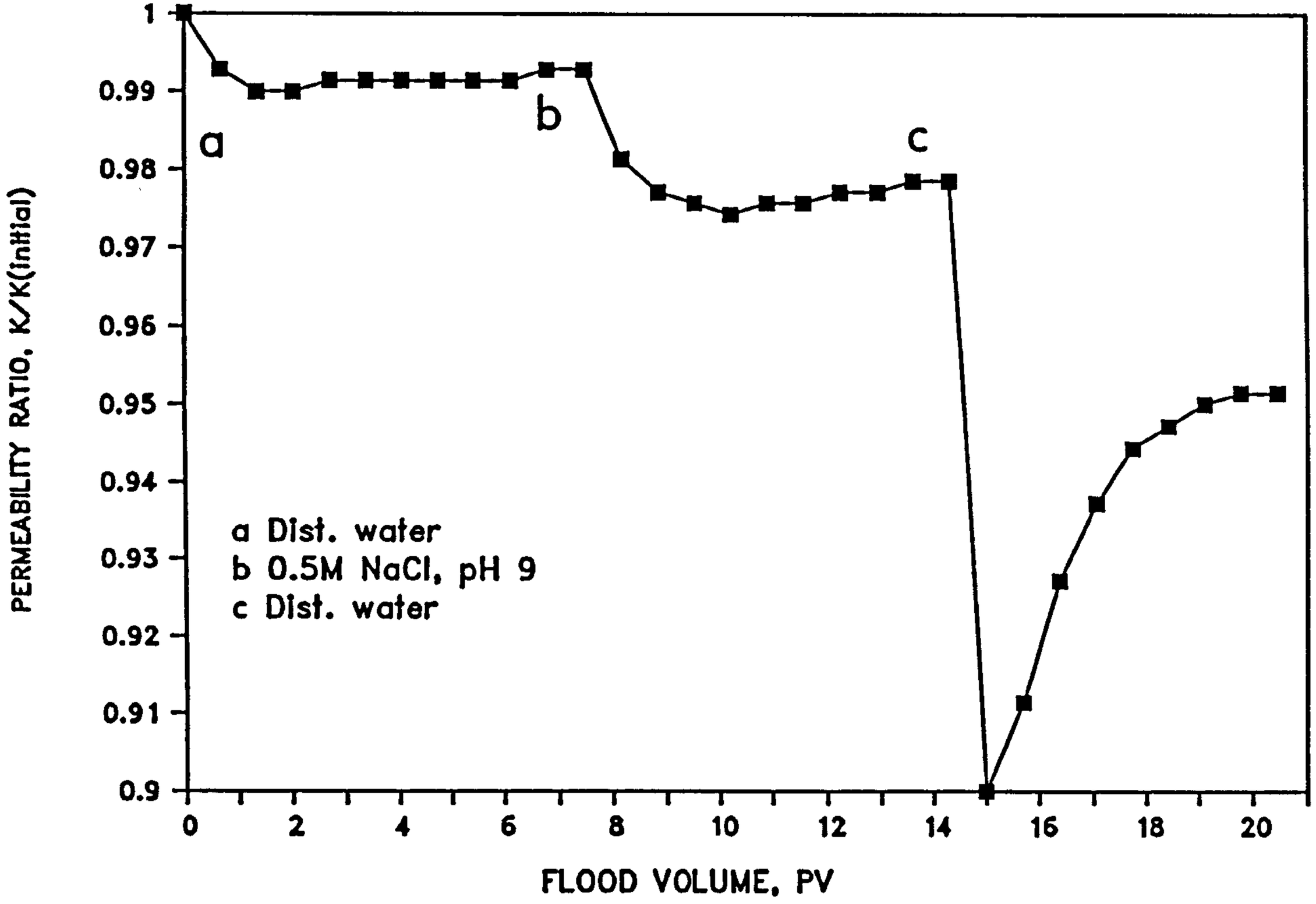

FIG. 37a Sandpack Permeability Profile for High pH Brine Flood

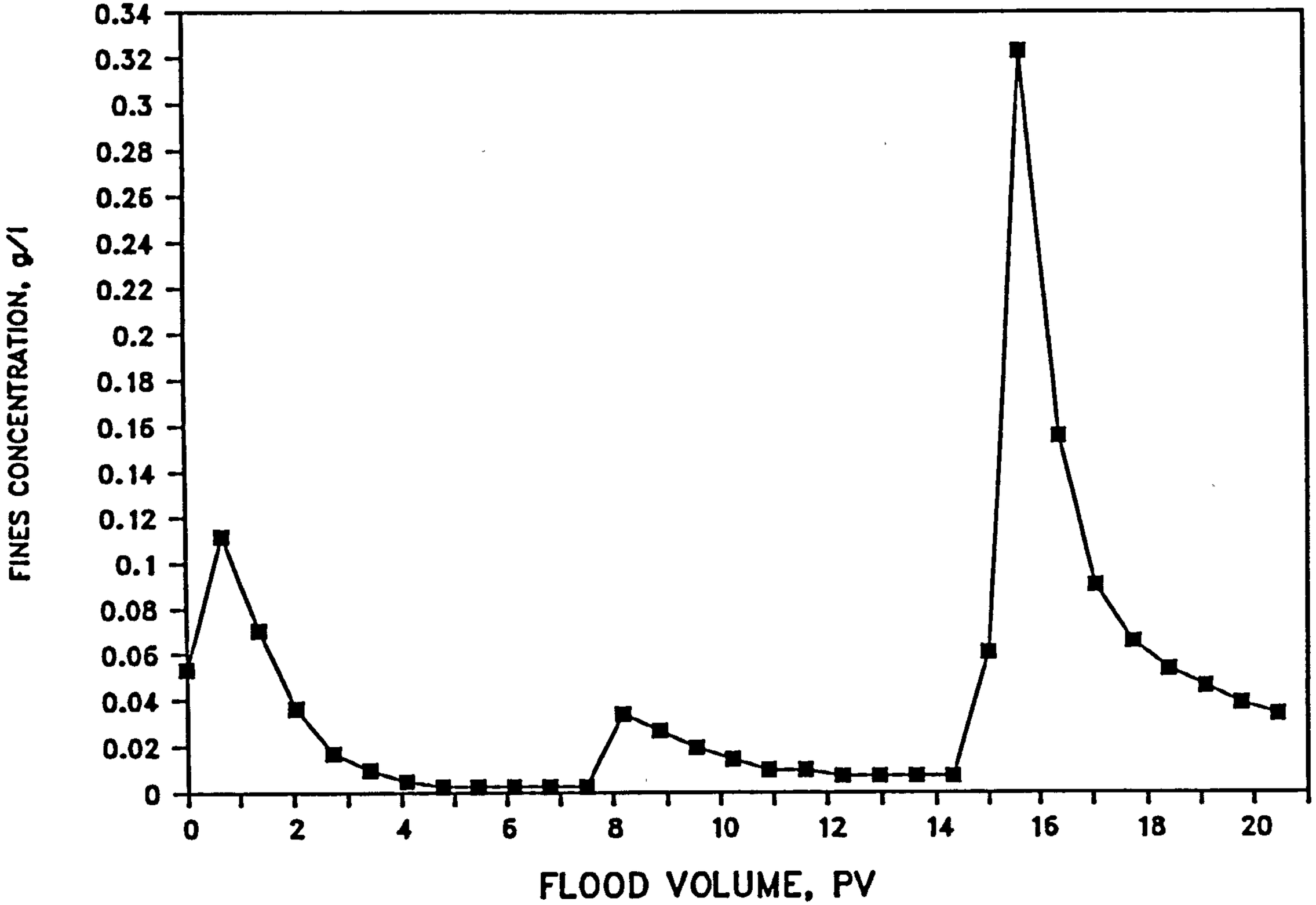

FIG. 37b Sandpack Effluent Fines Content for High pH Brine Flood

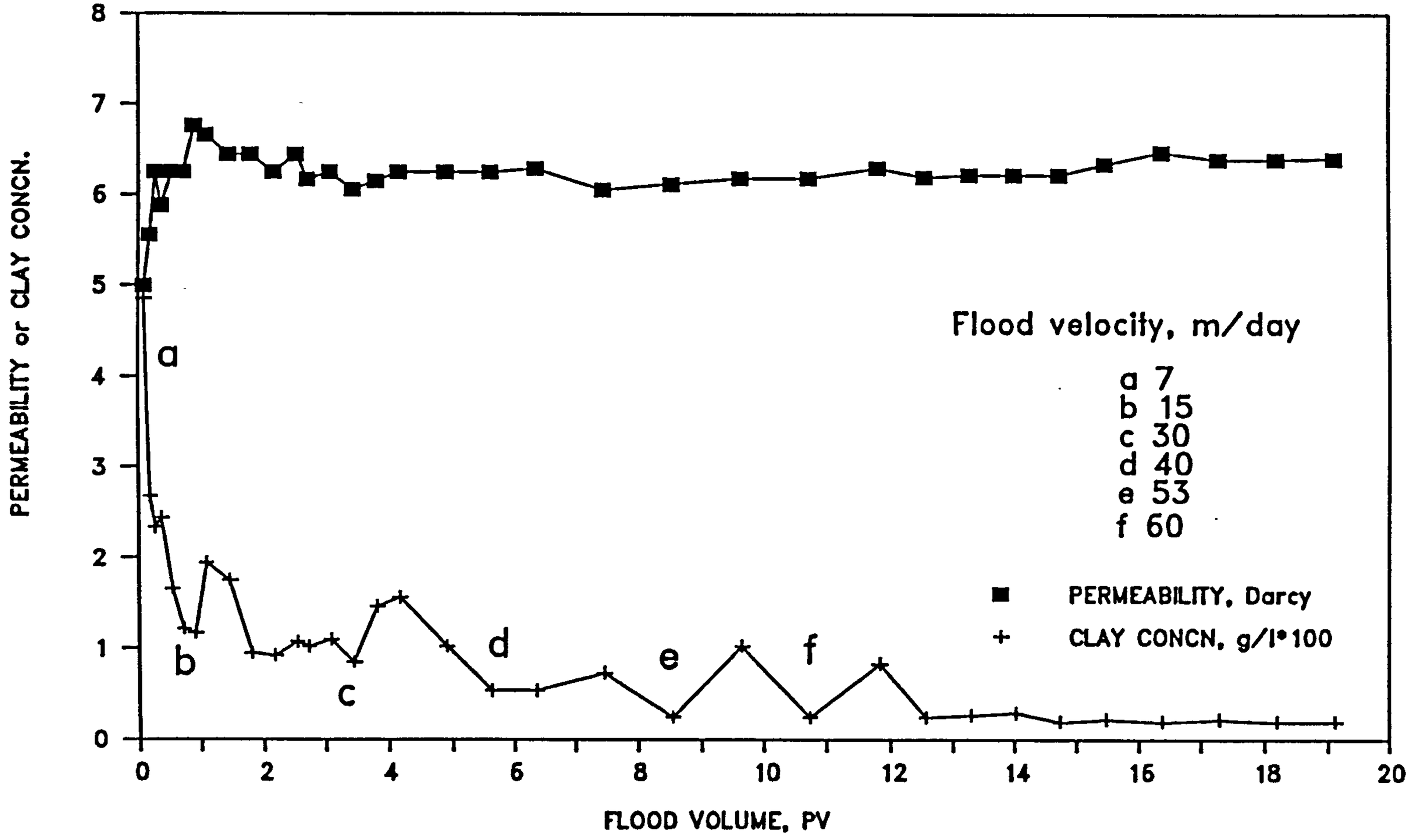

FIG. 38 Effect of Flowrate on Permeability and Fines Produced in Distilled Water Flood

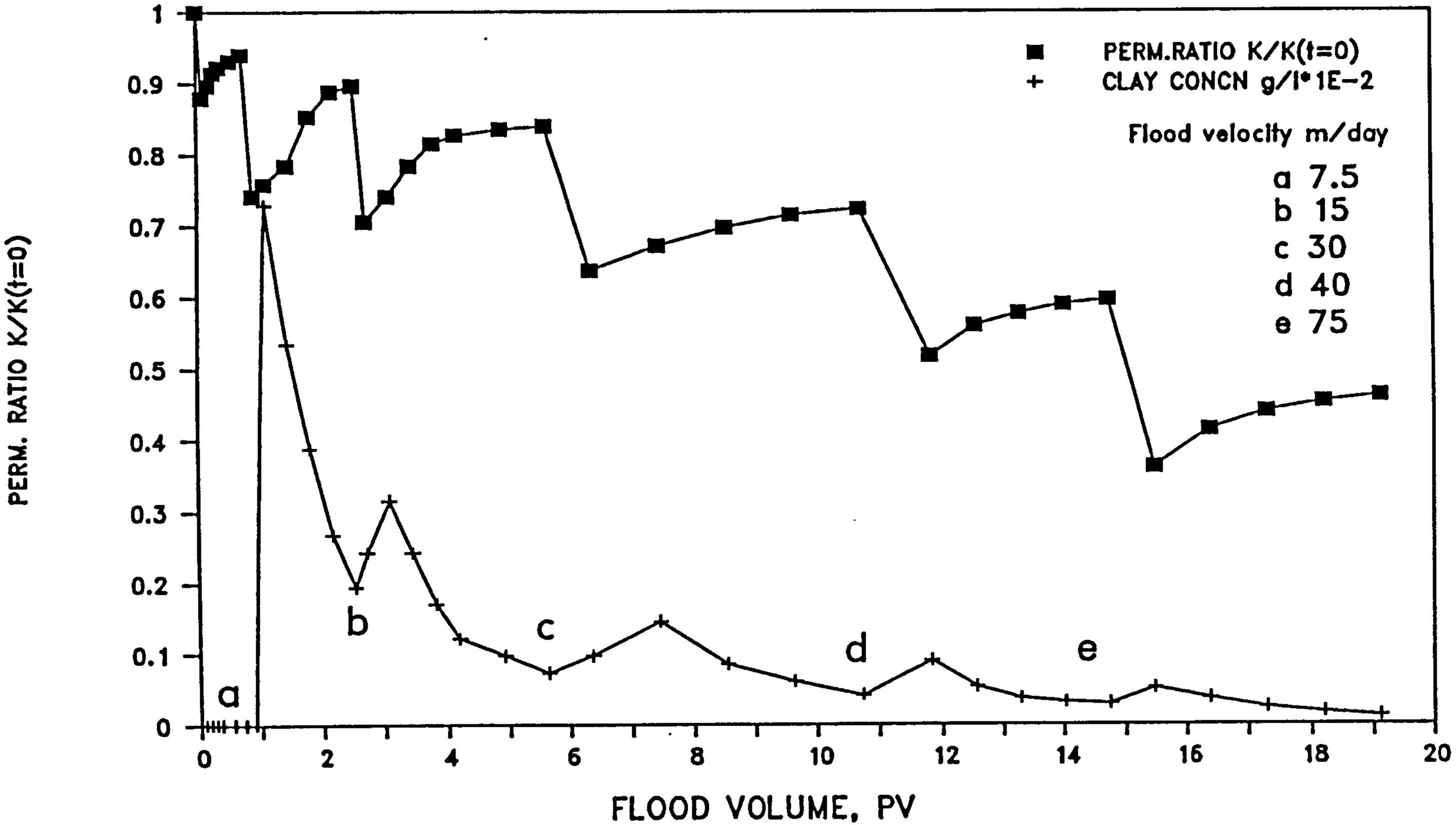

FIG. 39 Effect of Flowrate on Permeability and Fines Production in 'Mobilised clay' Sandpack

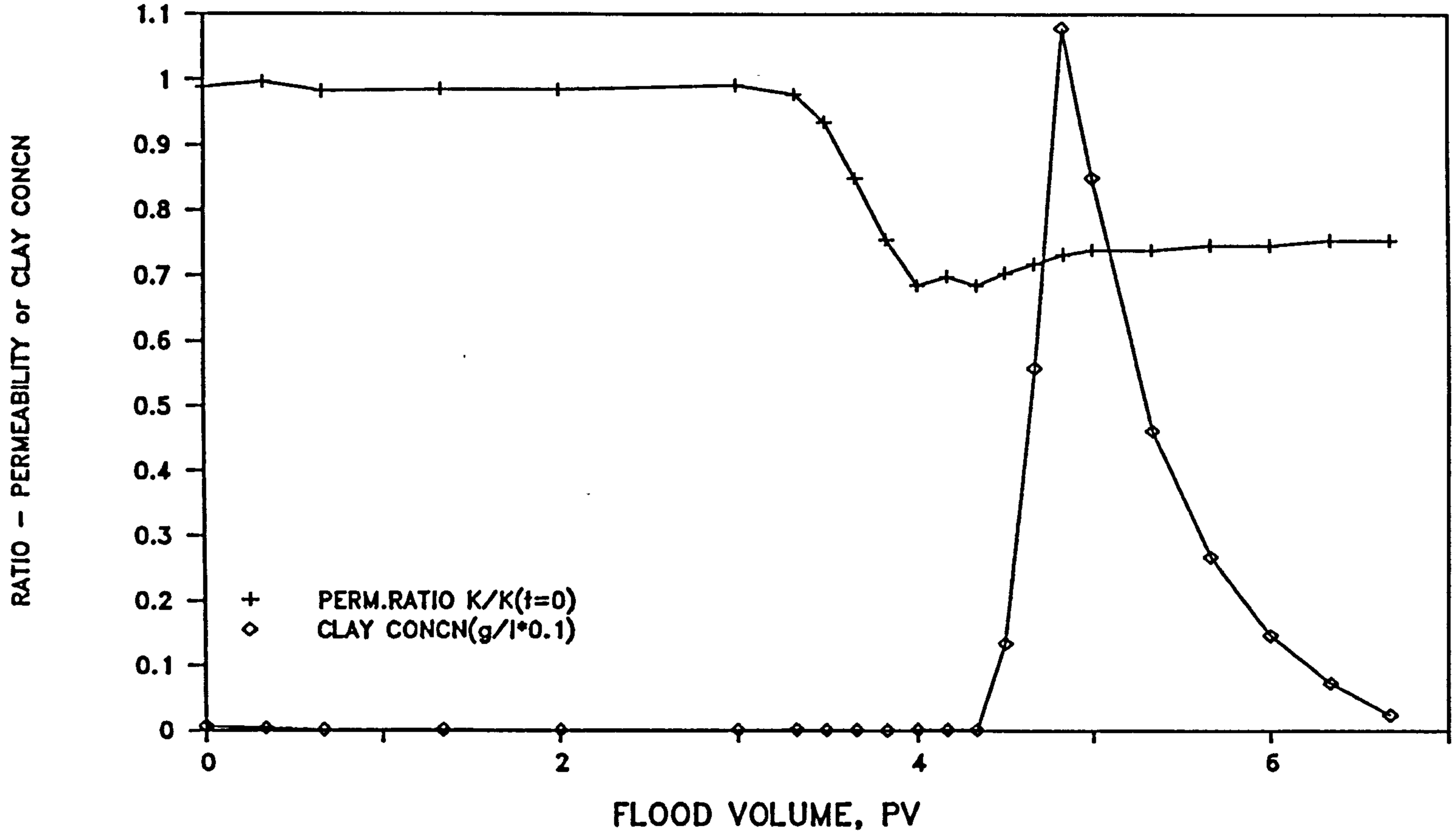

FIG. 40 Effect of Reverse Flow on Sandpack Permeability and Fines Production

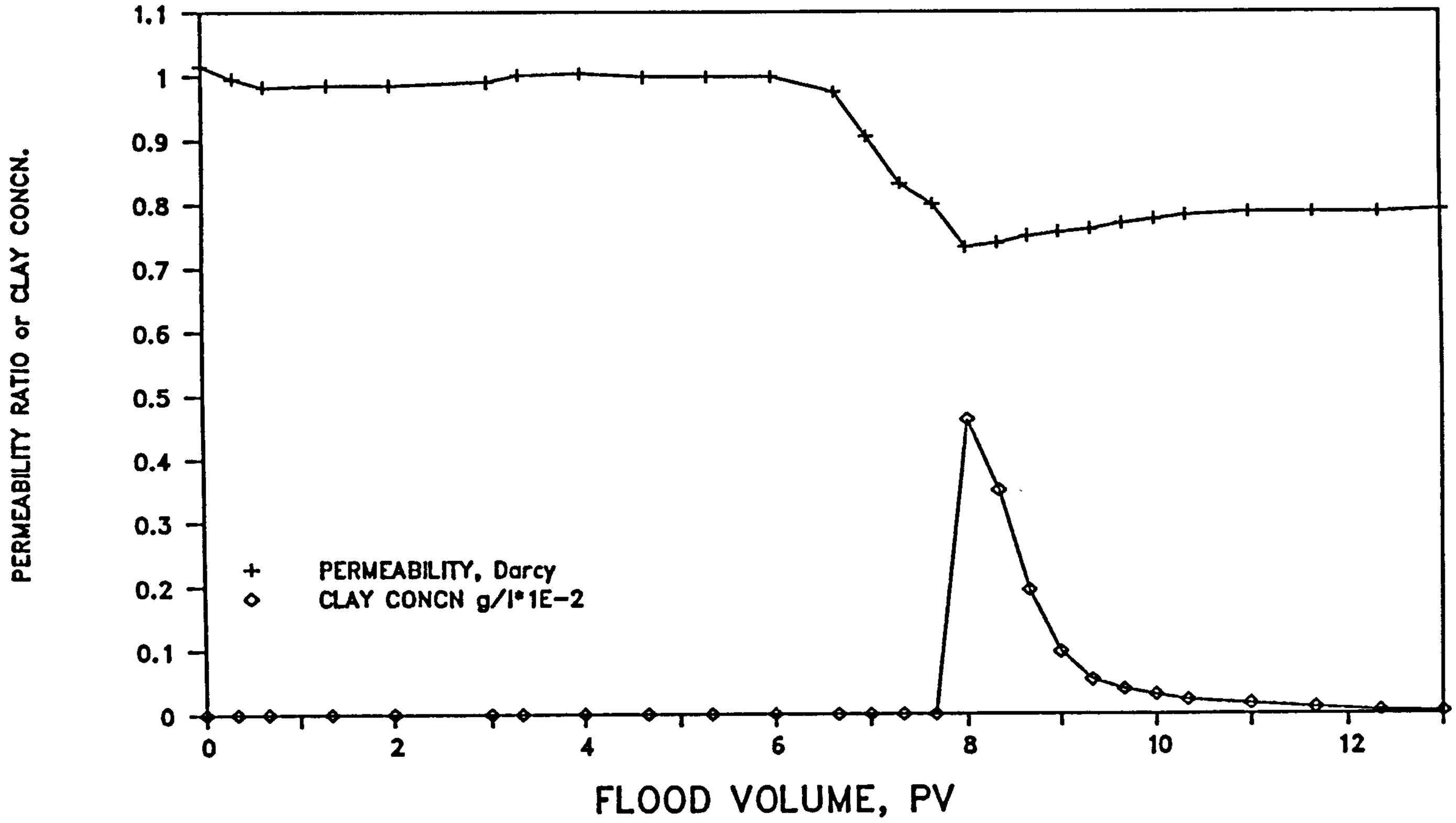

FIG. 41 Effect of Gravity on Permeability and Fines Production in Sandpacks

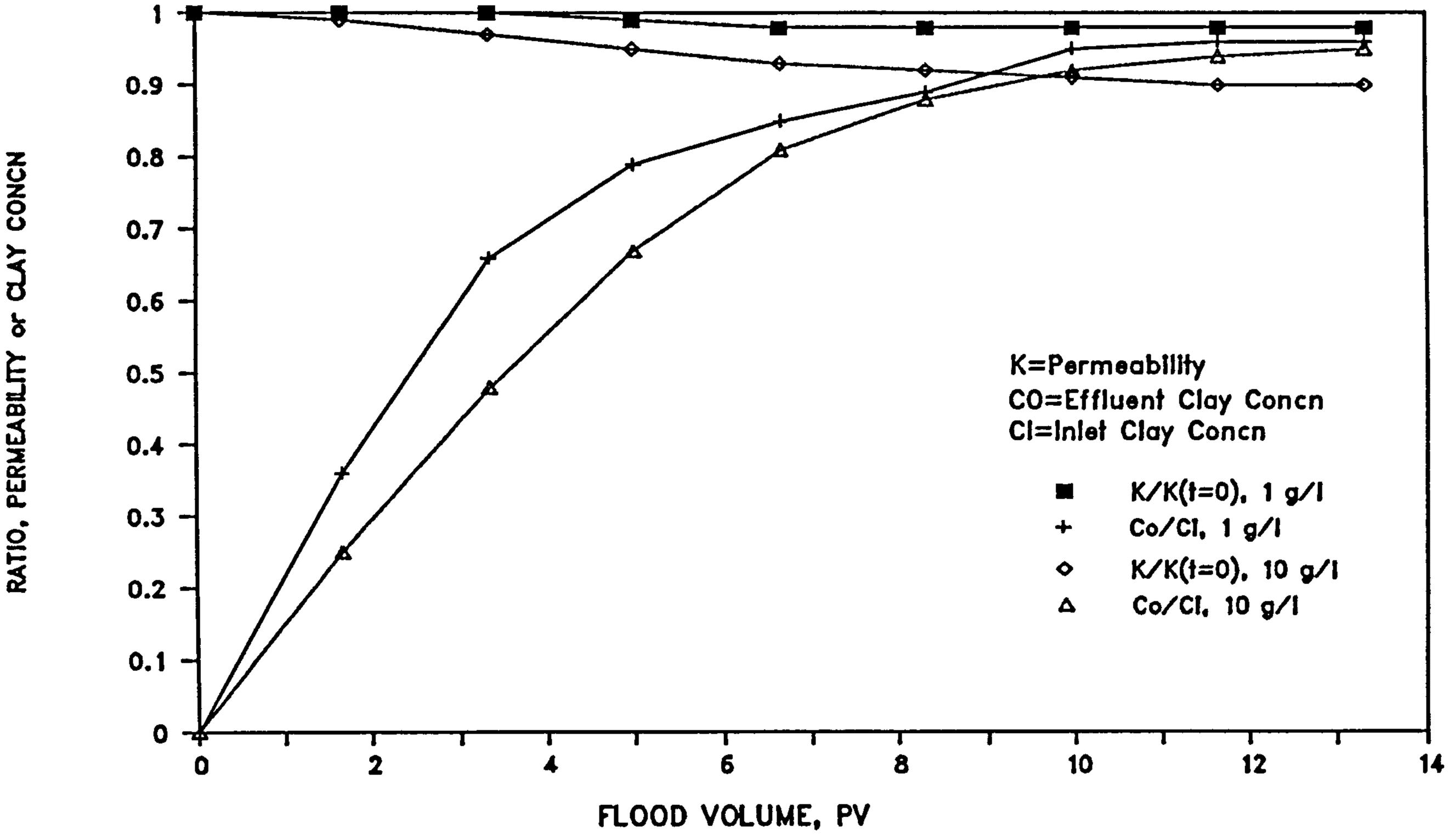

FIG. 42a Clay Filtration in 'Cleaned' Sandpacks From Distilled Water Suspensions

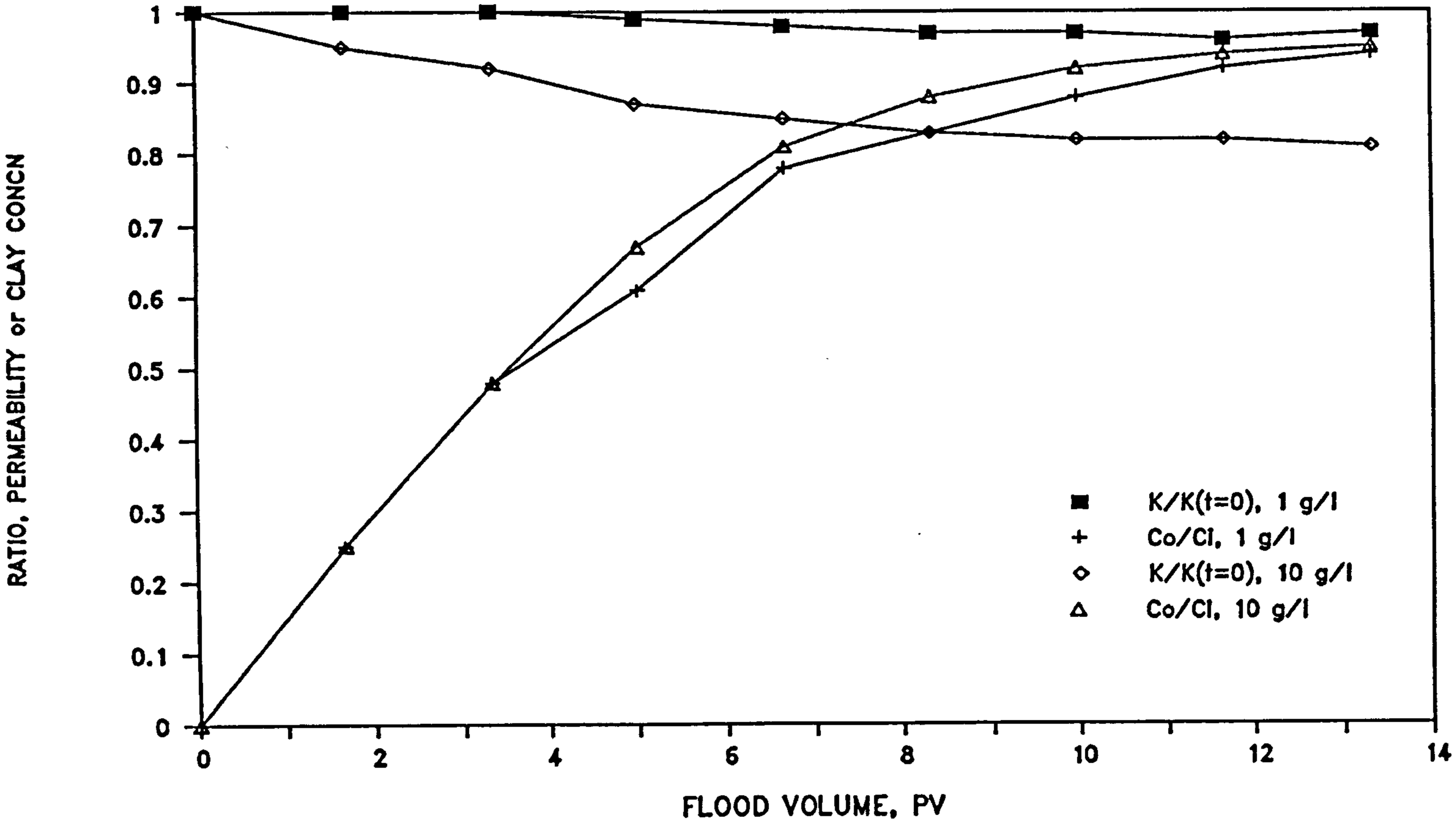

FIG. 42b Clay Filtration in 'Cleaned' Sandpacks From 0.01M Sodium Chloride Suspensions

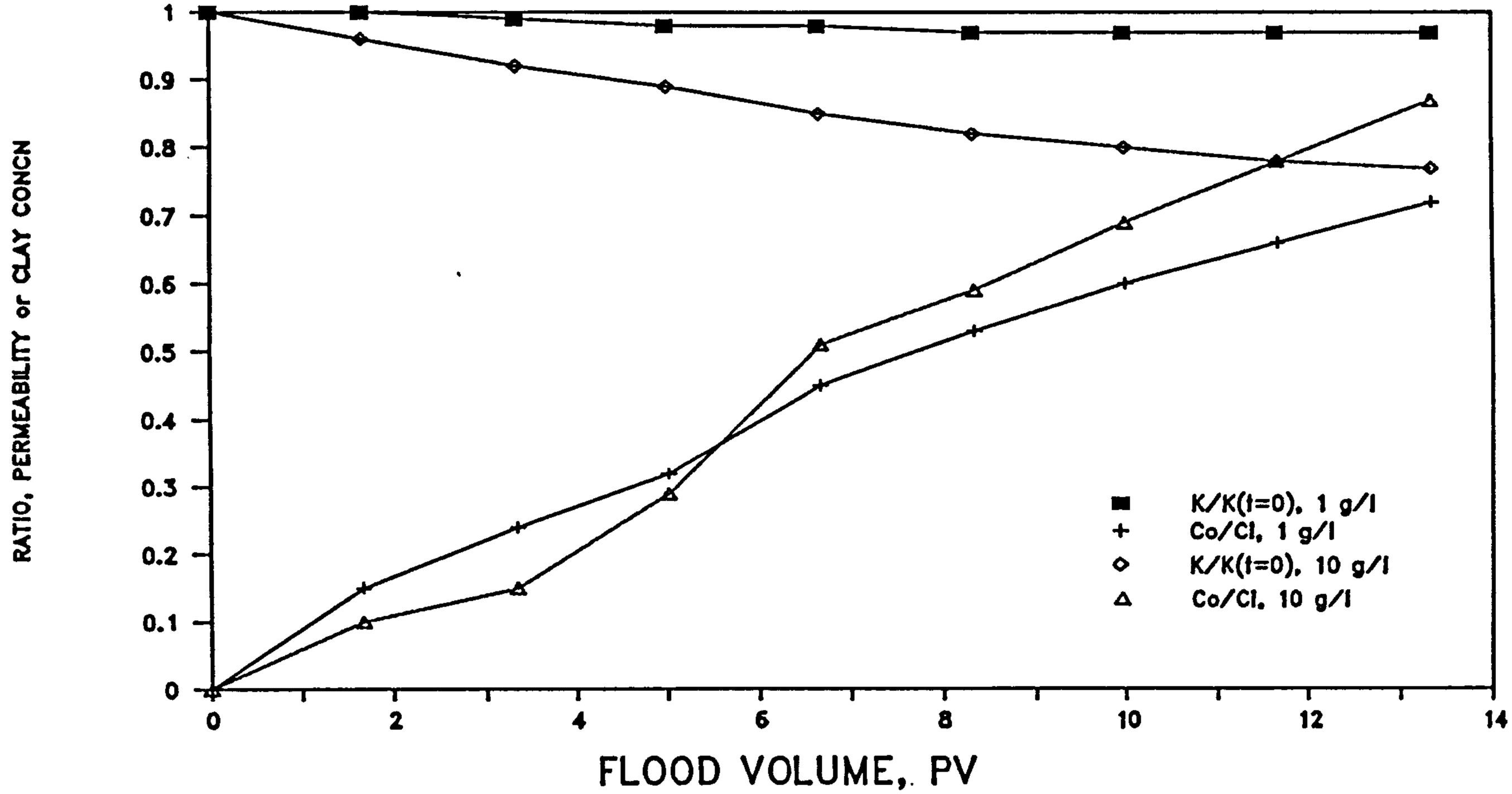

FIG. 43a Clay Filtration in 'Natural' Sandpacks From Distilled Water Suspensions

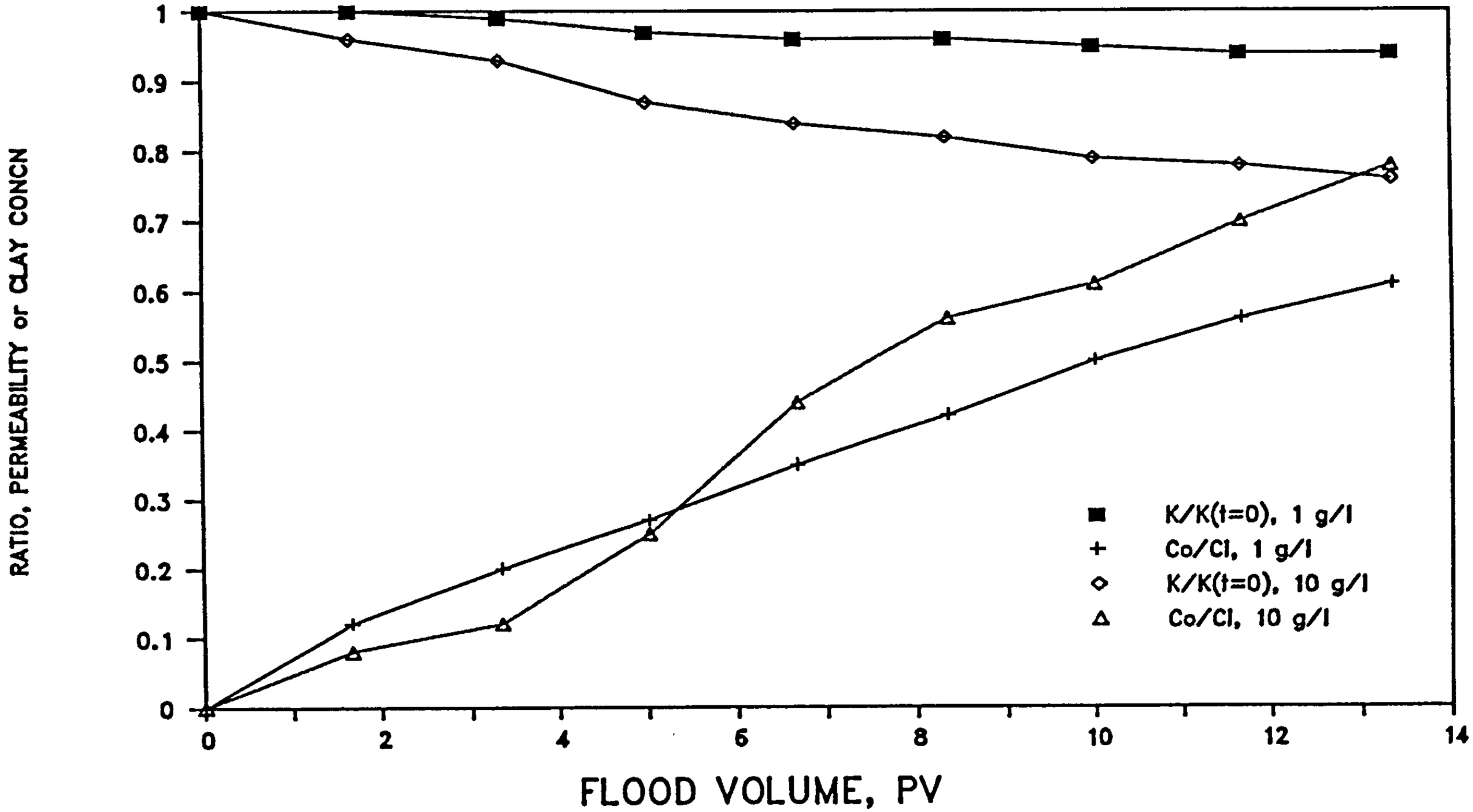

FIG. 43b Clay Filtration in 'Natural' Sandpacks From 0.01M Sodium Chloride Suspensions

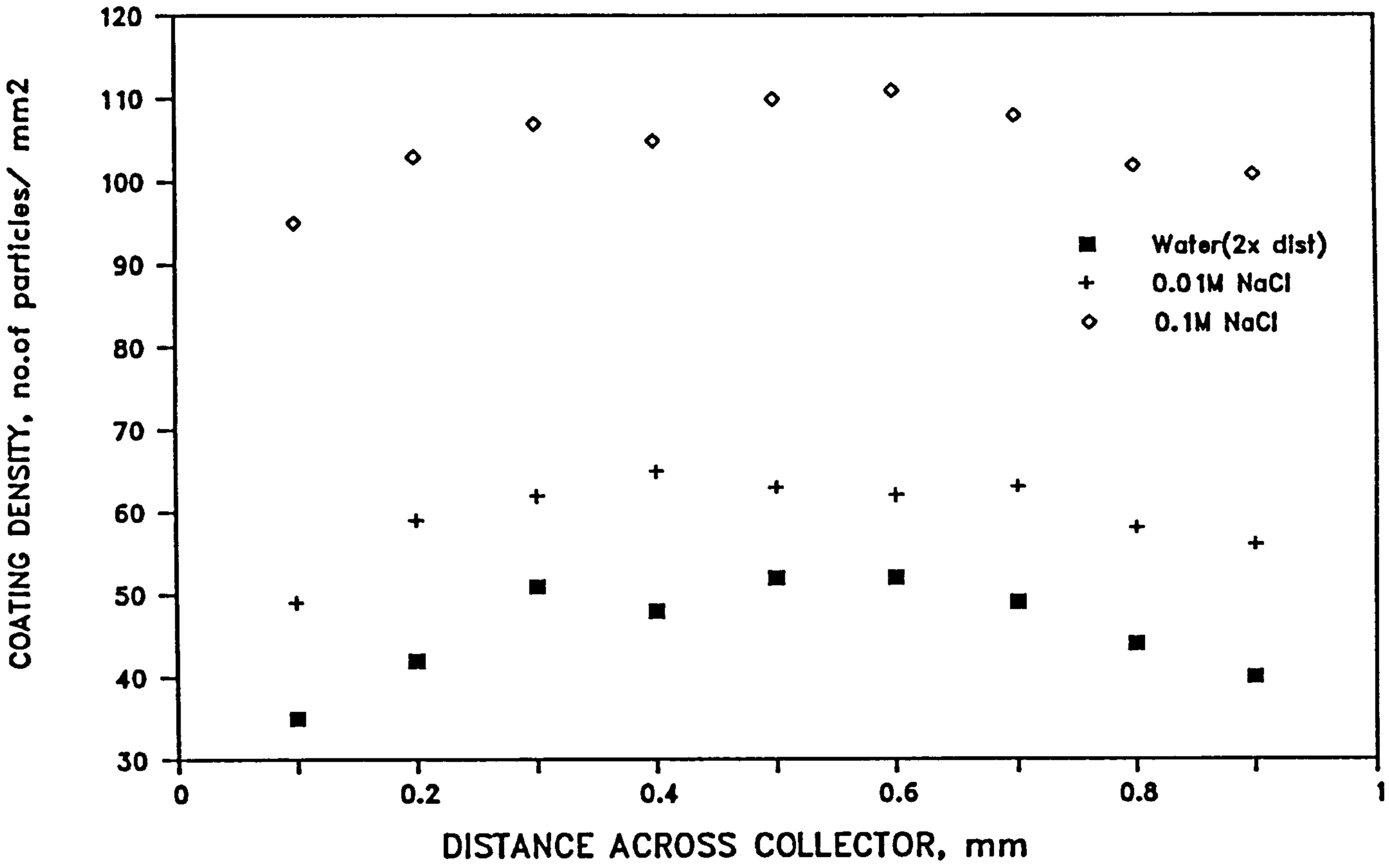

FIG. 44 Deposition of Latex onto Silica Discs

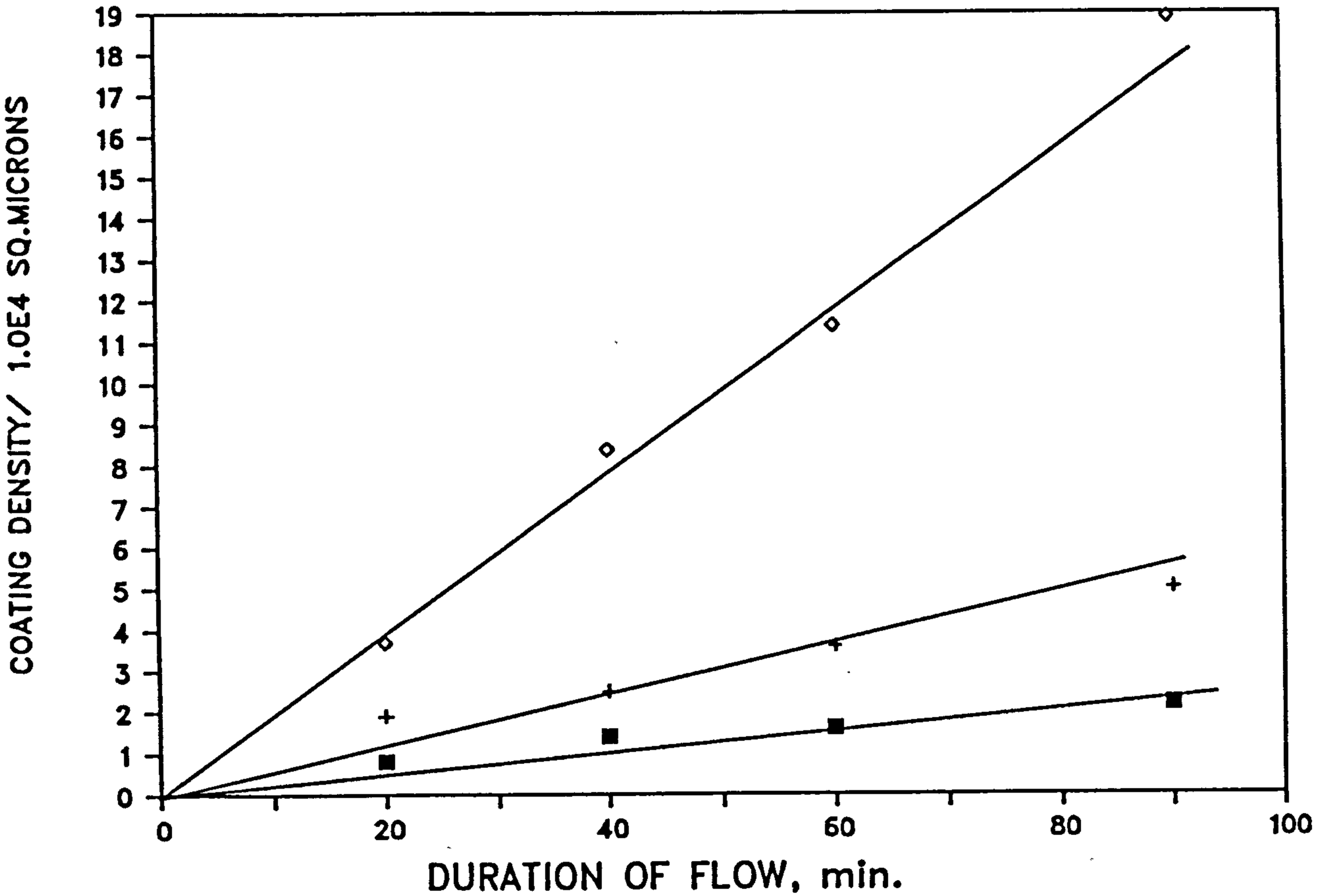

FIG. 45a Deposition of Kaolinite onto an Untreated Silica Disc

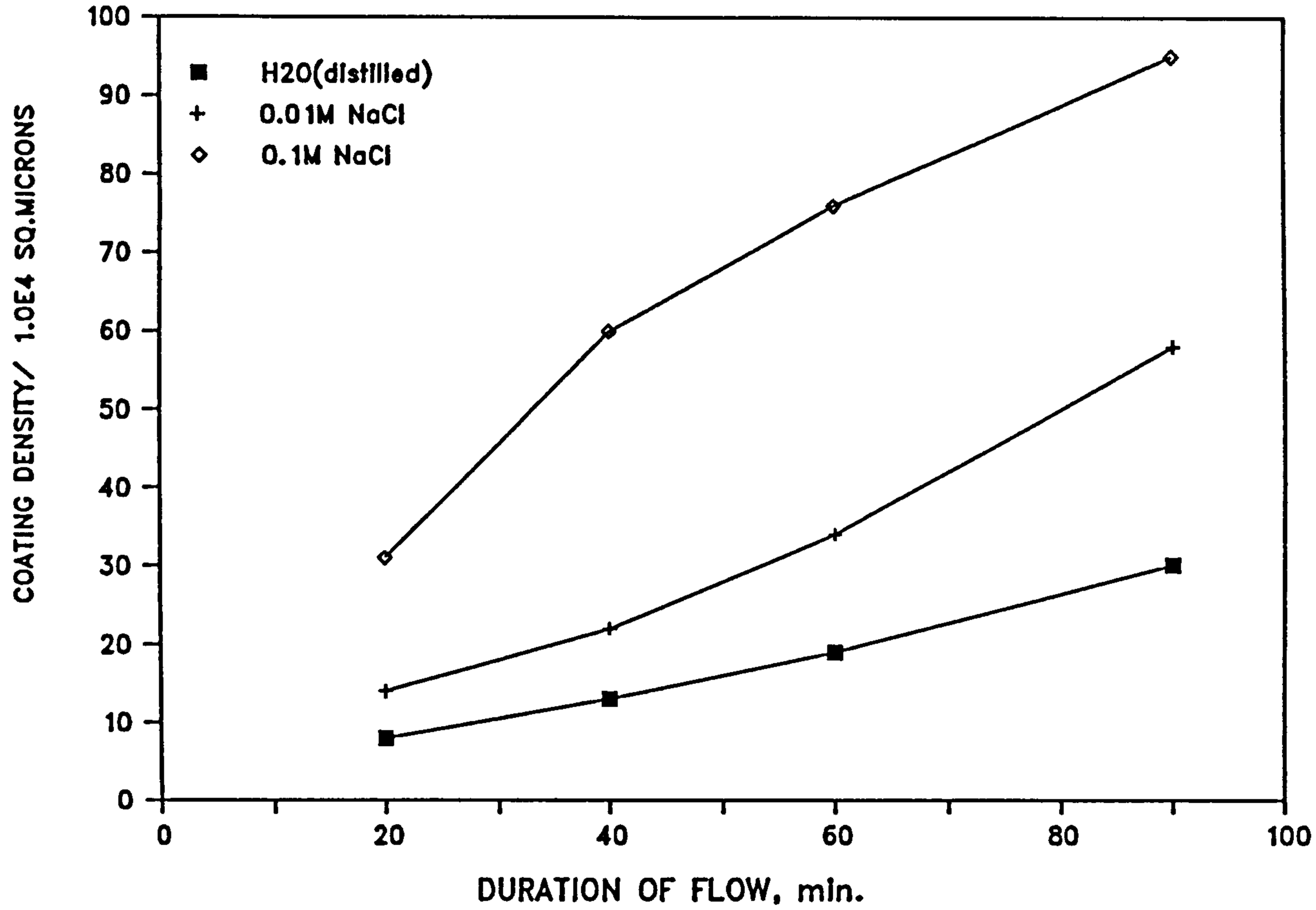

FIG. 45b Deposition of Kaolinite onto an Acid–Treated Silica Disc

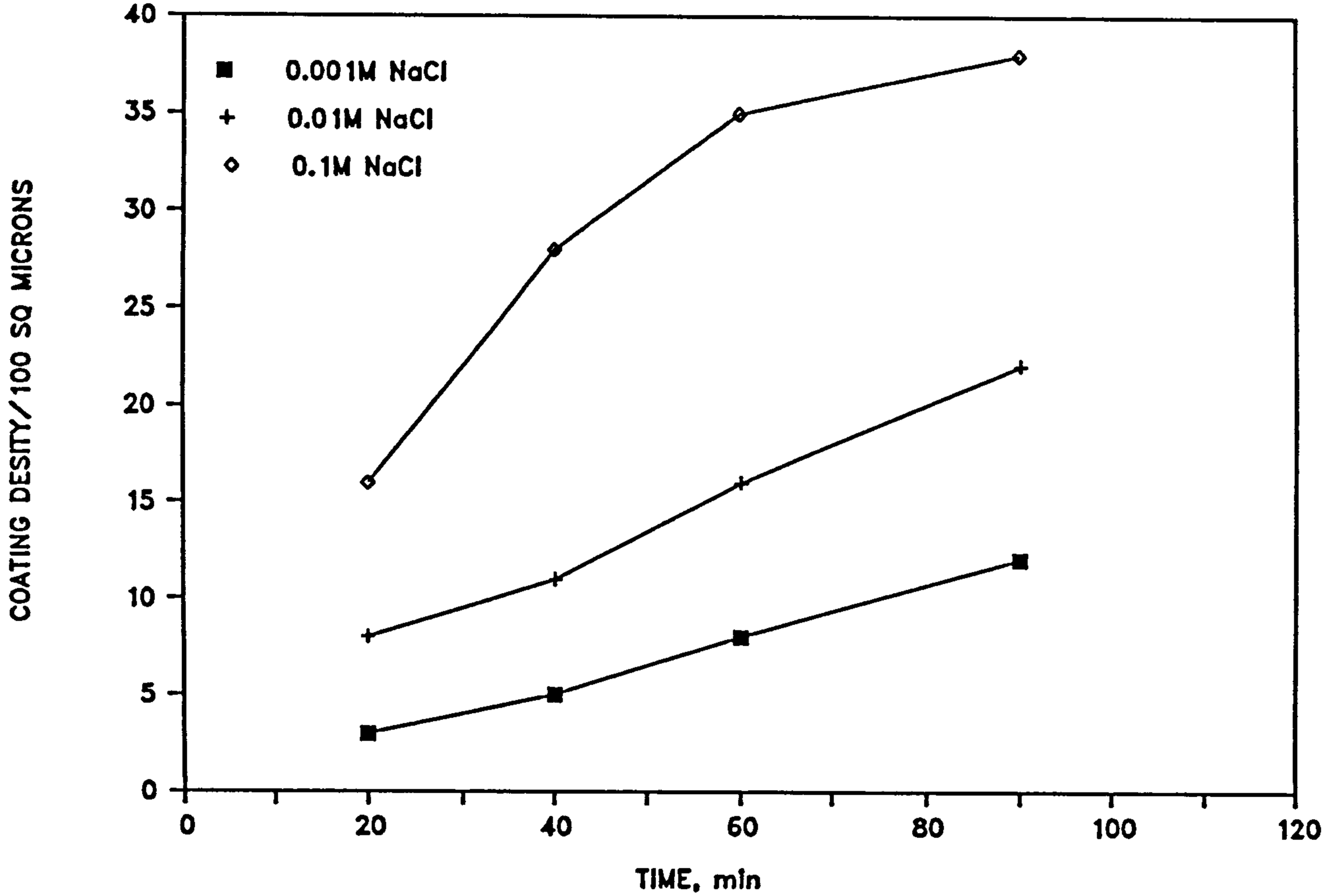

FIG. 46 Deposition of Kaolinite on a Silica Surface
Effect of Flow Duration and Salinity

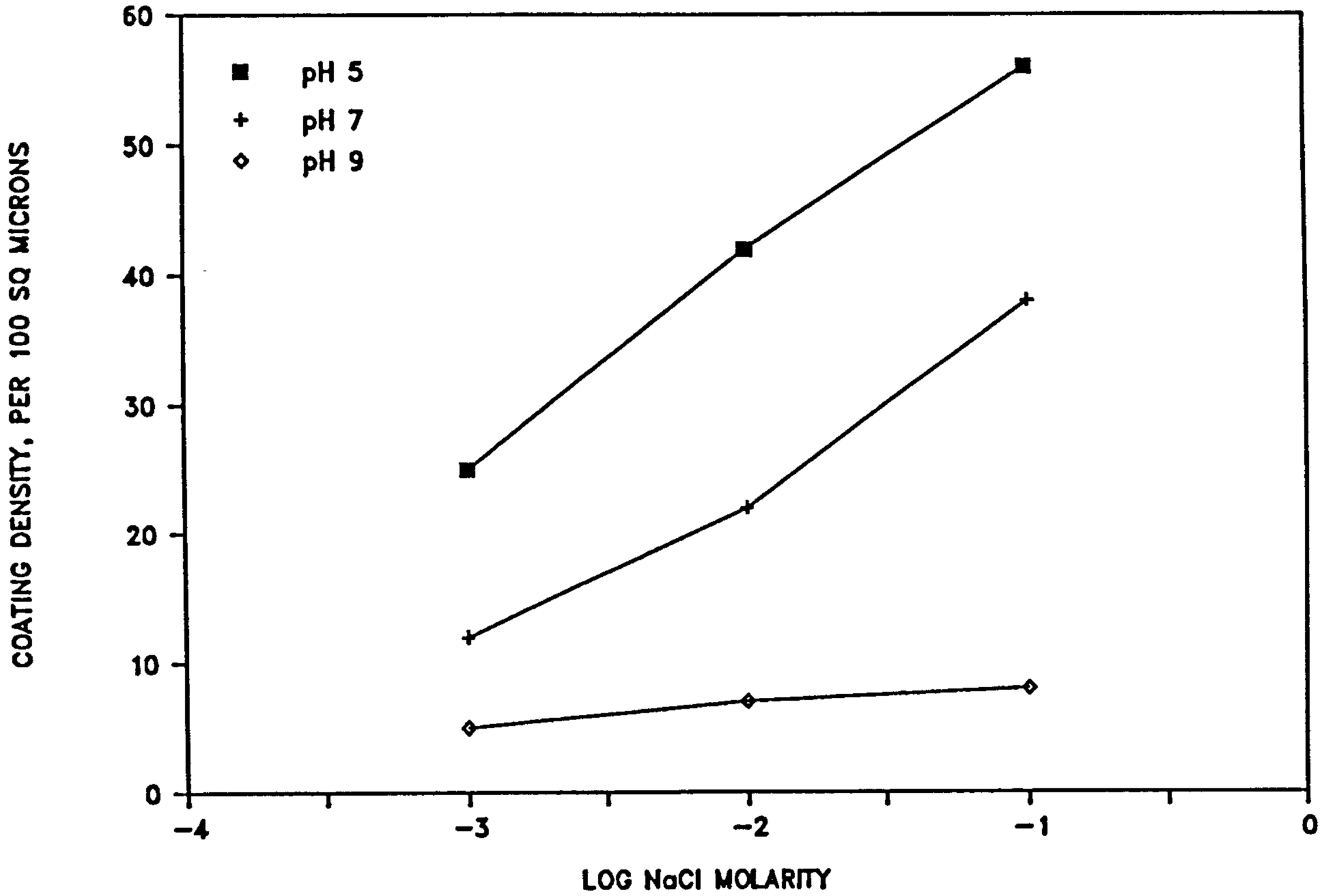

FIG. 47 Deposition of Kaolinite on a Silica Surface Effect of Salinity and pH

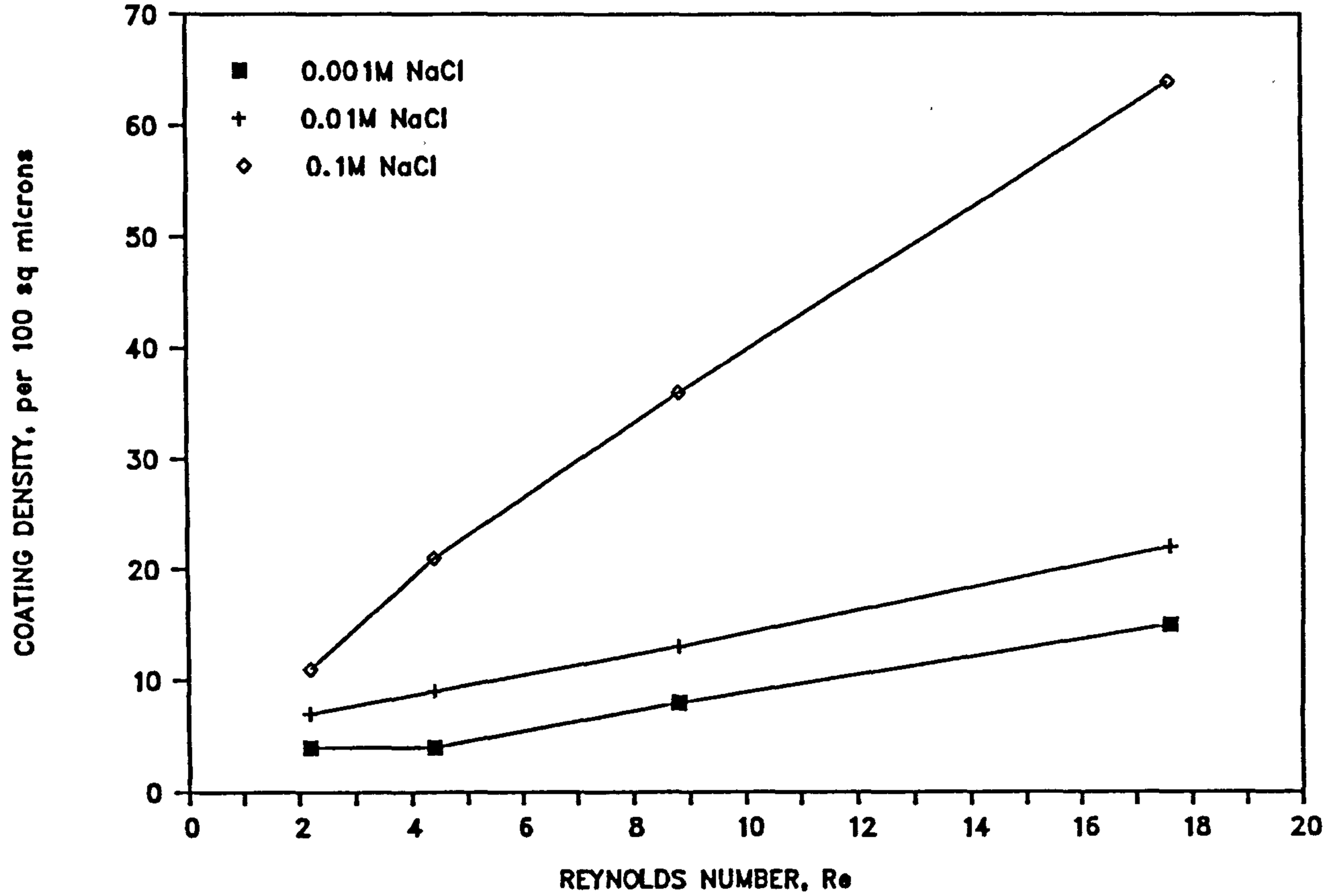

FIG. 48 Deposition of Kaolinite on a Silica Surface Effect of Reynolds Number

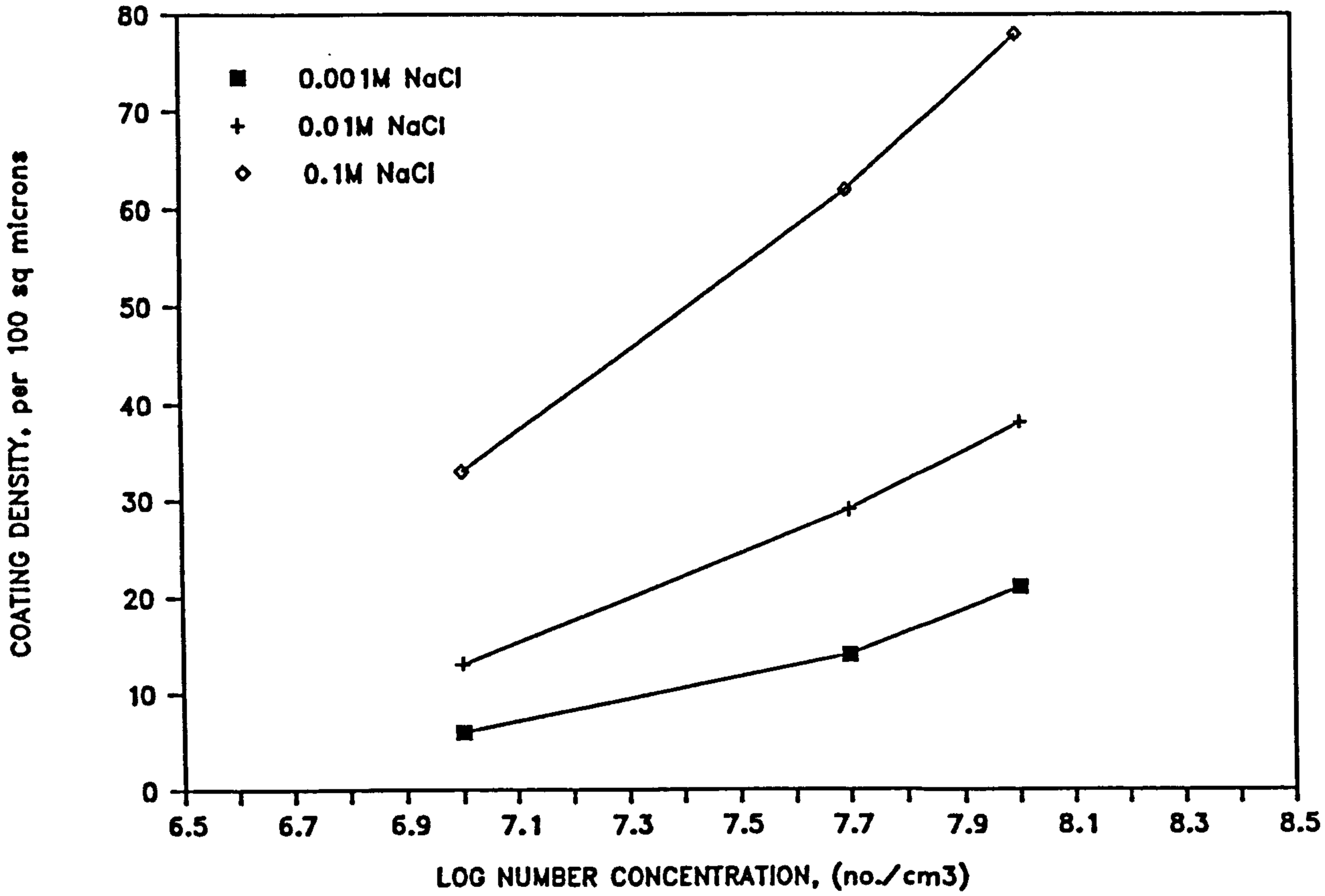

FIG. 49 Deposition of Kaolinite on a Silica Surface
Effect of Suspension Concentration

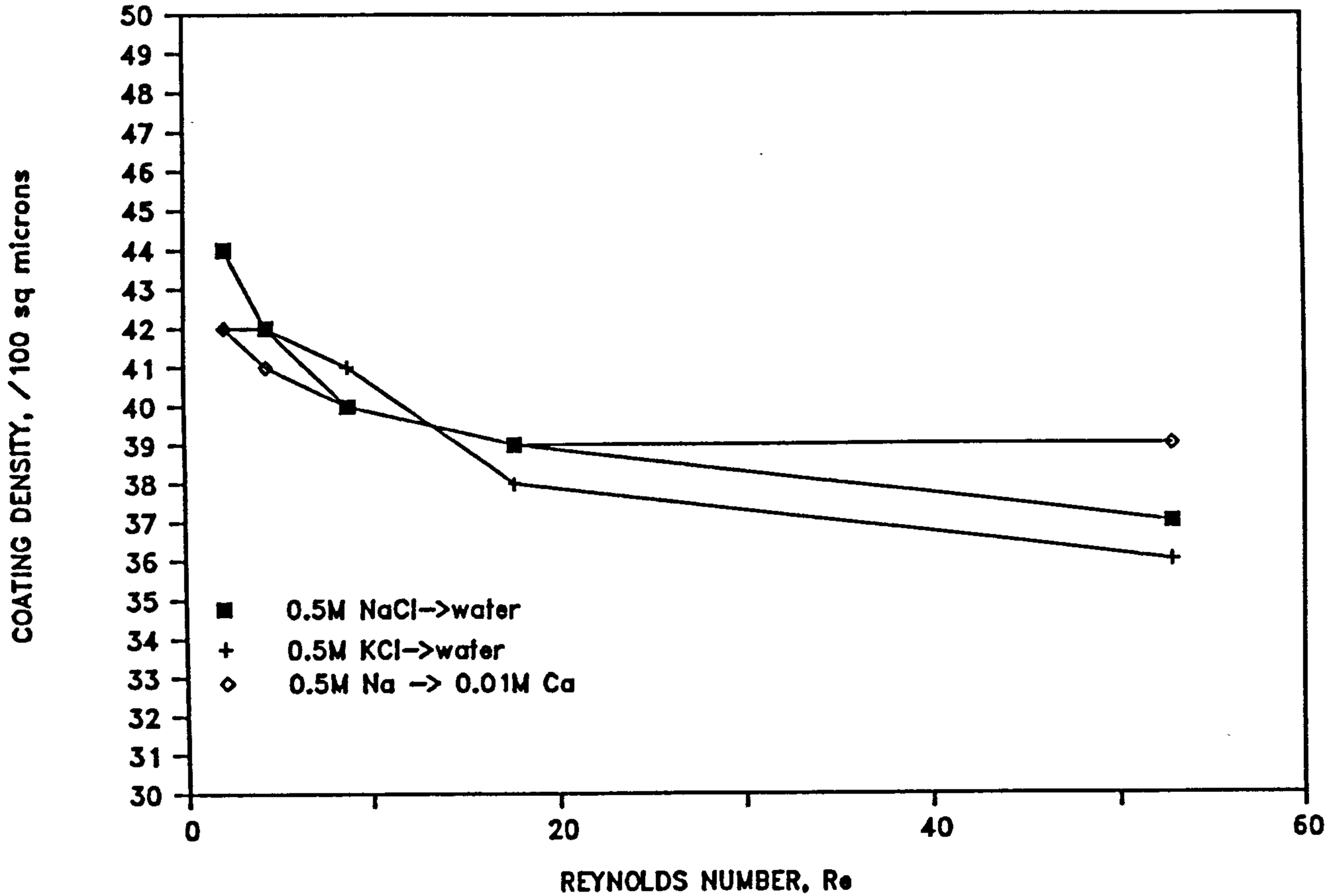

FIG. 50a Detachment of Kaolinite from Silica Surfaces
Effect of Different Brine Treatments

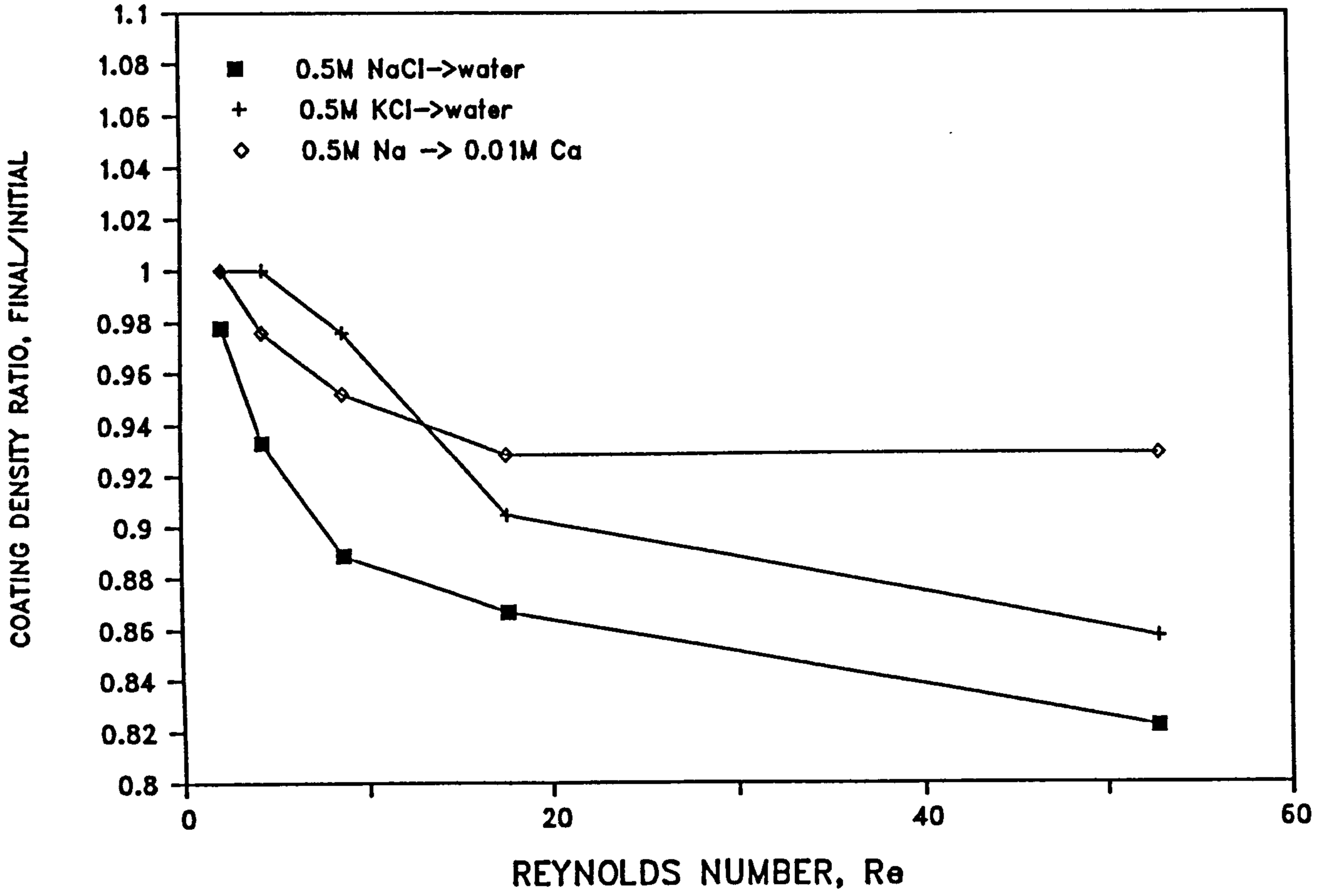

FIG. 50b Ratio of Final to Initial Coating Density for Fig. 50a

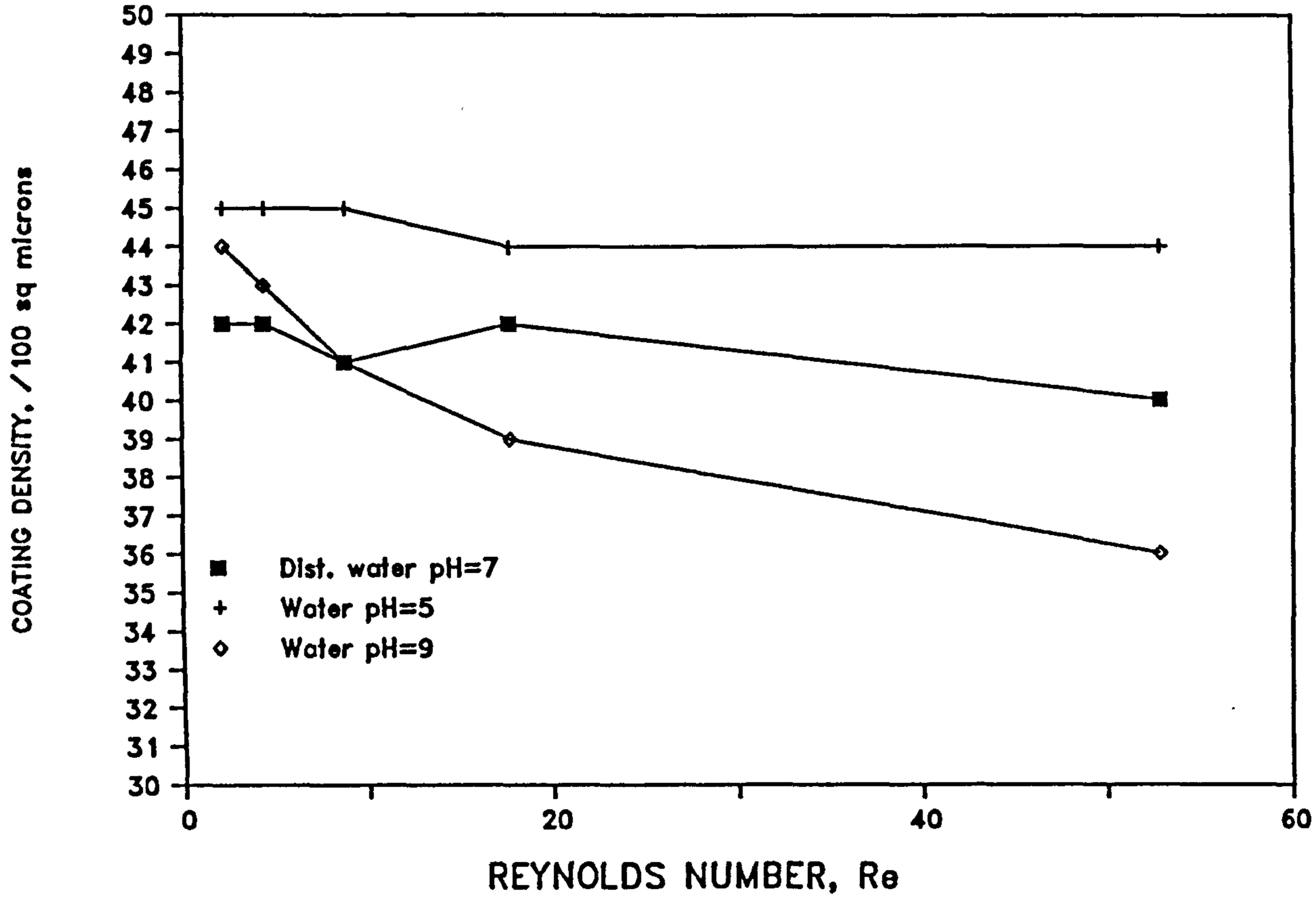

FIG. 51a Detachment of Kaolinite from Silica Surfaces
Effect of Reynolds Number and pH

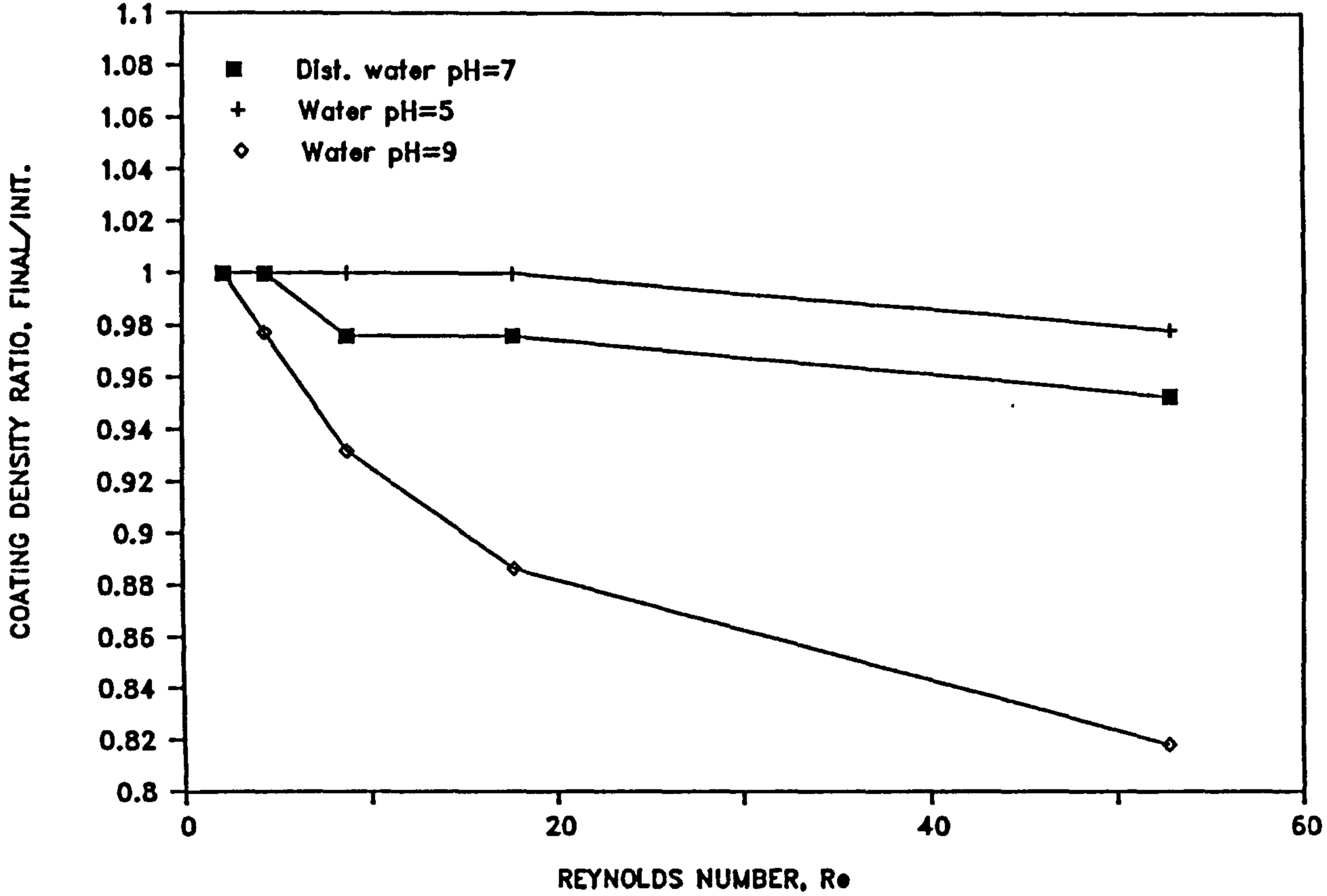

FIG. 51b Ratio of Final to Initial Coating Density for Fig. 51a

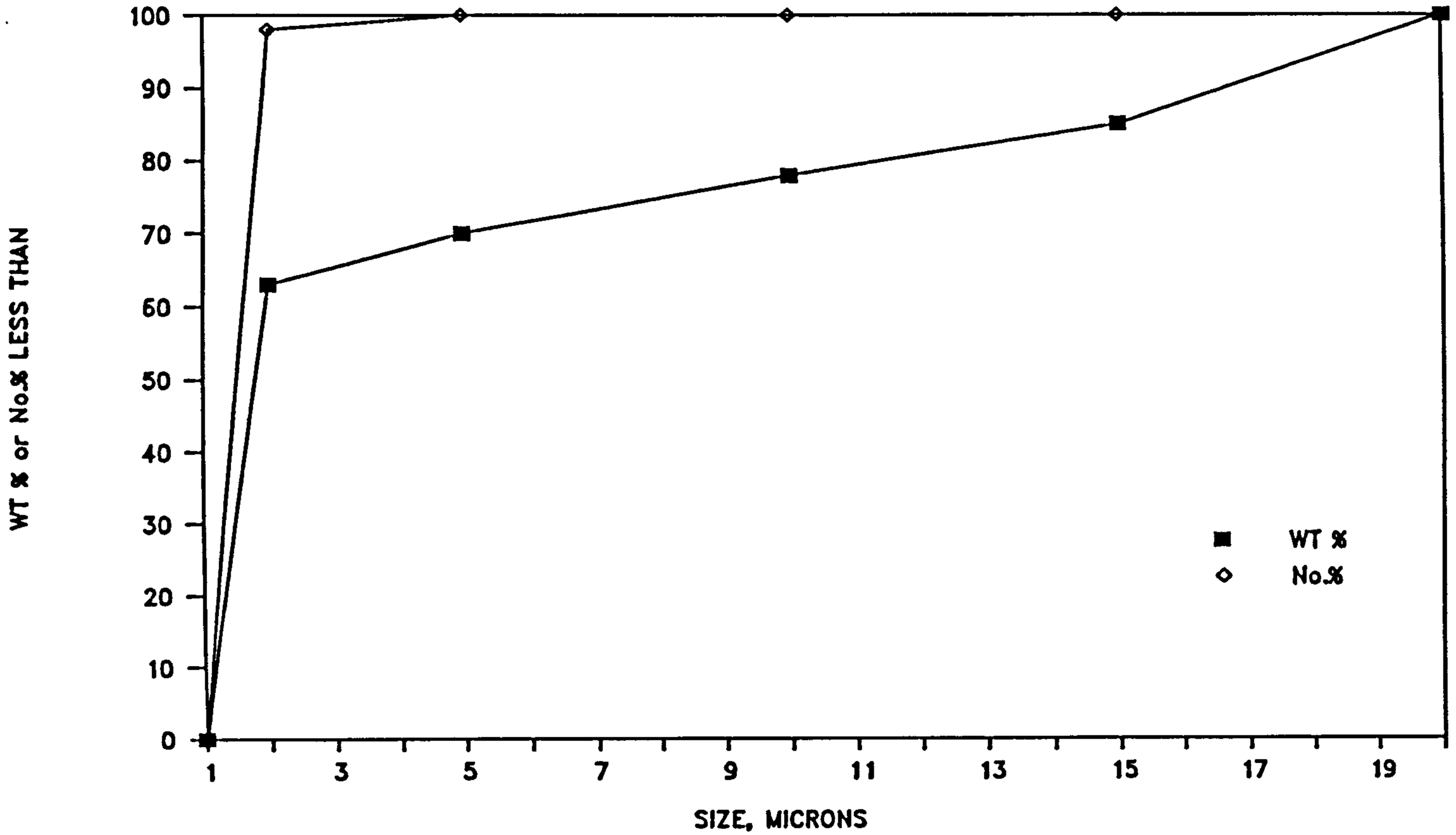

FIG. 52 Particle Size Distribution of Mobilised Clay from Separator Sand

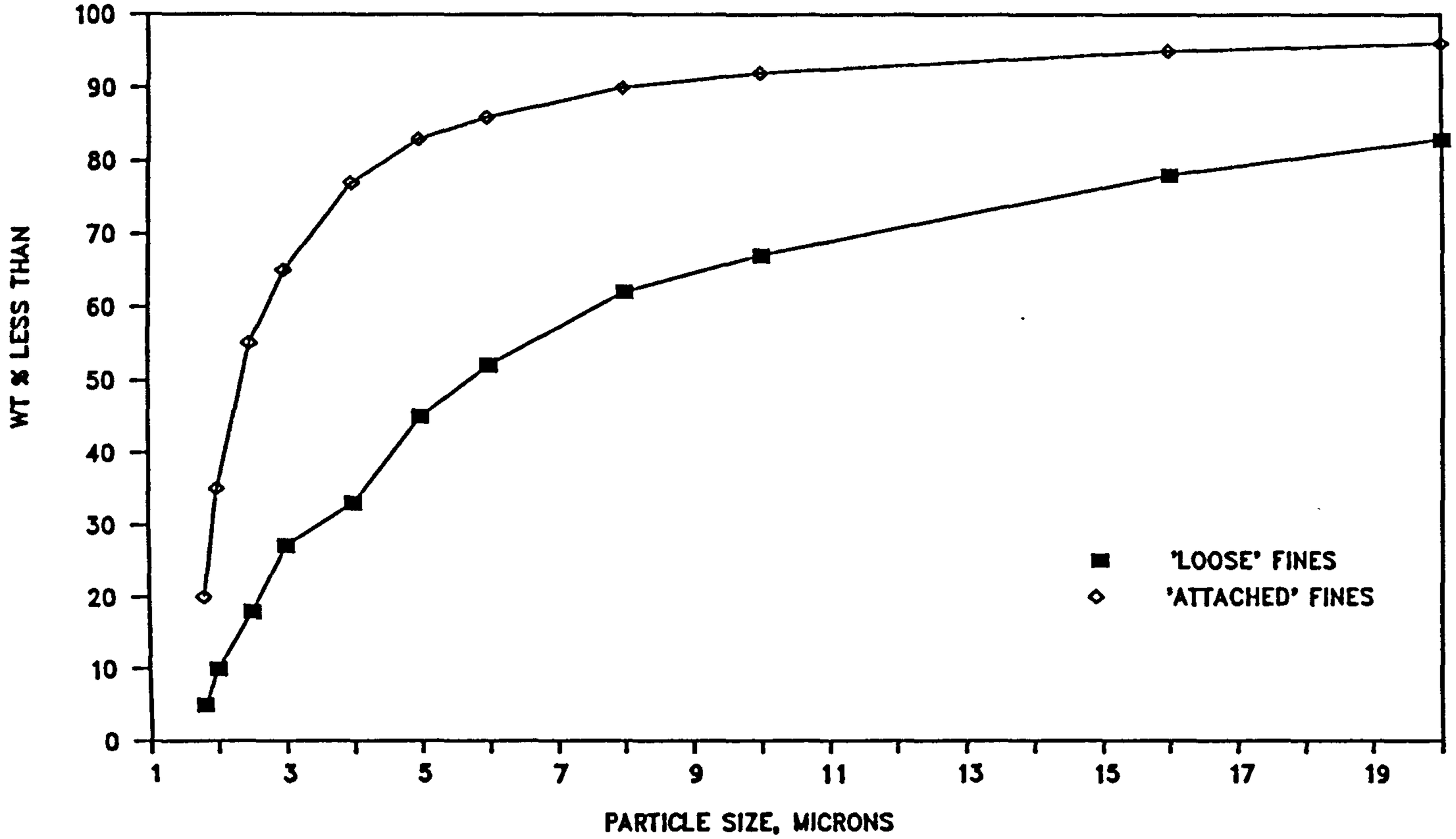

FIG. 53 Size Distribution of 'Loose' and 'Attached' Fines From Fine-Grey Sand

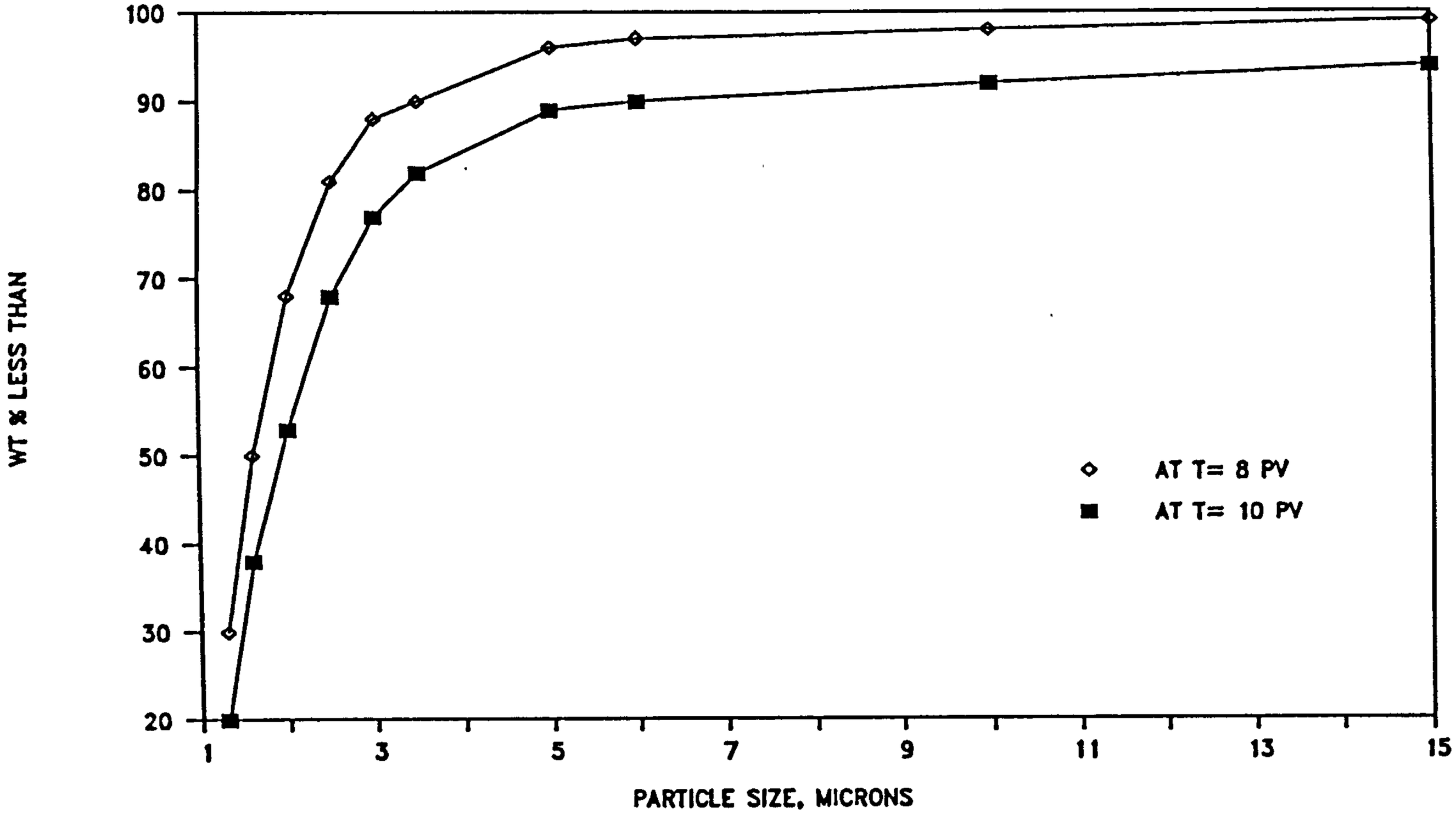

FIG. 54 Particle Size Distribution Across a Migrating Zone of Fines

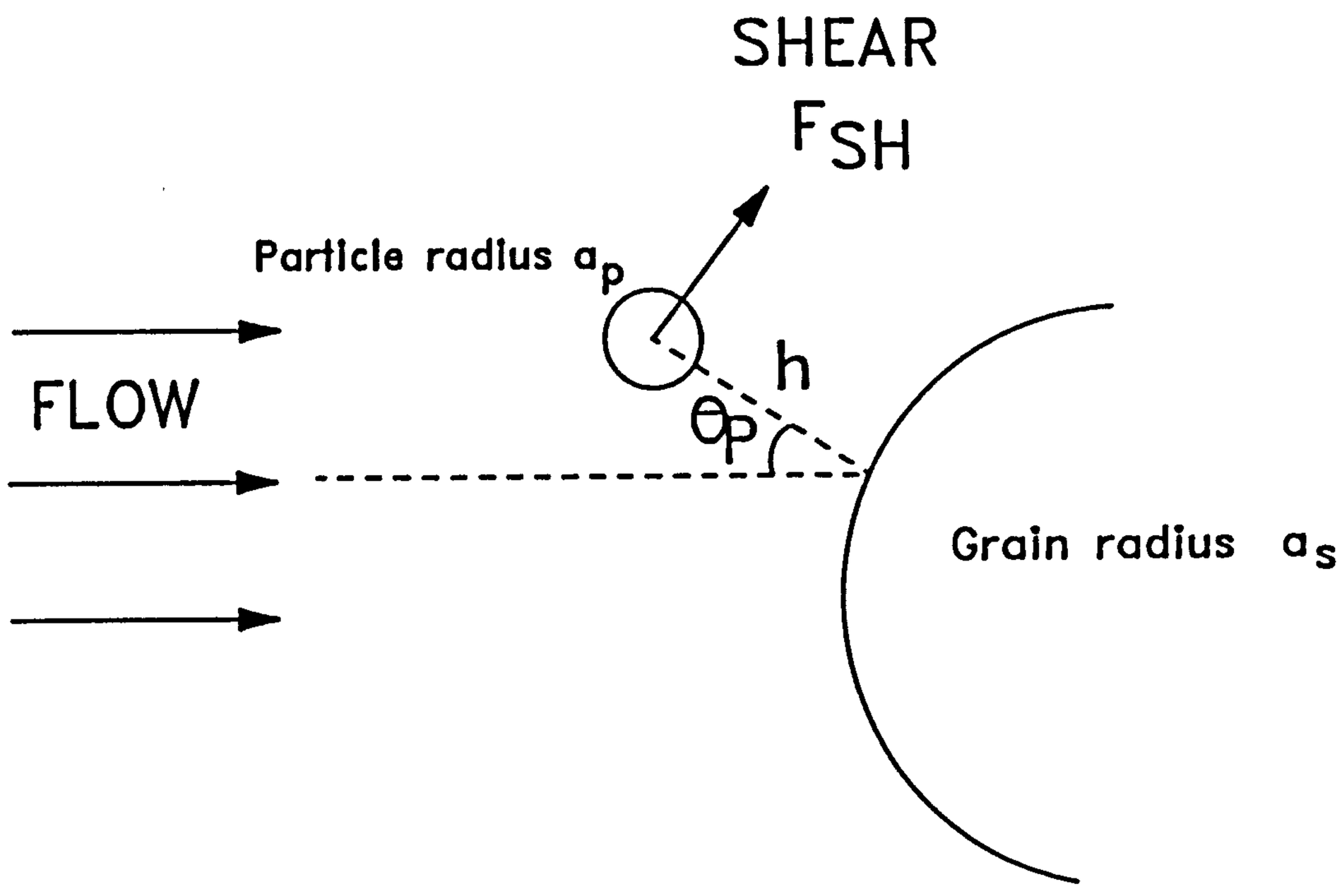

FIG. 55a Hydrodynamic Shear Force Acting on a Small Particle Near a Surface

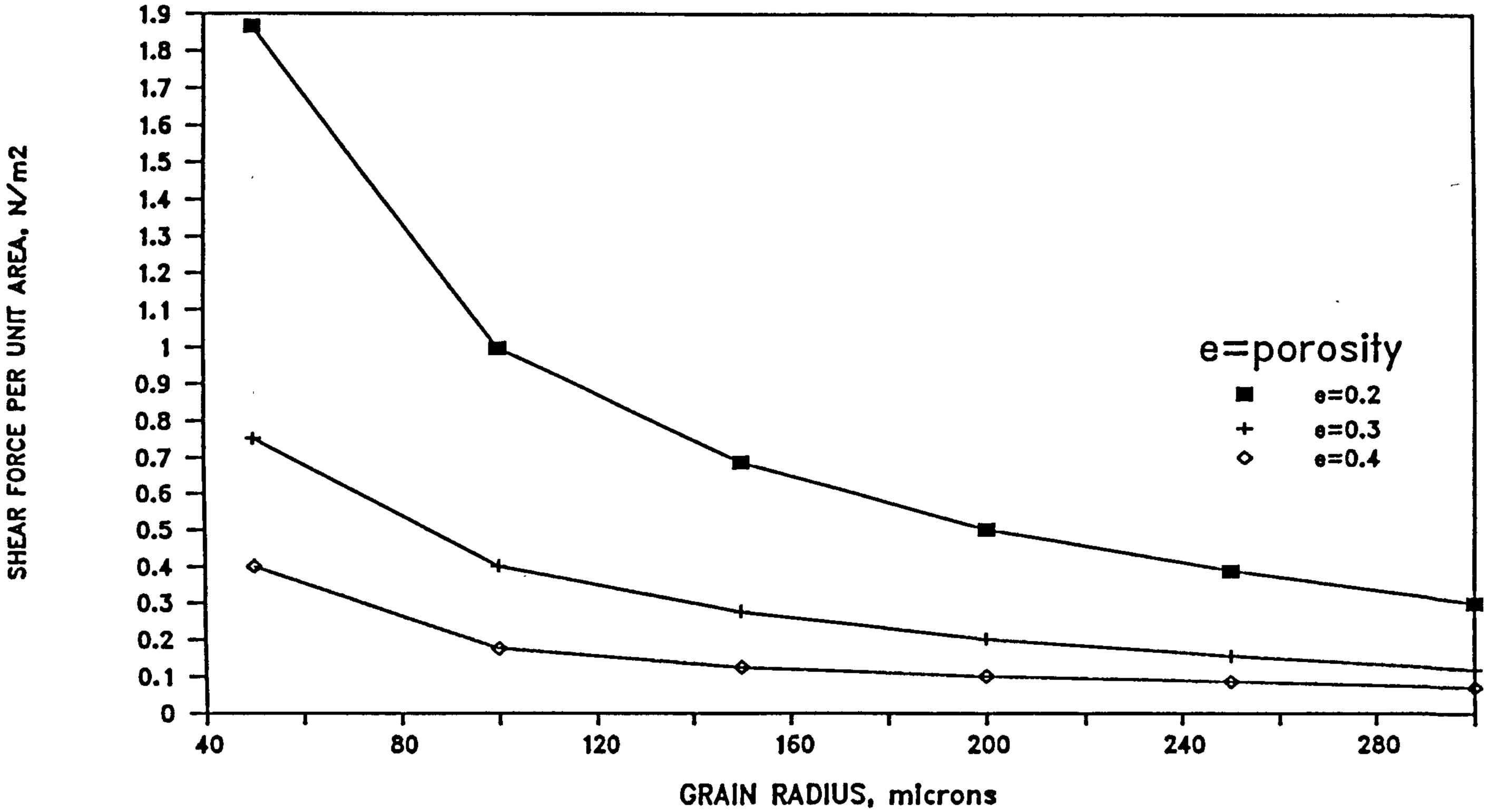

FIG. 55b The Fluid Shear Force on a Colloidal-Sized Particle Near the Surface of a Sand Grain

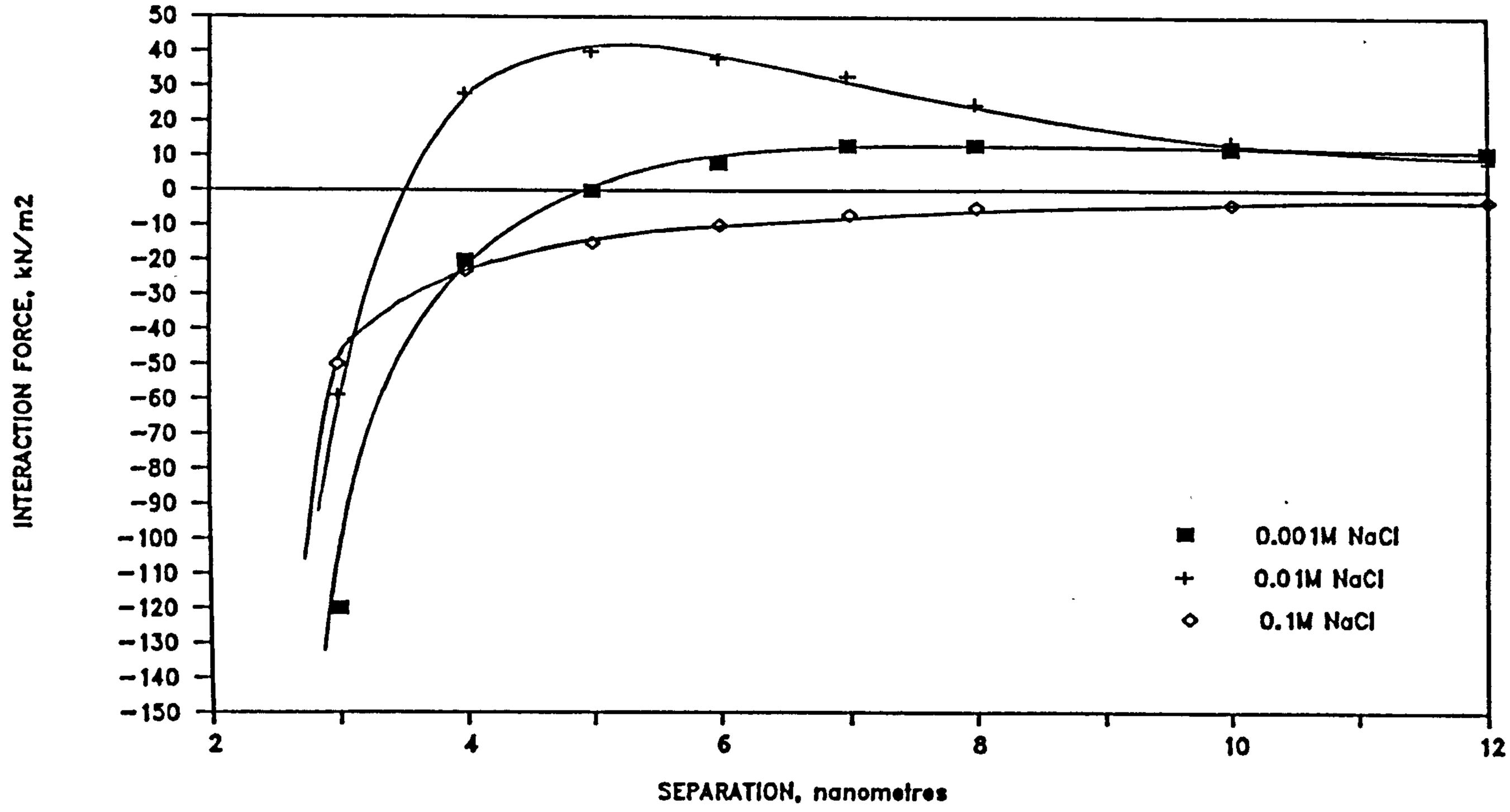

FIG. 56a Total Electrical Interaction Force
Kaolinite Face Association at pH 6

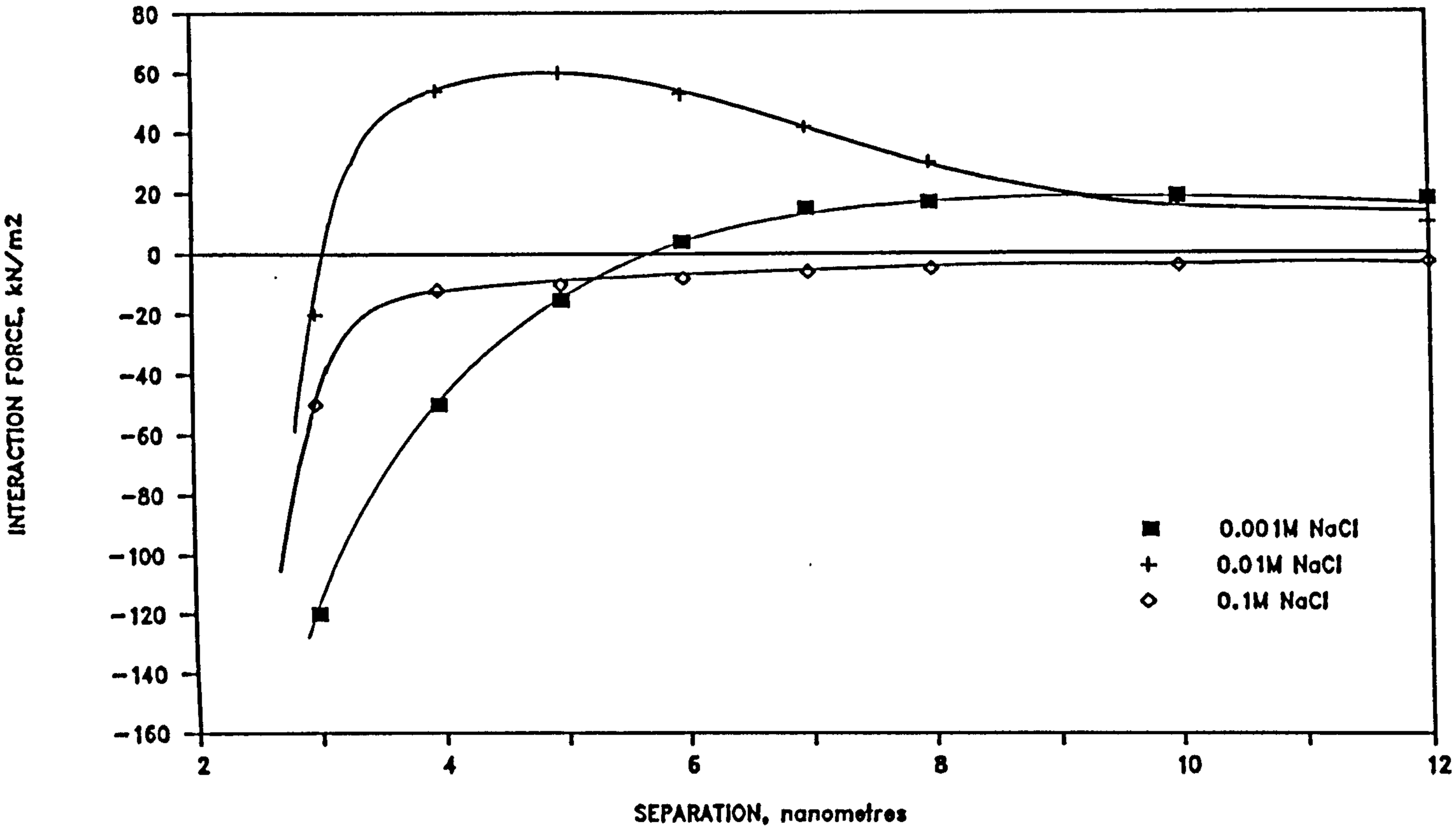

FIG. 56b Total Electrical Interaction Force
Kaolinite Face Association at pH 7

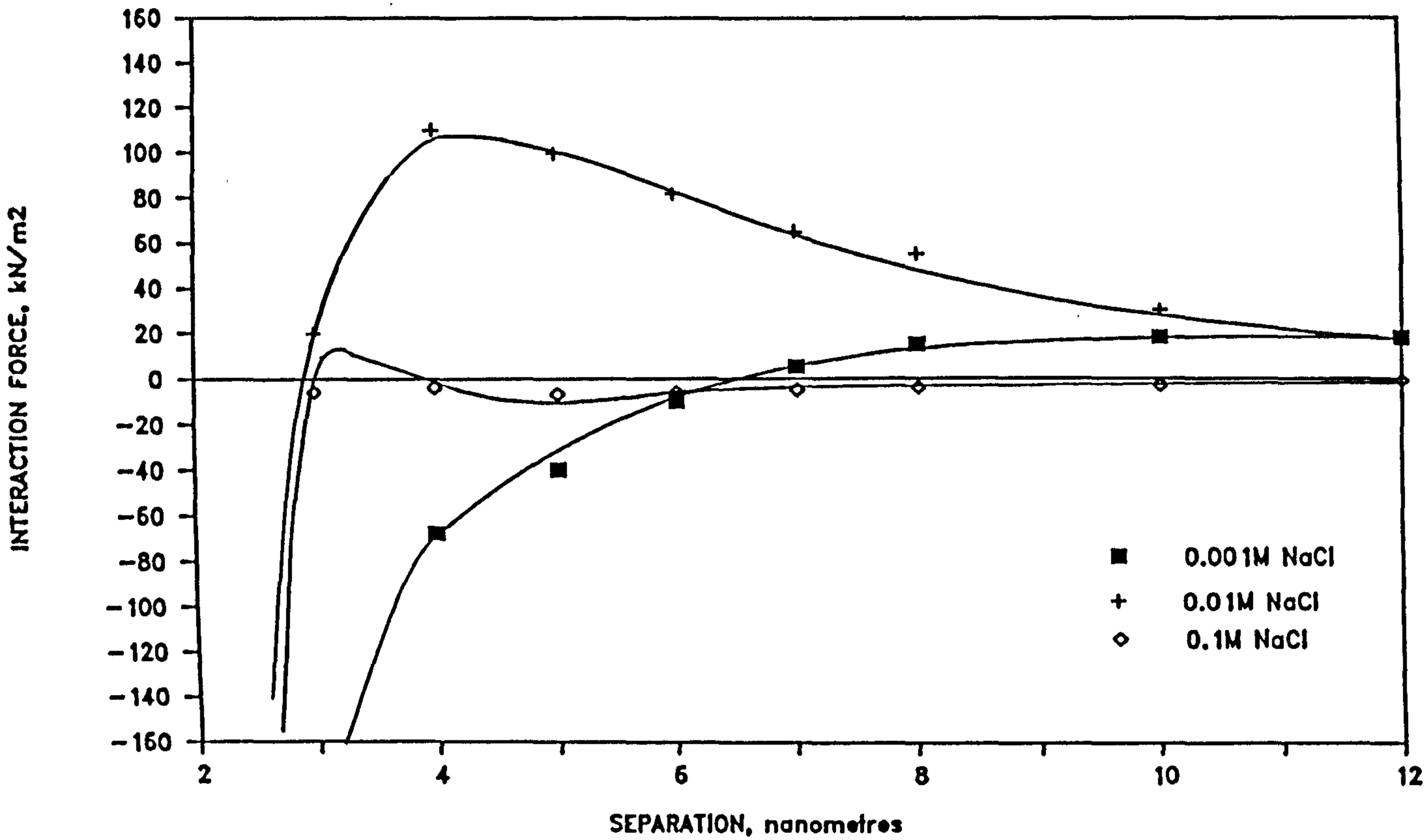

FIG. 56c Total Electrical Interaction Force
Kaolinite Face Association at pH 9

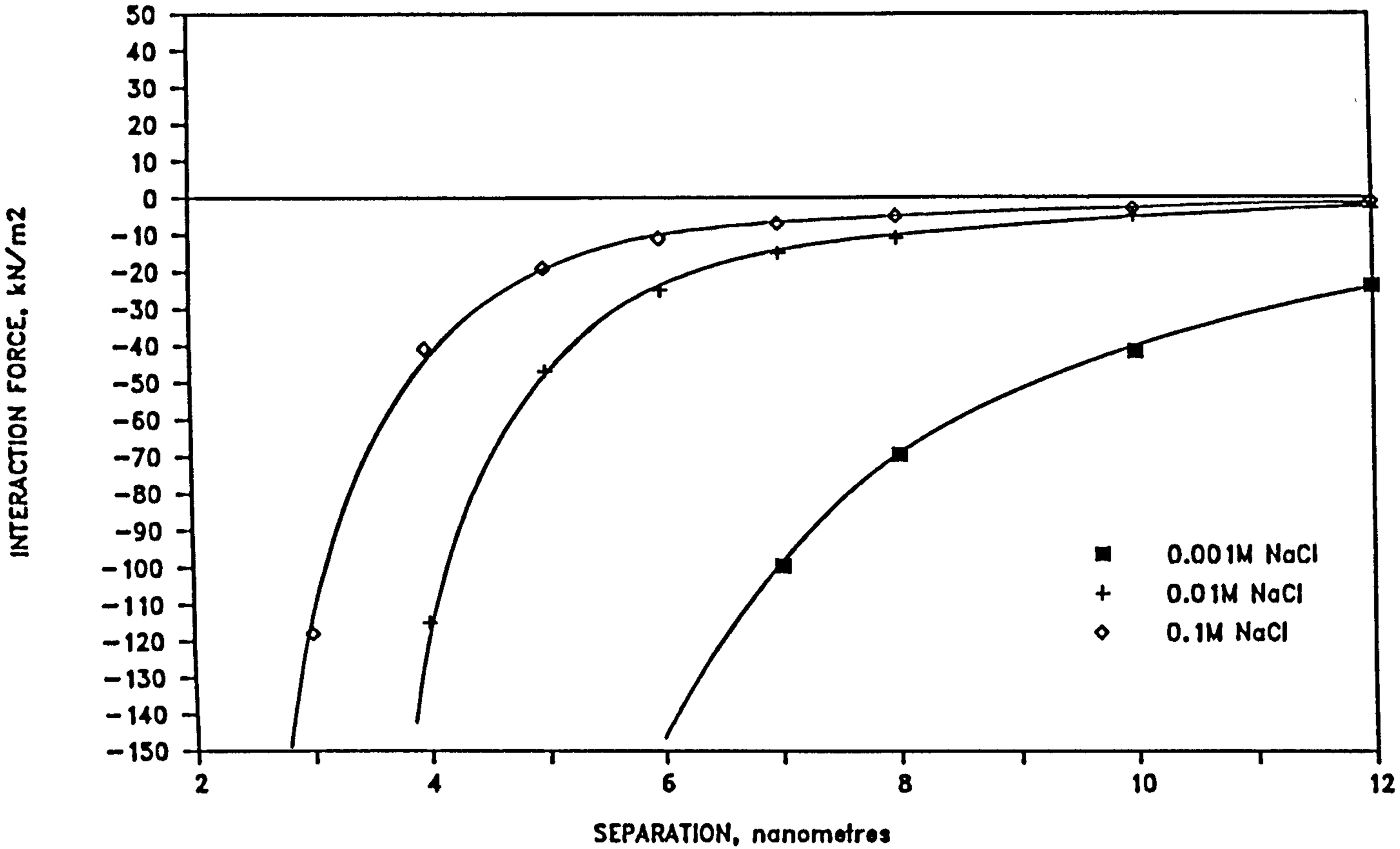

FIG. 57a Total Electrical Interaction Force
Kaolinite Edge Association at pH 7

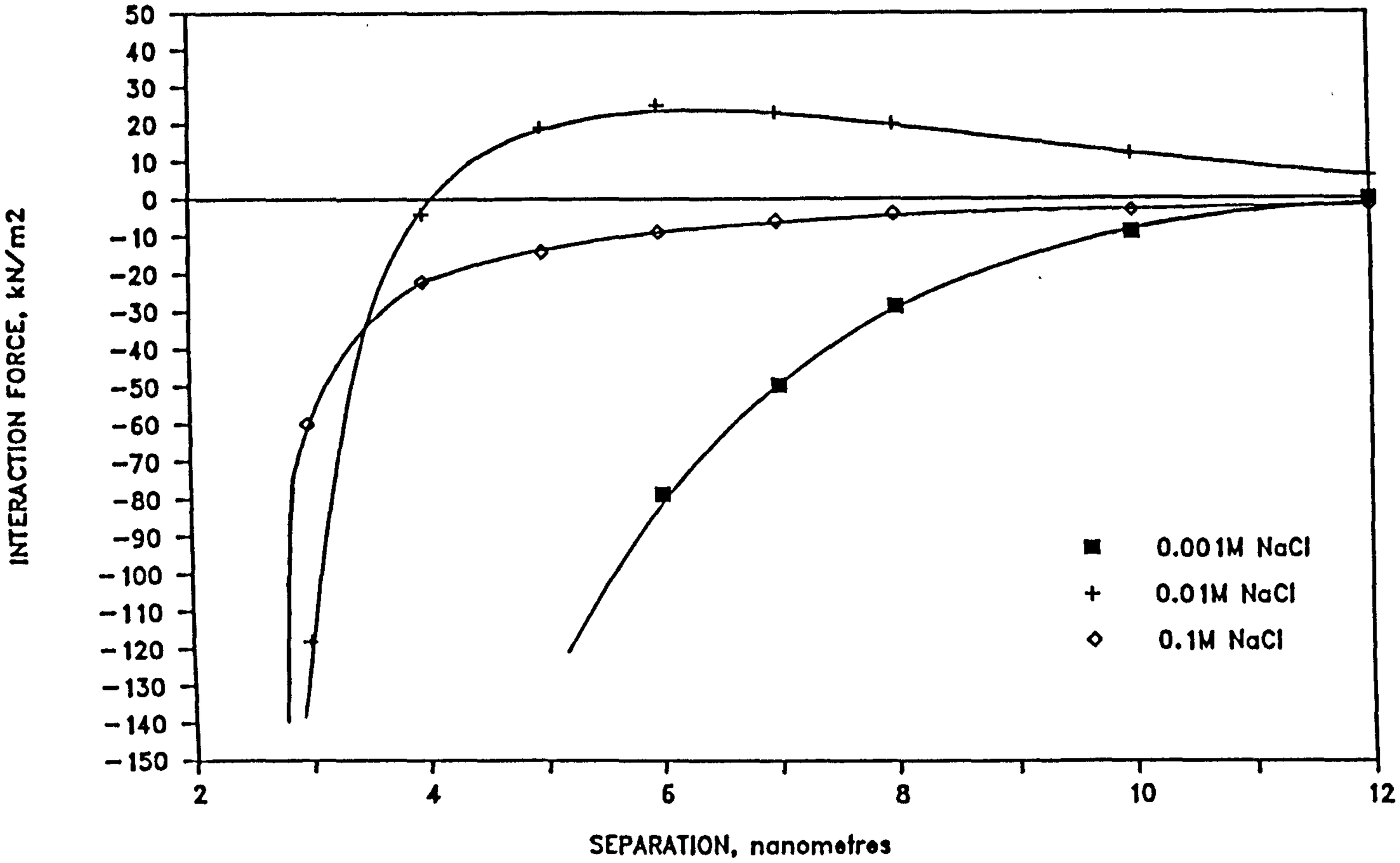

Fig. 57b Total Electrical Interaction Force
Kaolinite Edge Association at pH 9

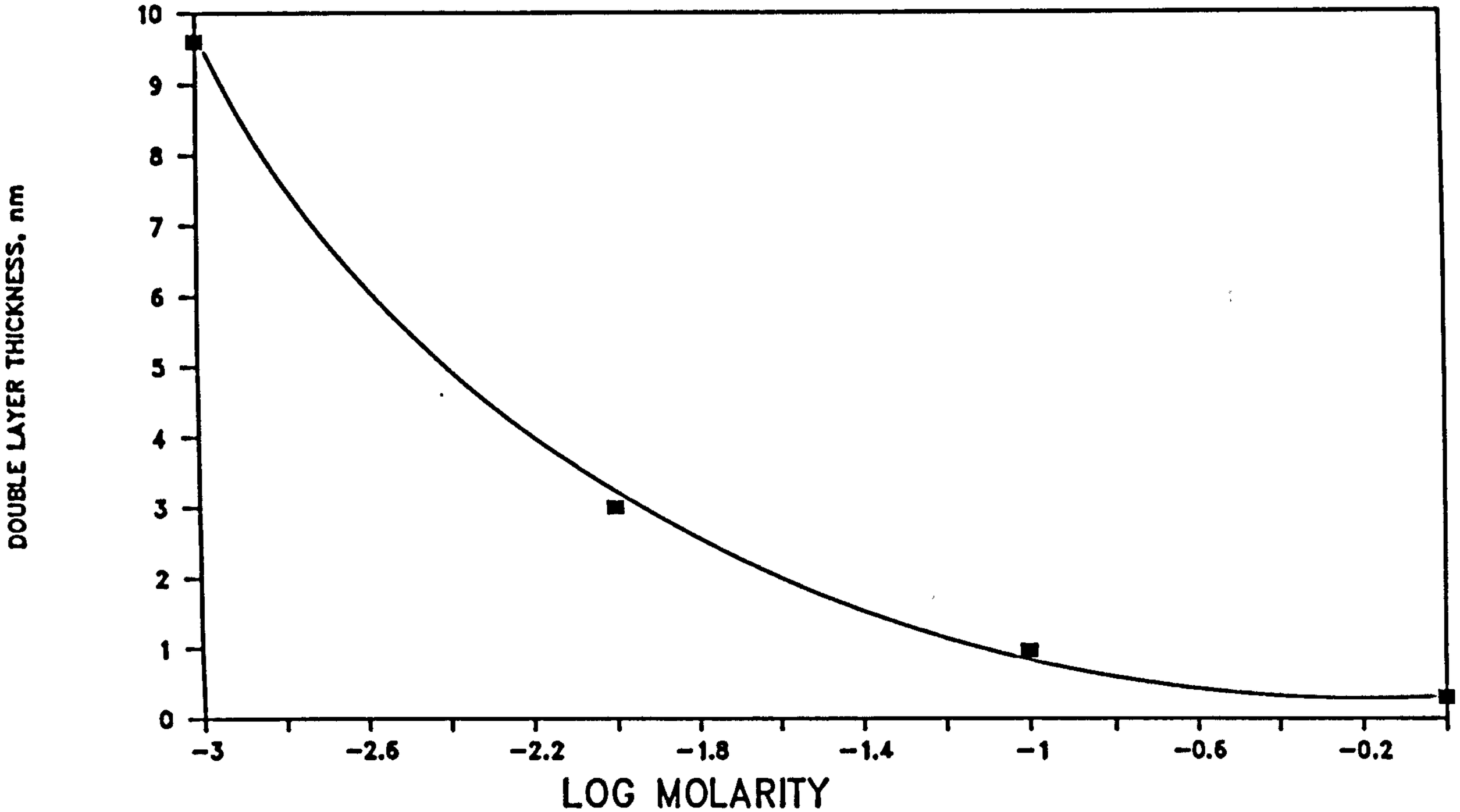

FIG. 58 Thickness of the Double Layer as Function of Aqueous Electrolyte(1:1) Strength at 25 Degrees Celsius

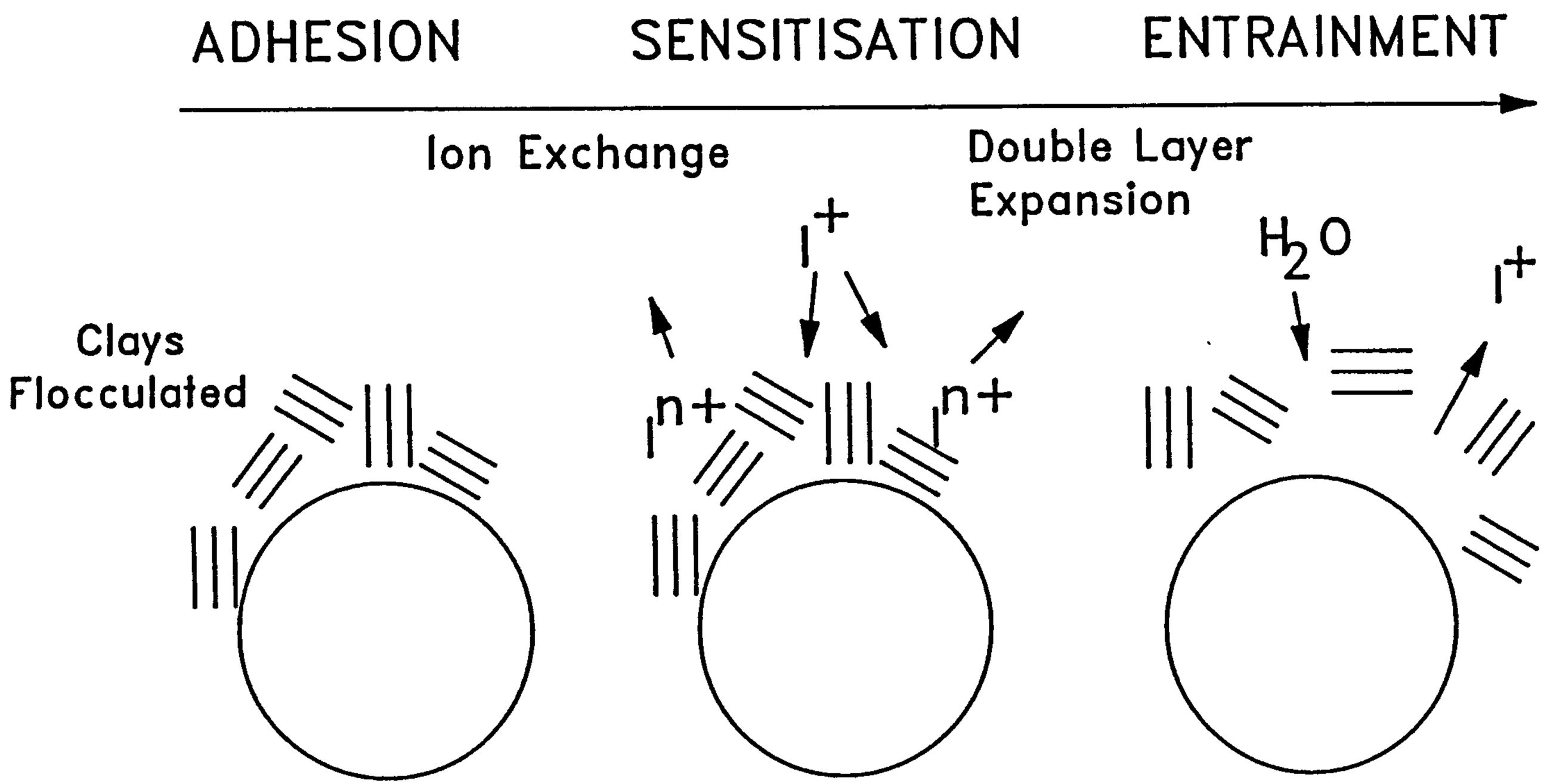

FIG. 59 A Model of Clay Mobilisation